2015

I. Synthesis of Ascarosides for Chemical Biology Studies in Caenorhabditis elegans, II. A Photochemical Approach to Delavayine, and III. Remote Hydroxylation by Radical Translocation and Polar Crossover

Kyle Allen Hollister
Louisiana State University and Agricultural and Mechanical College, kholl13@lsu.edu

I. SYNTHESIS OF ASCAROSIDES FOR CHEMICAL BIOLOGY STUDIES IN *CAENORHABDITIS ELEGANS*, II. A PHOTOCHEMICAL APPROACH TO DELAVAYINE, AND III. REMOTE HYDROXYLATION BY RADICAL TRANSLOCATION AND POLAR CROSSOVER

A Dissertation

Submitted to the Graduate Faculty of the
Louisiana State University and
Agricultural and Mechanical College
in partial fulfillment of the
requirements for the degree of
Doctor of Philosophy

in

The Department of Chemistry

by
Kyle Allen Hollister
B.S., University of Florida, 2010
December 2015

Dedicated to my

parents for unwavering love,

support, and guidance.

ACKNOWLEDGMENTS

I would first like to express great appreciation for my mentor and friend, Dr. Justin R. Ragains. His continued trust, support, and edification have been essential during my time at Louisiana State University. Without his patient yet testing tutelage I would not be the scientist I am today. I am excited to watch the Ragains lab grow, prosper, and produce exciting science in the future.

A grateful thank you to my committee members, Dr. George Stanley, Dr. Rendy Kartika, and Dr. Daniel Hayes for their assistance and encouragement. To Drs. George Stanley, William Crowe, Carol Taylor, Kermit Murray, and Julia Chan, thank you for essential fundamental knowledge passed on through instruction and/or conversation. Special thanks to the LSU faculty and staff who have provided wonderful assistance during my graduate career, especially Kim Mollere and Drs. Connie David, Thomas Weldeghioghis and Dale Treleaven. Thank you as well to our collaborators, Drs. Rebecca Butcher and Michael Miller, for their expertise and hard work.

Many thanks to past and present group members, Dr. Elizabeth Balapitiya, Mark Spell, Xiaoping Wang, Dr. Amir Wahba, Kristina Deveaux, Rashanique Quarels, John Crafton, Elizabeth Kimball and Shaofu Du, for their friendship, humor, and support. To my undergraduate and high school mentees, Gary Bernard, Michael Beal, Léa Maneval, and Pratik Patel, thank you for your bright and enthusiastic approach to learning.

Most vitally, I thank my family, especially my parents, Steve and Karen, for the immense amount of love and encouragement I have always received. It is impossible to describe how lucky and how proud I've been to have them in my life.

TABLE OF CONTENTS

LIST OF FIGURES

LIST OF ABBREVIATIONS

^{1}H……...proton NMR

^{13}C……carbon NMR

ACS……...……American Chemical Society

CD_3OD……...……...deuterated methanol

$CDCl_3$ ……..……...deuterated chloroform

CV……...……cyclic voltammetry

DCM……...…….dichloromethane

DMAP……...……4-dimethylaminopyridine

DMF……...……dimethylformamide

EC_{50}…….……half maximal effective concentration

EDG……...……..electron-donating group

E^{o}……...……standard reduction potential

EtOAc……...……ethyl acetate

EtOH……...……...ethanol

EWG……...……...electron-withdrawing group

GPCR……...…….G protein-coupled receptors

HPLC……...……high performance liquid chromatography

HRMS…….high resolution mass spectrometry

IC……...……indole-3-carboxyl

IGF-1……...……...insulin-like growth factor one

i-PrOH……...……...2-propanol

ISC……...……..intersystem crossing

LED……...…….light emitting diode

MeCN……...……acetonitrile

MeOH……...……...methanol

MK……...……...methyl ketone

NBS……...……...*N*-bromosuccinimide

NGM……...……nematode growth media

NIS……...……*N*-iodosuccinimide

NMR……...……...nuclear magnetic resonance

PABA……...……...*para*-aminobenzoic acid

PCC……...……pyridinium chlorochromate

Pd/C……...……palladium on activated carbon

RNA……...……..ribonucleic acid

S_0……...……..…singlet ground state

S_1……...……..…singlet excited state

SAR……...……..structure-activity relationship

SCE……...……...……..saturated calomel electrode

SET……...…….single electron transfer

T_1……...……..triplet excited state

t-BuOH……...……..2-methyl-2-propanol

TEMPO……...……...(2,2,6,6-tetramethyl-piperidin-1-yl)oxyl

TFA……...……...……trifluoroacetic acid

TGF-β……...……...transforming growth factor beta

THF……...……tetrahydrofuran

TLC……...……...thin layer chromatography

Tz^{o}Cl……...……*o*-tosyl triazene chloride

UV……...……..ultraviolet

LIST OF SCHEMES

ABSTRACT

The foci of this dissertation are the synthesis of analogs for chemical biology studies, synthetic chemistry method development (with an emphasis on photochemistry), and the application of these methods toward total synthesis. Chapter 1 outlines the synthesis of an array of pheromone analogs that are derivatives of the dideoxy sugar ascarylose. Referred to as ascarosides, such compounds have recently been shown to influence important biological processes in the model organism *Caenorhabditis elegans*. *C. elegans* secretes ascarosides into its environment, where the compounds then act as signaling molecules by providing information on factors like population density.

Chapter 2 describes the biological impact of naturally occurring and synthetic ascarosides in *C. elegans* developmental and reproductive assays. Chemosensation of ascarosides results in downregulation of important signaling pathways, which are conserved in higher organisms, and our studies provide data on the effects of these processes. We hypothesize that knowledge gained from these studies can be extrapolated to provide insight for similar processes in higher organisms such as humans.

In Chapter 3, a photochemical approach to total synthesis of the natural product delavayine is discussed. Alkaloids from the same family have shown biological activity via binding to human opioid receptors, which are responsible for producing analgesic and antidepressant effects. The photo-S_N1 reaction, a process which produces a triplet phenyl cation intermediate, was utilized as a central reaction for initiation of a cascade cyclization event en route to delavayine.

Chapter 4 details the development of a strategy for remote C-H functionalization using redox catalysis. The Tz^o directing group was used to effect 1,6- and 1,7-hydrogen

atom transfers from unactivated aliphatics. The resulting radicals were then oxidized by redox (or photoredox) catalysis to form a carbocation that was ultimately trapped by water or methanol. After loss of a proton, successfully hydroxylated or methoxylated products were isolated in moderate yields. This newly developed method was then applied to a concise total synthesis of the powerful antidepressant drug fluoxetine (Prozac®), beginning from a more inexpensive and simple starting material than current industrial methods.

CHAPTER 1: CHEMICAL GENETIC STUDIES ON CHEMOSENSATION IN THE MODEL ORGANISM *CAENORHABDITIS ELEGANS*, PART I: SYNTHESIS OF ASCAROSIDES

1.1 Introduction

Chemical biology, the utilization of chemical principals to examine biological processes, has been referred to as "the ultimate team sport."[1] This interdisciplinary field has emerged as a high-impact arena for all those with an interest in molecular biology. In 2005 and 2006 respectively, the journals entitled *Nature Chemical Biology* and *ACS Chemical Biology* were created in order to accommodate the bulk of new research in the area. By recognizing the potential of this field, scientists are developing the means to answer questions like, "How do small molecules play a role in complex biological processes?", "What can studying such relationships do to improve our overall understanding of chemistry and biology?", and ultimately, "Can we benefit by applying this knowledge to make advances in vital areas such as medicine?" Taking the first steps to resolving such questions has been the driving force for the research presented herein.

The common nematode *Caenorhabditis elegans* (Figure 1.1) has been widely used to study biological processes in animals for nearly half a century, and has facilitated the discovery of many important phenomena including RNA interference and programmed cell death.[2,3] Recently, it has been found that a series of small molecule pheromones regulates a variety of biological processes in *C. elegans*. Each of these molecules consists of the dideoxy sugar ascarylose linked to a fatty acid-like moiety of varying chain length, degree of unsaturation, and terminal functionality. Gathering information about these structural features and how they confer activity will be of the utmost importance in understanding the roles of these molecules in *C. elegans*. We furthermore anticipate that small molecule

studies will give insight into various biological processes in *C. elegans*, many of which are of importance in higher organisms.

Figure 1.1 *Caenorhabditis elegans* hermaphrodite

1.2 *C. elegans* Background

One of the most important choices facing scientists when exploring the realm of chemical biology is the selection of a model organism to study. In the early 1960s, Sydney Brenner sought to find a model organism that met certain criteria for studies of higher level biological functions such as development.[4] The organism needed to be easy to cultivate and manipulate in large numbers, have a short generation time, be easily studied under a microscope, and be complex enough to contain differentiated organs and a central nervous system.[5] Bacteria, though heavily used for molecular biology, did not meet the criterion of complexity. Brenner also stated that the fruit fly *Drosophila melanogaster* was too complex for his intentions, and its nervous system was not yet well-studied.[3] Through much searching, Brenner eventually identified the small nematode *Caenorhabditis elegans*. *C. elegans* can be easily cultivated in a laboratory and has a short generation time (2-3 days) and lifespan (2-3 weeks).[6] An adult hermaphrodite (Figure 1.1) is approximately 1 mm in length, contains exactly 959 somatic cells, and has a transparent body which can

be observed via light microscopy. In the 50 years since Brenner's seminal studies, the entire *C. elegans* genome has been sequenced, its cell lineage and nervous system have been completely reconstructed, and its use of RNA interference in the expression of genes has been revealed.[6] These discoveries have firmly established the worm's practicality as a model organism.

It has now been determined that *C. elegans* senses chemical cues, *e.g.* pheromones, via sensory organs located in its head.[7] When the correct pheromones are present, and when their antagonists are absent, it is believed that this process results in down regulation of pathways such as TGF-β[8] and IGF-1.[9] Homologous pathways to TGF-β and IGF-1 are known to influence growth, metabolism, development, longevity, and stress-resistance in higher organisms.[7] In 2005, the first structural elucidation and synthesis of a *C. elegans* pheromone took place.[10] This initially-discovered pheromone is one of no fewer than twelve additional compounds,[11,12,13,14] some published as recently as 2012.[15] Scheme 1.1 shows some key pheromones. Several of these additional compounds are potent inducers of dauer formation, and others have activity as sexual attractants (Chapter 2).[12] It has also been shown that these molecules work synergistically by binding to multiple receptors.[13,16]

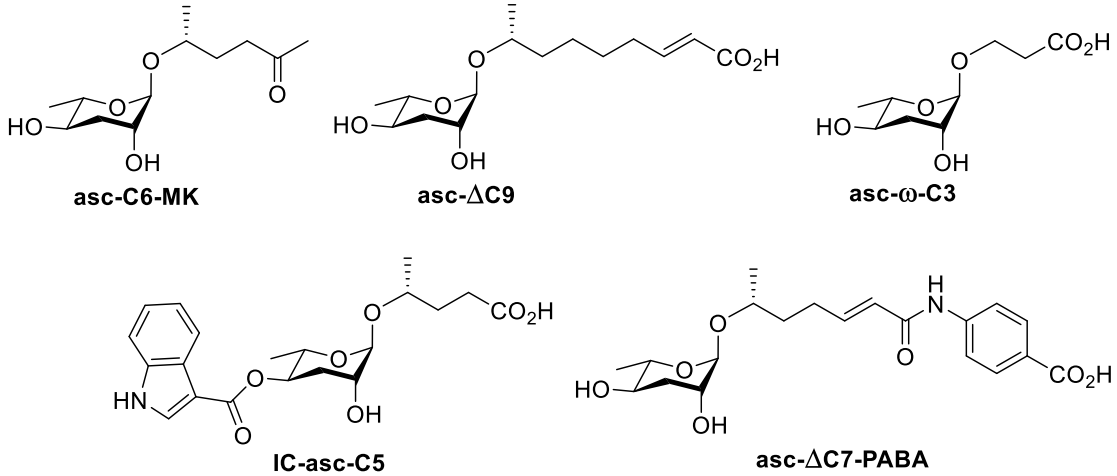

Scheme 1.1 Important *C. elegans* pheromone components

1.3 *C. elegans* Ascaroside Pheromones

To date, each pheromone molecule is a derivative of ascarylose, a dideoxy sugar which comprises the backbone of the structure (shown in red, Figure 1.2). Every ascaroside also has a fatty-acid like moiety attached by a glycosidic linkage to C1 of the sugar. Ascarosides can vary by many structural features, as shown in Figure 1.2, and the names reflect these variations. Structures can vary by having ω or ω–1 (R = H or Me, respectively) oxygenation of the side chain, of which ω–1 is more common and therefore left out of the name. Side chains may also contain α,β-unsaturation, which is denoted with a Δ in the name of the compound. The terminus of the side chain regularly varies and may include a carboxyc acid (common, not named), methyl ketone (MK), or *para*-aminobenzoic acid (PABA) group attached by amide linkage. Some ascarosides have been found to contain a head group at C4 of the sugar. The indole carboxyl group (IC) shown in Figure 1.2 is the most common head group other than the free hydroxyl. The systematic naming of ascarosides follows these differences in structure and is therefore given as (head group-)asc-(ω)(Δ)C(# of carbons in side chain)-(terminal group).

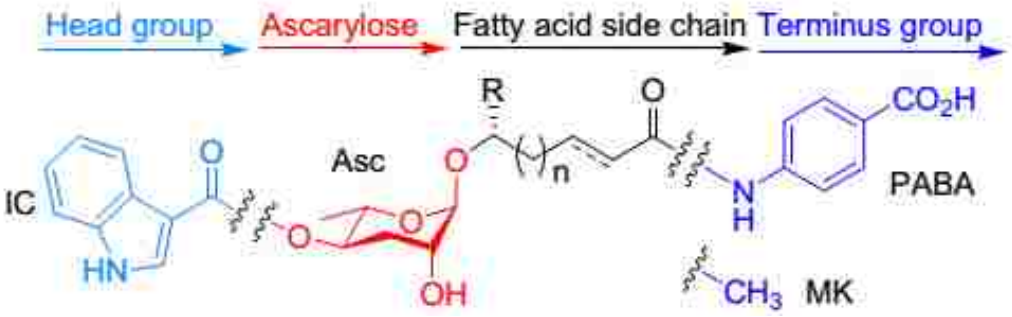

Figure 1.2 General structure of ascarosides

The key structural features of the ascaroside family addressed by these initial analog studies are 1) presence of IC head group, 2) side chain length, 3) degree of

unsaturation, 4) functionality at the terminus and 5) ω vs ω–1 oxygenation of the side chain. Study of activity conferred by specific structural features has produced an SAR for *C. elegans* pheromones dauer-inducing ability and given insight into receptor function. Naturally occuring ascarosides were also synthesized and used for study of sperm motility in *C. elegans*. See Chapter 2 for results of both the analog and sperm motility studies.

1.4 Results and Discussion

Analogs of the *C. elegans* dauer-inducing pheromones have been synthesized in 4-5 steps from dibenzoyl ascarylose, which was previously synthesized according to a known procedure. Ascaroside head group, side chain length, degree of unsaturation, and functionality at the terminus have been varied systematically to produce a series of similar compounds. By screening molecules with only slight structural differences from the natural products and from each other, we aimed to determine which structural features confer activity. Scheme 1.2 shows all targeted ascarosides, with boxes around targets synthesized by this researcher (a total of 12).

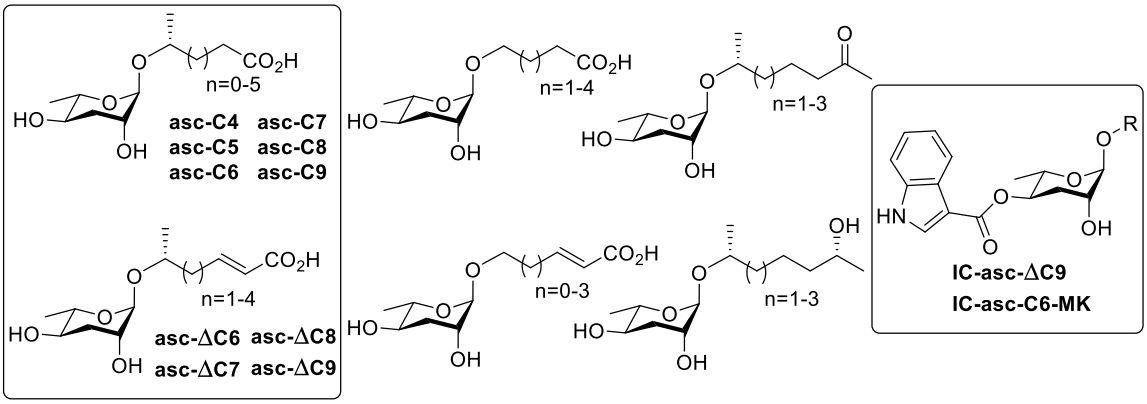

Scheme 1.2 Ascarosides targeted for synthesis

The first series of ascarosides produced has structures similar to naturally occurring pheromones **asc-C7** and **asc-ΔC9** (also synthesized in this study), shown in Scheme 1.2. The first series of targeted compounds range in chain length from four to nine carbons and

maintain the carboxylic acid terminal functionality. Both the saturated and α,β-unsaturated derivatives have been synthesized in 4-5 steps from dibenzoyl ascarylose. Shown in Scheme 1.3, enantioenriched, terminal alkene-bearing alcohols (*e.g.* the depicted (*R*)-(-)-4-Penten-2-ol (for n=1) were successfully attached to dibenzoyl ascarylose via BF_3-promoted glycosylation[10] to produce intermediate compounds such as **1.1**. Neighboring group participation from the adjacent benzoyl protecting group resulted in selective formation of the desired α anomer in moderate yields.

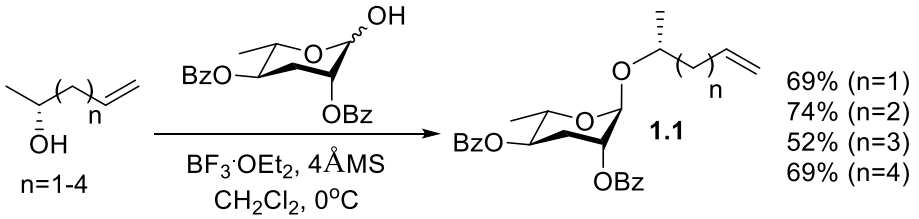

Scheme 1.3 Glycosylation

Olefin cross metathesis with Grubbs II catalyst and methyl acrylate in refluxing CH_2Cl_2 was used to install a methyl ester terminal functionality. Intermediate series **1.2**, shown in Scheme 1.4, was readily produced in good yields from this reliable reaction. To provide saturated analogs **1.3**, some of each analog **1.2** was hydrogenated with palladium on activated carbon in EtOAc. Scheme 1.4 depicts this high yielding reaction, which produced intermediates **1.3** in good yields. The methyl esters and benzoyl protecting groups of both intermediate series **1.2** and series **1.3** were hydrolyzed with 1M LiOH in *t*-BuOH to produce the final ascaroside analogs **asc-ΔC(n+5)** and **asc-C(n+5)** in moderate to good yields.[13]

The next set of analogs includes the indole carboxyl (IC) moiety of natural ascaroside **IC-asc-C5**, shown in Scheme 1.1. By creating analogs of **IC-asc-C5** that also contain a side chain of known activity, we intend to ascertain the significance of the indole

functionality. Therefore, two IC containing analogs (**IC-asc-ΔC9** & **IC-asc-C6-MK**, with side chains from **asc-ΔC9** & **asc-C6-MK** respectively) have been synthesized in 5 steps each from dibenzoyl ascarylose.

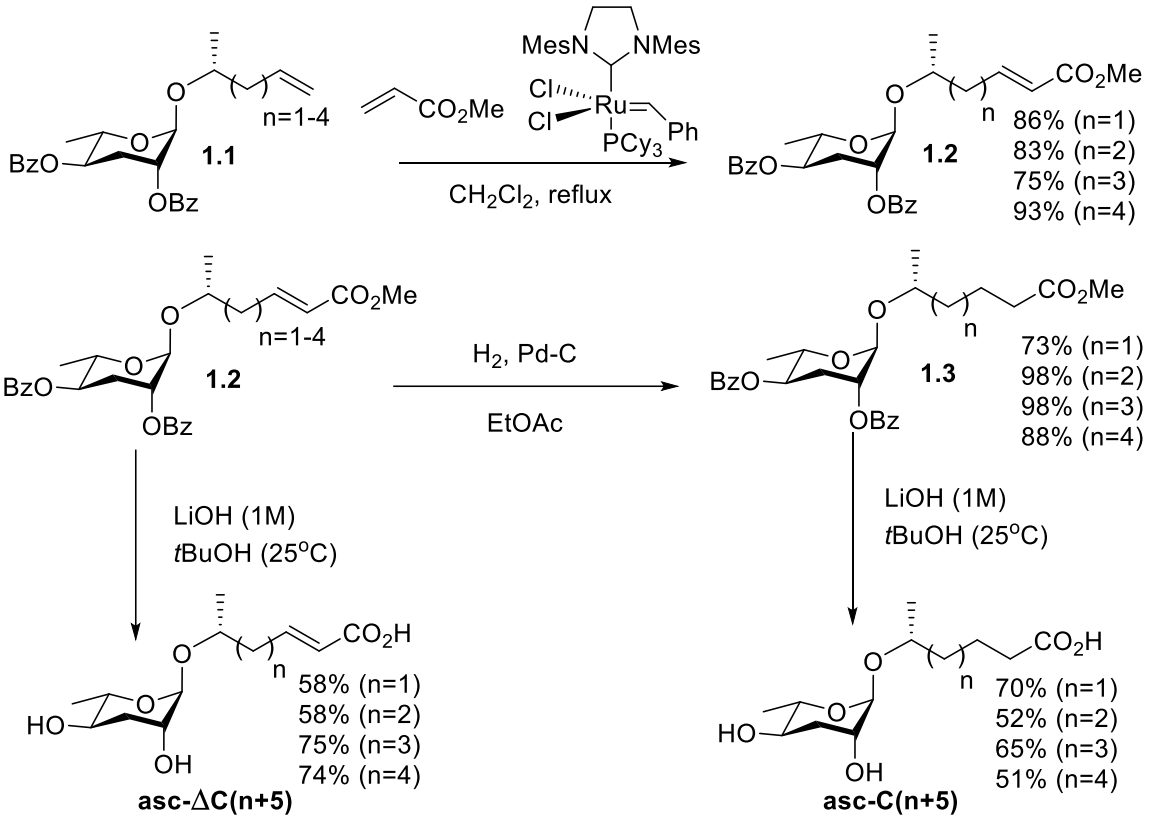

Scheme 1.4 Completion of first ascaroside series

For the synthesis of **IC-asc-C6-MK** (Scheme 1.5), the previously described glycosylation method was used, this time with (2R,5R)-2,5-hexanediol to produce alcohol intermediate **1.4**. PCC oxidation of **1.4** in CH_2Cl_2 gave ketone **1.5** in outstanding yield at which point the benzoyl protecting groups were removed via 1M LiOH hydrolysis in *t*-BuOH to produce naturally occurring ascaroside **asc-C6-MK**. At this stage, the indole carboxyl head group was to be attached at the equatorial free hydroxyl group. Unfortunately, the axial hydroxyl proved to be more reactive, (likely due to gauche interaction at the equatorial position) which prevented us from achieving monoacylation at

the desired position. Instead, diacylation of **asc-C6-MK** with freshly prepared indole-3-carbonyl chloride in dry CH_2Cl_2 afforded **1.6** in high yield.[14] In the last step of the synthesis, a difficult monohydrolysis of the C2 indole carboxyl group in intermediate **1.6** was accomplished to give **IC-asc-C6-MK**, the target analog. Aliquots of the reaction in progress were subjected to ^{1}H NMR where it was observed that an upfield chemical shift of the glycosidic proton at C2 correlated to hydrolysis. After testing several sets of conditions, the slightly more reactive axial indole moiety was cleaved in low yield with 1M LiOH in *i*-PrOH at 45°C and purified via HPLC. The isomer containing the indole carboxyl group solely at the axial position was never observed.

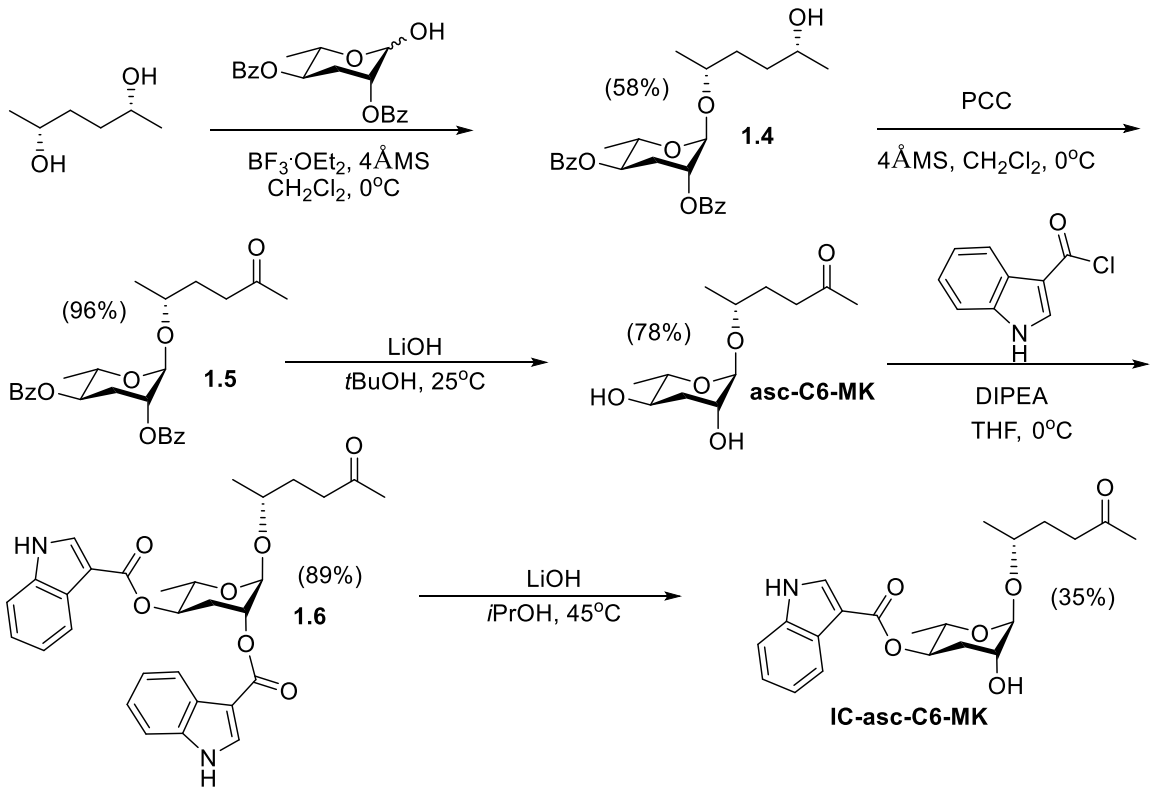

Scheme 1.5 Synthesis of **IC-asc-C6-MK**

Synthesis of **IC-asc-ΔC9** (Scheme 1.6) commenced with BF_3-promoted glycosylation with dibenzoyl ascarylose and (*R*)-(-)-7-Octan-2-ol to yield **1.1** at which point the benzoyl groups were hydrolyzed to obtain terminal alkene **1.7**. Diacylation with

indole-3-carbonyl chloride yielded **1.8**, and methyl ester **1.9** was produced in excellent yield using Grubbs II catalyst for olefin cross metathesis with methyl acrylate. Finally, monohydrolysis of the C2 indole carboxyl group (and simultaneous methyl ester cleavage) in intermediate **1.9** was accomplished to give target compound **IC-asc-ΔC9**. It is interesting to note that, while testing conditions for the monohydrolysis of the indole group at C2 during the synthesis of **IC-asc-C6-MK** (Scheme 1.5), it was found that *t*-BuOH was not a suitable solvent. The reaction did not proceed at room temperature and progressed too rapidly at elevated temperature in *t*-BuOH, and therefore *i*-PrOH was used as an acceptable alternative. However, for the quite similar transformation of **1.1** to **IC-asc-ΔC9** the same was not true. In fact, a much improved yield was obtained by using *t*-BuOH with 1M LiOH at 50°C. Again, none of the isomer containing the indole carboxyl solely at the axial position was ever observed.

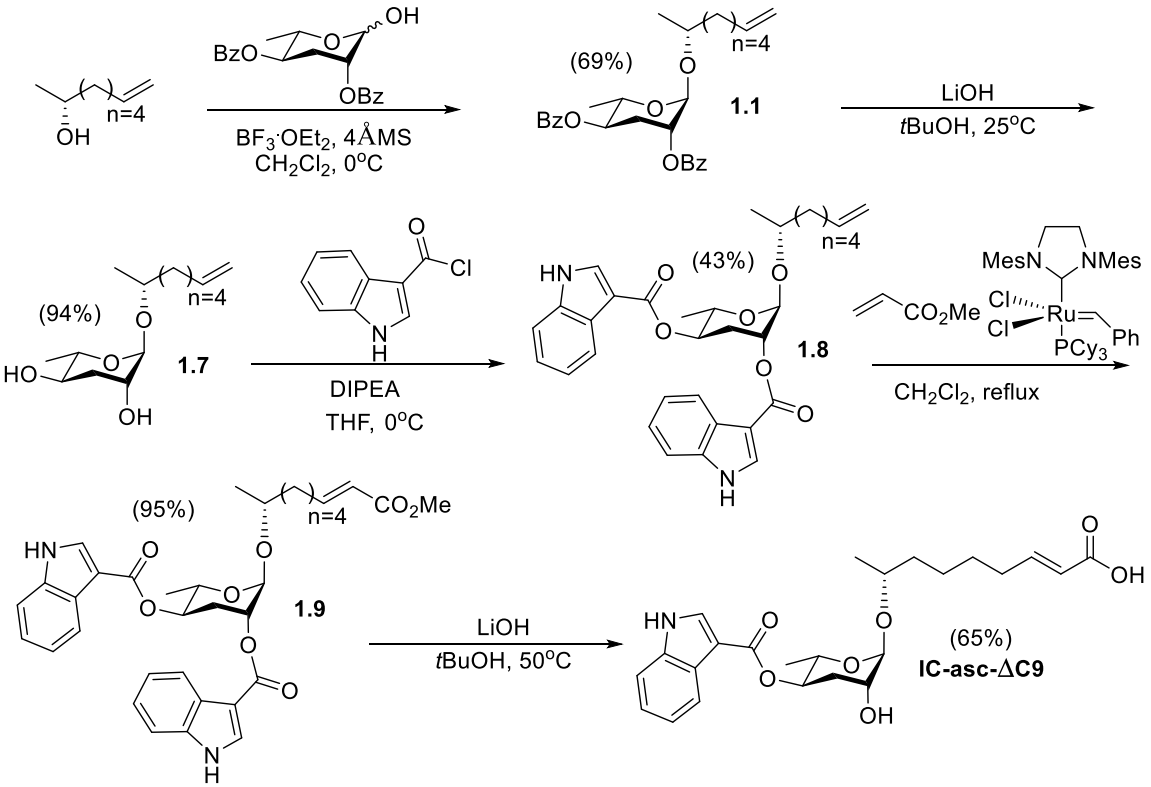

Scheme 1.6 Synthesis of **IC-asc-ΔC9**

To further understand the importance of the IC moiety, it was desirable to synthesize analogs with a very similar side chain to **IC-asc-C5** (Scheme 1.1), but which lacked the IC. One such analog had been previously synthesized (Scheme 1.4, **asc-C6**). This analog was one side-chain carbon longer (6 carbons total) than **IC-asc-C5**, and therefore additional analogs with 4 and 5 carbon side chains were synthesized. Scheme 1.7 shows the synthetic pathway beginning with previously accessed intermediates **1.1** undergoing ozonolysis in CH_2Cl_2 at -78°C. Upon workup with PPh_3, the desired aldehyde was obtained (unpurified, confirmed by ^1H NMR) and subjected to Pinnick oxidation conditions to afford carboxylic acid series **1.10**.[14] Hydrolysis under the customary set of conditions successfully generated target analogs **asc-C4** and **asc-C5**.

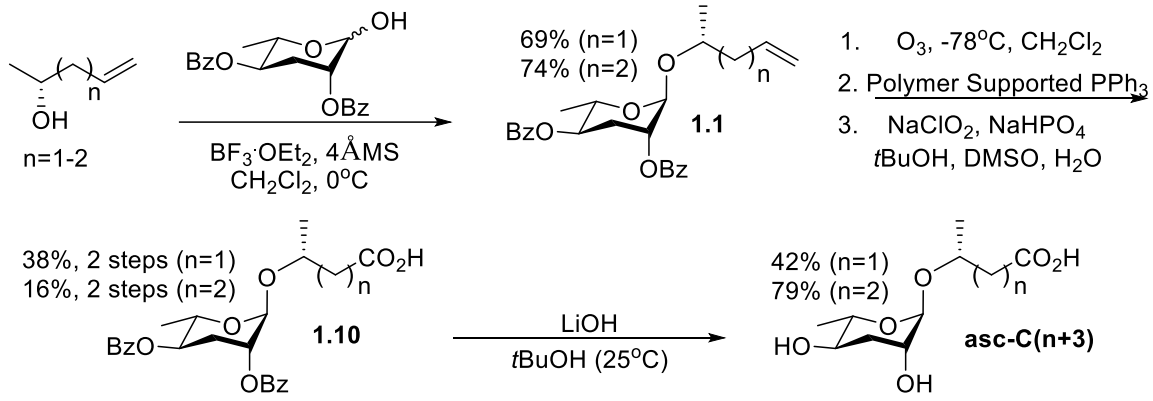

Scheme 1.7 Synthesis of **asc-C4** and **asc-C5**

In some instances, enantiomerically enriched alcohols for glycosylation were not commercially available. Thus, the 7 and 8 carbon chain alcohols, (*R*)-hept-6-en-2-ol and (*R*)-oct-7-en-2-ol respectively, were synthesized via organocuprate opening of commercially available (*R*)-(+)-propylene oxide as shown in Scheme 1.8. These reactions consistently produced the desired alcohols is high yield.

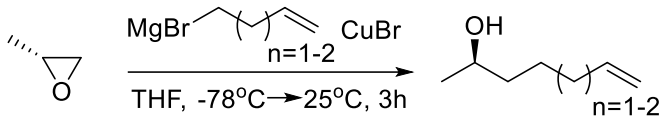

Scheme 1.8 Epoxide opening

1.5 Conclusions

Target ascarosides were successfully synthesized in 4-5 steps from dibenzoyl ascarylose. Both the equivalents of alcohol for glycosylation and equivalents of methyl acrylate for cross metathesis proved to be important and required significant optimization. In most cases, hydrolysis of benzoyl esters proved to be much higher yielding if *t*-butanol was used as solvent rather than methanol. By far the most challenging synthetic step involved placement of the indole carboxyl moiety in two of the analogs. It was necessary to diacylate both compounds due to the higher reactivity of the unwanted axial position. Then, removal of the indole group from the axial position proved to be extremely sensitive. Even though the two target analogs were very similar in structure, the same set of conditions did not work for both. Instead, careful optimization was required for each analog, including monitoring of the reaction by NMR.

Though many steps were challenging and required careful planning and optimization, all were finally accomplished. Most of the target analogs were quite polar and required HPLC purification. Also, during synthesis of analogs, it was discovered that analog target **IC-asc-ΔC9** was a natrually occuring ascaroside.

1.6 Experimental

Representative procedure for glycosylation:

A suspension of 1.0228 g (2.8720 mmol) dibenzoylascarylose, 0.54 mL (4.5 mmol) alcohol and 325.8 mg 4Å molecular sieves in 32 mL CH_2Cl_2 was cooled to 0°C. To this suspension

was added 1.54 mL (12.2 mmol) $BF_3{\cdot}OEt_2$ at once. The resulting suspension was stirred at 0°C for 7 h. 30 mL saturated $NaHCO_3$ solution was then added. Upon cessation of effervescence, the aqueous layer was separated from the organic layer and then extracted with 3 x 20 mL CH_2Cl_2. The resulting organic extracts were dried over $MgSO_4$ and filtered to obtain 1.5492 mg of oil. Column chromatography (35 g silica gel, gradient run from 50% hexanes in CH_2Cl_2 to 30% hexanes in CH_2Cl_2) afforded 1.1364 mg (90%) of a colorless syrup.

Synthesis of **1.1, n=1** (glycosylation):

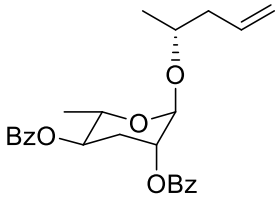

Began with 234.6 mg dibenzoyl ascarylose, column chromatography (14.5 g silica gel, 30% hexanes in CH_2Cl_2) yielded 193.8 mg (69%) of a colorless oil. $[\alpha]_D^{25}$ = -9.34, *c* 3.18 (MeOH); HRMS (*m/z*): $[M+Na]^+$ calcd. for $C_{25}H_{28}O_6Na$ 447.1778, found 447.1788; ^1H NMR (400 MHz, $CDCl_3$) δ 8.12 (d, *J* = 7.4 Hz, 2H), 8.05 (d, *J* = 7.5 Hz, 2H), 7.63 – 7.54 (m, 2H), 7.51 – 7.42 (m, 4H), 5.89 (ddt, *J* = 14.0, 5.1 Hz, 1H), 5.25 – 5.08 (m, 4H), 4.97 (s, 1H), 4.22 – 4.05 (m, 1H), 3.98 – 3.86 (m, 1H), 2.48 – 2.36 (m, 2H), 2.36 – 2.27 (m, 1H), 2.21 (ddd, *J* = 13.9, 11.1, 3.1 Hz, 1H), 1.28 (d, *J* = 6.1 Hz, 3H), 1.21 (d, *J* = 6.0 Hz, 3H); ^{13}C NMR (101 MHz, $CDCl_3$) δ 165.68, 165.56, 134.81, 133.15, 133.08, 129.94, 129.77, 129.52, 128.35, 117.13, 93.89, 72.35, 71.09, 70.57, 66.82, 41.53, 29.60, 18.84, 17.73.

Synthesis of **1.1, n=2** (glycosylation):

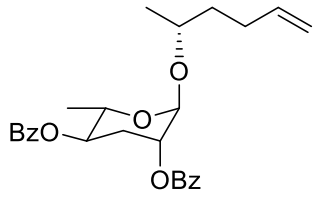

Began with 750.0 mg dibenzoyl ascarylose, column chromatography (55 g silica gel, 30% hexanes in CH_2Cl_2) yielded 684.1 mg (74%) of a colorless oil. $[\alpha]_D^{25}$ = 90.0, *c* 1.01 (CH_2Cl_2); HRMS (*m/*z): $[M+Na]^+$ calcd. for $C_{26}H_{30}O_6Na$ 461.1935, found 461.1931; ^1H NMR (400 MHz, $CDCl_3$) δ 8.12 (d, *J* = 7.6 Hz, 2H), 8.05 (d, *J* = 7.6 Hz, 2H), 7.59 (t, *J* = 7.2 Hz, 2H), 7.52 – 7.42 (m, 4H), 5.88 (ddt, *J* = 16.9, 10.2, 6.6 Hz, 1H), 5.25 – 5.13 (m, 2H), 5.09 (dd, *J* = 17.1, 2.0 Hz, 1H), 5.02 (d, *J* = 10.2 Hz, 1H), 4.96 (s, 1H), 4.13 (dq, *J* = 12.3, 6.3 Hz, 1H), 3.88 (h, *J* = 6.2 Hz, 1H), 2.42 (ddd, *J* = 13.4, 3.9 Hz, 1H), 2.31 – 2.13 (m, 3H), 1.83 – 1.69 (m, 1H), 1.68 – 1.58 (m, 1H), 1.29 (d, *J* = 6.3 Hz, 3H), 1.21 (d, *J* = 6.1 Hz, 3H); ^{13}C NMR (101 MHz, $CDCl_3$) δ 165.81, 165.69, 138.41, 133.25, 133.19, 130.01, 129.87, 129.63, 128.45, 114.77, 93.74, 72.01, 71.26, 70.66, 67.03, 36.37, 29.98, 29.75, 19.11, 17.89.

Synthesis of **1.1, n=3** (glycosylation):

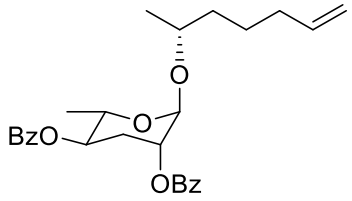

Began with 320.5 mg dibenzoyl ascarylose, column chromatography (30.5 g silica gel, gradient run from 5% ethyl acetate in hexanes to 10% ethyl acetate in hexanes) yielded 213.2 mg (52%) of a colorless oil. $[\alpha]_D^{25}$ = -55.7, *c* 0.60 (MeOH); HRMS (*m/*z): $[M+Na]^+$ calcd. for $C_{27}H_{32}O_6Na$ 475.2091, found 475.2083; ^1H NMR (250 MHz, $CDCl_3$) δ 8.18 – 8.08 (m, 2H), 8.08 – 7.98 (m, 2H), 7.66 – 7.53 (m, 2H), 7.53 – 7.39 (m, 4H), 5.86 (ddt, *J* = 16.9, 10.2, 6.6 Hz, 1H), 5.26 – 5.11 (m, 2H), 5.11 – 4.91 (m, 3H), 4.19 – 4.04 (m, 1H), 3.87 (dq, *J* = 13.2, 6.9, 6.2 Hz, 1H), 2.42 (dt, *J* = 13.0, 4.0 Hz, 1H), 2.30 – 2.00 (m, 3H),

1.74 – 1.39 (m, 4H), 1.28 (d, *J* = 6.1 Hz, 3H), 1.20 (d, *J* = 6.1 Hz, 3H); ^{13}C NMR (101 MHz, $CDCl_3$) δ 165.78, 165.65, 138.68, 133.21, 133.15, 130.01, 129.86, 129.84, 129.60, 128.42, 114.58, 93.76, 72.43, 71.24, 70.65, 66.97, 36.54, 33.60, 29.72, 24.95, 19.14, 17.86.

Synthesis of **1.1, n=4** (glycosylation):

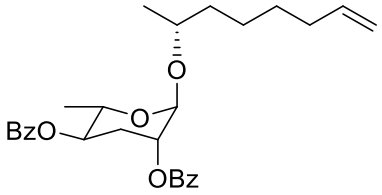

Began with 486.1 mg dibenzoyl ascarylose, column chromatography (20 g silica gel, 30% hexanes in CH_2Cl_2) yielded 440.0 mg (69%) of a colorless oil. $[\alpha]_D^{25}$ = 89.4, *c* 0.085 (CH_2Cl_2); HRMS (*m/*z): $[M+Na]^+$ calcd. for $C_{28}H_{34}O_6Na$ 489.2248, found 489.2250; ^{1}H NMR (250 MHz, $CDCl_3$) δ 8.19 – 8.09 (m, 2H), 8.09 – 7.99 (m, 2H), 7.61 – 7.49 (m, 2H), 7.51 – 7.37 (m, 4H), 5.85 (ddt, *J* = 16.9, 10.2, 6.7 Hz, 1H), 5.29 – 5.12 (m, 2H), 5.10 – 4.93 (m, 3H), 4.15 (dq, *J* = 12.3, 6.2 Hz, 1H), 3.87 (h, *J* = 5.9 Hz, 1H), 2.44 (dt, *J* = 13.4, 4.0 Hz, 1H), 2.23 (ddd, *J* = 13.8, 11.3, 3.1 Hz, 1H), 2.11 (d, *J* = 6.5 Hz, 2H), 1.70 – 1.41 (m, 6H), 1.31 (d, *J* = 6.3 Hz, 3H), 1.20 (d, *J* = 6.0 Hz, 3H); ^{13}C NMR (63 MHz, $CDCl_3$) δ 165.57, 165.45, 138.64, 133.06, 133.01, 129.89, 129.77, 129.71, 129.50, 129.45, 128.28, 114.34, 93.62, 72.35, 71.13, 70.53, 66.83, 36.85, 33.65, 29.60, 28.65, 25.10, 19.06, 17.76.

Synthesis of **1.4** (glycosylation):

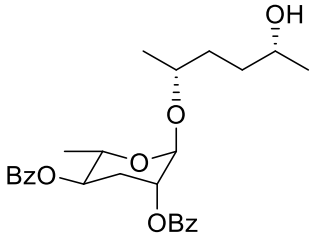

Began with 400.0 mg dibenzoyl ascarylose, column chromatography (50 g silica gel, gradient run from 20% EtOAc in hexanes to 100% EtOAc) yielded 297.5 mg (58%) of a

colorless oil. $[\alpha]_D^{25}$ = 3.1, *c* 1.46 (CH_2Cl_2); HRMS (*m/z*): $[M+Na]^+$ calcd. for $C_{26}H_{32}O_7Na$ 479.2040, found 479.2046; ^1H NMR (250 MHz, MeOD) δ 8.08 (d, *J* = 7.3 Hz, 2H), 8.00 (d, *J* = 7.7 Hz, 2H), 7.60 (t, *J* = 6.6 Hz, 2H), 7.56 – 7.40 (m, 4H), 5.21 – 5.03 (m, 2H), 4.96 (s, 1H), 4.16 (dq, *J* = 12.5, 6.4 Hz, 1H), 3.93 – 3.70 (m, 2H), 2.39 (dt, *J* = 13.4, 4.0 Hz, 1H), 2.19 (ddd, *J* = 13.9, 11.3, 3.1 Hz, 1H), 1.90 – 1.39 (m, 4H), 1.25 (d, *J* = 6.2 Hz, 3H), 1.20 (d, *J* = 6.1 Hz, 6H); ^{13}C NMR (101 MHz, $CDCl_3$) δ 165.75, 165.62, 133.21, 133.14, 129.89, 129.80, 129.75, 129.56, 128.39, 93.65, 72.49, 71.15, 70.56, 67.81, 67.02, 35.05, 33.01, 29.65, 23.57, 19.04, 17.81.

Representative procedure for cross metathesis:

To a solution of 40.0 mg (0.0734 mmol) terminal alkene and 33 µL (0.37 mmol) methyl acrylate in 4.0 mL CH_2Cl_2 was added 3.7 mg (0.0044 mmol) Grubbs 2nd generation ruthenium catalyst at once. The resulting solution was allowed to stir at reflux for 1.5 h. The reaction mixture was concentrated to 67.6 mg of brown-red oil. Column chromatography (4 g silica gel, gradient run from pure CH_2Cl_2 to 15% ethyl acetate in CH_2Cl_2) afforded 42.2 mg (0.0700 mmol) (95%) of a clear oil.

Synthesis of **1.2, n=1** (cross metathesis):

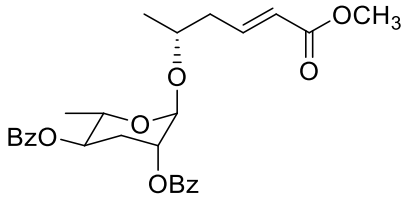

Began with 177.2 mg **1.1, n=1**, column chromatography (20.5 g silica gel, gradient run from 2% Et_2O in hexanes to 10% Et_2O in hexanes) yielded 173.6 mg (86%) of a colorless oil. $[\alpha]_D^{25}$ = 75.9, *c* 1.27 (CH_2Cl_2); HRMS (*m/z*): $[M+Na]^+$ calcd. for $C_{27}H_{30}O_8Na$ 505.1833, found 505.1838; ^1H NMR (250 MHz, $CDCl_3$) δ 8.11 (d, *J* = 7.5 Hz, 2H), 8.04

(d, *J* = 7.8 Hz, 2H), 7.66 – 7.52 (m, 2H), 7.50 – 7.39 (m, 4H), 7.14 – 6.94 (m, 1H), 5.96 (d, *J* = 15.8 Hz, 1H), 5.23 – 5.10 (m, 2H), 4.95 (s, 1H), 4.13 – 3.94 (m, 2H), 3.74 (s, 3H), 2.57 – 2.34 (m, 3H), 2.17 (t, *J* = 12.1 Hz, 1H), 1.32 – 1.19 (m, 6H); ^{13}C NMR (101 MHz, $CDCl_3$) δ 166.64, 165.73, 165.59, 145.42, 133.25, 133.15, 129.90, 129.81, 129.72, 129.61, 128.41, 128.39, 123.29, 93.89, 71.47, 70.95, 70.37, 67.06, 51.43, 39.74, 29.58, 19.19, 17.70.

Synthesis of **1.2, n=2** (cross metathesis):

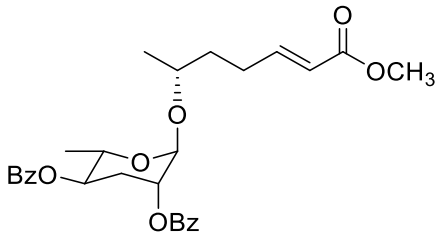

Began with 670.0 mg **1.1, n=2**, column chromatography (107 g silica gel, gradient run from 2% Et_2O in hexanes to 20% Et_2O in hexanes) yielded 630.5 mg (83%) of a colorless oil. $[\alpha]_D^{25}$ = 86.4, *c* 1.03 (CH_2Cl_2); HRMS (*m/*z): $[M+Na]^+$ calcd. for $C_{28}H_{32}O_8Na$ 519.1989, found 519.1990; ^{1}H NMR (250 MHz, $CDCl_3$) δ 8.11 (d, *J* = 7.3 Hz, 2H), 8.05 (d, *J* = 7.4 Hz, 2H), 7.59 (t, *J* = 7.0 Hz, 2H), 7.53 – 7.40 (m, 4H), 7.15 – 6.95 (m, 1H), 5.91 (d, *J* = 15.7 Hz, 1H), 5.27 – 5.09 (m, 2H), 4.96 (s, 1H), 4.06 (dq, *J* = 12.8, 6.3 Hz, 1H), 3.88 (h, *J* = 11.8, 6.3 Hz, 1H), 3.73 (s, 3H), 2.51 – 2.29 (m, 3H), 2.19 (ddd, *J* = 13.9, 10.9, 3.1 Hz, 1H), 1.90 – 1.61 (m, 2H), 1.28 (d, *J* = 6.2 Hz, 3H), 1.22 (d, *J* = 6.1 Hz, 3H); ^{13}C NMR (101 MHz, $CDCl_3$) δ 167.01, 165.80, 165.68, 148.95, 133.29, 133.22, 129.95, 129.87, 129.81, 129.65, 128.47, 121.28, 93.73, 71.73, 71.14, 70.56, 67.20, 51.47, 35.36, 29.71, 28.40, 19.07, 17.87.

Synthesis of **1.2, n=3** (cross metathesis):

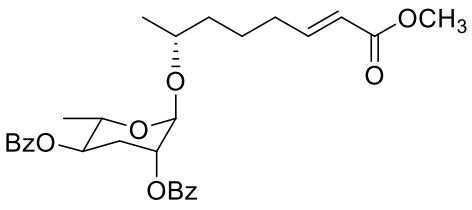

Began with 202.0 mg **1.1, n=3**, column chromatography (32 g silica gel, gradient run from 5% EtOAc in hexanes to 15% EtOAc in hexanes) yielded 170.8 mg (75%) of a colorless oil. $[\alpha]_D^{25}$ = -1.3, *c* 2.22 (MeOH); HRMS (*m/*z): $[M+Na]^+$ calcd. for $C_{29}H_{34}O_8Na$ 533.2146, found 533.2143; ^{1}H NMR (250 MHz, $CDCl_3$) δ 8.15 – 8.08 (m, 2H), 8.08 – 8.00 (m, 2H), 7.66 – 7.53 (m, 2H), 7.46 (td, *J* = 7.4, 6.8, 2.0 Hz, 4H), 7.02 (dt, *J* = 15.7, 6.9 Hz, 1H), 5.88 (d, *J* = 15.7 Hz, 1H), 5.25 – 5.10 (m, 2H), 4.95 (s, 1H), 4.16 – 4.01 (m, 1H), 3.93 – 3.79 (m, 1H), 3.72 (s, 3H), 2.42 (dt, *J* = 13.5, 4.0 Hz, 1H), 2.35 – 2.10 (m, 3H), 1.77 – 1.49 (m, 4H), 1.28 (d, *J* = 6.2 Hz, 3H), 1.20 (d, *J* = 6.0 Hz, 3H); ^{13}C NMR (63 MHz, $CDCl_3$) δ 167.04, 165.74, 165.63, 149.08, 133.21, 133.14, 129.92, 129.81, 129.59, 128.41, 121.16, 93.69, 72.20, 71.15, 70.56, 67.05, 51.39, 36.49, 32.05, 29.69, 24.12, 19.08, 17.86.

Synthesis of **1.2, n=4** (cross metathesis):

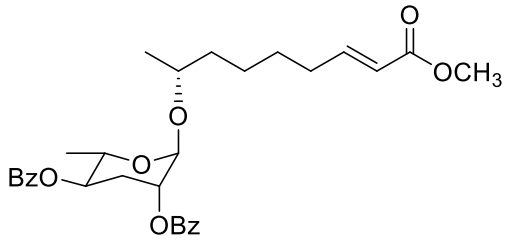

Began with 513.6 mg **1.1, n=4**, column chromatography (50 g silica gel, isocratic run of 100% CH2Cl2) yielded 534.4 mg (93%) of a colorless oil. $[\alpha]_D^{25}$ = -7.0, *c* 7.58 (CH2Cl2); HRMS (m/z): $[M+Na]^+$ calcd. for $C_{30}H_{36}O_8Na$ 547.2302, found 547.2317; ^{1}H NMR (250 MHz, $CDCl_3$) δ 8.16–8.09 (m, 2H), 8.09–8.02 (m, 2H), 7.64–7.56 (m, 2H), 7.48 (m, 4H), 7.01 (dt, J= 15.7, 7.0 Hz, 1H), 5.91–5.81 (m, 1H), 5.25–5.14 (m, 2H), 4.96 (s, 1H), 4.17–4.05 (m, 1H), 3.85 (t,J= 8.4 Hz, 1H), 3.72 (s, 3H), 2.44 (dt, J= 13.4, 4.0 Hz, 1H), 2.32–2.15 (m, 3H), 1.60–1.47 (m, 6H), 1.29 (d,J= 6.2 Hz, 3H), 1.21 (d,J= 6.0 Hz, 3H); ^{13}C NMR (101 MHz, $CDCl_3$) δ 167.17, 165.87, 165.77, 149.43, 133.36, 133.31, 130.10, 129.97, 129.73,

128.57, 121.18, 93.91, 72.63, 71.35, 70.76, 67.15, 51.49, 36.97, 32.28, 29.84, 28.09, 25.38, 19.28, 18.01.

Synthesis of **1.9** (cross metathesis):

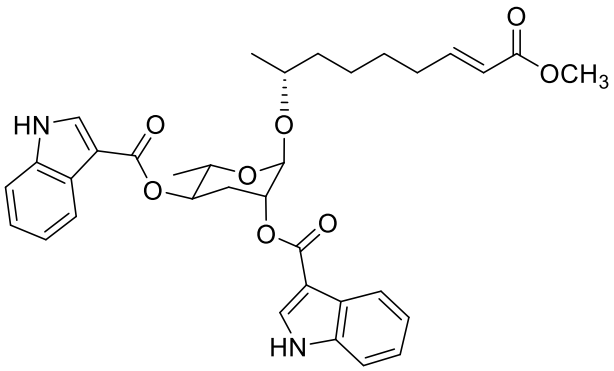

Began with 40.0 mg **1.8**, column chromatography (5 g silica gel, CH_2Cl_2, then a gradient from 5% EtOAc in CH_2Cl_2 to 15% EtOAc in CH_2Cl_2) yielded 42.2 mg (95%) of a white solid. $[\alpha]_D^{25}$ = 53.0, *c* 0.245 (CH_2Cl_2); HRMS (*m/*z): $[M+Na]^+$ calcd. for $C_{34}H_{38}N_2O_8Na$ 625.2520, found 625.2544; ^{1}H NMR (400 MHz, $CDCl_3$) δ 9.39 (s, 1H), 9.35 (s, 1H), 8.26 (d, *J* = 7.9 Hz, 1H), 8.17 – 8.12 (m, 1H), 7.94 (d, *J* = 2.7 Hz, 1H), 7.89 (d, *J* = 2.8 Hz, 1H), 7.43 – 7.36 (m, 2H), 7.30 – 7.19 (m, 4H), 7.03 (dt, *J* = 15.6, 6.9 Hz, 1H), 5.88 (d, *J* = 15.6 Hz, 1H), 5.32 (ddd, *J* = 14.4, 9.4, 4.0 Hz, 1H), 5.25 – 5.21 (m, 1H), 5.05 (s, 1H), 4.17 (dq, *J* = 12.2, 6.0 Hz, 1H), 3.91 – 3.85 (m, 1H), 3.72 (s, 3H), 2.56 – 2.49 (m, 1H), 2.32 – 2.24 (m, 3H), 1.72 – 1.63 (m, 1H), 1.59 – 1.49 (m, 4H), 1.49 – 1.42 (m, 1H), 1.35 (d, *J* = 6.2 Hz, 3H), 1.20 (d, *J* = 6.0 Hz, 3H); ^{13}C NMR (101 MHz, $CDCl_3$) δ 167.33, 164.65, 164.33, 149.63, 136.22, 136.18, 131.86, 131.77, 125.79, 125.70, 123.17, 123.03, 122.10, 122.05, 121.26, 121.11, 120.91, 111.82, 111.69, 108.10, 107.88, 94.10, 72.25, 70.01, 69.63, 67.35, 51.44, 36.87, 32.21, 30.12, 27.95, 25.36, 19.15, 18.01.

Representative procedure for hydrogenation:

A suspension of 376.7 mg (0.7377 mmol) unsaturated ester and 44.9 mg 10 % palladium on activated carbon in 41 mL EtOAc was vacuum purged and back filled with H_2 from a balloon. The resulting suspension was allowed to stir at 23°C for 24 h. The reaction mixture was filtered through Celite® and concentrated to obtain 375.4 mg (99%) of colorless oil that required no further purification.

Synthesis of **1.3, n=1** (hydrogenation):

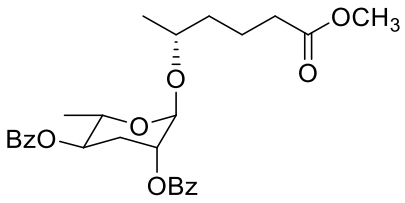

Began with 90.4 mg **1.2, n=1**, column chromatography (2.5 g silica gel, CH_2Cl_2) yielded 66.1 mg (73%) of a colorless oil. HRMS (*m/*z): $[M+Na]^+$ calcd. for $C_{27}H_{32}O_8Na$ 507.1989, found 507.1990; ^{1}H NMR (250 MHz, $CDCl_3$) δ 8.12 (d, *J* = 7.2 Hz, 2H), 8.06 (d, *J* = 7.1 Hz, 2H), 7.66 – 7.53 (m, 2H), 7.53 – 7.39 (m, 4H), 5.29 – 5.10 (m, 2H), 4.96 (s, 1H), 4.21 – 4.02 (m, 1H), 3.88 (h, *J* = 6.0 Hz, 1H), 3.70 (s, 3H), 2.51 – 2.30 (m, 3H), 2.21 (ddd, *J* = 13.9, 11.3, 3.1 Hz, 1H), 1.95 – 1.47 (m, 4H), 1.29 (d, *J* = 6.2 Hz, 3H), 1.22 (d, *J* = 6.0 Hz, 3H); ^{13}C NMR (101 MHz, $CDCl_3$) δ 173.89, 165.73, 165.62, 133.20, 133.13, 129.94, 129.81, 129.59, 128.39, 93.72, 72.12, 71.17, 70.56, 67.05, 51.48, 36.41, 33.90, 29.68, 21.14, 19.01, 17.82.

Synthesis of **1.3, n=2** (hydrogenation):

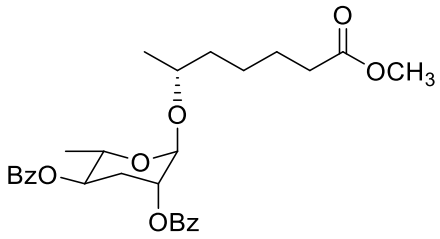

Began with 324.0 mg **1.2, n=2**, (no purification) yielded 318.4 mg (98%) of a colorless oil. $[\alpha]_D^{25}$ = -36.8, *c* 1.01 (MeOH); HRMS (*m/*z): $[M+Na]^+$ calcd. for $C_{28}H_{34}O_8Na$ 521.2146, found 521.2148 ^{1}H NMR (250 MHz, $CDCl_3$) δ 8.11 (d, *J* = 7.2 Hz, 2H), 8.05 (d, *J* = 7.3 Hz, 2H), 7.59 (t, *J* = 7.3 Hz, 2H), 7.53 – 7.39 (m, 4H), 5.27 – 5.09 (m, 2H), 4.95 (s, 1H), 4.10 (dq, *J* = 12.1, 6.4 Hz, 1H), 3.90 – 3.77 (m, 1H), 3.68 (s, 3H), 2.48 – 2.30 (m, 3H), 2.19 (ddd, *J* = 13.7, 11.3, 3.1 Hz, 1H), 1.69 (dq, *J* = 13.6, 7.3, 6.8 Hz, 2H), 1.61 – 1.37 (m, 4H), 1.28 (d, *J* = 6.2 Hz, 3H), 1.19 (d, *J* = 6.1 Hz, 3H); ^{13}C NMR (101 MHz, $CDCl_3$) δ 173.82, 165.58, 165.49, 133.08, 133.02, 129.87, 129.75, 129.69, 129.47, 128.29, 93.65, 72.26, 71.10, 70.51, 66.89, 51.30, 36.61, 33.87, 29.58, 25.11, 24.78, 18.98, 17.73.

Synthesis of **1.3, n=3** (hydrogenation):

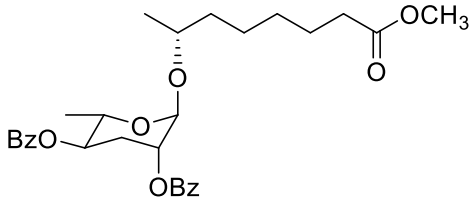

Began with 83.1 mg **1.2, n=3**, (no purification necessary) yielded 81.3 mg (98%) of a colorless oil. $[\alpha]_D^{25}$ = -1.1, *c* 0.355 (MeOH); HRMS (*m/*z): $[M+Na]^+$ calcd. for $C_{29}H_{36}O_8Na$ 535.2302, found 535.2305; ^{1}H NMR (250 MHz, $CDCl_3$) δ 8.14 – 8.07 (m, 2H), 8.07 – 7.99 (m, 2H), 7.60 – 7.50 (m, 2H), 7.50 – 7.39 (m, 4H), 5.25 – 5.10 (m, 2H), 4.95 (s, 1H), 4.18 – 4.03 (m, 1H), 3.91 – 3.76 (m, 1H), 3.64 (s, 3H), 2.42 (dt, *J* = 13.6, 4.0 Hz, 1H), 2.33 (t, *J* = 7.4 Hz, 2H), 2.20 (ddd, *J* = 13.7, 11.3, 3.1 Hz, 1H), 1.77 – 1.57 (m, 3H), 1.57 – 1.32 (m, 5H), 1.28 (d, *J* = 6.2 Hz, 3H), 1.18 (d, *J* = 6.0 Hz, 3H); ^{13}C NMR (63 MHz, $CDCl_3$) δ 173.97, 165.61, 165.51, 133.09, 133.03, 129.87, 129.75, 129.71, 129.48, 128.30, 93.64, 72.39, 71.13, 70.53, 66.87, 51.31, 36.80, 33.87, 29.60, 28.98, 25.28, 24.78, 19.02, 17.76.

Synthesis of **1.3, n=4** (hydrogenation):

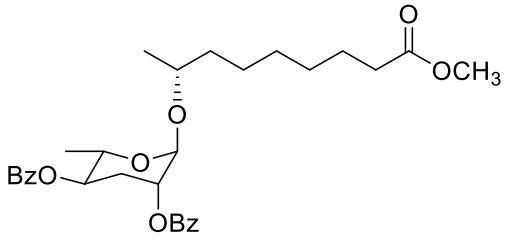

Began with 100.0 mg **1.2, n=4**, column chromatography (2.5 g silica gel, CH_2Cl_2) yielded 88.5 mg (88%) of a colorless oil. $[\alpha]_D^{25}$ = 35.5, *c* 0.80 (CH_2Cl_2); HRMS (*m/*z): $[M+Na]^+$ calcd. for $C_{30}H_{38}O_8Na$ 549.2459, found 549.2475; ^{1}H NMR (250 MHz, $CDCl_3$) δ 8.11 (d, *J* = 7.1 Hz, 2H), 8.04 (d, *J* = 7.1 Hz, 2H), 7.65 – 7.51 (m, 2H), 7.51 – 7.38 (m, 4H), 5.24 – 5.06 (m, 2H), 4.95 (s, 1H), 4.11 (dq, *J* = 12.5, 6.2 Hz, 1H), 3.84 (q, *J* = 5.9 Hz, 1H), 3.65 (s, 3H), 2.42 (dt, *J* = 13.4, 4.0 Hz, 1H), 2.32 (t, *J* = 7.4 Hz, 2H), 2.27 – 2.11 (m, 1H), 1.74 – 1.32 (m, 10H), 1.28 (d, *J* = 6.2 Hz, 3H), 1.18 (d, *J* = 6.0 Hz, 3H); ^{13}C NMR (101 MHz, $CDCl_3$) δ 174.17, 165.75, 165.63, 133.19, 133.13, 129.99, 129.84, 129.82, 129.57, 128.40, 93.76, 72.58, 71.23, 70.65, 66.93, 51.42, 37.04, 34.04, 29.70, 29.22, 29.10, 25.53, 24.89, 19.12, 17.84.

Representative procedure for hydrolysis:

To a suspension of 141.3 mg (0.2756 mmol) methyl ester in 20 mL *t*BuOH was added 20 mL 1M LiOH at once. The resulting solution was allowed to stir at 23°C for 24 h. 10 mL 20% *i*PrOH in CH_2Cl_2 was added to the reaction mixture, and the layers were separated. The aqueous layer was extracted with an additional 5x 10 mL 20% *i*PrOH in CH_2Cl_2. Solid NaCl was then added to the aqueous layer until saturation was obtained, and was further extracted with 3 x 10 mL 20% *i*PrOH in CH_2Cl_2. The combined organic layers were dried over Na_2SO_4 and filtered. Evaporation of solvent afforded 117.2 mg of an oil. Column

chromatography (47 g silica gel, gradient run from 5% *i*PrOH in CH_2Cl_2 to 20% *i*PrOH in CH_2Cl_2) afforded 78.9 mg (94%) of a colorless oil.

Synthesis of **asc-ΔC6** (hydrolysis):

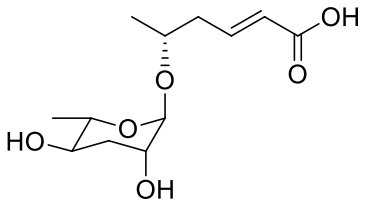

Began with 17.6 mg **1.2, n=1**, HPLC purification yielded 5.5 mg (58%) of a colorless oil. $[\alpha]_D^{25}$ = -59.5, *c* 0.82 (MeOH); HRMS (*m/z*): $[M-H]^-$ calcd. for $C_{12}H_{19}O_6$ 259.1187, found 259.1181 ^{1}H NMR (400 MHz, CD_3OD) δ 6.82 (dt, *J* = 15.0, 7.3 Hz, 1H), 5.87 (d, *J* = 15.6 Hz, 1H), 4.64 (s, 1H), 3.90 (h, *J* = 6.1 Hz, 1H), 3.72 (s, 1H), 3.68 – 3.56 (m, 1H), 3.47 (td, *J* = 10.7, 9.8, 4.6 Hz, 1H), 2.48 – 2.31 (m, 2H), 1.93 (dt, *J* = 13.1, 4.0 Hz, 1H), 1.77 (ddd, *J* = 13.3, 11.4, 3.1 Hz, 1H), 1.20 (d, *J* = 6.2 Hz, 3H), 1.15 (d, *J* = 6.1 Hz, 3H); ^{13}C NMR (101 MHz, CD_3OD) δ 170.79, 146.60, 125.71, 98.08, 72.42, 71.44, 69.91, 68.39, 40.81, 35.92, 19.51, 18.15.

Synthesis of **asc-C6** (hydrolysis):

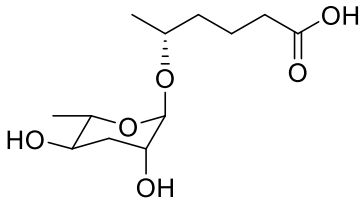

Began with 35.0 mg **1.3, n=1**, HPLC purification yielded 13.3 mg (70%) of a colorless oil. $[\alpha]_D^{25}$ = -74.9, *c* 0.81 (MeOH); HRMS (*m/z*): $[M-H]^-$ calcd. for $C_{12}H_{21}O_6$ 261.1344, found 261.1342; ^{1}H NMR (400 MHz, CD_3OD) δ 4.64 (s, 1H), 3.79 (d, *J* = 6.1 Hz, 1H), 3.71 (td, *J* = 3.1, 1.4 Hz, 1H), 3.62 (dq, *J* = 9.4, 6.2 Hz, 1H), 3.50 (ddd, *J* = 11.1, 9.3, 4.5 Hz, 1H), 2.34 – 2.25 (m, 2H), 1.94 (dt, *J* = 13.1, 3.7 Hz, 2H), 1.82 – 1.70 (m, 2H), 1.70 – 1.45 (m,

2H), 1.21 (d, *J* = 6.2 Hz, 3H), 1.12 (d, *J* = 6.1 Hz, 3H); ^{13}C NMR (101 MHz, CD_3OD) δ 174.92, 94.54, 69.23, 68.29, 67.00, 65.42, 34.81, 33.00, 32.23, 19.58, 16.29, 15.14.

Synthesis of **asc-ΔC7 (hydrolysis):**

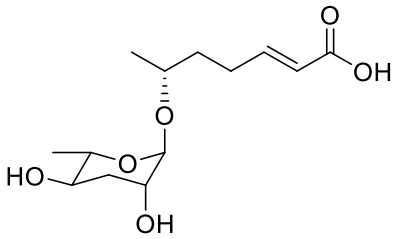

Began with 258.1 mg **1.2, n=2** , column chromatography (32 g silica gel, gradient run from 5% *i*PrOH in CH_2Cl_2 to from 50% *i*PrOH in CH_2Cl_2, then 10% 1:1:1 H_2O:CH_3CN:MeOH in ethyl acetate) yielded 83.3 mg (58%) of a colorless oil. $[\alpha]_D^{25}$ = -77.0, *c* 2.39 (MeOH); HRMS (*m/*z): $[M+Na]^+$ calcd. for $C_{13}H_{22}O_6Na$ 297.1309, found 297.1302; ^{1}H NMR (400 MHz, CD_3OD) δ 6.97 (dt, *J* = 15.5, 6.8 Hz, 1H), 5.83 (d, *J* = 15.6 Hz, 1H), 4.65 (s, 1H), 3.86 – 3.77 (m, 1H), 3.72 (d, *J* = 3.7 Hz, 1H), 3.66 – 3.54 (m, 1H), 3.51 (td, *J* = 10.1, 9.3, 4.6 Hz, 1H), 2.44 – 2.25 (m, 2H), 1.95 (dt, *J* = 12.8, 4.0 Hz, 1H), 1.76 (ddd, *J* = 17.2, 8.7, 3.4 Hz, 1H), 1.73 – 1.59 (m, 2H), 1.21 (d, *J* = 6.0 Hz, 3H), 1.15 (d, *J* = 6.0 Hz, 3H); ^{13}C NMR (101 MHz, CD_3OD) δ 170.42, 150.66, 123.06, 97.49, 71.72, 71.41, 70.02, 68.44, 36.86, 36.08, 29.51, 19.29, 18.24.

Synthesis of **asc-C7** (hydrolysis):

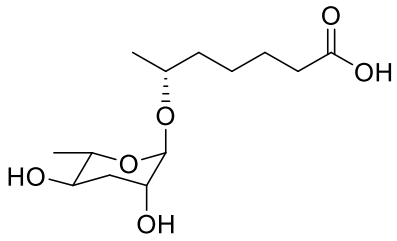

Began with 279.5 mg **1.3, n=2**, column chromatography (32 g silica gel, gradient run from 2% *i*PrOH in CH_2Cl_2 to 50% *i*PrOH in CH_2Cl_2) yielded 80.0 mg (52%) of a colorless oil.

$[\alpha]_D^{25}$ = -90.9, *c* 1.06 (MeOH); HRMS (*m/*z): $[M+Na]^+$ calcd. for $C_{13}H_{24}O_6Na$ 299.1465, found 299.1472; ^{1}H NMR (400 MHz, CD_3OD) δ 4.63 (s, 1H), 3.82 – 3.73 (m, 1H), 3.71 (s, 1H), 3.67 – 3.56 (m, 1H), 3.56 – 3.45 (m, 1H), 2.29 (t, *J* = 7.4 Hz, 2H), 1.94 (dt, *J* = 13.0, 3.8 Hz, 1H), 1.75 (ddd, *J* = 13.4, 11.3, 3.1 Hz, 1H), 1.68 – 1.35 (m, 6H), 1.21 (d, *J* = 6.1 Hz, 3H), 1.11 (d, *J* = 6.1 Hz, 3H); ^{13}C NMR (101 MHz, CD_3OD) δ 177.88, 97.63, 72.44, 71.30, 70.08, 68.48, 38.17, 36.08, 35.15, 26.52, 26.21, 19.45, 18.22.

Synthesis of **asc-ΔC8** (hydrolysis):

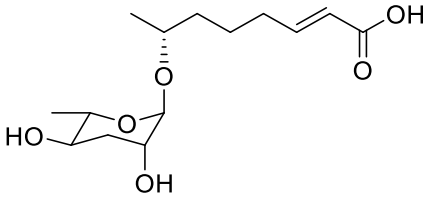

Began with 63.5 mg **1.2, n=3**, HPLC purification yielded 26.7 mg (75%) of a colorless oil. $[\alpha]_D^{25}$ = -60.2, *c* 0.165 (MeOH); HRMS (*m/*z): $[M+Na]^+$ calcd. for $C_{14}H_{24}O_6Na$ 311.1465, found 311.1469; ^{1}H NMR (400 MHz, CD_3OD) δ 6.94 (dt, *J* = 14.7, 6.9 Hz, 1H), 5.81 (d, *J* = 15.6 Hz, 1H), 4.64 (s, 1H), 3.79 (q, *J* = 5.8 Hz, 1H), 3.71 (s, 1H), 3.66 – 3.56 (m, 1H), 3.51 (td, *J* = 10.2, 4.2 Hz, 1H), 2.30 – 2.18 (m, 2H), 1.94 (dt, *J* = 13.2, 3.8 Hz, 1H), 1.81 – 1.69 (m, 1H), 1.68 – 1.43 (m, 4H), 1.21 (d, *J* = 6.1 Hz, 3H), 1.12 (d, *J* = 6.0 Hz, 3H); ^{13}C NMR (101 MHz, CD_3OD) δ 170.27, 150.91, 122.94, 97.65, 72.39, 71.36, 70.05, 68.45, 37.94, 36.07, 33.15, 25.57, 19.46, 18.26.

Synthesis of **asc-C8** (hydrolysis):

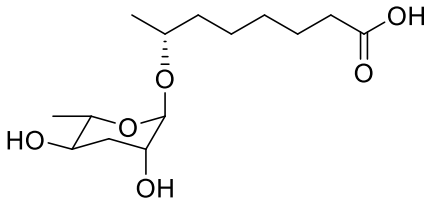

Began with 68.0 mg **1.3, n=3**, HPLC purification yielded 25.2 mg (65%) of a colorless oil. $[\alpha]_D^{25}$ = -81.5, *c* 0.955 (MeOH); HRMS (*m/*z): $[M+Na]^+$ calcd. for $C_{14}H_{26}O_6Na$ 313.1622, found 313.1627; ^{1}H NMR (250 MHz, CD_3OD) δ 4.63 (s, 1H), 3.81 – 3.66 (m, 2H), 3.66 – 3.44 (m, 2H), 2.28 (t, *J* = 7.4 Hz, 2H), 1.94 (dt, *J* = 13.0, 3.9 Hz, 1H), 1.75 (ddd, *J* = 13.3, 11.0, 3.0 Hz, 1H), 1.68 – 1.31 (m, 8H), 1.21 (d, *J* = 6.0 Hz, 3H), 1.11 (d, *J* = 6.0 Hz, 3H); ^{13}C NMR (63 MHz, CD_3OD) δ 177.83, 97.61, 72.53, 71.27, 70.07, 68.47, 38.35, 36.07, 35.13, 30.33, 26.70, 26.18, 19.47, 18.23.

Synthesis of **asc-ΔC9** (hydrolysis):

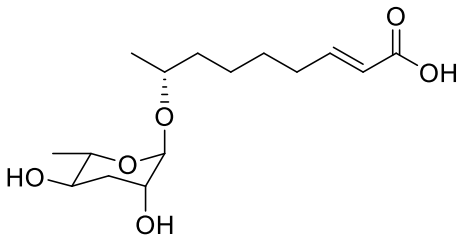

Began with 98.5 mg **1.2, n=4**, HPLC purification yielded 40.9 mg (72%) of a colorless oil. $[\alpha]_D^{25}$ = -61.0, *c* 0.53 (MeOH); HRMS (*m/*z): $[M+Na]^+$ calcd. for $C_{15}H_{26}O_6Na$ 325.1622, found 325.1633; ^{1}H NMR (400 MHz, CD_3OD) δ 6.93 (dt, *J* = 14.2, 6.8 Hz, 1H), 5.80 (d, *J* = 15.8 Hz, 1H), 4.63 (s, 1H), 3.84 – 3.73 (m, 1H), 3.71 (s, 1H), 3.61 (dq, *J* = 11.3, 5.7, 5.3 Hz, 1H), 3.51 (td, *J* = 10.2, 9.5, 4.5 Hz, 1H), 2.23 (q, *J* = 6.5 Hz, 2H), 1.94 (dt, *J* = 12.9, 4.0 Hz, 1H), 1.81 – 1.69 (m, 1H), 1.62 – 1.37 (m, 6H), 1.20 (d, *J* = 6.1 Hz, 3H), 1.11 (d, *J* = 6.1 Hz, 3H); ^{13}C NMR (101 MHz, CD_3OD) δ 170.55, 150.86, 123.04, 97.69, 72.54, 71.35, 70.10, 68.56, 68.47, 38.21, 36.09, 33.21, 29.31, 26.57, 19.49, 18.26.

Synthesis of **asc-C9** (hydrolysis):

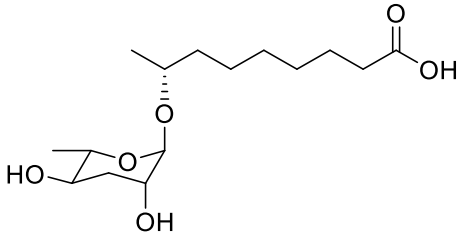

Began with 70.0 mg **1.3, n=4**, column chromatography (30 g silica gel, gradient run from 50% ethyl acetate in CH_2Cl_2 to 100% ethyl acetate, then from 2% 1:1:1 H_2O:CH_3CN:MeOH in ethyl acetate to 10% 1:1:1 H_2O:CH_3CN:MeOH in ethyl acetate) yielded 20.5 mg (51%) of a colorless oil. $[\alpha]_D^{25}$ = -58.4, *c* 0.23 (MeOH); HRMS (*m/*z): $[M+Na]^+$ calcd. for $C_{15}H_{28}O_6Na$ 327.1778, found 327.1778; ^{1}H NMR (400 MHz, CD_3OD) δ 4.63 (s, 1H), 3.81 – 3.73 (m, 1H), 3.71 (s, 1H), 3.62 (dq, *J* = 11.7, 6.0 Hz, 1H), 3.50 (td, *J* = 10.4, 9.6, 4.6 Hz, 1H), 2.27 (t, *J* = 7.2 Hz, 2H), 1.94 (dt, *J* = 12.8, 4.0 Hz, 1H), 1.81 – 1.70 (m, 1H), 1.65 – 1.29 (m, 10H), 1.20 (d, *J* = 6.2 Hz, 3H), 1.11 (d, *J* = 6.0 Hz, 3H); ^{13}C NMR (101 MHz, CD_3OD) δ 178.19, 97.70, 72.67, 71.32, 70.11, 68.49, 38.47, 36.09, 35.38, 30.53, 30.36, 26.87, 26.34, 19.50, 18.24.

Synthesis of **asc-C4** (hydrolysis):

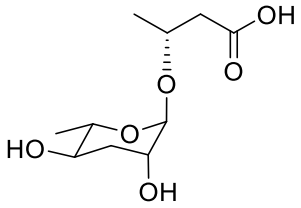

Began with 35.7 mg **1.10, n=1**, HPLC purification yielded 8.0 mg (42%) of a colorless oil. $[\alpha]_D^{25}$ = -98.8, *c* 0.25 (CH_2Cl_2); HRMS (*m/*z): $[M+Na]^+$ calcd. for $C_{10}H_{18}O_6Na$ 257.0996, found 257.1006; ^{1}H NMR (250 MHz, CD_3OD) δ 4.65 (s, 1H), 4.24 (h, *J* = 6.0 Hz, 1H), 3.76 – 3.55 (m, 2H), 3.48 (td, *J* = 10.4, 9.7, 4.6 Hz, 1H), 2.60 – 2.33 (m, 2H), 1.92 (dt, *J* = 13.1, 3.9 Hz, 1H), 1.74 (ddd, *J* = 13.2, 11.2, 3.0 Hz, 1H), 1.21 (d, *J* = 2.5 Hz, 3H), 1.18 (d, *J* = 2.6 Hz, 3H); ^{13}C NMR (126 MHz, CD_3OD) δ 175.88, 97.54, 71.28, 70.02, 70.00, 68.47, 43.97, 35.99, 19.35, 18.16.

Synthesis of **asc-C5** (hydrolysis):

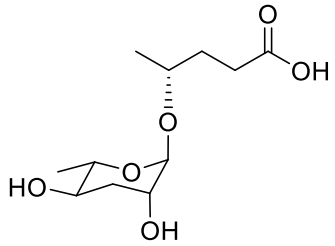

Began with 20.6 mg **1.10, n=2**, HPLC purification yielded 8.8 mg (79%) of a colorless oil. $[\alpha]_D^{25}$ = -62.2, *c* 0.51 (MeOH); HRMS (*m/*z): $[M+Na]^+$ calcd. for $C_{11}H_{20}O_6Na$ 271.1152, found 271.1150; ^{1}H NMR (250 MHz, CD_3OD) δ 4.64 (s, 1H), 3.93-3.75 (m, 1H), 3.71 (q, *J* = 2.7 1H), 3.68-3.41 (m, 2H), 2.41 (t, *J* = 7.4, 2H), 1.95 (dt, *J* = 13.1, 3.9 Hz, 1H), 1.87-1.67 (m, 3H), 1.21 (d, *J* = 2.5 Hz, 3H), 1.14 (d, *J* = 6.0 Hz, 3H).

Synthesis of **1.7** (hydrolysis):

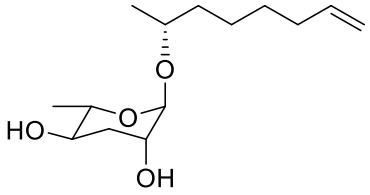

Began with 20.6 mg **1.1, n=4**, HPLC purification yielded 10.7 mg (69%) of a colorless oil. $[\alpha]_D^{25}$ = 76.8, *c* 0.09 (MeOH); HRMS (*m/*z): $[M+Na]^+$ calcd. for $C_{14}H_{26}O_4Na$ 281.1723, found 281.1732; ^{1}H NMR (250 MHz, CD_3OD) δ 5.81 (ddt, *J* = 17.0, 10.2, 6.8 Hz, 1H), 5.06 – 4.88 (m, 2H), 4.63 (s, 1H), 3.81 – 3.67 (m, 2H), 3.67 – 3.44 (m, 2H), 2.06 (q, *J* = 5.9, 5.4 Hz, 2H), 1.94 (dt, *J* = 13.0, 4.0 Hz, 1H), 1.75 (ddd, *J* = 13.3, 10.9, 3.0 Hz, 1H), 1.59 – 1.33 (m, 6H), 1.20 (d, *J* = 6.0 Hz, 3H), 1.11 (d, *J* = 6.1 Hz, 3H); ^{13}C NMR (63 MHz, CD_3OD) δ 139.94, 114.87, 97.57, 72.47, 71.15, 69.95, 68.30, 38.21, 35.94, 34.83, 30.02, 26.35, 19.37, 18.10.

Synthesis of **asc-C6-MK** (hydrolysis):

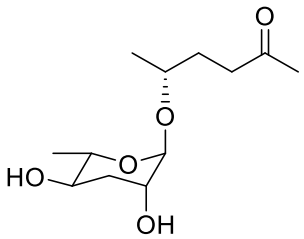

Began with 210.0 mg **1.5**, HPLC purification yielded 88.9 mg (78%) of a colorless oil. $[\alpha]_D^{25}$ = -138.5, *c* 0.895 (MeOH); HRMS (*m/z*): $[M+Na]^+$ calcd. for $C_{12}H_{22}O_5Na$ 269.1359, found 269.1355; ^{1}H NMR (400 MHz, CD_3OD) δ 4.63 (s, 1H), 3.78 (ddd, *J* = 8.0, 6.3, 4.7 Hz, 1H), 3.70 (td, *J* = 3.1, 1.5 Hz, 1H), 3.59 – 3.47 (m, 2H), 2.61 (t, *J* = 7.4 Hz, 2H), 2.15 (s, 3H), 1.94 (dt, *J* = 12.9, 3.6 Hz, 1H), 1.81 – 1.66 (m, 3H), 1.21 (d, *J* = 5.6 Hz, 3H), 1.12 (d, *J* = 6.1 Hz, 3H); ^{13}C NMR (101 MHz, CD_3OD) δ 211.77, 97.39, 71.63, 71.40, 69.94, 68.38, 40.58, 36.04, 32.20, 30.02, 19.22, 18.20.

Representative procedure for ozonolysis and Pinnick oxidation:

To a solution of 220.0 mg (0.512 mmol) terminal alkene in 80 mL dichloromethane was added a stream of O_3 at -78°C. After 4 min the solution turned a bright blue color, at which time the flow of O_3 was ceased. O_2 was then allowed to bubble through the mixture for an additional 4 minutes until the blue color had completely disappeared, and 518.7 mg Janda Jel™ polymer-supported PPh_3 (~1.555 mmol phosphine) was then added. The reaction mixture was then allowed to warm to 23°C and stir for 16h under an atmosphere of nitrogen. 50 mL H_2O was then added and the layers were separated. The aqueous layer was then extracted with 2 x 50 mL dichloromethane, and the organic layers were combined, dried over anhydrous Na_2SO_4 and filtered. Evaporation of volatiles afforded 240.0 mg of an oil (desired aldehyde confirmed with ^{1}H NMR) that was redissolved in 10 mL *t*BuOH and 2.5 mL dimethyl sulfoxide. To this mixture was added dropwise a solution of 440.2

mg (4.867 mmol) 80% $NaClO_2$ and 599.4 mg (3.842 mmol) $NaH_2PO_4 \cdot H_2O$ in 4.5 mL H_2O over the course of 2 min. The resulting solution was stirred at 23°C for 90 min after which the volatiles were evaporated in vacuo. The crude mixture was then suspended in 20 mL H_2O, and the pH was adjusted to 3 via the dropwise addition of 1N HCl. 25 mL EtOAc was then added and the layers were separated. The aqueous layer was then extracted with 3 x 25 mL EtOAc and the organic layers were combined, dried over anhydrous Na_2SO_4 and filtered. Evaporation of volatiles afforded 390 mg of an oil. Column chromatography of the oil afforded 190 mg of a residue that was suspended in 30 mL hexanes and filtered in order to remove contaminant dimethyl sulfone. Evaporation afforded 85.8 mg (38 %, 2 steps) of a colorless oil.

Synthesis of **1.10, n=1** (ozonolysis and Pinnick oxidation):

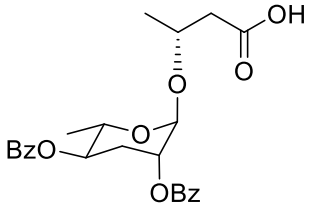

Began with 220.0 mg **1.1, n=1**, column chromatography (35 g silica gel, gradient run from 100% CH_2Cl_2 to 25% EtOAc in CH_2Cl_2) followed by filtration and evaporation afforded 85.8 mg (38%, 2 steps) of a colorless oil. $[\alpha]_D^{25}$ = 12.5, *c* 0.815 (CH_2Cl_2); HRMS (*m/z*): $[M+Na]^+$ calcd. for $C_{24}H_{26}O_8Na$ 465.1520, found 465.1535; ^1H NMR (500 MHz, $CDCl_3$) δ 9.61 (s, br, 1H), 8.11 (d, *J* = 7.8 Hz, 2H), 8.04 (d, *J* = 7.7 Hz, 2H), 7.63 – 7.53 (m, 2H), 7.49 – 7.41 (m, 4H), 5.17 (td, *J* = 10.6, 4.6 Hz, 1H), 5.11 (s, 1H), 4.98 (s, 1H), 4.35 (h, *J* = 5.3 Hz, 1H), 4.15 (dq, *J* = 12.0, 6.2 Hz, 1H), 2.70 (dd, *J* = 15.5, 8.1 Hz, 1H), 2.52 (dd, *J* = 15.5, 5.0 Hz, 1H), 2.39 (dt, *J* = 13.4, 3.9 Hz, 1H), 2.16 (ddd, *J* = 13.9, 11.3, 3.1 Hz, 1H), 1.28 (d, *J* = 2.5 Hz, 3H), 1.26 (d, *J* = 2.4 Hz, 3H); ^{13}C NMR (126 MHz, $CDCl_3$) δ 177.25,

165.70, 165.60, 133.25, 133.15, 129.88, 129.80, 129.67, 129.57, 128.40, 128.38, 93.48, 70.90, 70.44, 68.88, 67.09, 42.10, 29.52, 18.96, 17.63.

Synthesis of **1.10, n=2** (ozonolysis and Pinnick oxidation):

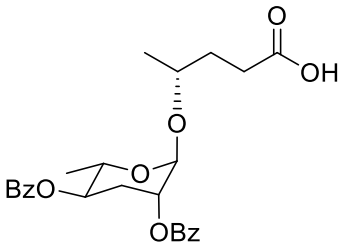

Began with 300.0 mg **1.1, n=2**, column chromatography (10 g silica gel, gradient run from 100% CH_2Cl_2 to 10% EtOAC in CH_2Cl_2) followed by filtration and evaporation afforded 51.2 mg (16%, 2 steps) of a colorless oil. $[\alpha]_D^{25}$ = -8.6, *c* 1.105 (CH_2Cl_2); HRMS (*m/*z): $[M+Na]^+$ calcd. for $C_{25}H_{28}O_8Na$ 479.1676, found 479.1670; ^{1}H NMR (250 MHz, $CDCl_3$) δ 8.17-7.99 (m, 4H), 7.66-7.52 (m, 2H), 7.52-7.38 (m, 4H), 5.24-5.09 (m, 2H), 4.96 (s, 1H), 4.19-4.01 (m, 1H), 3.93 (h, *J* = 5.9 Hz, 1H), 2.55 (t, *J* = 7.4 Hz, 2H), 2.42 (dt, *J* = 13.6, 3.9 Hz, 1H), 2.18 (ddd, *J* = 13.9, 11.3, 3.2 Hz, 1H), 1.92 (q, *J* = 7.1 Hz, 2H), 1.28 (d, *J* = 6.1 Hz, 3H), 1.22 (d, *J* = 6.0 Hz, 3H); ^{13}C NMR (101 MHz, $CDCl_3$) δ 179.10, 165.90, 165.80, 133.40, 133.31, 130.01, 129.97, 129.87, 129.77, 128.57, 128.55, 93.60, 71.25, 71.20, 70.59, 67.32, 31.87, 30.30, 29.79, 18.94, 17.92.

Synthesis of **1.5** (PCC oxidation):

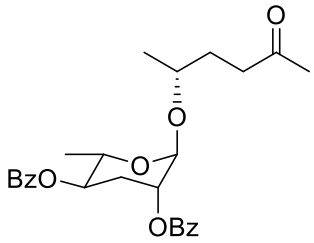

To a suspension of 400.0 mg (1.856 mmol) pyridinium chlorochromate and 340.0 mg 4Å molecular sieves in 12 mL CH_2Cl_2 at 0°C was added 220.0 mg (0.4819 mmol) **1.4** at once. The resulting suspension was allowed to stir at 0°C for 2 h. The reaction mixture was

concentrated to 250 mg of dark red oil. Column chromatography (8 g silica gel, 5% diethyl ether in CH_2Cl_2) afforded 210.0 mg (96%) of a colorless oil. $[\alpha]_D^{25}$ = 16.8, *c* 0.495 (CH_2Cl_2); HRMS (*m/z*): $[M+Na]^+$ calcd. for $C_{26}H_{30}O_7Na$ 477.1884, found 477.1905; ^1H NMR (400 MHz, $CDCl_3$) δ 8.09 (d, *J* = 7.4 Hz, 2H), 8.03 (d, *J* = 7.5 Hz, 2H), 7.58 – 7.52 (m, 2H), 7.47 – 7.40 (m, 4H), 5.21 – 5.10 (m, 2H), 4.93 (s, 1H), 4.06 (dq, *J* = 9.7, 6.3 Hz, 1H), 3.87 (h, *J* = 5.8 Hz, 1H), 2.58 (t, *J* = 7.4 Hz, 2H), 2.41 (dt, *J* = 13.3, 3.8 Hz, 1H), 2.21 – 2.13 (m, 4H), 1.85 (q, *J* = 7.6 Hz, 2H), 1.28 (d, *J* = 6.2 Hz, 3H), 1.19 (d, *J* = 6.1 Hz, 3H); ^{13}C NMR (101 MHz, $CDCl_3$) δ 208.11, 165.55, 165.44, 133.10, 133.04, 129.76, 129.66, 129.61, 129.43, 128.28, 93.40, 71.29, 70.92, 70.39, 66.96, 39.46, 30.67, 29.75, 29.51, 18.72, 17.71.

Representative procedure for diacylation:

To a solution of 43.5 mg (0.1766 mmol) diol and 250 μL (1.413 mmol) N,N-Diisopropylethylamine in 12.5 mL THF at 0 °C was added a solution of 190.3 mg (1.060 mmol) indole-3-carbonyl chloride in 1.5 mL THF dropwise over 3 minutes. The resulting solution was allowed to warm to 23 °C and stir for 6 h. During this time close monitoring of the reaction by TLC showed formation and disappearance of an intermediate, likely the monoacylated product at the axial position, followed by appearance of the desired product. 15 mL of H_2O was then added at once and the mixture was allowed to stir for an additional 30 minutes. 15 mL EtOAc was then added and the layers were separated. The aqueous layer was extracted with an additional 3 x 15 mL EtOAc. The combined organic layers were dried over Na_2SO_4, filtered and concentrated to a light orange oil. HPLC purification afforded 83.6 mg (89%) of a white solid.

Synthesis of **1.6** (diacylation):

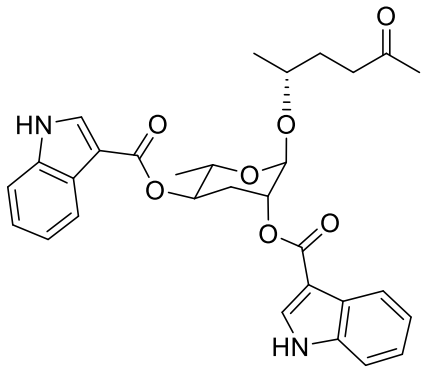

Began with 43.5 mg **asc-C6-MK**, HPLC purification afforded 83.6 mg (89%) of a white solid. $[\alpha]_D^{25}$ = 37.0, *c* 1.44 (CH_2Cl_2); HRMS (*m/*z): $[M+Na]^+$ calcd. for $C_{30}H_{32}N_2O_7Na$ 555.2102, found 555.2126; ^{1}H NMR (400 MHz, $CDCl_3$) δ 9.54 (s, 1H), 9.51 (s, 1H), 8.24 (d, *J* = 7.9 Hz, 1H), 8.14 (d, *J* = 7.3 Hz, 1H), 7.88 (d, *J* = 3.0 Hz, 1H), 7.85 (d, *J* = 3.1 Hz, 1H), 7.40 – 7.34 (m, 2H), 7.27 – 7.15 (m, 4H), 5.32 (td, *J* = 10.4, 4.5 Hz, 1H), 5.21 (s, 1H), 5.02 (s, 1H), 4.13 (dq, *J* = 12.2, 6.0 Hz, 1H), 3.91 (h, *J* = 6.0 Hz, 1H), 2.63 (t, *J* = 7.4 Hz, 2H), 2.51 (dt, *J* = 13.3, 3.7 Hz, 1H), 2.29 – 2.23 (m, 1H), 2.21 (s, 3H), 1.89 (q, *J* = 7.3 Hz, 2H), 1.34 (d, *J* = 6.3 Hz, 3H), 1.19 (d, *J* = 6.1 Hz, 3H); ^{13}C NMR (101 MHz, $CDCl_3$) δ 209.09, 164.73, 164.39, 136.26, 136.23, 131.96, 131.82, 125.76, 125.67, 123.16, 123.04, 122.10, 122.05, 121.17, 121.06, 111.87, 111.77, 107.96, 107.72, 93.98, 71.30, 69.94, 69.62, 67.51, 39.67, 30.84, 30.11, 29.90, 18.82, 17.98.

Synthesis of **1.8** (diacylation):

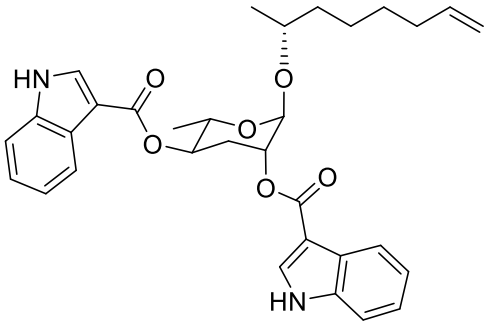

Began with 43.8 mg **1.7**, HPLC purification yielded 40.0 mg (43%) of a colorless oil. $[\alpha]_D^{25}$ = 43.0, *c* 0.40 (CH_2Cl_2); HRMS (*m/*z): $[M+Na]^+$ calcd. for $C_{32}H_{36}N_2O_6Na$ 567.2466, found 567.2474; ^{1}H NMR (400 MHz, $CDCl_3$) δ 9.19 (s, 1H), 9.16 (s, 1H), 8.25 (d, *J* = 7.8 Hz, 1H), 8.13 (d, *J* = 7.1 Hz, 1H), 7.91 – 7.88 (m, 1H), 7.88 – 7.83 (m, 1H), 7.41 – 7.32 (m, 2H), 7.28 – 7.16 (m, 4H), 5.85 (ddt, *J* = 16.9, 10.2, 6.5 Hz, 1H), 5.33 (td, *J* = 10.6, 4.6 Hz, 1H), 5.22 (s, 1H), 5.06 – 4.93 (m, 3H), 4.20 (dq, *J* = 10.8, 5.5, 5.0 Hz, 1H), 3.88 (h, *J* = 5.9 Hz, 1H), 2.51 (dt, *J* = 13.6, 4.0 Hz, 1H), 2.34 – 2.22 (m, 1H), 2.15 – 2.07 (m, 2H), 1.58 – 1.40 (m, 6H), 1.35 (d, *J* = 5.9 Hz, 3H), 1.19 (d, *J* = 5.8 Hz, 3H); ^{13}C NMR (101 MHz, $CDCl_3$) δ 164.65, 164.35, 139.01, 136.29, 136.27, 131.85, 131.57, 126.02, 125.83, 123.44, 123.28, 122.34, 122.32, 121.60, 121.48, 114.59, 111.82, 111.71, 108.71, 108.40, 94.34, 72.54, 70.24, 69.84, 67.46, 37.19, 33.97, 30.33, 28.98, 25.49, 19.39, 18.17.

Synthesis of **IC-asc-C6-MK**:

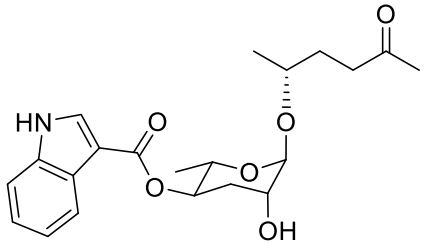

To a solution of 10.2 mg (0.0193 mmol) **1.6** in 3.0 mL *i*-PrOH at 23 °C was added 3.0 mL 1M LiOH at once. The resulting mixture was heated to 45 °C and allowed to stir for 6.5 h. The reaction was then permitted to cool to 23 °C at which time 5 mL 20% *i*-PrOH in CH_2Cl_2 was added and the layers were separated. The aqueous layer was extracted with an additional 2 x 5 mL 20% *i*-propanol in CH_2Cl_2. Solid NaCl was then added to the aqueous layer until saturation was obtained, and it was further extracted with 2 x 5 mL 20% *i*PrOH in CH_2Cl_2. The combined organic layers were dried over Na_2SO_4, filtered and concentrated

to yield 15.4 mg of an oil. HPLC purification afforded 2.6 mg (35%) of a colorless oil. $[\alpha]_D^{25}$ = -12.8, *c* 0.13 (CH_2Cl_2); HRMS (*m/*z): $[M+Na]^+$ calcd. for $C_{21}H_{27}NO_6Na$ 412.1731, found 412.1735; ^1H NMR (250 MHz, $CDCl_3$) δ 8.61 (s, 1H), 8.18 – 8.12 (m, 1H), 7.95 (d, *J* = 3.1 Hz, 1H), 7.46 – 7.40 (m, 1H), 7.33 – 7.28 (m, 2H), 5.18 – 5.06 (m, 1H), 4.77 (s, 1H), 4.08 – 3.98 (m, 1H), 3.92 – 3.84 (m, 2H), 2.62 (t, *J* = 7.5 Hz, 2H), 2.34 – 2.17 (m, 4H), 2.13 – 1.99 (m, 1H), 1.93 – 1.79 (m, 2H), 1.29 (d, *J* = 6.3 Hz, 3H), 1.19 (d, *J* = 6.1 Hz, 3H); ^{13}C NMR (126 MHz, $CDCl_3$) δ 208.52, 162.30, 136.09, 131.27, 125.75, 123.37, 122.21, 121.49, 111.58, 108.83, 96.22, 70.98, 69.38, 68.79, 68.01, 39.75, 32.31, 30.94, 29.99, 18.96, 17.76.

Synthesis of **IC-asc-ΔC9**:

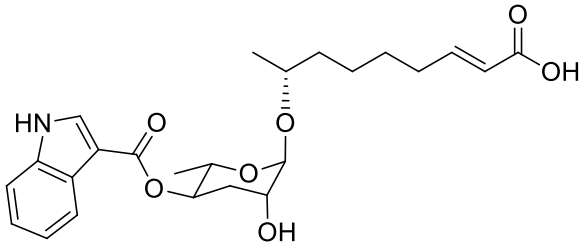

To a solution of 10.2 mg (0.0169 mmol) **1.9** in 2.5 mL *t*-BuOH at 23 °C was added 2.5 mL 1M LiOH at once. The resulting mixture was heated to 50 °C and allowed to stir for 11 h. The reaction was then permitted to cool to 23 °C at which time the pH was adjusted to 3 via dropwise addition of 1M HCl. 5 mL 20% *i*-PrOH in CH_2Cl_2 was then added and the layers were separated. The aqueous layer was extracted with an additional 2 x 5 mL 20% *i*-propanol in CH_2Cl_2. Solid NaCl was then added to the aqueous layer until saturation was obtained, and it was further extracted with 2 x 5 mL 20% *i*PrOH in CH_2Cl_2. The combined organic layers were dried over Na_2SO_4, filtered and concentrated to yield 17.3 mg of an oil. HPLC purification afforded 4.9 mg (65%) of a colorless oil. HRMS (*m/*z): $[M-H]^-$ calcd. for $C_{30}H_{32}N_2O_7Na$ 444.2028, found 444.2031. ^1H NMR (400 MHz, Methanol-d4)

δ 8.03 – 7.99 (m, 1H), 7.96 (s, 1H), 7.46 – 7.41 (m, 1H), 7.23 – 7.14 (m, 2H), 6.84 (dt, *J* = 15.4, 6.9 Hz, 1H), 5.83 (d, *J*= 15.6 Hz, 1H), 5.11 (td, *J* = 10.5, 4.7 Hz, 1H), 4.74 (s, 1H), 4.04 (dd, *J* = 9.6, 6.2 Hz, 1H), 3.89 – 3.81 (m, 1H), 3.79 (q, *J* = 2.9 Hz, 1H), 2.29 – 2.17 (m, 3H), 2.00 (ddd, *J* = 13.4, 11.2, 3.1 Hz, 1H), 1.70 – 1.58 (m, 1H), 1.58 – 1.42 (m, 5H), 1.23 (d, *J* = 6.3 Hz, 3H), 1.16 (d, *J* = 6.0 Hz, 3H).

Representative procedure for epoxide opening:

To a suspension of 82.4 mg (3.39 mmol) of magnesium turnings in 0.44 mL dry THF was added 0.52 mL (3.4 mmol) bromoalkene in 2.9 mL dry THF dropwise over the course of 4 minutes. The resulting suspension was brought to reflux and stirred for 12 h until all magnesium had been consumed. The resulting cloudy, pale-yellow mixture was allowed to cool to 25°C. To a separate flask was added 34.2 mg (0.238 mmol) CuBr in 5 mL dry THF. This suspension was cooled to -78°C. To this chilled suspension was added the previously synthesized Grignard reagent dropwise over 3 minutes via syringe. This resulting suspension was allowed to stir for 10 minutes, upon which it turned dark gray with black solids. To this suspension was added 0.17 mL (2.4 mmol) (R)-(+)-propylene oxide at once, upon which it turned from dark gray to black. The suspension was allowed to warm to 25°C and was stirred for 3 h. To the black suspension was added 4 mL sat. NH_4Cl at once. The aqueous layer was separated from the organic layer and then extracted with 3 x 10 mL THF. The resulting organic extracts were dried over MgSO4 and filtered to obtain 509.3 mg of yellow oil after rotary evaporation.

Synthesis of **(R)-hept-6-en-2-ol** (epoxide opening):

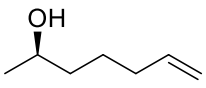

Began with 156.8 mg (R)-(+)-propylene oxide, (no purification necessary) yielded 175.4 mg (57%) of a light yellow liquid. $[\alpha]_D^{25}$ = 38.3, *c* 0.73 (CH_2Cl_2); ^{1}H NMR (250 MHz, $CDCl_3$) δ 5.81 (ddt, *J* = 16.9, 10.2, 6.7 Hz, 1H), 5.09 – 4.88 (m, 2H), 3.79 (h, *J* = 6.0 Hz, 1H), 2.16 – 1.95 (m, 2H), 1.95 (s, 1H), 1.60 – 1.31 (m, 4H), 1.18 (d, *J* = 6.2 Hz, 3H); ^{13}C NMR (63 MHz, $CDCl_3$) δ 138.63, 114.50, 67.87, 38.65, 33.62, 24.97, 23.42.

Synthesis of **(*R*)-oct-7-en-2-ol** (epoxide opening):

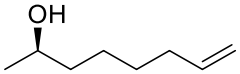

Began with 596.1 mg (R)-(+)-propylene oxide, (no purification necessary) yielded 322.5 mg (88%) of a light yellow liquid. $[\alpha]_D^{25}$ = 7.1, *c* 0.59 (CH_2Cl_2); ^{1}H NMR (250 MHz, $CDCl_3$) δ 5.77 (ddt, *J* = 16.9, 10.2, 6.7 Hz, 1H), 5.04 – 4.84 (m, 2H), 3.75 (q, *J* = 5.9 Hz, 1H), 2.01 (h, *J* = 5.7 Hz, 3H), 1.47 – 1.22 (m, 5H), 1.14 (d, *J* = 6.2 Hz, 3H); ^{13}C NMR (63 MHz, $CDCl_3$) δ 138.70, 114.18, 67.79, 38.98, 33.57, 28.74, 25.09, 23.26.

1.7 References

1. Marasco, C. A., Chemical Biology: Adventure Awaits. *Chemical & Engineering News* 2006, pp 47-49.

2. Fire, A.; Xu, S.; Montgomery, M. K.; Kostas, S. A.; Driver, S. E.; Mello, C. C., Potent and specific genetic interference by double-stranded RNA in Caenorhabditis elegans. *Nature* **1998,** *391*, 806-811.

3. Brenner, S., Nature's Gift to Science. *ChemBioChem* **2003,** *4*, 683.

4. Brenner, S.; Wolpert, L., *My Life in Science*. BioMed: London, 2001.

5. Brenner, S., *The Nematode Caenorhabditis elegans*. Cold Spring Harbor Laboratory Press: Cold Spring Harbor, 1988.

6. Hulme, S. E.; Whitesides, G. M., Chemistry and the worm: Caenorhabditis elegans as a platform for integrating chemical and biological research. *Angew. Chem. Int. Ed. Engl.* **2011,** *50* (21), 4774-807.

7. Fielenbach, N.; Antebi, A., C. elegans dauer formation and the molecular basis of plasticity. *Genes & development* **2008,** *22* (16), 2149-65.

8. Ren, P. e. a., Control of *C. elegans* larval development by neuronal expression of a TGFβ homolog. *Science* **1996,** *274*, 1389-1391.

9. Kimura, K. D., daf-2, an Insulin Receptor-Like Gene That Regulates Longevity and Diapause in Caenorhabditis elegans. *Science* **1997,** *277* (5328), 942.

10. Jeong, P.-Y.; Jung, M.; Yim, Y.-H.; Kim, H.; Park, M.; Hong, E.; Lee, W.; Kim, Y. H.; Park, K. K. Y.-K., Chemical structure and biological activity of the *Caenorhabditis elegans* dauer-inducing pheromone. *Nature* **2005,** *433* (7025), 541-545.

11. Butcher, R. A.; Fujita, M.; Schroeder, F. C.; Clardy, J., Small-molecule pheromones that control dauer development in Caenorhabditis elegans. *Nature chemical biology* **2007,** *3* (7), 420-2.

12. Srinivasan, J.; Kaplan, F.; Ajredini, R.; Zachariah, C.; Alborn, H. T.; Teal, P. E.; Malik, R. U.; Edison, A. S.; Sternberg, P. W.; Schroeder, F. C., A blend of small molecules regulates both mating and development in Caenorhabditis elegans. *Nature* **2008,** *454* (7208), 1115-8.

13. Butcher, R. A.; Ragains, J. R.; Kim, E.; Clardy, J., A potent dauer pheromone component in Caenorhabditis elegans that acts synergistically with other components. *Proceedings of the National Academy of Sciences of the United States of America* **2008,** *105* (38), 14288-92.

14. Butcher, R. A.; Ragains, J. R.; Clardy, J., An Indole-Containing Dauer Pheromone Component with Unusual Dauer Inhibitory Activity at Higher Concentrations. *Organic Letters* **2009,** *11* (14), 3100-3103.

15. Sengupta, P.; Srinivasan, J.; von Reuss, S. H.; Bose, N.; Zaslaver, A.; Mahanti, P.; Ho, M. C.; O'Doherty, O. G.; Edison, A. S.; Sternberg, P. W.; Schroeder, F. C., A Modular Library of Small Molecule Signals Regulates Social Behaviors in Caenorhabditis elegans. *PLoS biology* **2012,** *10* (1), e1001237.

16. Schackwitz, W. S.; Inoue, T.; Thomas, J. H., Chemosensory Neurons Function in Parallel to Mediate a Pheromone Response in C. elegans. *Neuron* **1996,** *17*, 719-728.

CHAPTER 2: CHEMICAL GENETIC STUDIES ON CHEMOSENSATION IN THE MODEL ORGANISM *CAENORHABDITIS ELEGANS*, PART II: IMPACT OF ASCAROSIDES ON DAUER FORMATION AND SPERM MOTILITY

2.1 Introduction

As previously mentioned in Chapter 1, *C. elegans* has been used as a model organism since the 1960s. Brenner developed and popularized its use as a model organism for biological research, and in 2002 he was awarded the Nobel Prize in Physiology and Medicine for his efforts.[1] *C. elegans* has now been used by molecular biologists to study development, aging, stress resistance, metabolism, neurobiology, cancer, pathways of signal transduction, anthelmintics, and genetics.[2] Now, the wealth of knowledge gained from the past 50 years of research is allowing a new field to emerge. Chemists have become interested in chemical genetics and chemical biology studies in *C. elegans* to explore how small molecules affect larger biological processes. This relatively new area of research helped to inspire the work presented herein.

Specifically, our interests concern how small molecule pheromones affect important signaling pathways in *C. elegans*. Both dauer formation and reduced sperm motility are shown to be inducible by treatment with ascaroside pheromones. Target ascaroside natural products and analogs were successfully synthesized in 4-5 steps each from dibenzoyl ascarylose and screened for activity in dauer formation assays and for activity regarding sperm function. Results from both studies, now published, are discussed in this chapter.

2.2 The *C. elegans* Dauer Stage

Though *C. elegans* has been used for biological research since the early 1960s, its use in chemical biology has emerged only recently. For example, it has been determined that small molecule pheromones control development[3] and behavior[4] in *C. elegans* via

regulation of important signaling pathways (TGF-β and IGF-1).[5] One of the most interesting and well-studied phenomena controlled by these pathways is an alternate larval stage during *C. elegans* early development. Referred to as the process of dauer diapause, the "dauerlarva" was first described by Cassada & Russel in 1975.[6] The word dauer is of German origin and means steady, continuous or permanent. Though the dauer larvae were studied to some extent, the exact reasons for diapause remained elusive for nearly a decade. Then, in 1984, Golden & Riddle determined that adverse environmental conditions such as food scarcity, high temperature, and overcrowding (high concentration of excreted pheromones) are triggers for dauer formation.[7] Figure 2.1 depicts the nematode life cycle.

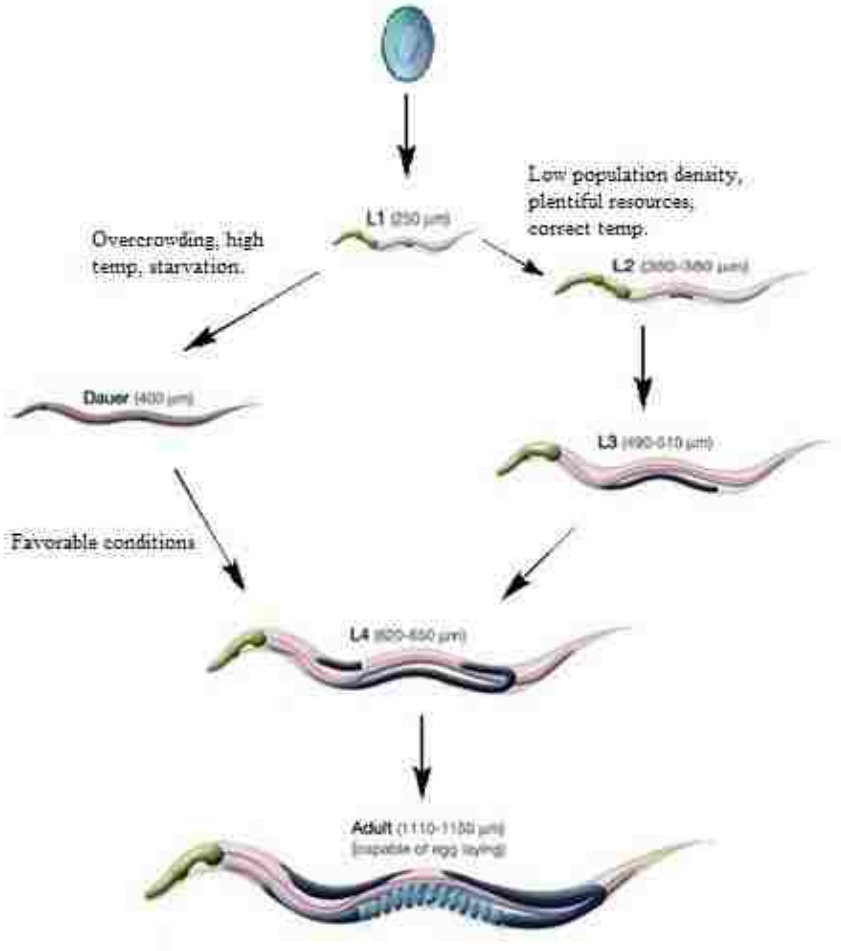

Figure 2.1 *Caenorhabditis elegans* developmental stages.

A normal development cycle begins with an egg, which hatches to become an L1 larva. The L1 then advances to become L2, L3, and L4 before finally reaching adulthood. However, when met with adverse conditions, an early stage larva (L1 or L2) may instead enter the dauer stage. While in the dauer stage, the larva rarely move, do not feed, and have thickened cuticles that protect against harsh environmental conditions. By surviving off of fat stores, the non-ageing dauer larva may persist for several months, much longer than the normal *C. elegans* lifespan of 2-3 weeks, until it is again met with favorable conditions.[8] At that time, the dauer larva can enter the L4 stage of development and progress into a normal adult.

C. elegans secretes ascaroside pheromones and senses their concentration via chemosensation with sensory neurons located in its head. In this way, the nematodes are able to gain important population information from their surroundings.[7] At high population density (high ascaroside concentration), dauer formation takes place as a preventative measure to ensure survival. The dauer larvae will then remain in that state of suspended animation until the concentration of pheromones in the environment is reduced. A competing, dauer-inducing signal, still of unknown origin, is referred to as the "food signal." The food signal gives *C. elegans* indications of the abundance of food in its environment and can prevent dauer formation even in cases when population density and ascaroside concentration are high. Both the ascaroside pheromone signal as well as the food signal are important for dauer formation and for the return to normal development.[3]

Sensory neurons located on the head of *C. elegans* express hundreds of G protein-coupled receptors (GPRCs) which sense ascaroside pheromones.[9] Ascaroside binding to

GPCRs has been documented in a few different ways. When *gpa-2* and *gpa-3* (two alpha subunits of GPCRs) were upregulated, dauer formation occurred; when those subunits were mutated, dauer formation was not induced.[10] Of the neurons associated with GPCR expression in *C. elegans*, the ASI and ASJ neurons are particularly significant because of their role in the regulation of IGF-1 and TGF-β signaling pathways.[5d, 11] When ascaroside pheromones are detected, the IGF-1 and TGF-β signaling pathways are downregulated due to neuron downregulation of secondary messengers such as TGF-β and insulin-like peptides.[11] As mentioned in Chapter 1, pathways like TGF-β and IGF-1 are known to influence growth, metabolism, development, longevity, and stress-resistance in higher organisms including humans.[12] IGF-1 has been shown to be important in the aging process of *C. elegans*. When the *C. elegans* IGF-1 receptor (DAF-2) was mutated, the lifespan of the worm doubled.[13] Increased lifespan was also observed when the IGF-1 pathway was manipulated in mice as well as the fruit fly *Drosphila melanogaster*.[14] The IGF-1 pathway also seems to affect cancer risk and growth of cancer cells. In fact, it has been demonstrated that when IGF levels are decreased, growth of cancer cells also decreases.[15] Also, there is evidence that diets which downregulate IGF-1 result in a lower risk of developing cancer at all.[16]

The TGF-β pathway is also conserved in higher organisms such as humans, and is associated with diseases such as cancer[17] and Alzheimer's disease.[18] Remarkably, for breast and skin cancers, TGF-β is upregulated in some cases and shown to aid in tumor progression. However, for gastric and pancreatic cancer, TGF-β is essentially turned off.[17] These conflicting results for different types of cancer speak to the complexity of the relationship between cancer and TGF-β. Furthermore, Alzheimer's patients have shown

higher concentrations of TGF-β in blood and cerebral fluid, suggesting a TGF-β relationship with the disease.[18] The study of IGF-1 and TGF-β pathways may indeed provide useful insight and perhaps aid in the fight against such diseases.

To assess downregulation of IGF-1 and TGF-β in *C. elegans*, we decided to screen the dauer-inducing ability of ascarosides. As shown in Chapter 1, we decided to synthesize a battery of natural and synthetic ascaroside analogs for screening in dauer formation assays. We hypothesized that these studies could help to develop an SAR between ascarosides and their GPCRs, as well as provide useful insight about the way *C. elegans* uses the IGF-1 and TGF-β signaling pathways. Results could be extrapolated to higher organisms and utilized in important research of diseases, aging, stress-resistance, development, and metabolism.

2.3 Results and Discussion of Dauer Studies

Upon synthesis of ascaroside pheromones and analogs, the dauer-inducing ability of each ascaroside was determined both at 220 nM, which is near the EC_{50} for already-identified compounds, and 6000 nM, a very high concentration that would show if any activity existed at all.[19] The ascarosides were mixed with nematode growth media (NGM) agar and previously heat-killed *E. coli* (food source) before being poured into plates. Live *C. elegans* nematodes were then exposed to the created environment and allowed to lay eggs. After 68-72 hours of incubation at 25ºC, plates were analyzed, with dauer larva being easily recognizable under microscope by their smaller size and lack of movement. In this way, dauer formation percentage was determined.

The activities of all synthesized compounds were screened in this manner, and the results are shown in Figure 2.2 (arrows at bottom of figure indicate compounds synthesized

by this researcher). Some naturally occurring ascarosides had activity up to 90% dauer formation at 220 nM and near 100% at 6000 nM. The highest activity for synthetic analogs at low concentration (220 nM) were **IC-asc-C6-MK** at 40% followed by **asc-C10-OH** at 20% and **asc-C10-MK** at 15%. At 6000 nM, several synthetic analogs showed activity with the maximum **of asc-C10-MK** remaining under 60%. Interestingly, none of the **asc-C#** or **asc-ΔC#** series had significant activity at 220 nM even when they only varied by one carbon or one degree of unsaturation. At 6000 nM, the most significant activity was about 40% for **asc-C9**, the saturated analog of naturally occurring **asc-ΔC9**. Synthetic analogs of these series showed the most activity when the chain length was 5, 7, or 9, all of which occur in one of the natural compounds. Thus, for this series, side chain length was more important than degree of unsaturation at 6000 nM, though both were extremely important at 220 nM.

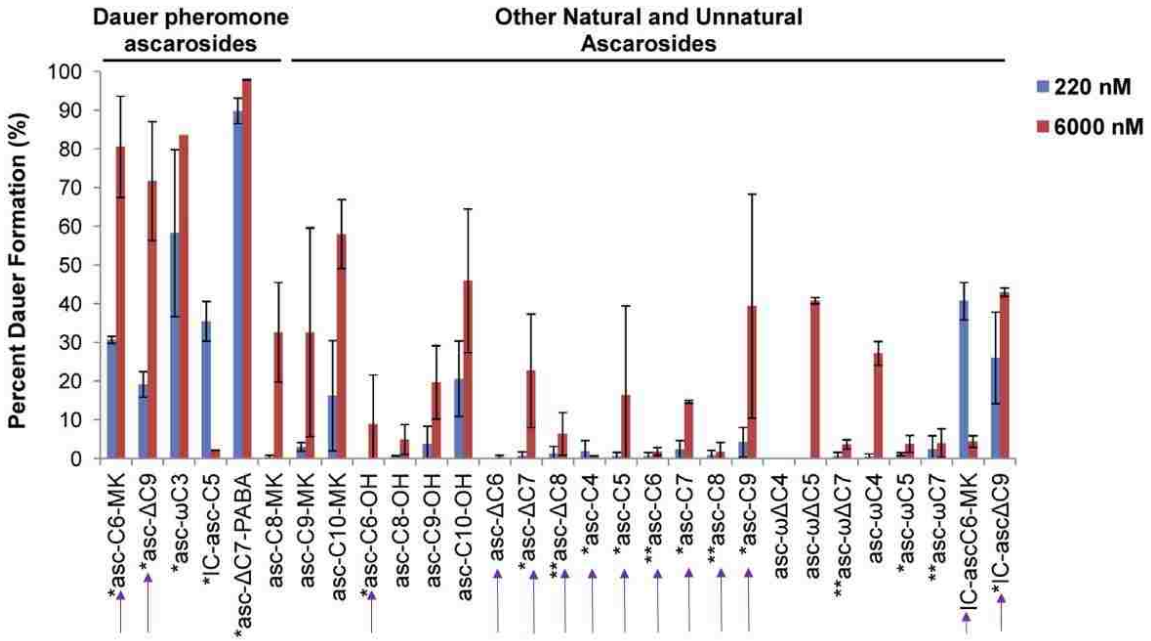

Figure 2.2 Dauer formation activity of naturally occurring and synthetic ascarosides*
*From reference 26, reprinted with permission from AAAS

Not surprisingly, **IC-asc-ΔC9**, shown to be a naturally occurring compound, had 25% dauer forming activity at 220 nM and 40% at 6000 nM. The only synthetic compound containing the IC head group also showed strong activity at 220 nM with about 40% dauer formation. Remarkably, at high concentration inhibited dauer formation, with less than 10% dauer formation at 6000 nM. This phenomenon was only observed with one other compound, the naturally occurring **IC-asc-C5**, possibly due to the IC moiety. Other than **IC-asc-C6-MK**, synthetic analogs showed very little activity at 220 nM across the board. Less than half showed significant activity at 6000 nM. These findings suggest that dauer formation activity of ascarosides is highly dependent on structure. Variance of a single carbon, one degree of unsaturation, or the terminal group in a side chain is enough to drastically alter activity. These results lead us to conclude that the GCPRs that bind ascarosides are highly selective despite the abundance and structural variation known to exist among these compounds.[20] This selectivity is not surprising considering the fact that *C. elegans* nematodes share their environment with other nematodes like *C. briggsae*, which produces similar compounds.[21] We hypothesize that, if receptor binding was promiscuous, misinformation by cross-talk between nematode species could be detrimental for survival.

2.4 Sperm Motility in *C. elegans*

Environmental factors are known to affect fertility in many animals, but the direct causes are not always well understood.[22] One important class of molecules that is known to influence reproduction in humans and other mammals is the set of fatty-acid derived signaling molecules called prostaglandins.[23] The specific role of prostaglandins in reproduction is not entirely understood, and monitoring gamete function in the

reproductive tract is considerably difficult. *C. elegans* is known to produce F-class prostaglandins, which have been shown to guide sperm to their fertilization site (spermatheca).[24] The transparent epidermis of *C. elegans*' allows for direct observation of fluorescently labeled sperm and it was shown that, when there is a mutation in the *daf-7* TGF-β ligand, sperm-targeting defects arise.[25]

2.5 Results and Discussion of Sperm Motility Studies

Figure 2.3 shows the anatomy and important fertilization regions of an adult nematode. Indicated are the sensory neurons (ASI), nerve ring (NR), oocytes (O), spermatheca (S, outlined in yellow), vulva (V), and fertilized eggs (E). Sperm, which are injected through the vulva, must find their way around the fertilized eggs and into the spermatheca. The nematode uterus is divided into three zones, Z1, Z2, and Z3 to further specify location and quantification of sperm.

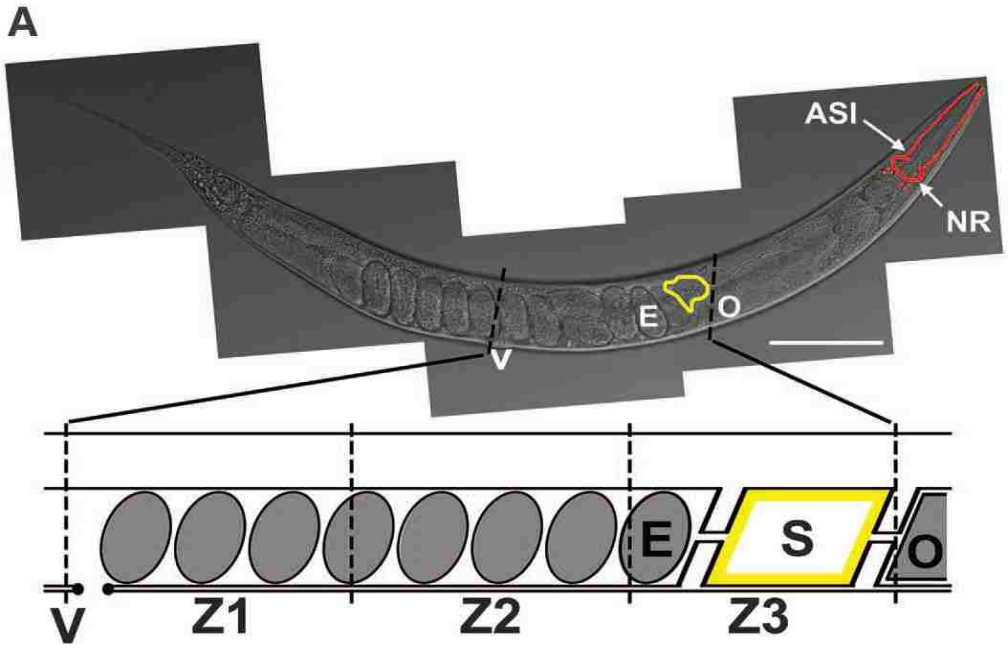

Figure 2.3 Anatomy of adult *C. elegans* hermaphrodite*
*From reference 26, reprinted with permission from AAAS

With this information in hand, we hypothesized that TGF-β promotes prostaglandin synthesis in *C. elegans*. In order to test this hypothesis, the previously mentioned ascarosides **asc-C6-MK** and **IC-asc-ΔC9** were used to study downregulation of TGF-β and observe any effect on sperm function.[26] Figure 2.4 shows the results of treatment with ascarosides. In the control experiment using wild type *C. elegans*, one hour after mating over 90% of sperm had found their way to Z3, the region of the uterus containing the spermatheca. When wild type *C. elegans* were treated with synthetic **asc-C6-MK** and **IC-asc-ΔC9** ascarosides, less than 60% of sperm were able to arrive in the Z3 region one hour after mating.

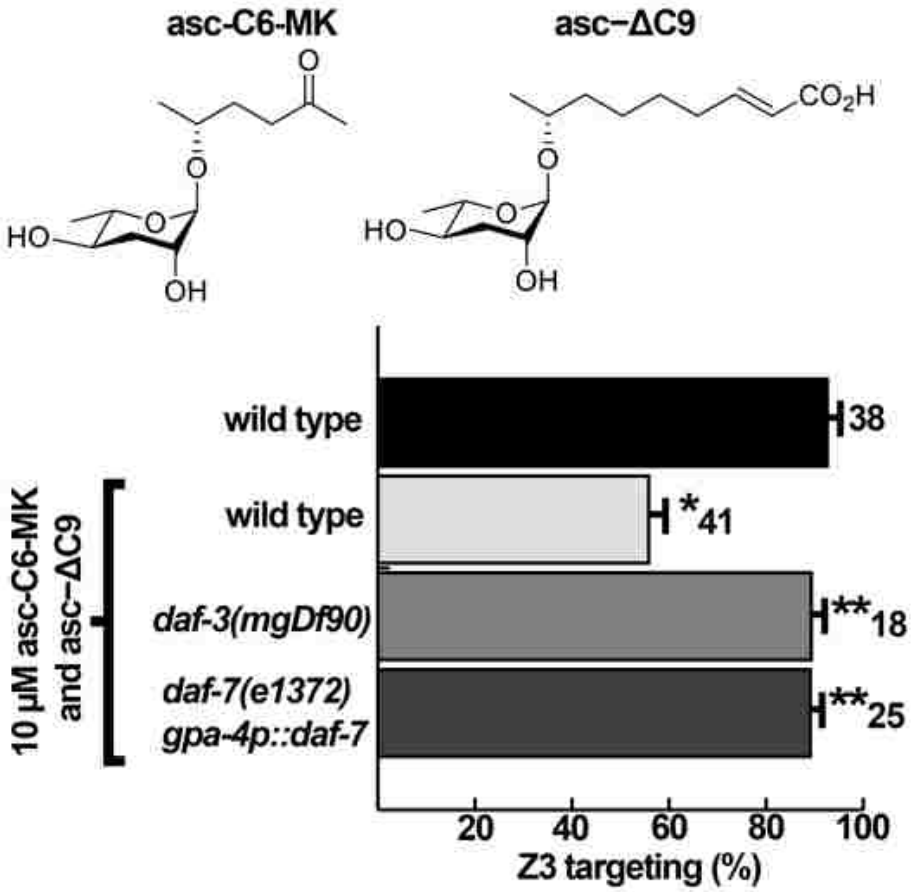

Figure 2.4 Ascaroside effects on sperm function*
*From reference 26, reprinted with permission from AAAS

This indicated a direct correlation between downregulation of the TGF-β pathway and decrease in sperm motility (likely via suppression of *daf-7*). Indeed, it was also shown that when *daf-7* mutants (mutants where *daf-7* was forced to express via the ASI-specific *gpa-4* promoter)[27] were given the same treatment, sperm function was unmolested, indicating that suppression of *daf-7* by **C6-MK** and **IC-asc-ΔC9** was almost certainly the cause of TGF-β downregulation.

2.6 Conclusions

In conclusion, 12 synthesized ascarosides were screened for activity in dauer formation assays. Analogs varied in chain length, degree of unsaturation, terminal functionality and head group. Generally speaking, synthetic analogs did not show high dauer-inducing ability unless they bore a high degree of similarity to naturally occurring ascarosides. This suggests that the GPCRs which bind these ascarosides are highly selective, possibly an evolutionary result that prevents cross-talk between nematode species. Side chain length was the most important factor for analogs not containing an IC moiety. When a synthetic side chain length was used, almost all activity ceased. However, some natural side chain lengths still had activity when the degree of unsaturation was altered. So far, all IC-containing compounds have been shown to induce dauer formation, though only one synthetic analog has been screened.

Sperm motility was reduced via treatment with two synthetic versions of naturally occurring ascarosides. Interestingly, a more detailed theoretical map of the TGF-β signaling pathway was elucidated, beginning with treatment by ascarosides and ultimately climaxing in reduced sperm motility. First, **asc-C6-MK** and **IC-asc-ΔC9** ascarosides were shown to repress expression of *daf-7*, an important TGF-β ligand normally present in ASI

sensory neurons. Suppression of *daf-7* is known to downregulate the TGF-β pathway, which is known to result in a decrease in production of prostaglandins. Specifically, F-class prostaglandins are known to play a critical role in guiding sperm to the fertilization site. Therefore, treatment with the two above mentioned ascarosides directly resulted in a decrease of prostaglandins, which led directly to decreased sperm function.

2.7 References

1. Brenner, S., Nature's Gift to Science. *ChemBioChem* **2003,** *4*, 683.

2. Hulme, S. E.; Whitesides, G. M., Chemistry and the worm: Caenorhabditis elegans as a platform for integrating chemical and biological research. *Angew. Chem. Int. Ed. Engl.* **2011,** *50* (21), 4774-807.

3. Golden, J. W.; Riddle, D. L., A pheromone influences larval development in the nematode *Caenorhabditis elegans*. *Science* **1982,** *218*, 578-580.

4. Simon, J. M.; Sternberg, P. W., Evidence of a mate-finding cue in the hermaphrodite nematode *Caenorhabditis elegans*. *Proceedings of the National Academy of Sciences of the United States of America* **2002,** *99* (3), 1598-1603.

5. (a) Golden, J. W.; Riddle, D. L., A pheromone-induced developmental switch in *Caenorhabditis elegans*: Temperature-sensitive mutants reveal a wild-type temperature-dependent process. *Proceedings of the National Academy of Sciences of the United States of America* **1984,** *81* (3), 819-823; (b) Vowels, J. J.; Thomas, J. H., Genetic analysis of chemosensory control of dauer formation in *Caenorhabditis elegans*. *Genetics* **1992,** *130*, 105-123; (c) Thomas, J. H.; Birnby, D. A.; Vowels, J. J., Evidence for parallel processing of sensory information controlling dauer formation in *Caenorhabditis elegans*. *Genetics* **1993,** *134*, 1105-1117; (d) Ren, P.; Lim, C.; Johnsen, R.; Albert, P. S.; Pilgrim, D.; Riddle, D. L., Control of *C. elegans* Larval Development by Neuronal Expression of a TGF-β Homolog. *Science* **1996,** *274* (5291), 1389-1391; (e) Kimura, K. D.; Tissenbaum, H. A.; Liu, Y.; Ruvkun, G., *daf-2*, an Insulin Receptor-Like Gene That Regulates Longevity and Diapause in *Caenorhabditis elegans*. *Science* **1997,** *277* (5328), 942.

6. Cassada, R. C.; Russell, R. L., The dauerlarva, a post-embryonic developmental variant of the nematode *Caenorhabditis elegans*. *Dev. Biol.* **1975,** *46*, 326.

7. Golden, J. W.; Riddle, D. L., The *Caenorhabditis elegans* dauer larva: developmental effects of pheromone, food, and temperature. *Dev. Biol.* **1984,** *102*, 368-378.

8. Klass, M.; Hirsh, D., Non-ageing developmental variant of *Caenorhabditis elegans. Nature* **1976,** *260*, 523-525.

9. Ward, S.; Thomson, N.; White, J.; Brenner, S., Electron Microscopical Reconstruction of the Anterior Sensory Anatomy of the Nematode *Caenorhabditis elegans*. *J. Comp. Neurol.* **1975,** *160* (313-337).

10. Zwaal, R.; Mendel, J.; Sternberg, P. W.; Plasterk, R., Two Neuronal G Proteins are Involved in Chemosensation of the *Caenorhabditis elegans* Dauer-Inducing Pheromone. *Genetics* **1997,** *145*, 715-727.

11. Larsen, P.; Albert, P.; Riddle, D., Genes that Regulate Both Development and Longevity in *Caenorhabditis elegans*. *Genetics* **1995,** *139*, 1567-1583.

12. Fielenbach, N.; Antebi, A., C. elegans dauer formation and the molecular basis of plasticity. *Genes & development* **2008,** *22* (16), 2149-65.

13. Dorman, J.; Albinder, B.; Shroyer, T.; Kenyon, C., The Age-1 and Daf-2 Genes Function in a Common Pathway to Control the Lifespan of *Caenorhabditis elegans. Genetics* **1995,** *141*, 1399-1406.

14. Bartke, A., Single-Gene Mutations and Healthy Ageing in Mammals. *Philos. Trans. R. Soc. London, Ser. B* **2011,** *366*, 28-34.

15. Arnaldez, F.; Helman, L., Targeting the Insulin Growth Factor Receptor 1. *Hematol. Oncol. Clin. North Am.* **2012,** *26*, 527-542.

16. McCarty, M., Vegan Proteins May Reduce Risk of Cancer, Obesity, and Cardiovascular Disease by Promoting Increased Glucagon Activity. *Med. Hypotheses* **1999,** *53*, 459-485.

17. Padua, D.; Massague, J., Roles of TGF-Beta in Metastasis. *Cell Res.* **2009,** *19*, 89.

18. Swardfager, W.; Lanctot, K.; Rothenburg, L.; Wong, A.; Cappel, J.; Herrmann, N., A Meta-Analysis of Cytokines in Alzheimer's Disease. *Biol. Pyschiatry* **2010,** *68*, 930-941.

19. Hollister, K. A.; Conner, E. S.; Zhang, X.; Spell, M.; Bernard, G. M.; Patel, P.; Carvalho, A. C. G. V. d.; Butcher, R. A.; Ragains, J. R., Ascaroside activity in *Caenorhabditis elegans* is highly dependent on chemical structure. *Biorg. Med. Chem.* **2013,** *21* (18), 5754-5769.

20. Schroeder, F. C., Modular Assembly of Primary Metabolic Building Blocks: A Chemical Language in C. elegans. *Chem. Biol.* **2014,** *22* (1), 7-16.

21. Felix, M.; Duveau, F., Population Dynamics and Habitat Sharing of Natural Populations of *Caenorhabditis elegans* and *C. briggsae*. *BMC Biol.* **2012,** *10*, 59.

22. (a) Cariboni, A.; Maggi, R.; Parnavelas, J. G., From nose to fertility: the long migratory journey of gonadotropin-releasing hormone neurons. *Trends Neurosci.* **2007,** *30*, 638-644; (b) Crain, D. A. e. a., Female reproductive disorders: the roles of endocrine-disrupting compounds and developmental timing. *Fertil. Steril.* **2008,** *90*, 911-940.

23. Funk, C. D., Prostaglandins and leukotrienes: advances in eicosanoid biology. *Science* **2001,** *294*, 1871-1875.

24. Hoang, H. D.; Prasain, J. K.; Dorand, D.; Miller, M. A., A heterogeneous mixture of F-series prostaglandins promotes sperm guidance in the *Caenorhabditis elegans* reproductive tract. *PLoS genetics* **2013,** *9*, e1003271.

25. Edmonds, J. W.; Prasain, J. K.; Dorand, D.; Yang, Y.; Hoang, H. D.; Vibbert, J.; Kubagawa, H. M.; Miller, M. A., Insulin/FOXO Signaling Regulates Ovarian Prostaglandins Critical for Reproduction. *Dev. Cell* **2010,** *19*, 858-871.

26. McKnight, K.; Hoang, H. D.; Prasain, J. K.; Brown, N.; Vibbert, J.; Hollister, K. A.; Moore, R.; Ragains, J. R.; Reese, J.; Miller, M. A., Neurosensory Perception of Environmental Cues Modulates Sperm Motility Critical for Fertilization. *Science* **2014,** *344*, 754-757.

27. You, Y.-j.; Kim, J.; Raizen, D. M.; Avery, L., Insulin, cGMP, and TGF-β Signals Regulate Food Intake and Quiescence in *C. elegans*: A Model for Satiety. *Cell Metab.* **2008,** *7*, 249-257.

CHAPTER 3: EFFORTS TOWARD SYNTHESIS OF THE HASUBANAN ALKALOID DELAVAYINE: A PHOTO-S_N1 APPROACH

3.1 Introduction

The hasubanan alkaloids are a family of over 40 structurally related compounds isolated from several species of vines belonging to the genus *Stephania*.[1] These structurally exciting synthetic targets are similar to the morphines, and some members of this class of alkaloids have demonstrated activity for human δ-opiod receptors.[2] We conceived a novel photochemical approach to gain efficient entry into the hasubanan tetracyclic ring system. Specifically, we imagined a cascade cyclization utilizing the photo-S_N1 reaction.[3] The photo-S_N1 reaction's ultraviolet light-promoted generation of a triplet phenyl cation leads to a unique manifold not usually accessible under thermal conditions.[3] To quickly provide proof of concept, a substrate for the proposed photocyclization was completed in 5 linear steps from 3,4,5-trimethoxybenzyl cyanide. If the proposed step were to give the desired result, the intermediate obtained would be only a few steps from hasubanan alkaloid delavayine and would open the door for many other substrates to be attempted.

3.2 Hasubanan Alkaloids

The alkaloid hasubanonine was first isolated from the Japanese vine *Stephania japonica* in 1951.[4] Its structure was erroneously assigned twice before Matsui *et. al* determined it correctly in 1964 using a combination of NMR techniques and degradation studies.[5] As a result of the striking similarity between the structure of morphine **3.1** (Scheme 3.1) and that of hasubanonine **3.2**, this alkaloid attracted considerable attention. Since that initial discovery, over 40 compounds sharing the same tetracyclic backbone have

been isolated from several species of the genus *Stephania*.[1] This structurally interesting family of compounds have become known as the hasubanan alkaloids.

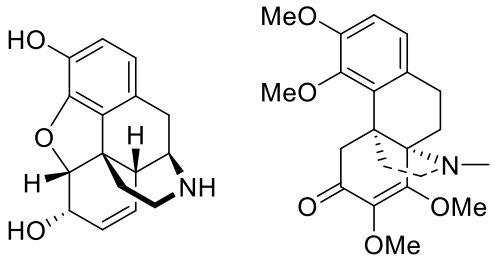

3.1 **3.2**

Scheme 3.1 Structures of morphine and hasubanonine

For some time, no biological acitivy was reported for these compounds, but in the late 1990s it was noticed by Shultz and coworkers that the orientation of the heterocyclic ring in relation to the aromatic ring in the hasubanan alkaloids was precisely inverse to that of the morphines.[6] For this reason, it was hypothesized that the unnatural enantiomers of the hasubanan alkaloids may be better suited to confer activity by having morphine-like analgesic effects. Shultz's 1998 synthesis of (+)-cepharamine, the mirror image of the natural product isolated from *Stephania cepharantha*, set the stage for testing this hypothesis.[6] Though several other hasubanan alkaloids were also synthesized in racemic or asymmetric fashion, no biological activity for these was reported. Then, in 2010, it was shown that several of the naturally occurring alkaloids, including two newly isolated, have binding activity for the δ-opiod receptor in humans.[2] This new information is rather thrilling given that binding to the δ-opiod receptor is known to produce analgesia and to cause antidepressant effects.[7] Besides being fascinating synthetic targets, the hasubanan alkaloids remain as promising leads for drug development.

3.3 Photo-S_N1 Reaction

Italian chemists Fagnoni and Albini have pioneered transformations via photochemical cleavage of aryl-diazonium salts, aryl chlorides, fluorides, mesylates, triflates, and phosphates leading to triplet phenyl cations.[3, 8] For electron-donating group (EDG)-substituted aryl chlorides and fluorides in polar media, flash photolysis studies have determined that cleavage occurs from the triplet state.[8] The difference between a singlet and triplet phenyl cation is important and leads to significant variances in chemical selectivity. A singlet phenyl cation is localized with a vacant σ-orbital and 6 π electrons (Scheme 3.2) and will often react with a lone pair-bearing nucleophile.[3] The triplet phenyl cation, however, is delocalized with 5 π electrons and a single electron in the σ-orbital. This gives the triplet phenyl cation carbene character at the dicoordinate carbon. Thus, the triplet phenyl cation is predisposed to react with a π-nucleophile, making it a better choice for C-C bond formation.[3]

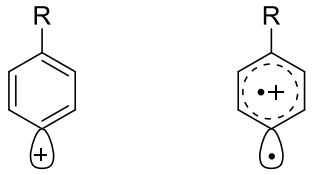

Scheme 3.2 Singlet vs. triplet phenyl cation

An example of the proposed mechanism for triplet phenyl cation reaction with π nucleophiles, known as photo-S_N1, is shown in Scheme 3.3. Vertical arrows over lines represent the spin of electrons in their orbitals, with higher energy orbitals shown above those of lower energy. First, a ground state singlet (**S_0**) molecule, a molecule in which all occupied orbitals contain two antiparallel spin (spin-paired) electrons, absorbs a photon of UV radiation. This absorbed energy causes an electron to be promoted to a higher energy

orbital, producing a singlet excited state ($\mathbf{S_1}$). The singlet excited state is defined by having two orbitals that are occupied by one electron each, with the spin of the electrons still paired. One electron then inverts its spin via intersystem crossing (ISC) and results in two orbitals that each contain one electron of parallel (unpaired) spin. This electronic state is referred to as the triplet excited state ($\mathbf{T_1}$).

Once the triplet excited state is achieved, heterolytic cleavage of the C-Cl bond results in a triplet phenyl cation. As previously discussed (Scheme 3.2), one electron is delocalized in the ring along with the positive charge while the other is localized in an orthogonal sp^2 orbital. This species behaves similarly to a triplet carbene. Addition of a π nucleophile results in a triplet diradical that must undergo intersystem crossing to the singlet excited state before the two radicals can unite to form a bond. The result of this radical termination is a singlet ground state cyclopropane intermediate which may undergo subsequent nucleophilic attack to rearomatize the ring and further construct complexity. This recently discovered chemistry inspired our photochemical approach to the synthesis of hasubanan alkaloid delavayine.

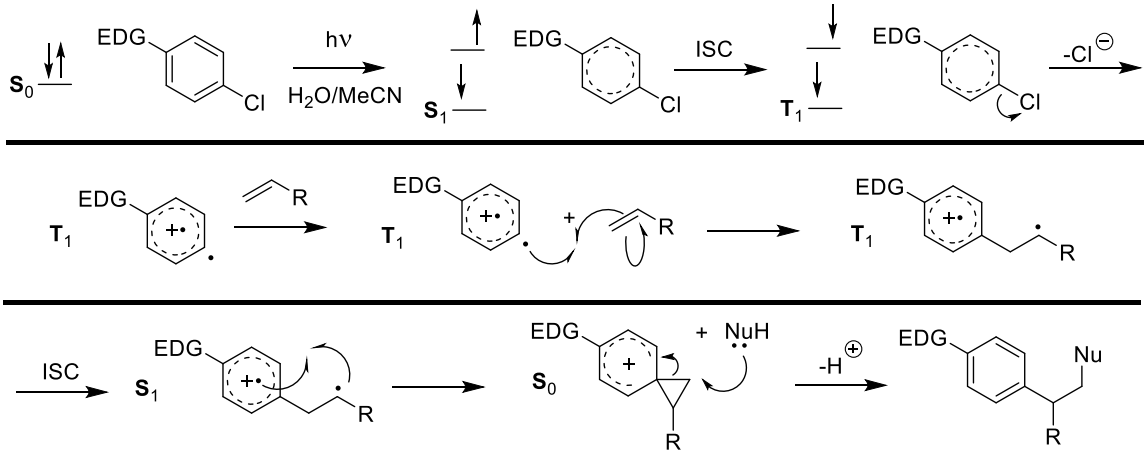

Scheme 3.3 Example of photo-S_N1 mechanism

3.4 Results and Discussion

Photo-S_N1 chemistry has now been used to accomplish arene cross-couplings, allylations, and alkynylations along with reactions such as the type shown in Scheme 3.3, and others.[9] In these ways, the photo-S_N1 has shown potential as a substitute for cross-couplings which are usually accomplished with metal catalysis.[8] While studying the photo-S_N1 mechanism, we realized that intramolecular examples of cyclization did not exist in the literature. Therefore, we proposed that intramolecular arene coupling could be followed by the addition of a nucleophile already present on the same structure. A reaction of this type would add considerable molecular complexity at once. Thus the hasubanan alkaloids were examined as synthetic targets, with delavayine (**3.3**, Scheme 3.4) being chosen as the first to attempt.

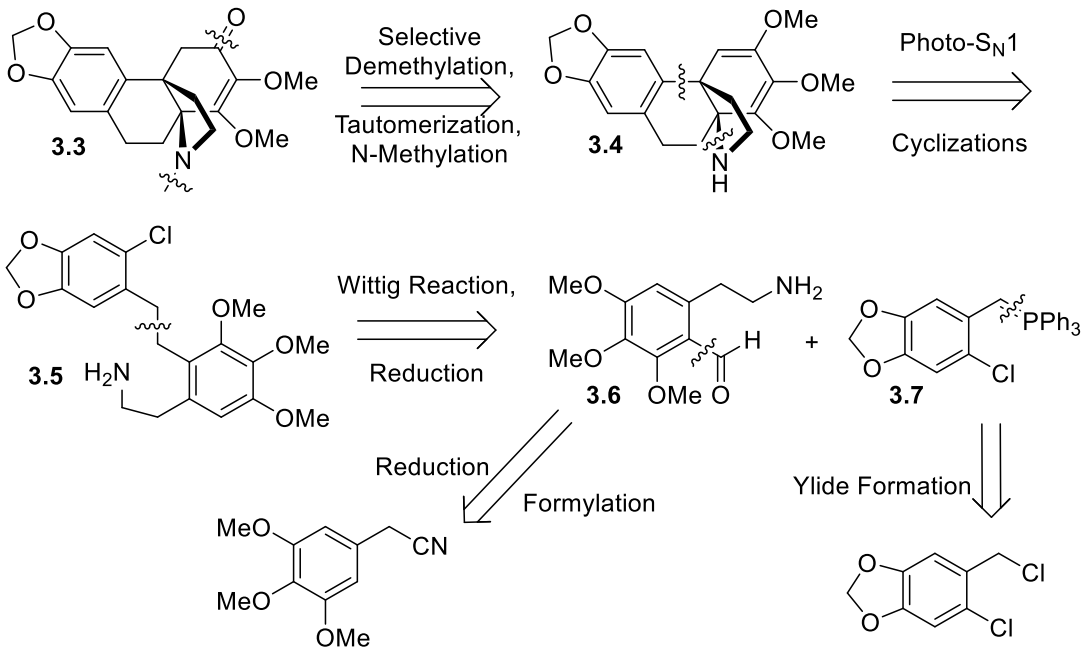

Scheme 3.4 Original retrosynthetic analysis of delavayine

The idea of arene coupling followed by nucleophilic attack from the nitrogen to access the tetracyclic core is shown in the retrosynthetic analysis in Scheme 3.4. If

intermediate **3.4** was in fact formed from **3.5** in this reaction, the structure would be only two steps from **3.3**. Photosubstrate **3.5** was to be synthesized via Wittig reaction between aldehyde **3.6**, attainable through reduction and formylation of 3,4,5-trimethoxybenzyl cyanide, and ylide **3.7**, accessible by reacting 6-chloropiperonyl chloride with triphenylphosphine followed by treatment with a strong base. It was unclear whether a protecting group would be necessary for the nitrogen during cyclization or even for the entire synthesis. If not, such a total synthesis would be only 7 linear steps, the shortest of any hasubanan alkaloid to date.

Synthesis of photosubstrate **3.5** began with the reduction of 3,4,5-trimethoxybenzyl cyanide. Reduction was attempted several times with lithium aluminum hydride to no avail, so a new method of reduction was sought out. Raney nickel reduction under 1 atm H_2 gave a quantitative yield of the primary amine **3.8** with no purification necessary (Scheme 3.5). Next, formylation of **3.8** was needed to produce proposed intermediate **3.6**. Although several methods for this transformation were attempted, including Duff reaction, Vilsmeier-Haack reaction, orthoester formylation, and lithiation/DMF formylation, no desired product was ever observed even with protection of the primary amine.

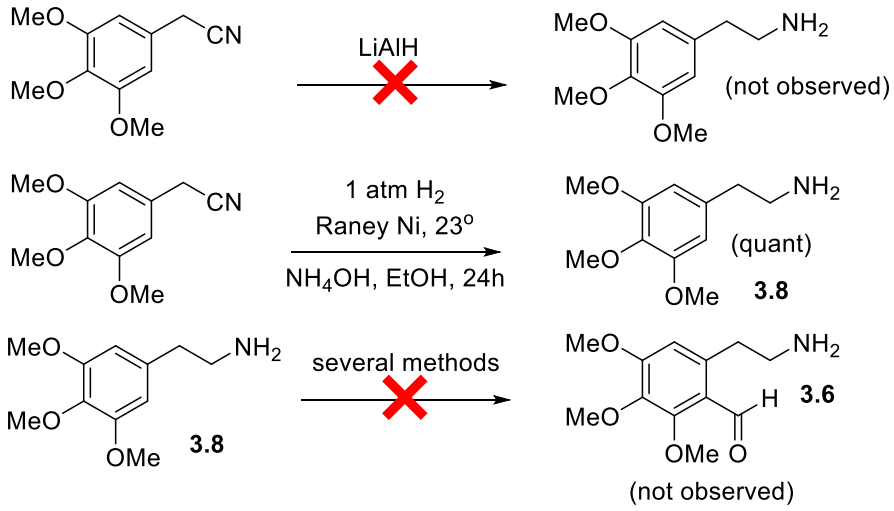

Scheme 3.5 Early synthetic work toward photosubtrate

We then devised an alternate route to photosubstrate **3.5**. Shown in Scheme 3.6, a methyl carbamate-protected version (**3.5a**) of photosubstrate **3.5** would now be constructed by Heck coupling of alkene **3.9**, to be formed via Wittig reaction of 6-chloropiperonal, and aryl bromide **3.10**, accessible by reduction, protection, and subsequent bromination of 3,4,5-trimethoxybenzyl cyanide.

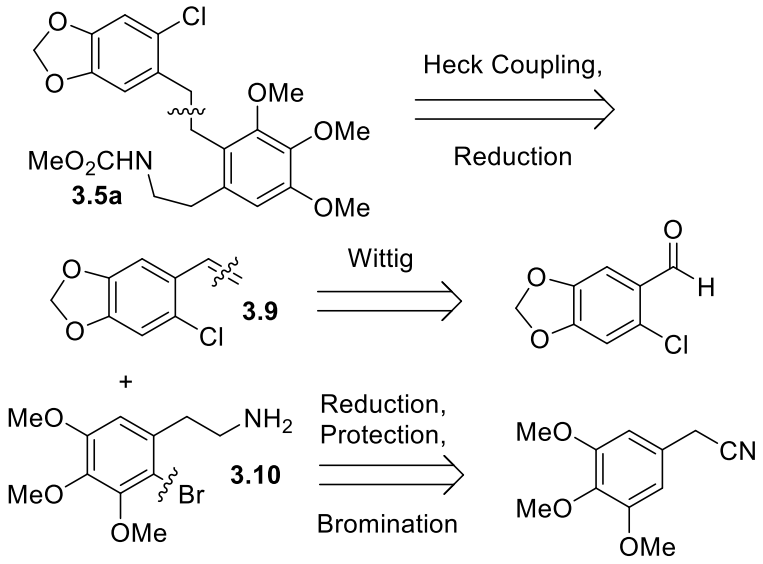

Scheme 3.6 New retrosynthetic plan for photosubstrate

Depicted in Scheme 3.7, 6-chloropiperonal was successfully converted into terminal alkene **3.9** via Wittig reaction with methylenetriphenylphosphorane. Aryl bromide **3.10** was also successfully synthesized via NBS bromination of intermediate **3.8a** (methyl carbamate-protected version of primary amine **3.8**). However, the Heck coupling of **3.8a** and **3.9** was not successful under any attempted conditions. At this point, we were concerned that the aryl bromide simply wasn't reactive enough. Thus, the aryl iodide analog **3.11** was synthesized via reaction of **3.8** with NIS. After failed Heck coupling with $Pd(PPh_3)_4$ as catalyst, successful Heck coupling of **3.9** and **3.11** was achieved using palladium acetate to give stilbene intermediate **3.12** as a single isomer. Reduction of **3.12**

with 10% palladium on activated carbon and 1 atm H_2 gave **3.5a**, the protected version of target photosubstrate **3.5**.

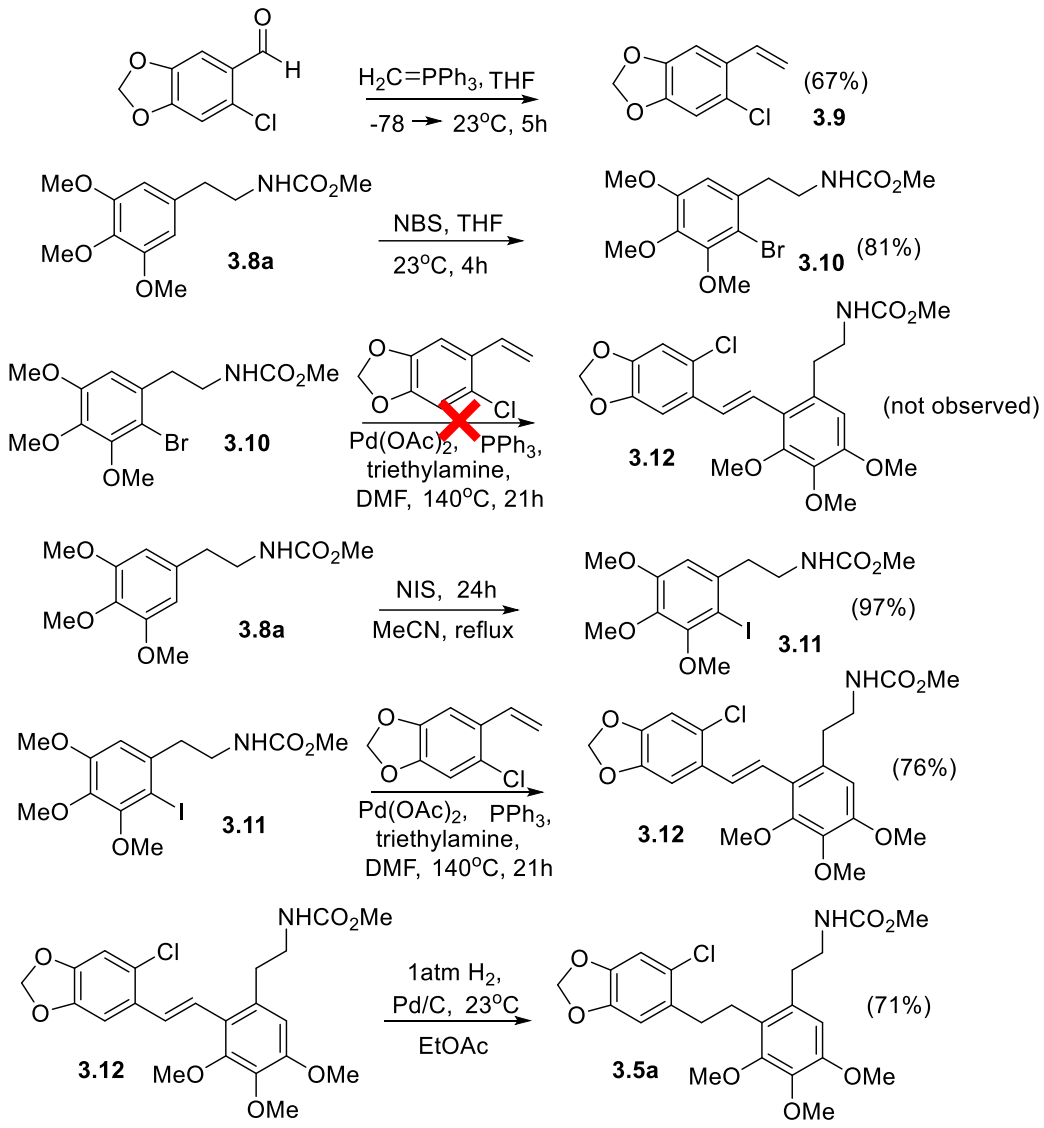

Scheme 3.7 Synthesis of target photosubstrate

After synthesis of the desired substrate was complete, we attempted the proposed photocyclizations. Thus, substrate **3.5a** was irradiated with an Hg arc lamp for 2 hours in an acetonitrile/water mixture. After irradiation, TLC showed that a single product had formed, though some starting material was still present. Isolation of the product showed

an unexpected result. It appeared that one of the methyl groups was no longer attached to the molecule, and that cyclization of the nitrogen did not occur. Indeed, upon 2D NMR studies along with mass spec, energy calculations, and NMR predictions the product was confirmed to be **3.13**, (29%, Scheme 3.8). These results led us to believe that our proposed pathway was indeed viable, but went astray at the last step.

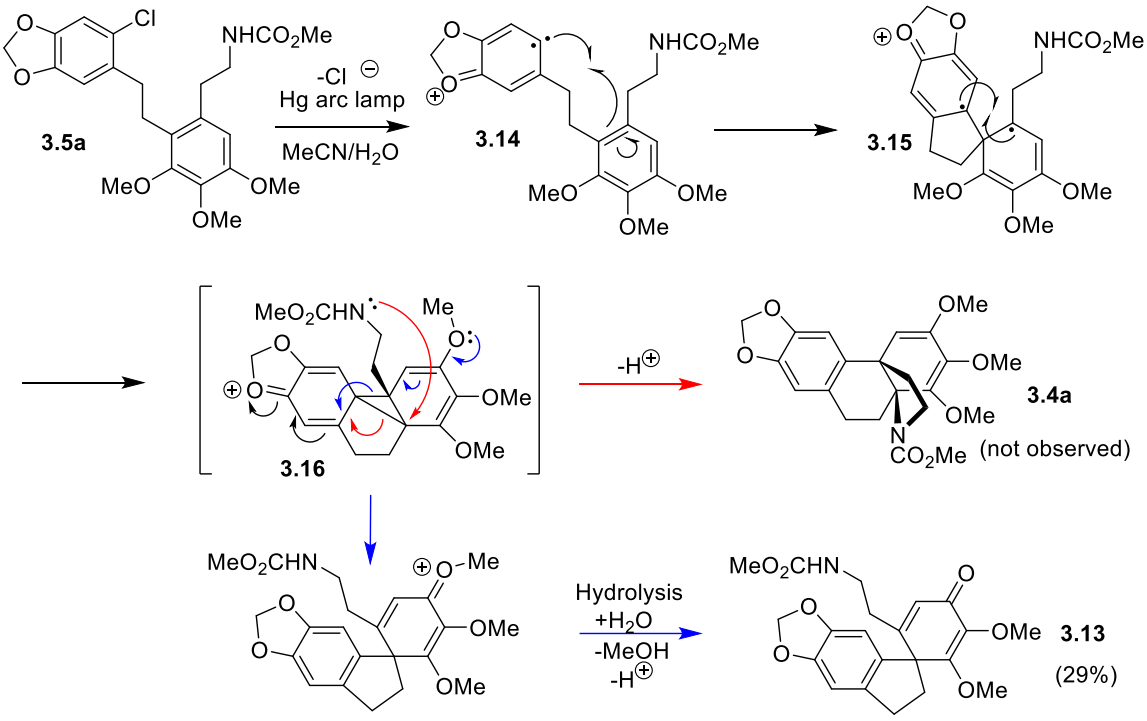

Scheme 3.8 Photochemical cyclization pathways

After expected generation of triplet phenyl cation **3.14**, cyclization occurred leading to diradical intermediate **3.15**. The two resulting radicals then formed a bond leading to predicted cyclopropane intermediate **3.16**. From intermediate **3.16**, we had anticipated cyclization of the nitrogen and loss of a proton to form a 5-membered heterocycle and give intermediate **3.4a** containing the hasubanan tertracyclic ring system. Instead, internal fragmentation of the cyclopropane intermediate formed an oxonium which was hydrolyzed

resulting in formation of **3.13**. These pathways are indicated in Scheme 3.8 by the blue and red arrows.

Strategies to promote cyclization and prevent loss of a methyl group included deprotection of the nitrogen to liberate the primary amine, and use of a polar but less nucleophilic solvent like trifluoroethanol. Deprotection of the nitrogen was performed, yet the free amine substrate gave analogous results. Also, when the less nucleophilic solvent trifluoroethanol was used, the reaction did not proceed. Another problem with the reaction was poor yield. Regardless of duration, yield for this reaction was never above 30%, and the remainder of the mass balance consisted of unconverted starting material. We attribute this to the product of the reaction acting as a triplet quencher, therefore rendering the formation of the triplet phenyl cation inoperable above a certain concentration of product. In an attempt to overcome this problem, photosensitizers like acetone were added to the reaction mixture, but no increase in yield was observed.

3.5 Experimental

3.5.1 General Methods

^{1}H NMR and ^{13}C NMR spectroscopy was conducted using a Bruker DPX-250, AV-400 or AV-500 spectrometer. Mass spectra were attained using an Agilent 6210 electrospray time-of-flight mass spectrometer. All materials were received from commercial suppliers and used without further purification. Flash column chromatography was accomplished using high purity grade 60 Å silica gel (Fluka® Analytical). Qualitative TLC was performed on aluminum sheets (Merck, silica gel, F254) and observed via UV absorption (254 nm) and staining with anisaldehyde or $KMnO_4$. Deuterated solvents were

acquired from Cambridge Isotope Labs. All reactions were carried out under an atmosphere of dry nitrogen.

3.5.2 Procedures and Characterization

Synthesis of **3.8**: 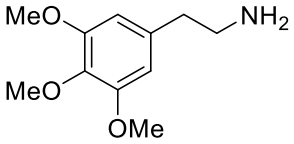

A vigorously stirred 20°C suspension of 500.0 mg (2.413 mmol) 3,4,5-trimethoxylphenylacetonitrile, 1.5 mL 50% Raney nickel slurry in H_2O, 15 mL NH_4OH (28% NH_3 basis), and 30 mL EtOH was vacuum-purged and backfilled with H_2 gas and allowed to stir for 18h at 1 atm. The suspension was then filtered and the volatiles evaporated *in vacuo* to afford 504.5 mg (quantitative yield) of a white solid that required no further purification. ^{1}H NMR (400 MHz, $CDCl_3$) δ 6.52 (s, 2H), 3.82 (s, 6H), 3.73 (s, 3H), 2.87 (t, *J* = 7.2 Hz, 2H), 2.69 (t, *J* = 7.1 Hz, 2H); ^{13}C NMR (101 MHz, $CDCl_3$) δ 154.65, 137.65, 137.31, 107.19, 61.22, 56.69, 44.26, 40.48; HRMS m/z calcd for $C_{11}H_{18}NO_3$ $[M+H]^+$ 212.1281 found 212.1291.

Synthesis of **3.8a**: 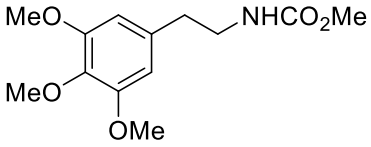

To a stirred 0°C solution of 268.1 mg (1.270 mmol) **3.8** in 10 mL 10% Na_2CO_3 and 5 mL THF was added 132 mg (1.40 mmol) methyl chloroformate in 5 mL THF. The resulting mixture was allowed to stir for 30 min before addition of 20 mL H_2O and subsequent extraction with 4 x 25 mL EtOAc. The combined organic layers were dried with anhydrous Na_2SO_4, filtered, and the solvent was removed *in vacuo* to yield 337.9 mg (quantitative yield) of a white solid that required no further purification. ^{1}H NMR (500 MHz, $CDCl_3$) δ 6.39 (s, 2H), 4.75 (s, 1H), 3.83 (s, 6H), 3.81 (s, 3H), 3.65 (s, 3H), 3.42 (q,

J = 6.8 Hz, 2H), 2.74 (t, *J* = 7.1 Hz, 2H); ^{13}C NMR (126 MHz, $CDCl_3$) δ 157.15, 153.47, 136.77, 134.61, 105.79, 60.99, 56.26, 52.22, 42.37, 36.70; HRMS m/z calcd for $C_{13}H_{20}NO_5$ $[M+H]^+$ 270.1336 found 270.1341.

Synthesis of **3.9**:

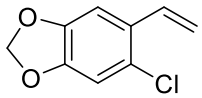

To a stirred -78°C solution of 788.4 mg (1.950 mmol) methyltriphenylphosphonium iodide in 20 mL dry THF was added 1.13 mL (2.28 mmol) *n*-butyllithium (2.02 M in hexane), resulting in a yellow mixture. After 1 h, 300.0 mg (1.625 mmol) 6-chloropiperonal dissolved in 5 mL THF was added dropwise over 2 minutes. The solution was allowed to stir for an additional 1 h at which time it was allowed to warm to 20°C (solution turned orange) and stir for 5 h. 15 mL of saturated NH_4Cl was then added at once and the resulting mixture was extracted with 3 x 20 mL CH_2Cl_2. The combined organic layers were dried with anhydrous Na_2SO_4, filtered, and the solvent was removed *in vacuo* to yield 950 mg of a crude yellow oil. Column chromatography (50 g silica gel, isocratic 30% CH_2Cl_2 in hexanes) afforded 199.5 mg (67%) of a clear liquid. Spectral data matched that previously reported in the literature.[10]

Synthesis of **3.11**:

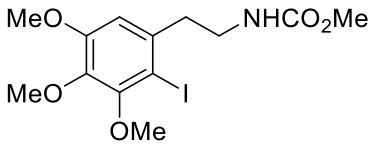

To a stirred solution of 828.7 mg (3.077 mmol) **3.8a** n 50 mL CH_3CN was added 900.0 mg (4.000 mmol) *N*-iodosuccinimide. The solution was then heated to reflux in the absence of light and allowed to stir for 15 h before being allowed to cool to 20°C, at which time the volatiles were removed. The mixture was then dissolved in 50 mL CH_2Cl_2 and 50 mL 1 M $Na_2S_2O_3$ and mixed vigorously. The layers were then separated, and the aqueous

layer was extracted with an additional 2 x 50 mL CH_2Cl_2. The combined organic layers were dried with anhydrous Na_2SO_4, filtered, and the solvent was removed *in vacuo* to yield 1.32 g of a light yellow/orange oil. Column chromatography (120 g silica gel, gradient run from pure CH_2Cl_2 to 10% EtOAc in CH_2Cl_2) afforded 1.18 g (97%) of colorless oil. ^{1}H NMR (400 MHz, $CDCl_3$) δ 6.62 (s, 1H), 4.87 (t, *J* = 6.4 Hz, 1H), 3.88 – 3.78 (m, 9H), 3.65 (s, 3H), 3.38 (q, *J* = 7.0 Hz, 2H), 2.94 (t, *J* = 7.4 Hz, 2H); ^{13}C NMR (101 MHz, $CDCl_3$) δ 157.18, 153.74, 153.29, 140.85, 137.21, 109.46, 88.28, 61.07, 60.85, 56.29, 52.21, 41.10, 41.05. HRMS m/z calcd for $C_{13}H_{19}INO_5$ $[M+H]^+$ 396.0302 found 396.0306.

Synthesis of **3.12**:

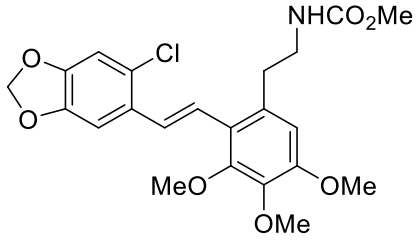

A stirred 20°C solution of 242.3 mg (0.6130 mmol) **3.11**, 167.9 mg (0.9195 mmol) **3.9**, 4.1 mg (0.018 mmol) palladium(II) acetate, 9.7 mg (0.037 mmol) triphenylphosphine and 172 μL (1.23 mmol) triethylamine in 30 mL DMF was sparged with nitrogen for 10 min then heated to 140°C. After 1 h, an additional 4.1 mg palladium(II) acetate was added. The solution turned dark and was allowed to stir for an additional 13 h. It was then cooled to 20°C and 60 mL H_2O was added followed by 90 mL CH_2Cl_2. The layers were separated and the aqueous layer was extracted with 2 x 90 mL CH_2Cl_2. The combined organic layers were dried with anhydrous Na_2SO_4, filtered, and the solvent was removed *in vacuo* to yield 380 mg of a red oil. Column chromatography (35 g silica gel, gradient run from 100% CH_2Cl_2 to 10% EtOAc in CH_2Cl_2) afforded 210 mg (76%) of a colorless oil. ^{1}H NMR (500 MHz, $CDCl_3$) δ 7.45 (d, *J* = 16.3 Hz, 1H), 7.23 (s, 1H), 6.91 (d, *J* = 16.4 Hz, 1H), 6.86 (s, 1H), 6.54 (s, 1H), 5.99 (s, 2H), 4.75 (s, 1H), 3.89 (s, 3H), 3.87 (m, 6H), 3.65 (s, 3H), 3.41

(q, *J* = 7.0 Hz, 2H), 2.94 (t, *J* = 7.4 Hz, 2H); ^{13}C NMR (126 MHz, $CDCl_3$) δ 157.21, 152.82, 152.72, 147.77, 147.39, 141.53, 133.16, 130.11, 129.19, 125.91, 123.55, 123.24, 110.04, 109.56, 105.65, 101.99, 61.15, 60.80, 56.23, 52.27, 42.17, 34.53; HRMS m/z calcd for $C_{22}H_{25}ClNO_7$ $[M+H]^+$ 450.1314 found 450.1302.

Synthesis of **3.5a**:

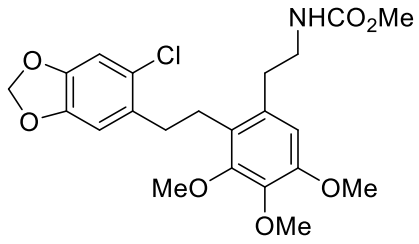

To a flask containing 34.5 mg (0.0767 mmol) **3.12** and 13.2 mg 10% palladium on activated carbon was added 10 mL EtOAc. Stirring was then begun and the flask was vacuum-purged and back-filled with H_2 gas, and allowed to stir for 17 h at 1 atm. The suspension was then filtered through Celite® and volatiles were evaporated *in vacuo* to yield 59.3 mg of a crude oil. Column chromatography (15 g silica gel, gradient run from 100% CH_2Cl_2 to 5% EtOAc in CH_2Cl_2) afforded 26.4 mg (71%) of a colorless oil. ^{1}H NMR (500 MHz, $CDCl_3$) δ 6.84 (s, 1H), 6.71 (s, 1H), 6.48 (s, 1H), 5.95 (s, 2H), 4.70 (s, 1H), 3.92 (s, 3H), 3.86 (s, 3H), 3.84 (s, 3H), 3.68 (s, 3H), 3.43 – 3.31 (m, 2H), 2.78 (m, 6H); ^{13}C NMR (126 MHz, $CDCl_3$) δ 157.18, 152.58, 151.92, 146.86, 146.72, 141.03, 132.98, 132.43, 125.98, 125.30, 110.24, 109.96, 108.79, 101.76, 61.20, 60.89, 56.21, 52.31, 42.29, 35.16, 33.38, 27.35; HRMS m/z calcd for $C_{22}H_{27}ClNO_7$ $[M+H]^+$ 452.1471 found 452.1460.

Synthesis of **3.13**:

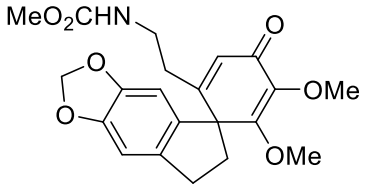

A solution of 3.1 mg (0.01 mmol) **3.5a** in 4.5 mL previously irradiated and distilled CH_3CN and 2.0 mL micron-filtered H_2O was sparged with nitrogen for 20 min. The solution was then irradiated with an Hg arc lamp for 2 h at which time the volatiles were removed *in vacuo* to yield 3.9 mg of a light yellow oil. HPLC purification (Waters 1525 Binary HPLC Pump, 2489 UV/Vis Detector, XBridge Prep C18 5µm 10x100 mm Reverse Phase Column, 20 min gradient from 95% H_2O/MeCN to 5% H_2O/MeCN) afforded 0.8 mg (29%) of a pale yellow oil. ^{1}H NMR (400 MHz, $CDCl_3$) δ 6.71 (s, 1H), 6.23 (s, 1H), 6.08 (s, 1H), 5.94 (s, 2H), 4.65 (s, 1H), 3.89 (s, 3H), 3.74 (s, 3H), 3.61 (s, 3H), 3.33 – 2.95 (m, 4H), 2.54 (m, 1H), 2.30 (m, 2H), 2.01 (m, 1H); ^{13}C NMR (101 MHz, $CDCl_3$) δ 184.31, 166.03, 158.32, 156.86, 148.50, 147.45, 138.68, 136.92, 134.90, 124.81, 105.34, 103.10, 101.59, 61.32, 61.25, 60.73, 52.23, 39.43, 34.85, 32.71, 31.38; HRMS m/z calcd for $C_{21}H_{23}NNaO_7$ $[M+Na]^+$ 424.1391 found 424.1368.

3.5.3 DFT Calculations

To gather more evidence for the structural assignment of **3.13**, DFT calculations were performed on two possible isomers, referred to here as 6-membered and spiro. Gaussian 2009 (version C.01, 64 bit, Windows multiprocessor) was used with GaussView 5 to perform molecular orbital calculations on the two isomeric structures. The DFT method was used with the B3YLP hybrid functional and 6-311G(d,p) basis set functions on all atoms. Cambridge Crystallographic searches using the 2015 database found related structures for each proposed isomer that were used as one of the starting points for the Gaussian geometry optimization. For the 6-membered ring isomer the related CCDC structure refcode OMEDEP was imported and modified using GaussView to produce the starting point for the optimization.[11] CCDC structure refcode QOHJOO was imported,

modified, and used as the starting point for the geometry optimization on the spiro isomers.[12] The methyl carbamate group was replaced with a simple NH_2 group for both isomers. Both isomers were also manually drawn in GaussView to generate somewhat different starting structures and conformations on which optimizations were also run. Figure 3.1 shows three dimensional structures of the two isomers.

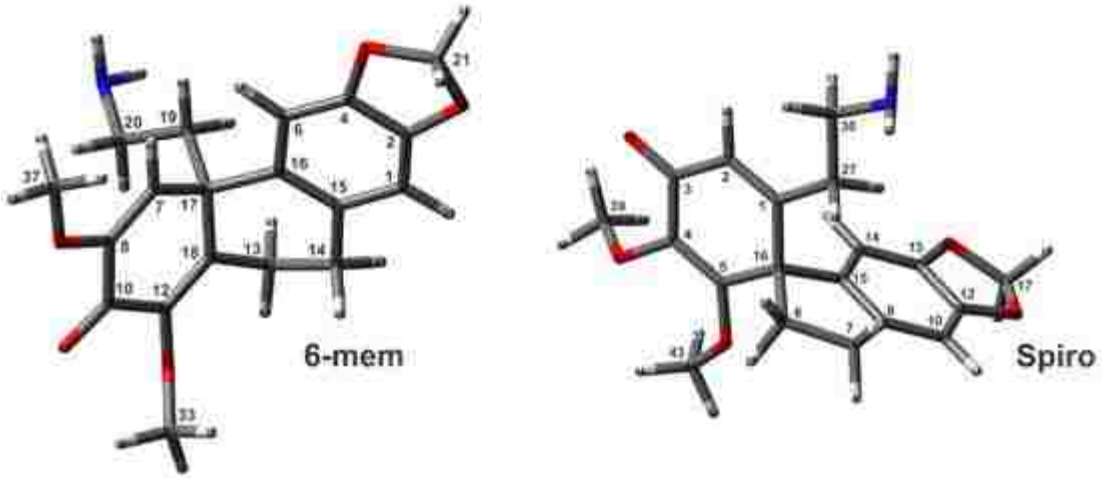

Figure 3.1 Possible isomers of **3.13**

The optimizations and frequency calculations on the two starting spiro isomer structures ended up with the same final structures that had the same overall energy. Optimization on the 6-membered ring isomer derived from the OMEDEP X-ray structure had the lower ΔG energy by 1.6 kcals/mol relative to the "hand-drawn" 6-membered ring isomer. All stretching frequencies calculated for the isomers were positive, indicating ground state structures. The spiro isomer was calculated to have the lowest overall ΔG energy, with the most stable 6-membered ring isomer higher by 2.9 kcals/mol. This non-trivial difference in relative energies is possibly due to extra ring strain induced by the quaternary center (Figure 3.1, 6-mem, carbon number 17) contained in the fused 6-membered ring system. The added rigidity of the 6-membered fused system compared to

the spiro may also cause increased steric interactions. For example, the hydrogen atoms on carbons number 6 and 7 of the 6-membered isomer are forced toward each other.

To gain additional evidence for the structural assignment of **3.13**, NMR chemical shift calculations were carried out on the lowest energy isomers and the absolute ^{13}C chemical shifts calculated were corrected using the internal Gaussian TMS ^{13}C standard based on a DFT 6-311+G(2d,p) basis set. Although the basis set used for the TMS reference differs somewhat from the 6-311G(d,p) basis set used for our calculation, we believed that it was close enough to allow a good relative comparison for the two isomers to the experimental ^{13}C NMR data. Figure 3.2 shows calculated ^{13}C NMR chemical shifts compared to experimental, with the spiro isomer being a considerably better match. This calculation provided additional evidence for the structural assignment, and together with the energy calculation allowed us to confidently assign the structure of compound **3.13** as the spiro isomer.

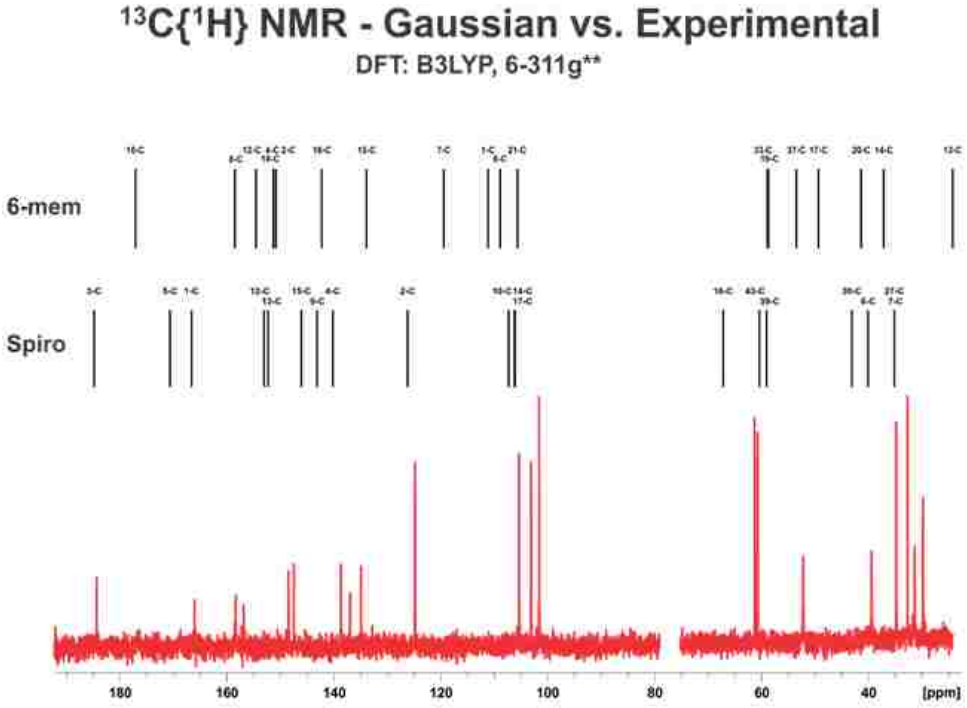

Figure 3.2 NMR comparison

3.6 References

1. Matsui, M., *The Alkaloids*. Academic Press: New York, 1988; Vol. 33.

2. Carroll, A. R.; Arumugan, T.; Redburn, J.; Ngo, A.; Guymer, G. P.; Forster, P. I.; Quinn, R. J., Hasubanan Alkaloids with δ-Opioid Binding Affinity from the Aerial Parts of *Stephania japonica*. *J. Nat. Prod.* **2010,** *73* (5), 988.

3. Fagnoni, M., The Photo SN1 Reaction *Via* Phenyl Cation. *Lett. Org. Chem.* **2006,** *3*, 253-259.

4. Kondo, H.; Satomi, M.; Odera, T., *Annu. Rep. ITSUU Lab* **1951,** *2*, 35.

5. Tomita, M.; Ibuka, T.; Inubushi, Y.; Watanabe, Y.; Matsui, M., Structure of Hasubanonine. *Tetrahedron Lett.* **1964,** *40*, 2937-2944.

6. Shultz, A. G.; Wang, A., First Asymmetric Synthesis of a Hasubanan Alkaloid. Total Synthesis of (+)-Cepharamine. *J. Am. Chem. Soc.* **1998,** *120*, 8259.

7. (a) Varga, E. V.; E.Navratilova; Stropova, D.; Jambrosic, J.; Roeske, W. R.; Yamamura, H. I., Agonist-specific regulation of the δ-opioid receptor. *Life Sci.* **2004,** *76* (6), 599-612; (b) Broom, D. C.; Jutkiewicz, E. M.; Rice, K. C.; Traynor, J. R.; Woods, J. H., Behavioral Effects of δ-Opioid Receptor Agonists: Potential Antidepressants? *Jpn. J. Pharmacol.* **2002,** *90*, 1-6.

8. FAGNONI, M.; ALBINI, A., Arylation Reactions: The Photo-SN1 Path via Phenyl Cation as an Alternative to Metal Catalysis. *Acc. Chem. Res.* **2005,** *38*, 713-721.

9. (a) Dichiarante, V.; Salvaneschi, A.; Protti, S.; Dondi, D.; Fagnoni, M.; Albini, A., The β Effect of Silicon in Phenyl Cations. *J. Am. Chem. Soc.* **2007,** *129*, 15919-15926; (b) Protti, S.; Dondi, D.; Fagnoni, M.; Albini, A., Photochemical Arylation of Alkenols: Role of Intermediates and Synthetic Significance. *Eur. J. Org. Chem.* **2008,** *2008* (13), 2240-2247; (c) Lazzaroni, S.; Protti, S.; Fagnoni, M.; Albini, A., Photoinduced Three-Component Reaction: A Convenient Access to 3-Arylacetals or 3-Arylketals. *Org. Lett.* **2009,** *11* (2), 349-352; (d) Dichiarante, V.; Fagnoni, M.; Albini, A., *Solar*ylations via 4-Aminophenyl Cations. *J. Org. Chem.* **2010,** *75*, 1271-1276.

10. Gerlach, M.; Przewosny, M.; Englberger, W.; Reissmueller, E.; P., B.-F.; Maul, C.; Jagusch, U.-P. *PCT Int. Appl.;* (Gruenenthal G.m.b.H., Germany) Wo. 2001, p 152.

11. Blanchfield, J. T.; Sands, D. P. A.; Kennard, C. H. L.; Byriel, K. A.; Kitching, W., *Phytochemistry* **2003,** *63*, 711-720.

12. Lin, Y.-C.; Cheng, Y.-B.; Liaw, C.-C.; Lo, I.-W.; Kuo, Y.-H.; Chiang, M. Y.; Chou, C.-H.; Shen, Y.-C., *Molecules* **2013,** *18*, 6573.

CHAPTER 4: REMOTE HYDROXYLATION BY RADICAL TRANSLOCATION AND POLAR CROSSOVER

4.1 Introduction

Functionalization of aliphatic C-H bonds is a widely utilized and vitally important process in nature.[1] Although the synthetic manipulation of unactivated C-H bonds was first discovered in the 1800s, use of these bonds in the synthesis of target molecules remains limited. Indeed, for quite some time synthetic methods for C-H functionalization were harsh (highly reactive, prone to decomposition), low-yielding and unselective.[2] Therefore the view persisted that this process could only be made selective and high-yielding by mimicking enzymes.[3] In the past two decades, however, improvements to reaction conditions, selectivity, and yields have begun to render aliphatic C-H functionalization an advantageous step in synthetic planning.[4]

The benefits of incorporating C-H functionalization in total synthesis arise from shedding the usual constraints of retrosynthetic analysis. Step-, atom-, and redox-economy can all be significantly improved by viewing the C-H bond as a useful functional group rather than an inert bystander.[5] Employment of such strategies serves to improve overall synthetic efficiency. By alleviating problems with scalability and the cost of production of complex drugs, the economic viability of such compounds can be realized to a greater extent.[4]

Two main strategies exist for the conversion of aliphatic C-H bonds. The first strategy relies on the innate properties of the bond and its inherent reactivity while the second strategy uses external reagents to guide or direct the activation.[6] A directing approach which has received considerable attention in recent years incorporates functionality which directs either the inner sphere of a transition metal or a metal-oxo

species to a remote C-H bond.[7] Alternatively, a covalently attached directing group can be activated thermally, chemically, or photochemically to produce a radical which will translocate via hydrogen abstraction.[8] A radical-promoted hydrogen atom transfer of this sort is often referred to as a radical translocation event. Our recently developed approach to site-selective C-H functionalization falls into this category.

4.2 Important Examples of Radical Translocation

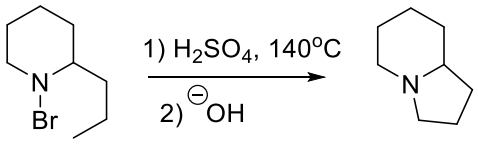

Scheme 4.1 Hofmann's pioneering radical translocation

Though this reaction was discovered in the late 1800s and expanded upon in the early 1900s, the mechanism was not understood until much later. In 1950, Wawzonek and Thelen researched and correctly predicted the mechanism which was studied further and confirmed by Corey and Hertler in 1960.[9]

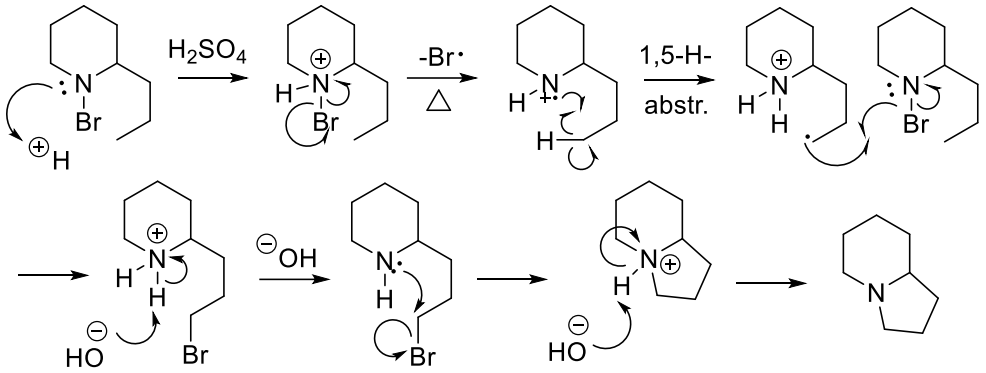

Scheme 4.2 Radical translocation mechanism

As shown in Scheme 4.2, the mechanism begins with amine protonation followed by homolysis of the N-Br bond. The resulting nitrogen radical cation abstracts hydrogen intramolecularly from an energetically favored carbon atom yielding an ammonium ion and a primary carbon-centered radical. The primary radical begins a chain process by

abstracting bromine from another substrate molecule. Finally, basic workup liberates the free amine which cyclizes via S_N2 onto the bromine-bearing carbon, and loss of a final proton results in the observed product.

Breslow and coworkers famously employed guided radical translocation, which they referred to as remote oxidation, as a method for steroid functionalization in the early 1970s.[10] Cholestanols were esterified with various benzophenone acids which could be activated phototchemically for use as directing groups. Among various results, ultraviolet irradiation of the benzophenone-4-acetic ester of 3α-cholestanol gave an impressive 55% yield of a single olefin between carbons 14 and 15 in ring D of the steroid backbone (Scheme 4.3).[10] This groundbreaking site-selective remote functionalization led to increased interest in directed radical translocation.

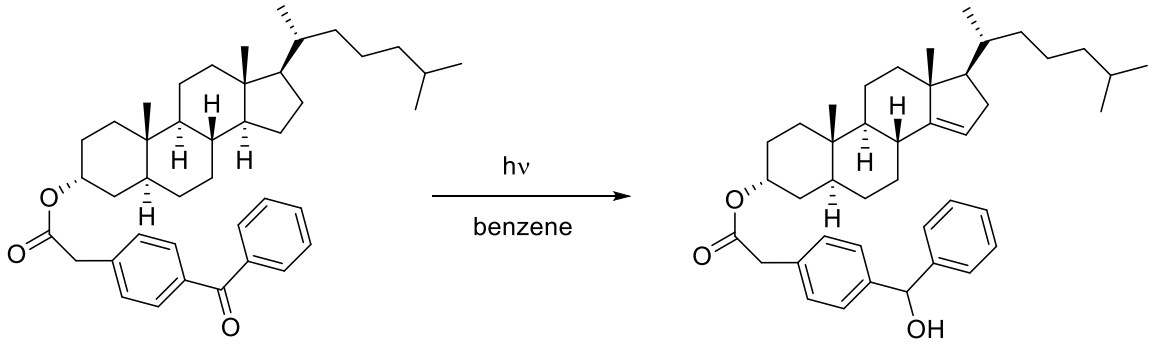

Scheme 4.3 Breslow's photochemical remote olefination

Recently, a radical translocation method for desaturation has been developed by Baran and coworkers.[11] This guided desaturation makes use of a novel benchtop-stable "portable desaturase" which can be attached to a substrate molecule where it facilitates C-H bond functionalization. The newly devised Tz^{o}Cl (*o*-tosyl triazene chloride) group exhibits an aryl sulfonyl chloride for attachment to alcohol or amine moieties of a substrate before further reaction (Scheme 4.4).

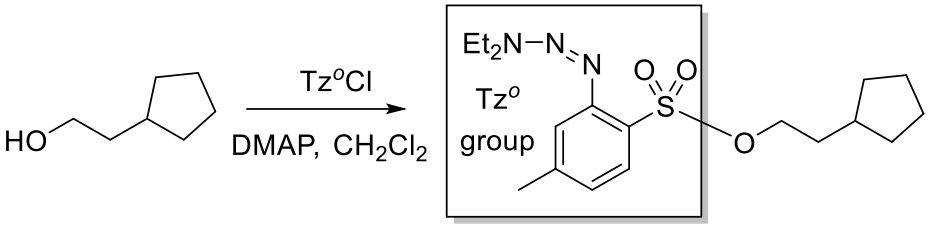

Scheme 4.4 Attachment of Tz^o directing group

Ortho to the sulfonyl is a diethyl triazene which, upon treatment with two equivalents of strong acid, produces an aryl diazonium salt. The redox-active aryl diazonium is reduced by TEMPO to release nitrogen and yield the aryl radical which performs an (unusual 1,7) intramolecular hydrogen abstraction at a nearby tertiary carbon. Oxidation of the resulting tertiary radical to carbocation by TEMPO$^+$ and subsequent elimination give the desired olefin product. When the reaction is complete, the Tz^o directing group leaves behind a synthetically useful tosyl group. Depicted in Scheme 4.5, this intriguing radical-polar crossover reaction helped to inspire our foray into remote C-H bond functionalization.

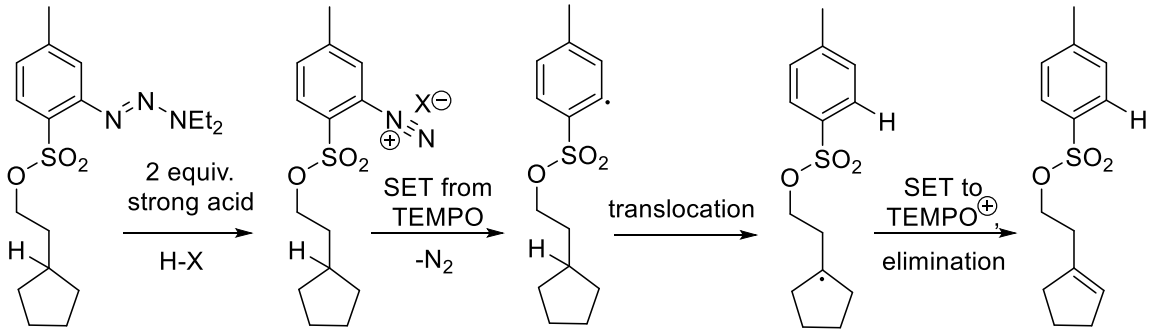

Scheme 4.5 Baran's remote desaturation process

4.3 Results and Discussion

Our initial goal for C-H functionalization was to create a mild and versatile method for the selective installation of important functionalities at relatively unreactive positions. We recognized that there was ample room for expansion to the guided desaturation work completed by Baran and coworkers, and we thought to employ photoredox catalysis toward

that goal. An approach involving a controlled hydrogen abstraction followed by oxidation to carbocation and subsequent rearrangement, elimination, or nucleophilic attack would open pathways to a plethora of desired bond formations. One can imagine using such a reaction to replace C-H bonds with carbon bonds to oxygen (hydroxylation, etherification), nitrogen (Ritter amidation), carbon, fluorine and many others.

We envisioned a process to form an electron-poor aryl radical which could translocate via hydrogen abstraction to a nearby alkyl group. Such translocations from relatively unstable aryl radicals to more stable alkyl radicals are known to be favorable and selective under the correct conditions.[6-9, 11, 12] The low oxidation potential of the resulting alkyl radical allows mild reagents to effect SET oxidation to carbocation.[13] To accomplish this goal, we proposed a pathway like that shown in Scheme 4.6.

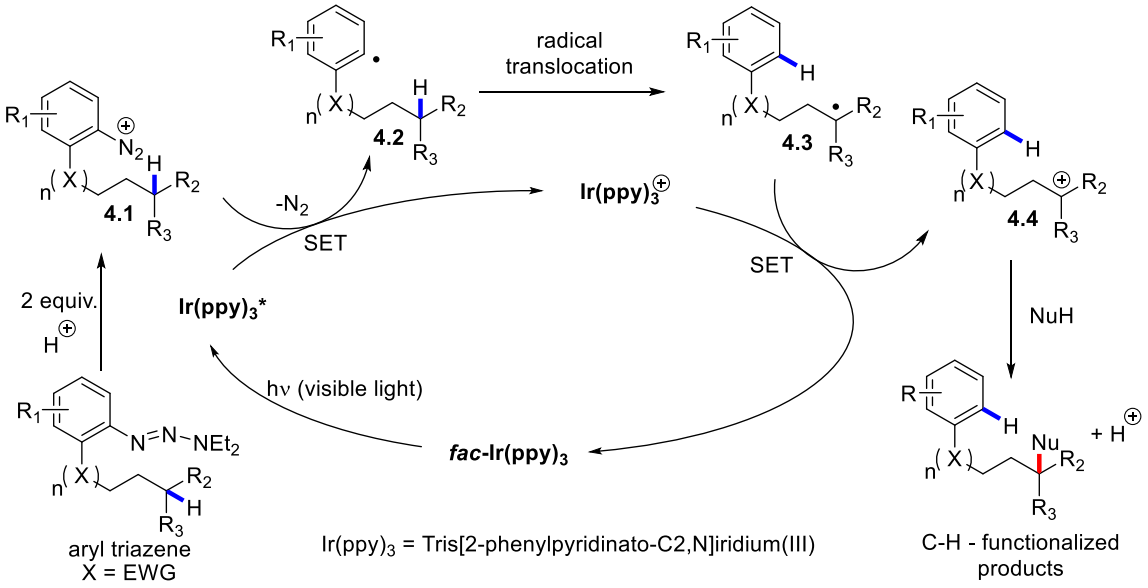

Scheme 4.6 Proposed pathway for remote functionalization

En route to our goal of mild conditions, we chose to employ visible light photoredox catalysis, a set of techniques which have gained recent traction by solving several challenging problems in organic synthesis.[14] Beginning with an established directing group (See Tz^o, Scheme 4.4), an arene diazonium **4.1** could be generated upon addition of

two equivalents of strong acid. A diazonium of this type, with a reduction potential (E^o) in the range of -0.1 to +0.5 V vs. SCE could favorably undergo single electron reduction from an excited state photocatalyst such as *fac*-$Ir(ppy)_3^*$, which has a E^o of -1.73 V vs. SCE in the excited state.[14f, 15] After release of nitrogen, the resulting aryl radical **4.2** would then abstract hydrogen from an attached alkyl moiety. This radical translocation event would generate alkyl radical **4.3** (E_{ox} = 0-0.75 V vs. SCE) which could be oxidized to carbocation by the oxidatively quenched photocatalyst $Ir(ppy)_3^+$ (E^o = +0.77 V vs. SCE), thus completing the catalytic cycle.[13, 14f] Carbocation **4.4** would then intercept a nucleophile and yield the desired C-H functionalized product.

For our initial experiments, we synthesized isoamyl Tz*o* sulfonate ester **4.5** in one step from the corresponding alcohol. We then degassed and irradiated (4 W blue LEDs, λ=455 nm) **4.5** and two equivalents of tetrafluoroboric acid in the presence of *fac*-$Ir(ppy)_3$ as photocatalyst, nitromethane as solvent, and methanol as nucleophile and cosolvent.

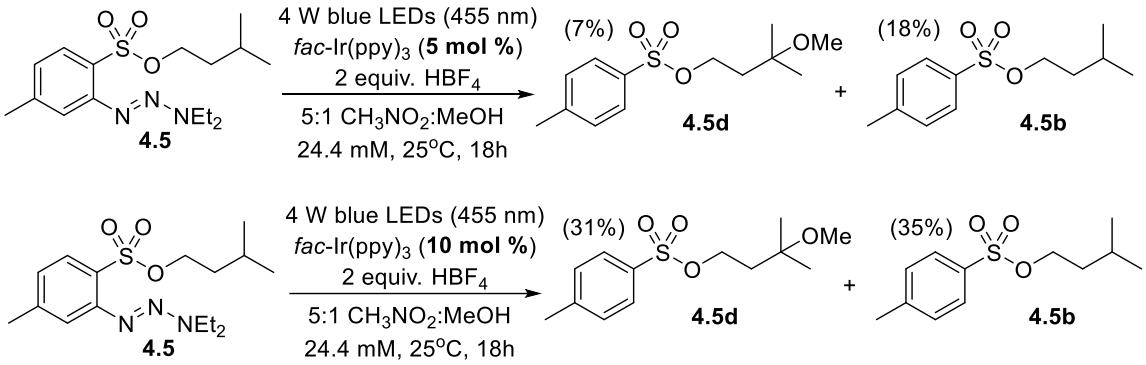

Scheme 4.7 Initial experiments

Shown in Scheme 4.7, an initial 7% yield of desired product **4.5d** was obtained along with 18% of trivial reduction product **4.5b**. However, increasing the loading of photocatalyst had an immediate influence on yield. 10 mol% catalyst gave 31% yield of desired product and a similar amount of trivial reduction product. Further increases of

photocatalyst as well as changes to the acid used (TFA, TfOH) did not have a noticeable effect on yield. Any modifications to the solvent system or reduction of methanol equivalents led to no desired product formation.

To test this system outside of a single substrate, we synthesized cyclopentyl Tz^o ester **4.6** and menthyl Tz^o ester **4.7** (Scheme 4.8). While the cylopentyl substrate gave 25% of desired product **4.6d**, the menthol derivative gave just 13% desired product **4.7d** and 32% of desaturation product **4.7c**. Both substrates produced noticeable amounts (not isolated) of trivial reduction products.

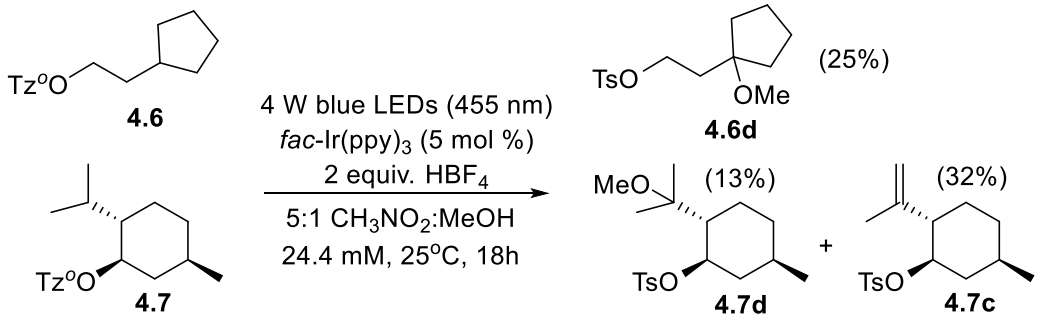

Scheme 4.8 Additional preliminary results

After these initial results, it was clear to us that this remote functionalization system was in need of improvement. The most problematic issue was the consistent production of trivial reduction products (See Scheme 4.7, structure **4.5b**). These products are likely formed when a radical intermediate abstracts hydrogen from the electron-rich C-H bonds of methanol.

To remedy this problem we decided to look for a nucleophile which lacked electron-rich C-H bonds while also being neutral and relatively non-basic. Though water has low miscibility with nitromethane, we attempted the same reaction conditions from Scheme 4.8, replacing methanol with water. We were pleased to find that, on the first attempt of the new reaction conditions, isoamyl Tz^o ester **4.5** yielded 57% of desired

hydroxylation product **4.5a** with only trace evidence of trivial reduction product **4.5b** or desaturation product **4.5c** (Scheme 4.9).[16]

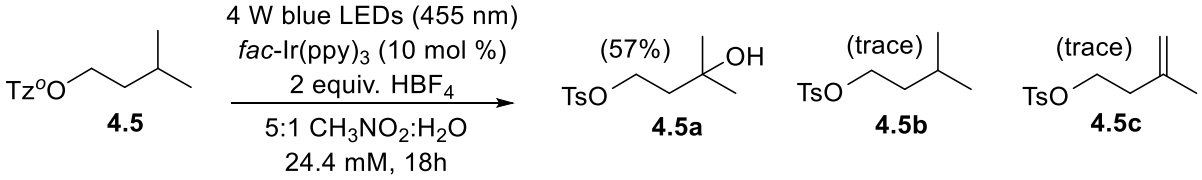

Scheme 4.9 Initial remote hydroxylation experiment

At this point we decided to further optimize conditions for remote hydroxylation (Figure 4.1). We found that a reaction time of less than 6 hours decreased yield (incomplete consumption of starting material) while anything more gave a consistent yield in the high 50s (entries 1-4). Decrease in photocatalyst loading resulted in significantly decreased yields (entries 5-6). Exclusion of acid resulted in no observed conversion of starting material, (entry 7) while exclusion of photocatalyst gave 11% of desired product (entry 8).

Interestingly, reactions run in the absence of light gave results of 40% after 4 hours and 50% after 18 hours (entries 9-10). The ground state photocatalyst, *fac*-Ir(ppy)$_3$ (E^o = +0.77 V vs. SCE), was not expected to undergo SET to reduce the generated aryl diazonium species (E^o range of -0.1 to +0.5 V vs. SCE), yet that seemed to be the case. The unanticipated yields of this "dark reaction" prompted us to further investigate the reduction potential of the specific diazonium being generated during the reaction. As shown in Scheme 4.10, diazonium **4.5e** was generated from isoamyl Tz^o ester **4.5** by addition of 2 equivalents of strong acid. Cyclic voltammetry of **4.5e** was then performed (See section **4.6.2** for experimental data) and E^o was found to be -0.12 V vs. SCE. These findings tell us that, as expected, an electron transfer from ground state *fac*-Ir(ppy)$_3$ to diazonium **4.5e** would be energetically unfavorable (by 890 mV). However, because this electron transfer

Entry	Deviation from Std. Cond.	Irradiation Time (h)	yield of 6 (%)
1	1h irradiation	1	36
2	2h irradiation	2	49
3	6h irradiation	6	54
4	18.5h irradiation	18	57
5	5 mol % *fac*-Ir(ppy)$_3$	18	12
6	1 mol % *fac*-Ir(ppy)$_3$	18	4
7	no acid	18	none observed
8	no *fac*-Ir(ppy)$_3$	18	11
9	light excluded	4	40
10	light excluded	18	50
11	no freeze-pump-thaw	18	57
12	48.8 mM 5	18	40
13	10 mM 5	18	57
14	DMF as solvent	4	none observed
15	CH_3CN as solvent	4	none observed
16	DMSO as solvent	18	none observed
17	20 equiv. H_2O	4	trace
18	Ru(phen)$_3$(PF_6)$_2$ as catalyst	18	trace
19	Ir[dF(CF_3)ppy]$_2$(dtbbpy)(PF_6) as catalyst	18	trace
20	ethyl eosin as catalyst	18	none observed
21	Ru(bpy)$_3$(PF_6)$_2$ as catalyst	18	16
22	TFA replaces HBF_4	18	54
23*	Baran's conditions + 2 mL H_2O	N/A	18

Figure 4.1 Optimization of reaction conditions
Isolated yields. *1 equiv. of TEMPO, 2 equiv. TFA at 60^{o}C for 1.5 h without irradiation.

is coupled to a highly favorable and irreversible fragmentation (loss of nitrogen), the overall process is energetically favorable and precedents of similar events exist.[17]

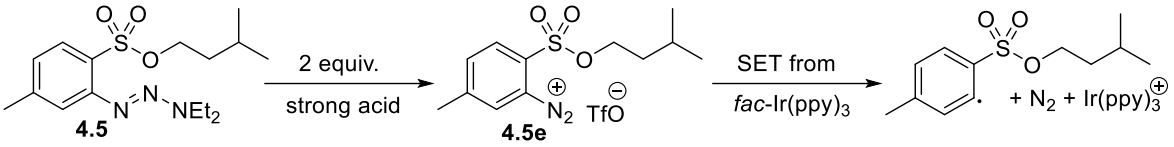

Scheme 4.10 Generation of diazonium and subsequent fragmentation

Entry 11 showed that degassing of the reaction was unnecessary as 57% yield was observed under nitrogen with no freeze-pump-thaw procedure. Entries 12 and 13 showed that higher concentration decreased yield while lower concentration had no observable effect. The strong effect of solvent choice was apparent by the lack of any desired product isolated from entries 14-16. Entry 17 showed the importance of water as a cosolvent when only trace amounts of desired product formed with 20 equivalents of water added. Choice of photocatalyst was also imperative, with entries 18-21 resulting in a yield of 16% or less. Replacement of HBF_4 with TFA resulted in a slight decrease in yield (entry 22). Finally, and of great significance, we showed that this transformation could not be efficiently accomplished using the conditions of Baran and coworkers with the addition of water.[11]

Even under optimized conditions for remote hydroxylation, yields of **4.5a** did not exceed 60%. Considering these results, the possibility of side products/pathways needed to be explored. To this end, we irradiated **4.5** in CD_3NO_2 and D_2O with 48% HBF_4 and 10 mol% *fac*-Ir(ppy)$_3$ for 18 hours (Scheme 4.11). The resulting crude mixture's ^{1}H NMR spectrum (in CD_3NO_2 after separating layers) showed desired product **4.5a** as well as small amounts of desaturation product **4.5c** and some unknown species. Desaturation product **4.5f** and trivial reduction product **4.5b** were not observed. Hydrolysis product **4.8** (isoamyl alcohol) was observed although neither of its desaturated derivatives (**4.8c**, **4.8f**) nor hydroxylated derivative **4.8a** were detected.

Baran and coworkers also mentioned the possibility that an allylic tosylate like **4.5f** may decompose.[11] An expected product of such a pathway would be allylic alcohol **4.9**, but none was detected during NMR studies. In order to determine NMR yields of the observed products, use of various internal standards was attempted yet none gave useful data. Instead, relative ratios of products were calculated and found to be 5.1 to 1.1 to 1 respectively for **4.5a**, **4.8**, and **4.5c**. These findings, along with the notable presence of *p*-toluenesulfonate salts in the D_2O layer, suggested that a reaction intermediate was sensitive to hydrolysis while translocation products were stable under the reaction conditions.

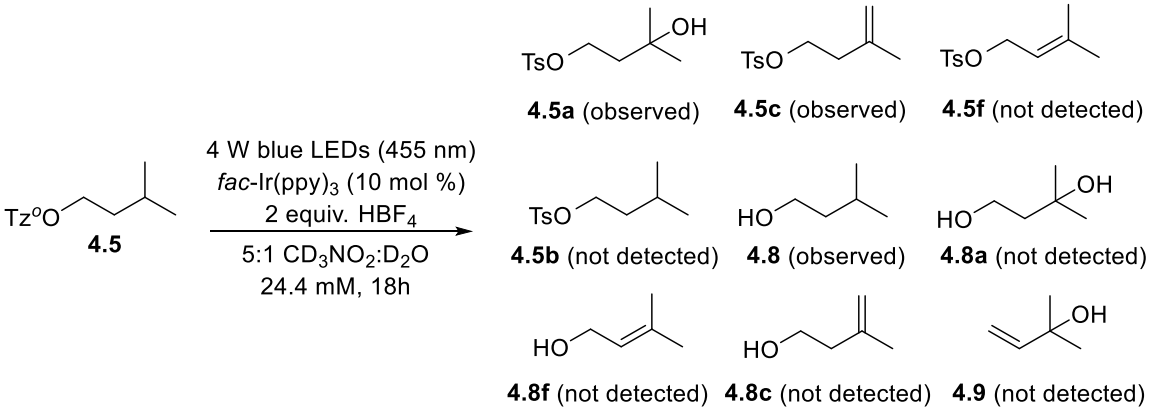

Scheme 4.11 NMR studies

In order to confirm the stability of hydroxylation product **4.5a** and desaturation product **4.5c**, each was resubmitted to standard reaction conditions (Scheme 4.9) and no degradation was observed in either case. However, when Tz^o ester **4.5** was subjected to standard conditions without photocatalyst (Scheme 4.12), considerable quantities of isoamyl alcohol **4.8** and diazonium **4.5e** were observed. Considering these results, the possibility of an electron-poor diazonium intermediate like **4.5e** undergoing hydrolysis is much more likely than hydrolysis of a Tz^o ester like **4.5** or translocation products like **4.5a** and **4.5c** (Scheme 4.11).

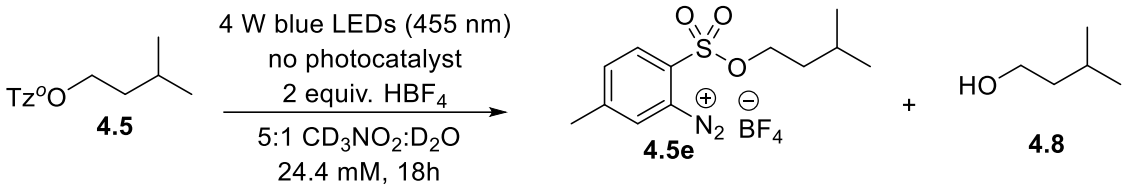

Scheme 4.12 Control experiment with absence of photocatalyst

Next, we tested our photocatalytic remote hydroxylation method on several additional substrates to determine the scope. Using our standard conditions (Scheme 4.9), we found that yields of this reaction ranged from 31-63% over a broad range of structures. We also tested lower temperatures intended to suppress the competing desaturation reaction (Figure 4.2). Cyclopentyl substrate **4.6** yielded 41% of desired hydroxylation product **4.6a**. The same substrate gave a slightly increased yield of 48% when run at 6ºC for 3 days, (slow consumption of triazene Tz^o ester) but reaction of Tz^o esters at temperatures lower than 0ºC were unreasonably slow. This slowed consumption of starting material, in addition to the absence of diazonium or other intermediates in crude ^{1}H NMRs, led us to believe that acid-promoted liberation of the diazonium ion from the triazene is the rate-determining step of the overall process. Menthyl subtrate **4.7** afforded 31% hydroxylation product while citronellol derivative **4.10** gave 38%. Leucine-derived substrate **4.11** gave exclusively lactone product **4.11a** in 47% yield. Higher yields resulted from benzylic Tz^o esters **4.12, 4.13,** and **4.15** (41-63%). Tz^o sulfonamides (substrates **4.14**, **4.15**, **4.16**) also successfully underwent remote hydroxylation to give 34-56% yields. Substrates **4.16**, **4.17** and **4.18** demonstrated that secondary benzylic systems were effectively converted to the corresponding alcohols (52-56% yields), while substrate **4.18** (56%) also revealed that 1,6-abstractions are feasible with this method.

Figure 4.2 Substrate Scope
Unless otherwise stated, reaction conditions were 0.2929 mmol substrate, 10 mol % *fac*-$Ir(ppy)_3$, 10 mL CH_3NO_2, 2 mL H_2O and 2 equiv. of 48 % HBF_4 were employed for 18 h irradiation. *Experiment was conducted at 6^oC for 3 days irradiation.

Entry	Substrate	Product (% yield)
1	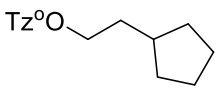 **4.6**	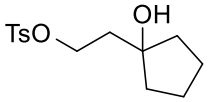 **4.6a** (41 %)
2*	**4.6**	**4.6a** (48 %)
3	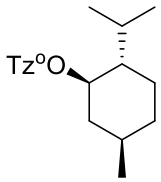 **4.7**	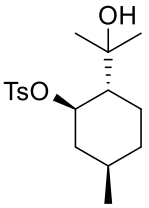 **4.7a** (31 %)
4	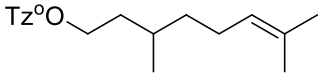 **4.10**	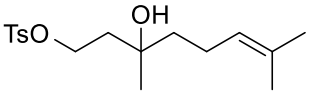 **4.10a** (38 %)
5	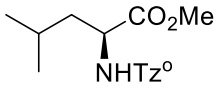 **4.11**	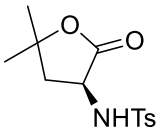 **4.11a** (47 %)
6 (R=CH_3) 7 (R=Ph)	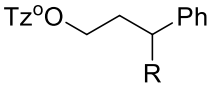 **4.12** (R=CH_3) **4.13** (R=Ph)	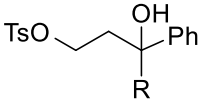 **4.12a** (R=CH_3, 63 %) **4.13a** (R=Ph, 56 %)
8 (R=CH_3) 9 (R=Ph)	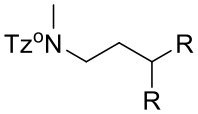 **4.14** (R=CH_3) **4.15** (R=Ph)	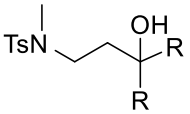 **4.14a** (R=CH_3, 34 %) **4.15a** (R=Ph, 41 %)
10	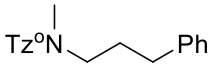 **4.16**	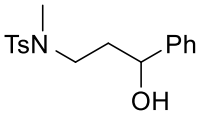 **4.16a** (56%)
11	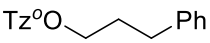 **4.17**	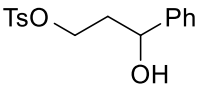 **4.17a** (52%)
12	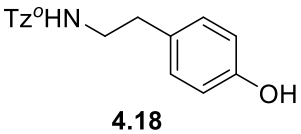 **4.18**	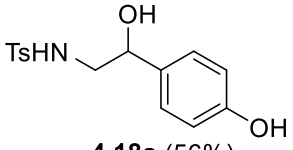 **4.18a** (56%)

To confirm that the suggested pathway for this transformation was indeed feasible, an isotopic labeling experiment was conducted. Shown in Scheme 4.13, 97% ^{18}O-containing water was used along with standard conditions. The result of the experiment was hydroxylation with 90% ^{18}O incorporation, which agreed with the original mechanistic hypothesis that water is trapping a carbocation.

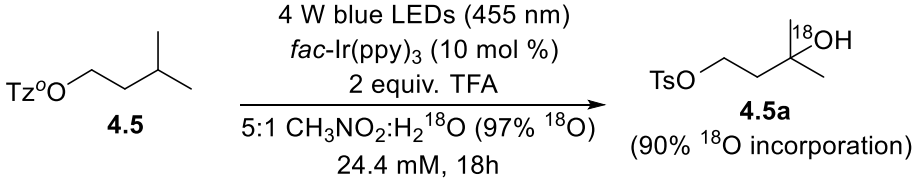

Scheme 4.13 ^{18}O labeling experiment

After establishing photocatalytic remote hydroxylation we looked forward to demonstrating its useful application in organic synthesis. We recognized that many important molecules contain the 1,3-aminoalcohol structural feature that our method can expediently construct. Therefore, we converted hydroxylation product **4.17a** (Figure 4.2) to the powerful antidepressant drug (±)-fluoxetine (Prozac®) in two steps.[18] Shown in Scheme 4.14, the tosyl group resulting from conversion of Tz^o triazene was used as a leaving group for nucleophilic addition of methylamine to give aminoalcohol **4.19**. This intermediate was then deprotonated with sodium hydride and converted to fluoxetine via nucleophilic aromatic substitution reaction with 4-chlorobenzotrifluoride. Proceeding in only 4 steps from the inexpensive and simple 3-phenyl-1-propanol, this synthesis displays the rapid complexity introduced by our directed C-H functionalization method.

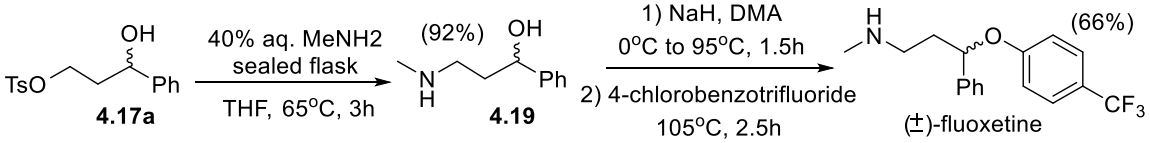

Scheme 4.14 Unoptimized synthesis of fluoxetine

4.4 Future Work

Additional work toward C-H functionalization strategies will likely employ sulfones in place of previously used sulfonate esters and sulfonamides. In this way, we aim to eliminate the problem of hydrolysis of our intermediates and increase yields. Sulfones may conceivably be prepared by modifying Baran's procedure for production of Tz^{o}Cl from the bromotriazene precursor.[11] Alternatively, sulfones could be prepared from previously made Tz^{o}Cl.[19] Shown in Scheme 4.15, both methods for production of Tz^o sulfones would go through sulfinate anion intermediates (structure **4.20)**. Reaction of sulfinates with alkyl iodides would produce desired Tz^o sulfone substrates with pendant alkyl chains such as **4.21.** We would then endeavor to direct a nucleophile to a desired location via our standard conditions (Scheme 4.9) to yield structures such as **4.22**.

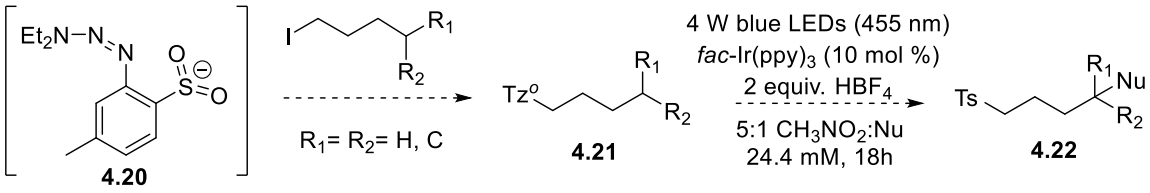

Scheme 4.15 Proposed remote functionalization of sulfones

4.5 Conclusions

Activation of relatively inert aliphatic C-H bonds plays a vital role in nature and is becoming increasingly useful in organic synthesis. The abundance of this type of bond in organic structures makes it a desirable target for manipulation. Currently, many existing synthetic methods for functionalization of C-H bonds are harsh and/or unselective. As a step toward a solution to these problems, we have developed a photocatalytic directed hydroxylation (and methoxylation) of aliphatic C-H bonds which proceeds under mild conditions. Our method has been tested on a variety of substrates and also applied to the total synthesis of the antidepressant drug fluoxetine (Prozac®). This and similar systems

will be explored in the future to produce new and better ways for functionalizing aliphatic C-H bonds.

4.6 Experimental

4.6.1 General Methods

^{1}H NMR and ^{13}C NMR spectroscopy was conducted using a Bruker AV-400 or AV-500 spectrometer. Mass spectra were attained using an Agilent 6210 electrospray time-of-flight mass spectrometer. Optical rotation was measured using a JASCO P-2000 polarimeter. All materials were received from commercial suppliers and used without further purification. Flash column chromatography was accomplished using high purity grade 60 Å silica gel (Fluka® Analytical). Qualitative TLC was performed on aluminum sheets (Merck, silica gel, F254) and observed via UV absorption (254 nm) and staining with anisaldehyde or $KMnO_4$. Deuterated solvents were acquired from Cambridge Isotope Labs. Tz^{o}Cl and CH_3NO_2 (reagent grade, 96%) were received from Sigma-Aldrich. Unless otherwise noted, all Tz^{o}-containing compounds were synthesized according to literature procedure.[1] All reactions were carried out under an atmosphere of dry nitrogen. Photocatalyzed remote hydroxylation reactions were conducted in round bottom flasks and irradiated with 4W blue LEDs (Creative Lighting Solutions, λ_{max}=455 nm) which were wrapped around a beaker or crystallizing dish as pictured in Figure 4.3.

4.6.2 Procedures and Characterization

Representative procedure for remote hydroxylation - synthesis of **4.5a**:

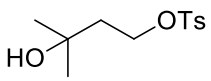

To a vigorously stirred 20^{o}C solution of 100.0 mg (0.2929 mmol) triazene **4.5** and 19.2 mg (0.0293 mmol) *fac*-Ir(ppy)$_3$ in 10 mL CH_3NO_2 and 2 mL deionized H_2O was added

77 μL (0.59 mmol) 48% HBF_4 via gas-tight syringe. After 4 minutes, irradiation of the solution with blue LEDs (λ_{max}=455 nm) commenced and the reaction mixture was stirred

Figure 4.3 Experimental Setup

vigorously for 18.5 h. 10 mL of 5% $NaHCO_3$(aq.) was then added at once followed by 10 mL CH_2Cl_2 and the resulting layers were separated. The aqueous layer was extracted with an additional 2 x 10 mL CH_2Cl_2. The combined organic layers were dried over Na_2SO_4, filtered and concentrated to yield 117.3 mg of a brown residue. Silica gel chromatography (gradient run from 20% EtOAc in hexanes to 30% EtOAc in hexanes) of the residue afforded 43.4 mg (57%) of a yellow oil. ^{1}H NMR (400 MHz, $CDCl_3$) δ 7.79 (d, *J* = 8.2

Hz, 2H), 7.34 (d, *J* = 8.0 Hz, 2H), 4.20 (t, *J* = 6.8 Hz, 2H), 2.44 (s, 3H), 1.85 (t, *J* = 6.8 Hz, 2H), 1.67 (br s, 1H), 1.21 (s, 6H); ^{13}C NMR (101 MHz, $CDCl_3$) δ 145.0, 133.1, 130.1, 128.0, 69.8, 67.8, 41.8, 29.8, 21.8; HRMS (m/z) calcd for $C_{12}H_{18}NaO_4S$ $[M+Na]^+$ 281.0818, found 281.0805.

Representative procedure for NMR studies:

To a vigorously stirred 20°C solution of 22.0 mg (0.0644 mmol) triazene **4.5** and 4.2 mg (0.0064 mmol) *fac*-Ir(ppy)$_3$ in 2.2 mL CD_3NO_2 and 0.44 mL D_2O was added 17 μL (0.13 mmol) 48% HBF_4 via gas-tight syringe. After 4 minutes, irradiation of the solution with blue LEDs (λ_{max}=455 nm) commenced and the reaction mixture was stirred vigorously for 18.5 h. The aqueous and organic layers were then separated and placed directly into NMR tubes for analysis.

Unless specifically noted, all Tz^o-containing compounds were synthesized according to literature procedure.[11] Synthesis and spectral data of known compounds **4.6** and **4.7** can also be found in reference 11.

Synthesis of **4.5**:

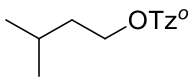

Started with 2000.0 mg (6.902 mmol) Tz^{o}Cl, 486.7 mg (5.521 mmol) isoamyl alcohol, 1349.0 mg (11.04 mmol) DMAP and 11.1 mL CH_2Cl_2. Silica gel chromatography (gradient run from 10% EtOAc in hexanes to 20% EtOAc in hexanes) afforded 1724.3 mg (91%) of a yellow oil. ^{1}H NMR (500 MHz, $CDCl_3$): δ 7.81 (d, *J* = 8.1 Hz, 1H), 7.34 (s, 1H), 6.96 (d, *J* = 8.1 Hz, 1H), 4.02 (t, *J* = 6.6 Hz, 2H), 3.80 (q, *J* = 7.2 Hz, 4H), 2.36 (s, 3H), 1.66 (m, 1H), 1.48 (q, *J* = 6.7 Hz, 2H), 1.32 (t, *J* = 7.3 Hz, 3H), 1.24 (t, *J* = 7.3 Hz, 3H), 0.80 (d, *J* = 7.0 Hz, 6H); ^{13}C NMR (126 MHz, $CDCl_3$): δ 149.3, 145.1, 130.5, 126.0,

125.0, 118.4, 68.7, 49.3, 42.2, 37.6, 24.4, 22.1, 21.7, 14.5, 11.3; HRMS (m/z) calcd for $C_{16}H_{27}N_3NaO_3S$ $[M+Na]^+$ 364.1665, found 364.1658.

Synthesis of **4.10**:

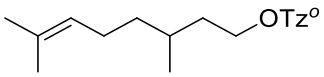

Started with 500.0 mg (1.725 mmol) Tz^{o}Cl, 0.25 mL (1.4 mmol) citronellol, 337.0 mg (2.758 mmol) DMAP and 2.8 mL CH_2Cl_2. Silica gel chromatography (20% CH_2Cl_2 and 5% Et_2O in hexanes) afforded 521.0 mg (91%) of a red oil. ^{1}H NMR (400 MHz, $CDCl_3$) δ 7.85 (d, *J* = 8.1 Hz, 1H), 7.37 (s, 1H), 7.00 (d, *J* = 8 Hz 1H), 5.02 (t, *J* = 7.2Hz, 1H), 4.13 – 3.99 (m, 2H), 3.83 (q, *J* = 7.2 Hz, 4H), 2.39 (s, 3H), 1.98-1.79 (m, 2H), 1.78-1.46 (m, 2H), 1.66 (s, 3H), 1.56 (s, 3H), 1.45-1.19 (m, 2H), 1.36 (t, 3H), 1.27 (t, 3H), 1.16 – 1.02 (m, 1H), 0.80 (d, *J* = 6.6 Hz, 3H); ^{13}C NMR (101 MHz, $CDCl_3$) δ 149.4, 145.2, 131.5, 130.7, 126.3, 125.3, 124.6, 118.5, 68.8, 49.5, 42.5, 37.0, 36.0, 29.1, 25.9, 25.5, 21.9, 19.2, 17.8, 14.7, 11.5; HRMS (m/z) calcd for $C_{21}H_{36}N_3O_3S$ $[M+H]^+$ 410.2472, found 410.2475.

Synthesis of **4.11**:

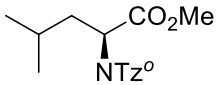

To a round bottom flask containing 804.2 mg (4.427 mmol) L-leucine methyl ester HCl salt (prepared according to reference 2), 11.8 mL sat. $NaHCO_3$ and 9.8 mL CH_2Cl_2 was added a solution of 944.8 mg (3.162 mmol) Tz^{o}Cl in 2 mL CH_2Cl_2 dropwise. The resulting mixture was allowed to stir under N_2 at room temperature for 15 h until complete consumption of starting material was observed via TLC. The aqueous layer was then separated from the organic layer and extracted with 3x10 mL CH_2Cl_2. The combined organic layers were dried over Na_2SO_4, filtered and concentrated *in vacuo*. Silica gel chromatography (gradient run from 10% EtOAc in hexanes to 20% EtOAc in hexanes)

afforded 866.8 mg (49%) of the desired product. Spectral data matched that previously reported in literature.[11]

Synthesis of **4.12**:

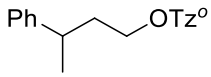

Started with 350.0 mg (1.208 mmol) Tz^{o}Cl, 0.15 mL (0.97 mmol) 3-phenyl-1-butanol, 294.9 mg (2.414 mmol) DMAP and 1.9 mL of CH_2Cl_2. Silica gel chromatography (gradient run from 8% EtOAc in hexanes to 10% EtOAc in hexanes) afforded 261.5 mg (67%) of a red oil. ^{1}H NMR (400 MHz, $CDCl_3$) δ 7.79 (d, *J* = 8.0 Hz, 1H), 7.39 (s, 1H), 7.20 (t, *J* = 7.4 Hz, 2H), 7.14 (d, *J* = 6.9 Hz, 1H), 7.04 (d, *J* = 8 Hz, 2H), 6.95 (d, *J* = 8 Hz, 1H), 3.99 (dt, *J* = 9.7, 6.0 Hz, 1H), 3.92 – 3.85 (m, 1H), 3.81 (q, *J* = 7.2 Hz, 4H), 2.81 (q, *J* = 7.2 Hz, 1H), 2.38 (s, 3H), 1.92 – 1.81 (m, 2H), 1.33 (t, *J* = 7.3 Hz, 3H), 1.26 (t, *J* = 7.2 Hz, 3H), 1.17 (d, *J* = 6.9 Hz, 3H); ^{13}C NMR (101 MHz, $CDCl_3$) δ 149.3, 145.8, 145.2, 130.6, 128.5, 126.9, 126.3, 126.0, 125.1, 118.4, 68.6, 49.4, 42.4, 37.3, 35.8, 21.9, 21.8, 14.6, 11.4; HRMS (m/z) calcd for $C_{21}H_{30}N_3O_3S$ $[M+H]^+$ 404.2002, found 404.2000.

Synthesis of **4.13**:

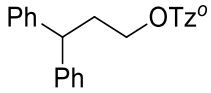

Started with 350.0 mg (1.208 mmol) Tz^{o}Cl, 0.19 mL (0.97 mmol) 3,3-diphenyl-1-propanol, 294.9 mg (2.414 mmol) DMAP and 1.9 mL of CH_2Cl_2. Silica gel chromatography (20% DCM and 5% Et_2O in hexanes) afforded 307.9 mg (68%) of a red oil. ^{1}H NMR (500 MHz, $CDCl_3$) δ 7.76 (d, *J* = 8.1 Hz, 1H), 7.38 (s, 1H), 7.20 (dd, *J* = 8.3, 6.7 Hz, 4H), 7.17 – 7.11 (m, 2H), 7.08 (d, *J* = 7.5 Hz, 4H), 6.95 (d, *J* = 7.8 Hz, 1H), 4.05 – 3.96 (m, 3H), 3.80 (dq, *J* = 13.9, 7.3 Hz, 4H), 2.40 (s, 3H), 2.34 (dt, *J* = 7.8, 6.2 Hz, 2H), 1.33 (t, *J* = 7.3 Hz, 3H), 1.24 (t, *J* = 7.2 Hz, 3H); ^{13}C NMR (126 MHz, $CDCl_3$) δ 149.4,

145.3, 143.7, 130.8, 128.7, 128.0, 126.6, 126.3, 125.3, 118.6, 68.6, 49.5, 46.9, 42.6, 35.0, 21.9, 14.7, 11.6; HRMS (m/z) calcd for $C_{26}H_{32}N_3O_3S$ $[M+H]^+$ 466.2159, found 466.2156.

Synthesis of **des-methyl-4.14**:

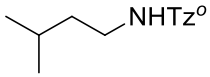

Started with 155.0 mg (0.5349 mmol) Tz^{o}Cl, 90 µL (0.75 mmol) isoamyl amine, 2 ml sat. $NaHCO_3$ and 2 mL CH_2Cl_2. Silica gel chromatography (20% EtOAc in hexanes) afforded 169.4 mg (93%) of a yellow oil. ^{1}H NMR (400 MHz, $CDCl_3$) δ 7.81 (d, *J* = 8.0 Hz, 1H), 7.40 (s, 1H), 7.01 (d, *J* = 8.0 Hz, 1H), 5.52 (t, *J* = 6.4 Hz, 1H), 3.85 (q, *J* = 7.0 Hz, 2H), 3.76 (q, *J* = 7.2 Hz, 2H), 2.88 (q, *J* = 7.0 Hz, 2H), 2.38 (s, 3H), 1.68-1.50 (m, 1H), 1.43-1.17 (m, 8H), 0.82 (d, *J* = 6.7 Hz, 6H); ^{13}C NMR (101 MHz, $CDCl_3$) δ 147.3, 143.7, 128.8, 128.8, 125.3, 118.0, 49.8, 42.1, 41.8, 38.3, 25.4, 22.2, 21.5, 14.3, 11.0; HRMS m/z calcd for $C_{16}H_{29}N_4O_2S$ $[M+H]^+$ 341.2012, found 341.2003.

Synthesis of **4.14**:

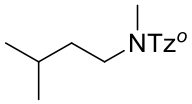

To a stirred 0°C solution of 222.6 mg (0.6537 mmol) **des-methyl-4.14** in 10 mL dry THF was added 17.4 mg (0.727 mmol) 95% sodium hydride. After 1 hour the reaction mixture was removed from the ice bath and placed in an 80°C oil bath. 90 µL (1.5 mmol) iodomethane was then added. After 2 hours the reaction mixture was removed from the oil bath and allowed to cool. 15 mL H_2O was then added at once followed by 15mL CH_2Cl_2 and the layers were separated. The aqueous layer was extracted with an additional 2 x 15 mL CH_2Cl_2. The combined organic layers were dried over Na_2SO_4, filtered and concentrated to yield 283.4 mg crude yellow oil. Silica gel chromatography (12 g silica gel, gradient run from 5% EtOAc in hexanes to 10% EtOAc in hexanes) of the residue

afforded 163.8 mg (76%) of a pale yellow oil. ^{1}H NMR (400 MHz, $CDCl_3$) δ 7.78 (d, *J* = 8.1 Hz, 1H), 7.27 (s, 1H), 6.98 (d, *J* = 8.0 Hz, 1H), 3.82 (q, *J* = 7.2 Hz, 4H), 3.17 (t, *J* = 8.0 Hz, 2H), 2.81 (s, 3H), 2.37 (s, 3H), 1.69 – 1.53 (m, 1H), 1.41 (q, *J* = 7.0 Hz, 2H), 1.32 – 1.23 (m, 6H), 0.88 (d, *J* = 6.7 Hz, 6H); ^{13}C NMR (101 MHz, $CDCl_3$) δ 149.3, 143.6, 130.7, 128.6, 125.2, 119.6, 49.0, 48.5, 41.7, 36.8, 34.5, 25.6, 22.5, 21.5, 14.6, 11.5; HRMS m/z calcd for $C_{17}H_{31}N_4O_2S$ $[M+H]^+$ 355.2162, found 355.2175.

Synthesis of **des-methyl-4.15**:

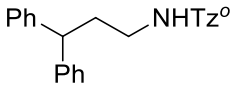

Started with 155.0 mg (0.5349 mmol) Tz^{o}Cl, 158.5 mg (0.7501 mmol) 3,3-diphenylpropylamine, 2 ml sat. $NaHCO_3$ and 2 mL CH_2Cl_2. Silica gel chromatography (15% EtOAc in hexanes) afforded 192.0 mg (77%) of an off-white residue. ^{1}H NMR (400 MHz, $CDCl_3$) δ 7.76 (d, *J* = 8.0 Hz, 1H), 7.39 (s, 1H), 7.26-7.00 (m, 10H), 6.93 (d, *J* = 8.0 Hz, 1H), 5.64 (t, *J* = 6.2 Hz, 1H), 3.97 (t, *J* = 7.8 Hz, 1H), 3.75 (q, *J* = 7.3 Hz, 2H), 3.64 (q, *J* = 7.3 Hz, 2H), 2.85 (q, *J* = 6.7 Hz, 2H), 2.31 (s, 3H), 2.20 (q, *J* = 7.2 Hz, 2H), 1.27 (t, *J* = 7.2 Hz, 3H), 1.20 (t, *J* = 7.3 Hz, 3H); ^{13}C NMR (101 MHz, $CDCl_3$) δ 147.2, 143.8, 129.1, 128.8, 128.4, 127.6, 126.2, 125.3, 118.0, 49.8, 47.9, 42.2, 41.9, 35.4, 21.5, 14.4, 11.0; HRMS m/z calcd for $C_{26}H_{32}N_4NaO_2S$ $[M+Na]^+$ 487.2144, found 487.2142.

Synthesis of **4.15**:

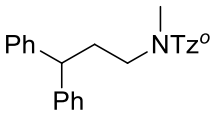

For procedure see synthesis of **4.14**. Started with 400.0 mg (0.8609 mmol) **des-methyl-4.15**, 24.8 mg (1.03 mmol) 95 % sodium hydride, 150 μL (2.07 mmol) iodomethane and 18 mL dry THF. Obtained 410.1 mg (quantitative yield) of a pale yellow oil. ^{1}H NMR (400 MHz, $CDCl_3$) δ 7.71 (d, *J* = 8.1 Hz, 1H), 7.28 – 7.18 (m, 9H), 7.18 –

7.10 (m, 2H), 6.93 (d, *J* = 8.2 Hz, 1H), 3.95 (t, *J* = 7.8 Hz, 1H), 3.74 (s, 2H), 3.61 (s, 2H), 3.15 (t, *J* = 7.5 Hz, 2H), 2.81 (s, 3H), 2.35 (s, 3H), 2.32 – 2.25 (m, 2H), 1.29 (s, 3H), 1.09 (s, 3H). ^{13}C NMR (126 MHz, $CDCl_3$) δ 149.1, 144.2, 143.6, 130.7, 128.4, 128.4, 127.7, 126.2, 125.1, 119.3, 48.9, 48.4, 41.5, 34.8, 34.0, 21.5, 14.4, 11.2; HRMS m/z calcd for $C_{27}H_{35}N_4O_2S$ $[M+H]^+$ 479.2475, found 479.2483.

Synthesis of **4.16**:

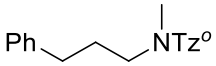

Started with 277.4 mg (0.9573 mmol) Tz^{o}Cl, 200.0 mg (1.340 mmol) *N*-methyl-3-phenylpropylamine, 4 ml sat. $NaHCO_3$ and 4 mL CH_2Cl_2. Silica gel chromatography (100% EtOAc) afforded 368.9 mg (96%) of an orange oil. ^{1}H NMR (500 MHz, $CDCl_3$) δ 7.79 (d, *J* = 8.1 Hz, 1H), 7.36 – 7.22 (m, 3H), 7.20 – 7.11 (m, 3H), 6.99 (d, *J* = 8.1 Hz, 1H), 3.80 (s, 4H), 3.24 (t, *J* = 7.2 Hz, 2H), 2.85 (s, 3H), 2.63 (t, *J* = 8.0 Hz, 2H), 2.38 (s, 3H), 1.86 (t, *J* = 7.7 Hz, 2H), 1.34 (s, 3H), 1.23 (s, 3H**)**; ^{13}C NMR (126 MHz, $CDCl_3$) δ 149.3, 143.8, 141.7, 130.8, 128.5, 128.4, 125.9, 125.3, 119.6, 49.8, 49.1, 41.8, 34.7, 32.9, 29.7, 21.6, 14.6, 11.5; HRMS (m/z) calcd for $C_{21}H_{31}N_4O_2S$ $[M+H]^+$ 403.2162, found 403.2162.

Synthesis of **4.17**:

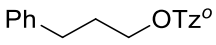

Started with 500.0 mg (1.725 mmol) Tz^{o}Cl, 187.9 mg (1.380 mmol) 3-phenyl-1-propanol, 337.3 mg (2.761 mmol) DMAP and 3.0 mL CH_2Cl_2. Silica gel chromatography (gradient run from 5% EtOAc in hexanes to 10% EtOAc in hexanes) afforded 375.5 (70%) of a yellow oil. ^{1}H NMR (400 MHz, $CDCl_3$) δ 7.85 (d, *J* = 8.1 Hz, 1H), 7.39 (s, 1H), 7.26 – 7.20 (m, 2H), 7.18 – 7.14 (m, 1H), 7.06 (d, *J* = 6.9 Hz, 2H), 7.00 (d, *J* = 8.0 Hz, 1H), 4.06 (t, *J* = 6.2 Hz, 2H), 3.83 (q, *J* = 7.6 Hz, 4H), 2.64 (t, *J* = 7.7 Hz, 2H), 2.41 (s, 3H),

2.12 – 1.74 (m, 2H), 1.35 (t, *J* = 6.9 Hz, 3H), 1.29 (t, *J* = 7.1 Hz, 3H); ^{13}C NMR (101 MHz, $CDCl_3$) δ 149.5, 145.3, 141.0, 130.8, 128.6, 126.2, 126.2, 125.3, 118.6, 69.6, 49.5, 42.5, 31.8, 30.9, 21.9, 14.7, 11.6; HRMS (m/z) calcd for $C_{20}H_{28}N_3O_3S$ $[M+H]^+$ 390.1846, found 390.1860.

Synthesis of **4.18**:

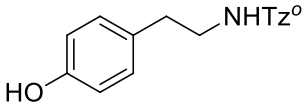

Started with 100.0 mg (0.3347 mmol) Tz^{o}Cl, 64.3 mg (0.469 mmol) tyramine, 3 ml sat. $NaHCO_3$ and 3 mL CH_2Cl_2. Silica gel chromatography (gradient run from 20% EtOAc in hexanes to 40% EtOAc in hexanes) afforded 109.3 mg (83%) of a yellow oil. ^{1}H NMR (400 MHz, $CDCl_3$) δ 7.81 (d, *J* = 8.0 Hz, 1H), 7.35 (s, 1H), 7.00 (d, *J* = 8.0 Hz, 1H), 6.90 (d, *J* = 7.9 Hz, 2H), 6.70 (d, *J* = 7.9 Hz, 2H), 5.83 (br s, 1H), 5.48 (t, *J* = 6.8 Hz, 1H), 3.75 (s, 2H), 3.20 (s, 2H), 3.11 (q, *J* = 6.7 Hz, 2H), 2.70 (t, *J* = 6.7 Hz, 2H), 2.38 (s, 3H), 1.30 (s, 3H), 1.06 (s, 3H); ^{13}C NMR (101 MHz, $CDCl_3$) δ 155.0, 147.6, 144.3, 130.0, 129.8, 129.1, 128.6, 125.5, 118.0, 115.6, 49.9, 44.8, 42.2, 34.9, 21.9, 14.6, 11.1; HRMS (m/z) calcd for $C_{19}H_{27}N_4O_3S$ $[M+H]^+$ 391.1798, found 391.1783.

Synthesis of **4.5c**:

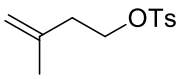

To a round bottom flask containing a previously degassed solution of 100.1 mg (0.2929 mmol) **4.5**, 45.8 mg (0.293 mmol) TEMPO, 2.3 mL deionized H_2O and 11.7 mL CH_3NO_2 was added 67 µL (0.88 mmol) TFA at once. The reaction was warmed to 60°C and allowed to stir for 1.5 h with monitoring by TLC. The reaction mixture was then concentrated *in vacuo* and 15 mL EtOAc and 15 mL 1 N HCl were added. The resulting layers were separated and the aqueous layer was washed with 3 x 15 mL EtOAc. The combined organic layers were dried over Na_2SO_4, filtered and concentrated. Silica gel

chromatography (gradient run from 20% CH_2Cl_2 in hexanes to 30% EtOAc in hexanes) afforded 20.9 mg (30%) **4.5c** as a colorless oil. ^{1}H NMR (400 MHz, $CDCl_3$): δ 7.79 (d, *J* = 8.0 Hz, 2H), 7.35 (d, *J* = 7.9 Hz, 2H), 4.79 (br s, 1H), 4.68 (br s, 1H), 4.13 (t, *J* = 6.8 Hz, 2H), 2.45 (s, 3H), 2.35 (t, *J* = 7.0 Hz, 2H), 1.66 (s, 3H); ^{13}C NMR (126 MHz, $CDCl_3$): δ 144.6, 140.0, 133.1, 129.7, 127.8, 113.0, 68.4, 36.7, 22.2, 21.5; HRMS m/z calcd for $C_{12}H_{17}O_3S$ $[M+H]^+$ 241.0893, found 241.0897, and 12.8 mg (18%) of **4.5a**.

Synthesis of **4.16a**:

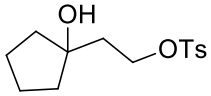

Started with 107.6 mg (0.2929 mmol) **4.16**, 19.2 mg (0.0293 mmol) *fac*-Ir(ppy)$_3$, 77 µL (0.59 mmol) 48% HBF_4, 2 mL deionized H_2O and 10 mL CH_3NO_2. Irradiated for 18 h. Silica gel chromatography (gradient run from 100% hexanes to 25% EtOAc in hexanes) afforded 34.2 mg (41%) **4.16a** as a pale yellow oil ^{1}H NMR (500 MHz, $CDCl_3$): δ 7.79 (d, *J* = 8.2 Hz, 2H), 7.35 (d, *J* = 8.1 Hz, 2H), 4.24 (t, *J* = 6.8 Hz, 2H), 2.45 (s, 3H), 1.97 (t, *J* = 7.3 Hz, 2H), 1.76 (m, 2H), 1.64 (m, 4H), 1.55 (m, 2H); ^{13}C NMR (126 MHz, $CDCl_3$): δ 144.7, 133.0, 129.8, 127.8, 80.5, 68.0, 40.0, 39.7, 23.4, 21.6; HRMS m/z calcd for $C_{14}H_{20}NaO_4S$ $[M+Na]^+$ 307.0975, found 307.0974, and 14.6 mg (19%) of an inseparable mixture of desaturation and reduced products (**4.16c**:**4.16b** = 3.5:1). Spectral data matched that previously reported in literature.[11]

Synthesis of **4.17a**:

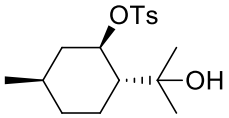

Started with 120.0 mg (0.2929 mmol) **4.17**, 19.2 mg (0.0293 mmol) *fac*-Ir(ppy)$_3$, 77 µL (0.59 mmol) 48% HBF_4, 2 mL deionized H_2O and 10 mL CH_3NO_2. Irradiated for 18 h. Silica gel chromatography (20% EtOAc in hexanes) afforded 30.0 mg (31%) **4.17a**

as a yellow oil $[\propto]_D^{25}$ = -20.8°, *c* 1.14 (CH_2Cl_2); ^{1}H NMR (500 MHz, $CDCl_3$) δ 7.80 (d, *J* = 8.0 Hz, 2H), 7.33 (d, *J* = 8.0 Hz, 2H), 4.83 (td, *J* = 10.8, 4.3 Hz, 1H), 2.56 (s, 1H), 2.43 (s, 3H), 2.20 (d, *J* = 11.8 Hz, 1H), 1.92 (m, 1H), 1.67 (m, 2H), 1.48 (m, 1H), 1.25 (s, 2H) 1.20 (s, 3H), 1.16 (s, 3H), 1.05 (qd, *J* = 13.1, 3.5 Hz, 1H), 0.88 (d, *J* = 6.5 Hz, 3H); ^{13}C NMR (126 MHz, $CDCl_3$) δ 145.0, 134.9, 130.0, 127.6, 84.7, 72.7, 52.3, 42.3, 34.0, 31.7, 28.9, 27.3, 25.9, 21.8, 21.8; HRMS m/z calcd for $C_{17}H_{26}NaO_4S$ $[M+Na]^+$ 349.1444, found 349.1446, and 19.9 mg (22%) desaturation product **4.17c** as a white solid. Spectral data matched that previously reported in literature.[11]

Synthesis of **4.10a**:

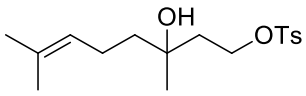

Started with 112.0 mg (0.2929 mmol) **4.10**, 19.2 mg (0.0293 mmol) of *fac*-Ir(ppy)$_3$, 77 µL (0.59 mmol) 48% HBF_4, 2 mL deionized H_2O and 10 mL CH_3NO_2. Irradiated for 18 h. Silica gel chromatography (gradient run from 10% EtOAc in hexanes to 30% EtOAc in hexanes) afforded 19.3 mg (22%) **4.10a** as a colorless oil. ^{1}H NMR (500 MHz, $CDCl_3$) δ 7.79 (d, *J* = 8.5 Hz, 2H), 7.35 (d, *J* = 8.0 Hz, 2H), 5.07 (t, *J* = 7 Hz, 1H), 4.20 (tq, *J* = 5.5, 3.0 Hz, 2H), 2.45 (s, 3H), 2.00 (q, *J* = 7.7 Hz, 2H), 1.85 (q, *J* = 6.9 Hz, 2H), 1.68 (s, 3H), 1.59 (s, 3H), 1.48 – 1.42 (m, 3H), 1.16 (s, 3H); ^{13}C NMR (126 MHz, $CDCl_3$) δ 145.0, 133.2, 132.5, 130.1, 128.1, 124.0, 71.9, 67.6, 42.4, 40.2, 27.1, 25.9, 22.8, 21.9, 17.9; HRMS (m/z) calcd for $C_{17}H_{26}NaO_4S$ $[M+Na]^+$ 349.1444, found 349.1443, and 5 mg (6%) of the trivial reduction product **15b**, a colorless oil. Spectral data matched that previously reported in literature.[20]

Synthesis of **4.11a**:

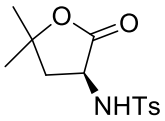

Started with 116.7 mg (0.2929 mmol) **4.11**, 19.2 mg (0.0293 mmol) *fac*-Ir(ppy)$_3$, 77 µL (0.59 mmol) 48% HBF_4, 2 mL deionized H_2O and 10 mL CH_3NO_2. Irradiated for 18 h. Silica gel chromatography (gradient run from 100% hexanes to 30% EtOAc in hexanes) afforded 39.0 mg (47%) of a pale yellow oil. $[\propto]_D^{25}$ = 59.1°, *c* 0.915; ^{1}H NMR (500 MHz, $CDCl_3$): δ 7.79 (d, *J* = 8.0 Hz, 2H), 7.34 (d, *J* = 8.0 Hz, 2H), 5.32 (br s, 1H), 4.10 (m, 1H), 2.57 (dd, *J* = 12.8, 8.7 Hz, 1H), 2.44 (s, 3H), 2.05 (t, *J* = 12.1 Hz, 1H), 1.47 (s, 3H), 1.37 (s, 3H); ^{13}C NMR (126 MHz, $CDCl_3$): δ 173.3, 144.1, 136.0, 129.9, 127.2, 83.4, 52.9, 43.2, 28.8, 26.9, 21.6; HRMS m/z calcd for $C_{13}H_{18}NO_4S$ $[M+H]^+$ 284.0951, found 284.0951.

Synthesis of **4.12a**:

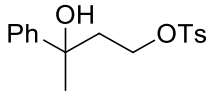

Started with 118.0 mg (0.2929 mmol) **4.12**, 19.2 mg (0.0293 mmol) of *fac*-Ir(ppy)$_3$, 77 µL (0.59 mmol) 48% HBF_4, 2 mL deionized H_2O and 10 mL of CH_3NO_2. Irradiated for 18 h. Silica gel chromatography (gradient run from 15% EtOAc in hexanes to 30% EtOAc in hexanes) afforded 59.1 mg (63%) of a white solid. ^{1}H NMR (400 MHz, $CDCl_3$) δ 7.68 (d, *J* = 8.4 Hz, 2H), 7.35 – 7.18 (m, 7H), 4.10 (dt, *J* = 10.1, 7.1 Hz, 1H), 3.95 (dt, *J* = 10.0, 6.6 Hz, 1H), 2.43 (s, 3H), 2.19 (td, *J* = 6.9, 1.9 Hz, 2H), 2.06 (s, 1H), 1.53 (s, 3H); ^{13}C NMR (101 MHz, $CDCl_3$) δ 146.5, 144.9, 133.0, 130.0, 128.5, 128.0, 127.1, 124.6, 73.6, 67.7, 42.5, 31.0, 21.8; HRMS (m/z) calcd for $C_{17}H_{21}O_4S$ $[M+H]^+$ 321.1155, found 321.1154.

Synthesis of **4.13a**:

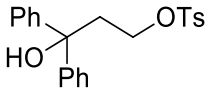

Started with 136.4 mg (0.2929 mmol) **4.13**, 19.2 mg (0.0293 mmol) of *fac*-Ir(ppy)$_3$, 77 µL (0.59 mmol) 48% HBF_4, 2 mL deionized H_2O and 10 mL CH_3NO_2. Irradiated for 18 h. Silica gel chromatography (gradient run from 10% EtOAc in hexanes to 20% EtOAc in hexanes) afforded 63.2 mg (56%) of a colorless oil. ^{1}H NMR (400 MHz, $CDCl_3$) δ 7.66 (d, *J* = 7.9 Hz, 2H), 7.34 – 7.16 (m, 12H), 4.08 (t, *J* = 7.3 Hz, 2H), 2.69 (t, *J* = 7.4 Hz, 2H), 2.42 (s, 3H), 2.39 (s, 1H); ^{13}C NMR (101 MHz, $CDCl_3$) δ 145.9, 144.9, 133.0, 130.0, 128.5, 128.0, 127.4, 125.8, 77.0, 67.9, 40.7, 21.8; HRMS (m/z) calcd for $C_{22}H_{22}NaO_4S$ $[M+Na]^+$ 405.1131, found 405.1125.

Synthesis of **4.14a**:

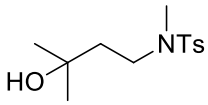

Started with 102.6 mg (0.2894 mmol) **4.14**, 19.2 mg (0.0293 mmol) *fac*-Ir(ppy)$_3$, 77 µL (0.59 mmol) 48% HBF_4, 2 mL deionized H_2O and 10 mL CH_3NO_2. Irradiated for 18 h. Silica gel chromatography (gradient run from 30% EtOAc in hexanes to 40% EtOAc in hexanes) afforded 26.4 mg (34%) of a yellow oil. ^{1}H NMR (400 MHz, $CDCl_3$) δ 7.67 (d, *J* = 7.9 Hz, 2H), 7.31 (d, *J* = 8.0 Hz, 2H), 3.14 (t, *J* = 7.5 Hz, 2H), 2.72 (s, 3H), 2.42 (s, 3H), 1.81 (br s, 1H), 1.72 (t, *J* = 7.5 Hz, 2H), 1.25 (s, 6H); ^{13}C NMR (126 MHz, $CDCl_3$) δ 143.4, 134.0, 129.7, 127.5, 70.1, 46.5, 40.2, 34.8, 29.5, 21.5; HRMS m/z calcd for $C_{13}H_{22}NNaO_3S$ $[M+H]^+$ 272.1315, found 272.1322.

Synthesis of **4.15a**:

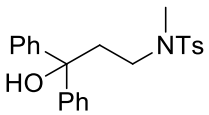

Started with 140.2 mg (0.2929 mmol) **4.15**, 19.2 mg (0.0293 mmol) *fac*-Ir(ppy)$_3$, 77 µL (0.59 mmol) 48% HBF_4, 2 mL deionized H_2O and 10 mL CH_3NO_2. Irradiated for 18 h. Silica gel chromatography (gradient run from 10% EtOAc in hexanes to 30% EtOAc in hexanes) afforded 47.9 mg (41%) of a pale yellow solid. ^{1}H NMR (500 MHz, $CDCl_3$) δ 7.58 (d, *J* = 8.3 Hz, 2H), 7.42 (d, *J* = 6.9 Hz, 2H), 7.34 (t, *J* = 7.8 Hz, 4H), 7.30 – 7.21 (m, 4H), 3.08 – 3.02 (m, 2H), 2.72 (s, 3H), 2.66 – 2.60 (m, 2H), 2.55 (s, 1H), 2.43 (s, 3H); ^{13}C NMR (126 MHz, $CDCl_3$) δ 146.2, 143.3, 134.4, 129.6, 128.3, 127.4, 127.1, 125.7, 64.0, 46.7, 39.9, 35.6, 21.5; HRMS m/z calcd for $C_{23}H_{25}NNaO_3S$ $[M+Na]^+$ 418.1447, found 418.1439.

Synthesis of **4.16a**:

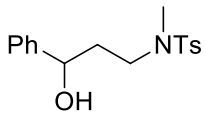

Started with 120.8 mg (0.3000 mmol) **4.16**, 19.6 mg (0.030 mmol) *fac*-Ir(ppy)$_3$, 79 µL (0.60 mmol) 48% HBF_4, 2 mL deionized H_2O and 10 mL CH_3NO_2. Irradiated for 18 h. Silica gel chromatography (20% EtOAc in hexanes) afforded 53.7 mg (56%) of a yellow oil. ^{1}H NMR (500 MHz, $CDCl_3$) δ 7.67 (d, *J* = 8.1 Hz, 2H), 7.40 – 7.30 (m, 6H), 7.29 – 7.23 (m, 1H), 4.88 (dd, *J* = 9.3, 3.9 Hz, 1H), 3.53 – 3.35 (m, 1H), 2.93 – 2.86 (m, 1H), 2.84 (br s, 1H), 2.76 (s, 3H), 2.43 (s, 3H), 1.95 – 1.83 (m, 2H); ^{13}C NMR (126 MHz, $CDCl_3$) δ 144.1, 143.6, 134.2, 129.8, 128.6, 127.6, 127.5, 125.8, 70.8, 47.3, 37.0, 35.2, 21.6; HRMS m/z calcd for $C_{17}H_{21}NNaO_3S$ $[M+Na]^+$ 342.1134, found 342.1132.

Synthesis of **4.17a**:

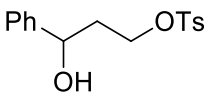

Started with 114.1 mg (0.2929 mmol) **22**, 19.2 mg (0.0293 mmol) of *fac*-Ir(ppy)$_3$, 77 µL (0.59 mmol) 48% HBF_4, 2 mL deionized H_2O and 10 mL of CH_3NO_2. Irradiated

for 18 h. Silica gel chromatography (gradient run from 10% EtOAc in hexanes to 30% EtOAc in hexanes) afforded 46.7 mg (52%) of a yellow oil. Spectral data (^{1}H and ^{13}C NMR) matched that previously reported in the literature.[21]

Synthesis of **4.18a**:

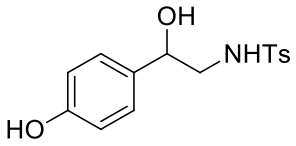

Started with 114.4 mg (0.2929 mmol) **4.18**, 19.2 mg (0.0293 mmol) *fac*-Ir(ppy)$_3$, 77 µL (0.59 mmol) 48% HBF_4, 2 mL deionized H_2O and 10 mL CH_3NO_2. Irradiated for 18 h. Silica gel chromatography afforded 50.2 mg (56%) of a yellow oil. ^{1}H NMR (500 MHz, MeOD) δ 7.68 (d, *J* = 8.3 Hz, 2H), 7.34 (d, *J* = 8.0 Hz, 2H), 7.07 (d, *J* = 8.5 Hz, 2H), 6.70 (d, *J* = 8.5 Hz, 2H), 4.53 (t, *J* = 6.4 Hz, 1H), 2.98 (d, *J* = 6.3 Hz, 2H), 2.41 (s, 3H); ^{13}C NMR (126 MHz, MeOD) δ 158.3, 144.8, 139.1, 134.3, 130.8, 128.6, 128.2, 116.2, 73.7, 51.5, 21.6; HRMS m/z calcd for $C_{15}H_{16}NO_3S$ $[M+H]^+$ 290.0845, found 290.0845.

Synthesis of **4.5d**:

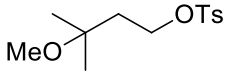

Started with 100.0 mg (0.2929 mmol) **4.5**, 19.2 mg (0.0293 mmol) *fac*-Ir(ppy)$_3$, 77 µL (0.59 mmol) 48% HBF_4, 2 mL MeOH and 10 mL CH_3NO_2. Irradiated for 18 h. Silica gel chromatography (gradient run from 5% EtOAc in hexanes to 10% EtOAc in hexanes) afforded 24.5 mg (31%) of a yellow oil. ^{1}H NMR (400 MHz, $CDCl_3$) δ 7.79 (d, *J* = 8.3 Hz, 2H), 7.34 (d, *J* = 8.1 Hz, 2H), 4.13 (t, *J* = 7.3 Hz, 2H), 3.10 (s, 3H), 2.45 (s, 3H), 1.87 (t, *J* = 7.3 Hz, 2H), 1.13 (s, 6H); ^{13}C NMR (101 MHz, $CDCl_3$) δ 144.9, 133.4, 130.0, 128.1, 73.4, 67.5, 49.4, 38.9, 25.3, 21.8; HRMS m/z calcd for $C_{13}H_{20}NaO_4S$ $[M+Na]^+$ 295.0975, found 295.0967.

Synthesis of **4.6d**:

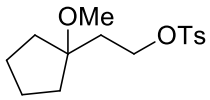

Started with 100.0 mg (0.2721 mmol) **4.6**, 17.8 mg (0.0272 mmol) *fac*-Ir(ppy)$_3$, 71 µL (0.54 mmol) 48% HBF_4, 2 mL MeOH and 10 mL CH_3NO_2. Irradiated for 18 h. Silica gel chromatography (gradient run from 5% EtOAc in hexanes to 10% EtOAc in hexanes) afforded 20.3 mg (25%) of a yellow oil. ^{1}H NMR (400 MHz, $CDCl_3$) δ 7.79 (d, *J* = 8.0 Hz, 2H), 7.34 (d, *J* = 8.0 Hz, 2H), 4.10 (t, *J* = 7.6 Hz, 2H), 3.04 (s, 3H), 2.44 (s, 3H), 1.98 (t, *J* = 7.6 Hz, 2H), 1.77 (m, 2H), 1.66 (m, 2H), 1.56 (m, 2H), 1.35 (p, *J* = 7.3 Hz, 2H); ^{13}C NMR (101 MHz, $CDCl_3$) δ 144.9, 133.4, 130.0, 128.1, 85.0, 67.9, 49.6, 36.0, 34.8, 23.6, 21.8.; HRMS m/z calcd for $C_{15}H_{22}NaO_4S$ $[M+Na]^+$ 321.1131 found 321.1135.

Synthesis of **4.19**:

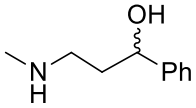

Procedure similar to that found in reference 17a. A solution of 82.1 mg (0.2680 mmol) **4.17a**, 6.5 mL 40% methylamine in H_2O, and 6.5 mL THF was sealed in a flask containing a stir bar. The mixture was lowered into a 65ºC oil bath and stirred for 3 h after which it was removed and allowed to cool. 25 mL Et_2O was then added followed by 10 mL sat. $NaHCO_3$ and the layers were separated. The organic layer was then washed with 15 mL sat. NaCl, dried over anhydrous K_2CO_3, filtered, and the solvent was removed *in vacuo* yielding 48.1 mg of a crude yellow oil. The oil was resuspended in 10 mL Et_2O and extracted with 3 x 10 mL portions of 1 M HCl. 20% NaOH was then added to the combined aqueous layers until the pH reached 13 and the basic solution was extracted with 3 x 10 mL portions of Et_2O. The combined organic layers were dried over anhydrous Na_2SO_4,

filtered, and the solvent was removed *in vacuo* to afford 40.8 mg (92%) of a pale yellow oil that required no further purification. Spectral data (^{1}H NMR) matched that previously reported in the literature.[18a]

Synthesis of (±)-fluoxetine:

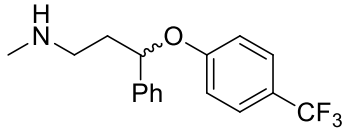

Procedure similar to that found in reference 17a. To a stirred 0°C solution of 30.8 mg (0.186 mmol) **4.19** in 2 mL *N*,*N*-dimethylacetamide was added 5.4 mg (0.22 mmol) 95% sodium hydride and the mixture was allowed to warm to room temperature over 45 min. The solution was then placed in a 95°C oil bath and stirred for an additional 30 min. 60 µL (0.45 mmol) 4-chlorobenzotrifluoride was then added at once and the reaction was heated to 105°C. After 2.5 h the reaction mixture was removed from the oil bath and allowed to cool. 10 mL toluene was then added followed by 10 mL H_2O and the layers were separated. The aqueous layer was extracted with an additional 2 x 10 mL toluene and the combined organic layers were then washed with 10 mL sat. $NaHCO_3$ followed by 10 mL sat. NaCl. The solution was then dried over anhydrous Na_2SO_4, filtered, and the solvent removed *in vacuo* to afford 50.8 mg of a crude orange oil. The oil was dissolved in MeCN (20 mg per 200 µL injection) and HPLC purification (Waters 1525 Binary HPLC Pump, 2489 UV/Vis Detector, XBridge Prep C18 5µm 10x100 mm Reverse Phase Column, 20 min gradient from 95% H_2O/MeCN to 5% H_2O/MeCN) yielded 37.8 mg (66%) fluoxetine as a colorless oil. The oil was suspended in Et_2O and 0.5 mL 2 M HCl in Et_2O was added after which the solvent was removed *in vacuo* to afford fluoxetine hydrochloride as a colorless oil. ^{1}H NMR (400 MHz, $CDCl_3$) δ 9.66 (br s, 2H), 7.41 (d, J = 8.3 Hz, 2H),

7.37 – 7.21 (m, 5H), 6.89 (d, J = 8.4 Hz, 2H), 5.52 – 5.41 (m, 1H), 3.12 (br s, 2H), 2.62 (s, 3H), 2.56 – 2.40 (m, 2H). ^{13}C NMR (126 MHz, $CDCl_3$) δ 159.8, 139.2, 129.2, 128.6, 127.00 (q, $J_{C\text{-}F}$ = 3.7 Hz), 125.9, 124.4 (q, $J_{C\text{-}F}$ = 271.2 Hz), 123.41 (q, $J_{C\text{-}F}$ = 32.8 Hz), 116.0, 77.1, 46.4, 34.8, 33.4. HRMS m/z calcd for $C_{17}H_{19}F_3NO$ $[M]^+$ 310.1413, found 310.1422.

4.6.3 Cyclic Voltammetry

Synthesis of **4.5e** *in situ***:**

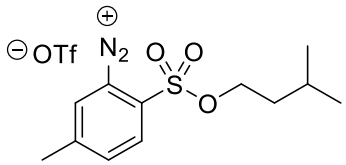

To a stirred 20°C solution of 50.0 mg (0.1464 mmol) triazene **4.5** in 5 mL CH_3CN (CD_3CN was used when obtaining NMR spectrum, page S78) was added 26 μL (0.29 mmol) triflic acid via gas-tight syringe. The light pink solution was allowed to stir for 20 hours in the absence of light. ^{1}H NMR (400 MHz, CD_3CN) δ 8.68 (s, 1H), 8.26 (s, 2H), 4.34 (t, J = 6.6 Hz, 2H), 2.61 (s, 3H), 1.62 (m, 3H), 0.85 (d, J = 6.6 Hz, 6H).

CV of 0.1 mM of **4.5e** in acetonitrile was performed on an AUTOLAB PGSTAT302 as a scan rate of 0.1 V/s with Ag/Ag^+ reference electrode, Pt counter electrode and glassy carbon working electrode. See Figure 4.4. Electrodes were mechanically polished then cleaned with acetone. The electrolyte used was tetrabutylammonium tetrafluoroborate at 0.1 M concentration. Observed E^o of **4.5e** vs Ag/Ag^+ was -0.42 V (-.035 V measurement – 0.07 V ferrocene calibration offset). Ag/Ag+ was converted to SCE by adding 0.30 V to the Ag/Ag+ potential.[22]

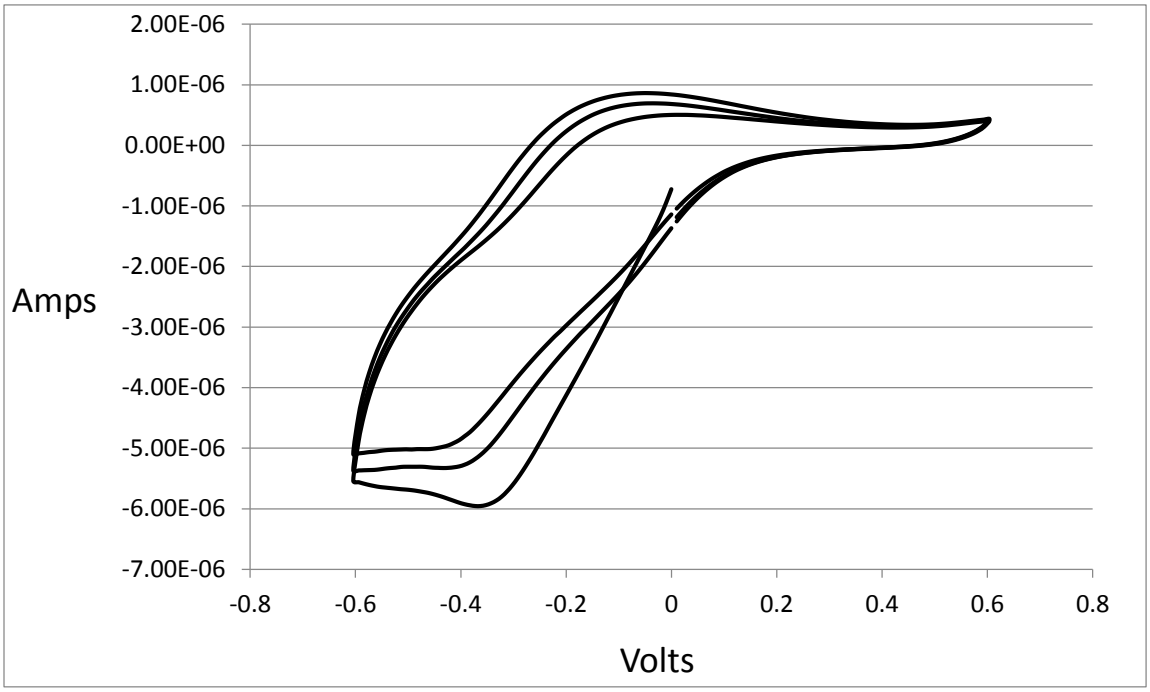

Figure 4.4 Cyclic Voltammetry of **4.5e**
E^o of **4.5e** was found to be -0.12 V vs. SCE.

4.6.4 ^{18}O Labeling Experiment

To determine the source of oxygen incorporation at the generated hydroxyl position, a labeling experiment using 97% ^{18}O water was performed. Standard reactions conditions were used with the replacement of HBF_4 by TFA and the replacement of H_2O by $H_2{}^{18}O$. ^{18}O incorporation of 90% was estimated based on the relative abundance of the peaks at 283.0866 and 281.0776 (Figure 4.5, Mass Spectrum-^{18}O Labeling Experiment). A correction was made to account for the peak at 283.0801 in the analysis of **4.5a** prepared under standard conditions (Mass Spectrum-Standard Conditions). This experiment confirmed our hypothesis that water purposely added to the system was the primary source of oxygen for hydroxylation. The 7% difference between the added ^{18}O labeled water and the determined incorporation is likely due to atmospheric water and/or water contained in the TFA used in the experiment.

HRMS (ESI+) for 6:

Ion	Formula	Ion Formula	Calc m/z	Score	Mass	Diff (ppm)	Abs Diff (ppm)	m/z
(M+Na)+	C12 H18 O4 S	C12 H18 Na O4 S	281.0818	97.85	258.0922	1.41	1.41	281.0814

Mass Spectrum – Standard Conditions:

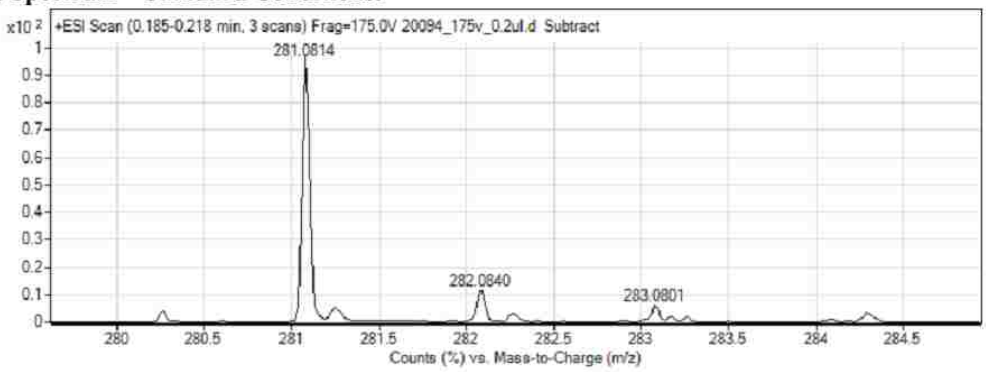

Mass Spectrum - ^{18}O Labeling Experiment:

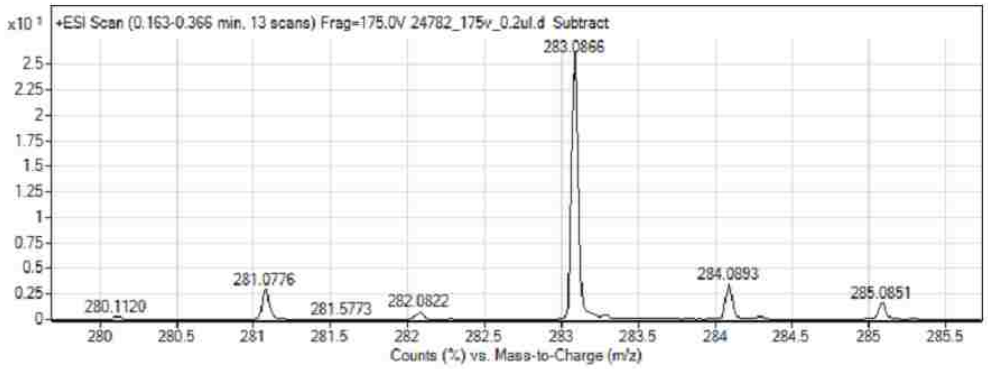

Peak list – Standard Conditions:

m/z	Abund
281.0814	11884
282.084	1424
283.0801	675

Peak list - ^{18}O Labeling Experiment:

m/z	Abund
281.0776	1970
282.0822	504
283.0866	17007

Figure 4.5 ^{18}O labeling data

4.7 References

1. Newhouse, T.; Baran, P. S., If C-H bonds could talk: selective C-H bond oxidation. *Angew. Chem. Int. Ed. Engl.* **2011,** *50* (15), 3362-74.

2. White, M. C., Adding Aliphatic C-H Bond Oxidations to Synthesis. *Science* **2012,** *335*, 807-809.

3. Breslow, R., Biomimetic Control of Chemical Selectivity. *Acc. Chem. Res.* **1979,** *13*, 170-177.

4. Gaich, T.; Baran, P. S., Aiming for the ideal synthesis. *J. Org. Chem.* **2010,** *75* (14), 4657-73.

5. Gutekunst, W. R.; P.S., B., C–H functionalization logic in total synthesis. *Chem. Soc. Rev.* **2011,** *40*, 1976-1991.

6. Fujiwara, Y.; Dixon, J. A.; O'Hara, F.; Funder, E. D.; Dixon, D. D.; Rodriguez, R. A.; Baxter, R. D.; Herle, B.; Sach, N.; Collins, M. R.; Ishihara, Y.; Baran, P. S., Practical and innate carbon-hydrogen functionalization of heterocycles. *Nature* **2012,** *492* (7427), 95-99.

7. (a) Ishii, Y.; Sakaguchi, S.; Iwahama, T., Innovation of Hydrocarbon Oxidation with Molecular Oxygen and Related Reactions. *Adv. Synth. Catal.* **2001,** *343*, 393-427; (b) Fokin, A. A.; Schreiner, P. R., Selective Alkane Transformations via Radicals and Radical Cations: Insights into the Activation Step from Experiment and Theory. *Chem. Rev.* **2002,** *102*, 1551-1593; (c) Crabtree, R. H., Alkane C–H activation and functionalization with homogeneous transition metal catalysts: a century of progress—a new millennium in prospect. *J. Chem. Soc., Dalton Trans.* **2001,** (17), 2437-2450; (d) Chen, X.; Engle, K. M.; Wang, D. H.; Yu, J. Q., Palladium(II)-catalyzed C-H activation/C-C cross-coupling reactions: versatility and practicality. *Angew. Chem. Int. Ed. Engl.* **2009,** *48* (28), 5094-115; (e) Jazzar, R.; Hitce, J.; Renaudat, A.; Sofack-Kreutzer, J.; Baudoin, O., Functionalization of Organic Molecules be Transition-Metal-Catalyzed C(sp^3)-H Activation. *Chem. Eur. J.* **2010,** *16*, 2654-2672.

8. Robertson, J.; Pillai, J.; Lush, R. K., Radical translocation reactions in synthesis. *Chem. Soc. Rev.* **2001,** *30*, 94-103.

9. (a) Wawzonek, S.; Thelen, P. J., Preparation of N-Methylgranatanine. *J. Am. Chem. Soc.* **1950,** *72*, 2118-2120; (b) Corey, E. J.; Hertler, W. R., A Study of the Formation of Haloamines and Cyclic Amines by the Free Radical Chain Decomposition of N-Haloammonium Ions (Hofmann-Loffler Reaction). *J. Am. Chem. Soc.* **1960,** *82*, 1657-1668.

10. Breslow, R.; Baldwin, S.; Rechtner, T.; P. Kalicky; Liu, S.; Washburnle, W., Remote Oxidation of Steroids by Photolysis of Attached Benzophenone Groups. *J. Am. Chem. Soc.* **1973,** *95*, 3251-3262.

11. Voica, A. F.; Mendoza, A.; Gutekunst, W. R.; Fraga, J. O.; Baran, P. S., Guided desaturation of unactivated aliphatics. *Nature chemistry* **2012,** *4* (8), 629.

12. Chen, K.; Richter, J. M.; Baran, P. S., 1,3-Diol Synthesis via Controlled, Radical-Mediated C-H Functionalization. *J. Am. Chem. Soc.* **2008,** *130*, 7247–7249.

13. Wayner, D. D. M.; McPhee, D. J.; Griller, D., Oxidation and Reduction Potentials of Transient Free Radicals. *J. Am. Chem. Soc.* **1988,** *110*, 132-137.

14. (a) Reckenthäler, M.; Griesbeck, A. G., Photoredox Catalysis for Organic Syntheses. *Adv. Synth. Catal.* **2013,** *355*, 2727 – 2744; (b) Yoon, T. P.; Ischay, M. A.; Du, J., Visible light photocatalysis as a greener approach to photochemical synthesis. *Nat. Chem.* **2010,** *2*, 527-532; (c) Hari, D. P.; Konig, B., The photocatalyzed Meerwein arylation: classic reaction of aryl diazonium salts in a new light. *Angew. Chem. Int. Ed. Engl.* **2013,** *52* (18), 4734-43; (d) Hu, J.; Wang, J.; Nguyen, T. H.; Zheng, N., The chemistry of amine radical cations produced by visible light photoredox catalysis. *Beilstein J. Org. Chem.* **2013,** *9*, 1977-2001; (e) Narayanam, J. M.; Stephenson, C. R., Visible light photoredox catalysis: applications in organic synthesis. *Chem. Soc. Rev.* **2011,** *40* (1), 102-13; (f) Prier, C. K.; Rankic, D. A.; MacMillan, D. W., Visible light photoredox catalysis with transition metal complexes: applications in organic synthesis. *Chem. Rev.* **2013,** *113* (7), 5322-63; (g) Teplý, F., Photoredox catalysis by [Ru(bpy)3]2+ to trigger transformations of organic molecules. Organic synthesis using visible-light photocatalysis and its 20th century roots. *Collect. Czech. Chem. Commun.* **2011,** *76* (7), 859-917; (h) Tucker, J. W.; Stephenson, C. R., Shining light on photoredox catalysis: theory and synthetic applications. *J. Org. Chem.* **2012,** *77* (4), 1617-22; (i) Xuan, J.; Xiao, W. J., Visible-light photoredox catalysis. *Angew. Chem. Int. Ed. Engl.* **2012,** *51* (28), 6828-38; (j) Zeitler, K., Photoredox catalysis with visible light. *Angew. Chem. Int. Ed. Engl.* **2009,** *48* (52), 9785-9.

15. Galli, C., Radical Reactions of Arenediazonium Ions: An Easy Entry into the Chemistry of the Aryl Radical. *Chem. Rev.* **1988,** *88*, 765-792.

16. Hollister, K. A.; Conner, E. S.; Spell, M. L.; Deveaux, K.; Maneval, L.; Beal, M. W.; Ragains, J. R., Remote Hydroxylation through Radical Translocation and Polar Crossover. *Angew. Chem. Int. Ed.* **2015,** *Early View*, DOI : 10.1002/anie.201500880.

17. (a) Sahoo, B.; Hopkinson, M. N.; Glorius, F., Combining gold and photoredox catalysis: visible light-mediated oxy- and aminoarylation of alkenes. *J. Am. Chem. Soc.* **2013,** *135* (15), 5505-8; (b) Verberne-Sutton, S. D.; Quarels, R. D.; Zhai, X.; Garno, J. C.; Ragains, J. R., Application of visible light photocatalysis with particle lithography to generate polynitrophenylene nanostructures. *J. Am. Chem. Soc.* **2014,** *136* (41), 14438-44.

18. (a) Gao, Y.; Sharpless, K. B., Asymmetric Synthesis of Both Enantiomers of Tomoxetine and Fluoxetine. Selective Reduction of 2,3-Epoxycinnamyl Alcohol with Red-A1. *J. Org. Chem.* **1988,** *53*, 4081-4084; (b) Benfield, P.; Heel, R. C.; Lewis, S. P., Fluoxetine. A review of its pharmacodynamic and pharmacokinetic properties, and therapeutic efficacy in depressive illness. *Drugs* **1986,** *32*, 481-508; (c) Wolen, R. L.; Farid, N. A.; Lemberger, L.; Bergstrom, R. F., Clinical pharmacology and pharmacokinetics of fluoxetine: a review. *Br. J. Psychiatry Suppl.* **1988,** *153*, 47-50.

19. Ates-Alagoz, Z.; Coleman, N.; Martin, M.; Wan, A.; Adejare, A., Syntheses and In Vitro Anticancer Properties of Novel Radiosensitizers. *Chem. Biol. Drug Des.* **2012,** *80*, 853-861.

20. Denmark, S. E.; Kobayashi, T.; Regens, C. S., Total Synthesis of (+)-Papulacandin D. *Tetrahedron* **2010,** *66* (26), 4745-4759.

21. Ali, I. S.; Sudalai, A., Pd-catalyzed kinetic resolution of benzylic alcohols: a practical synthesis of (R)-tomoxetine and (S)-fluoxetine hydrochlorides. *Tetrahedron Lett.* **2002,** *43*, 5435–5436.

22. Crabtree, R. H., *Energy Production and Storage: Inorganic Chemical Strategies for a Warming World*. Wiley: 2010.

APPENDIX A: COPYRIGHT RELEASES

ELSEVIER LICENSE
TERMS AND CONDITIONS

Jun 11, 2015

This is a License Agreement between Kyle A Hollister ("You") and Elsevier ("Elsevier") provided by Copyright Clearance Center ("CCC"). The license consists of your order details, the terms and conditions provided by Elsevier, and the payment terms and conditions.

All payments must be made in full to CCC. For payment instructions, please see information listed at the bottom of this form.

Supplier	Elsevier Limited The Boulevard,Langford Lane Kidlington,Oxford,OX5 1GB,UK
Registered Company Number	1982084
Customer name	Kyle A Hollister
Customer address	1388 Harwich Dr BATON ROUGE, LA 70820
License number	3646090152431
License date	Jun 11, 2015
Licensed content publisher	Elsevier
Licensed content publication	Bioorganic & Medicinal Chemistry
Licensed content title	Ascaroside activity in Caenorhabditis elegans is highly dependent on chemical structure
Licensed content author	Kyle A. Hollister,Elizabeth S. Conner,Xinxing Zhang,Mark Spell,Gary M. Bernard,Pratik Patel,Ana Carolina G.V. de Carvalho,Rebecca A. Butcher,Justin R. Ragains
Licensed content date	15 September 2013
Licensed content volume number	21
Licensed content issue number	18
Number of pages	16
Start Page	5754
End Page	5769
Type of Use	reuse in a thesis/dissertation
Portion	figures/tables/illustrations
Number of figures/tables/illustrations	2
Format	both print and electronic
Are you the author of this Elsevier article?	Yes

Will you be translating?	No
Order reference number	1
Original figure numbers	Figure 2, Figure 4
Title of your thesis/dissertation	I. Synthesis of Ascarosides for Chemical Genetics Studies in C. elegans and II. Photochemical Methodology and Synthesis
Expected completion date	Aug 2015
Estimated size (number of pages)	200
Elsevier VAT number	GB 494 6272 12
Permissions price	0.00 USD
VAT/Local Sales Tax	0.00 USD / 0.00 GBP
Total	0.00 USD
Terms and Conditions	

JOHN WILEY AND SONS LICENSE TERMS AND CONDITIONS

Jun 11, 2015

This Agreement between Kyle A Hollister ("You") and John Wiley and Sons ("John Wiley and Sons") consists of your license details and the terms and conditions provided by John Wiley and Sons and Copyright Clearance Center.

License Number	3646091284580
License date	Jun 11, 2015
Licensed Content Publisher	John Wiley and Sons
Licensed Content Publication	Angewandte Chemie International Edition
Licensed Content Title	Remote Hydroxylation through Radical Translocation and Polar Crossover
Licensed Content Author	Kyle A. Hollister,Elizabeth S. Conner,Mark L. Spell,Kristina Deveaux,Léa Maneval,Michael W. Beal,Justin R. Ragains
Licensed Content Date	May 26, 2015
Pages	1
Type of use	Dissertation/Thesis
Requestor type	Author of this Wiley article
Format	Print and electronic
Portion	Figure/table
Number of figures/tables	3
Original Wiley figure/table number(s)	Scheme 1, Table 1, Table 2
Will you be translating?	No
Order reference number	2

Title of your thesis / dissertation	I. Synthesis of Ascarosides for Chemical Genetics Studies in C. elegans and II. Photochemical Methodology and Synthesis
Expected completion date	Aug 2015
Expected size (number of pages)	200
Requestor Location	Kyle A Hollister 1388 Harwich Dr BATON ROUGE, LA 70820 United States Attn: Kyle A Hollister
Billing Type	Invoice
Billing Address	Kyle A Hollister 1388 Harwich Dr BATON ROUGE, LA 70820 United States Attn: Kyle A Hollister
Total	0.00 USD
Terms and Conditions	

APPENDIX B: NMR SPECTRA OF COMPOUNDS FOUND IN CHAPTER 1

Spectral data for compound **(*R*)-hept-6-en-2-ol**:

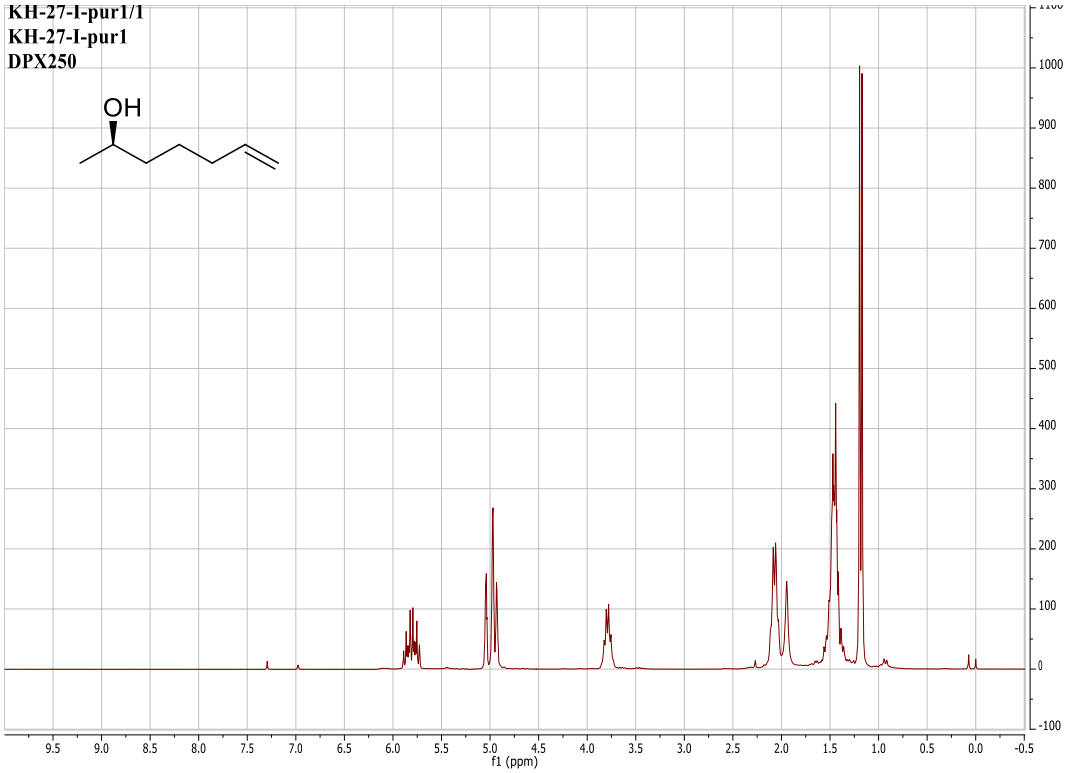

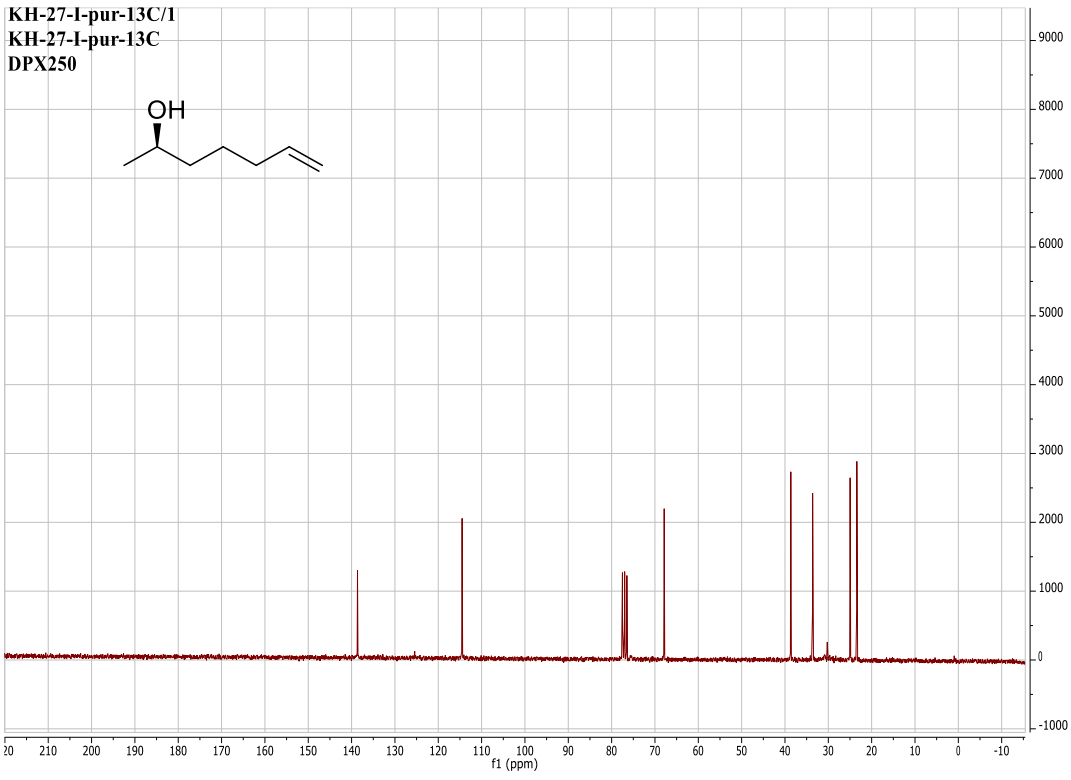

Spectral data for compound **(*R*)-oct-7-en-2-ol**:

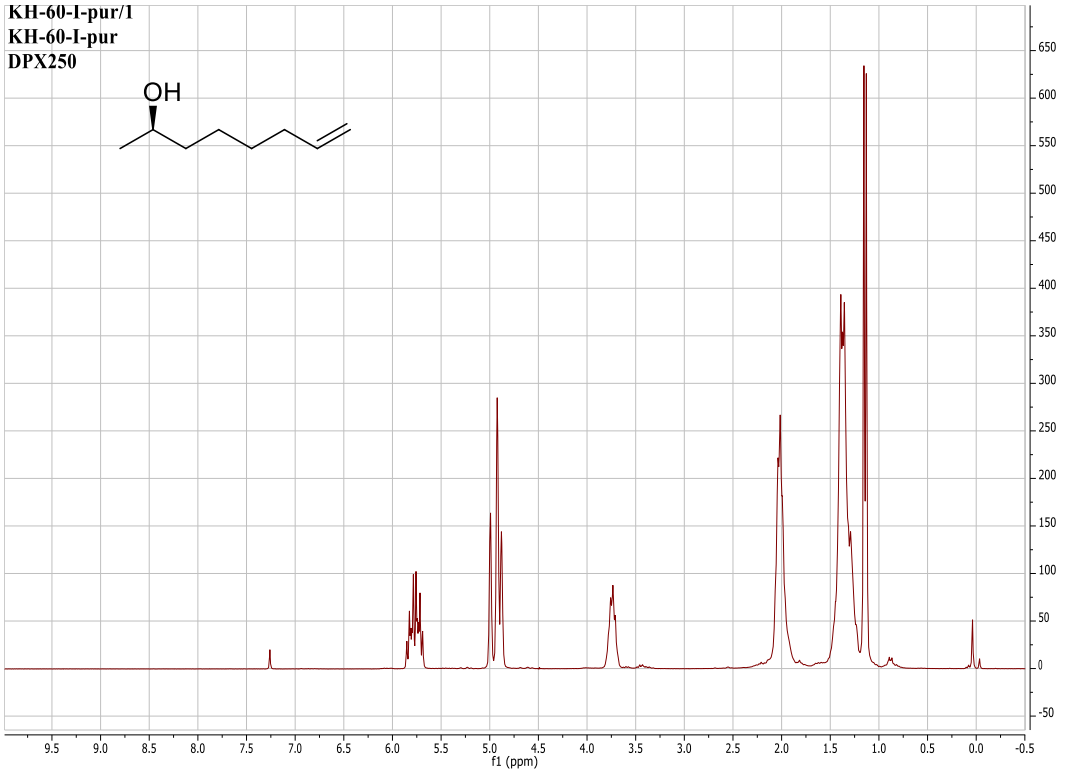

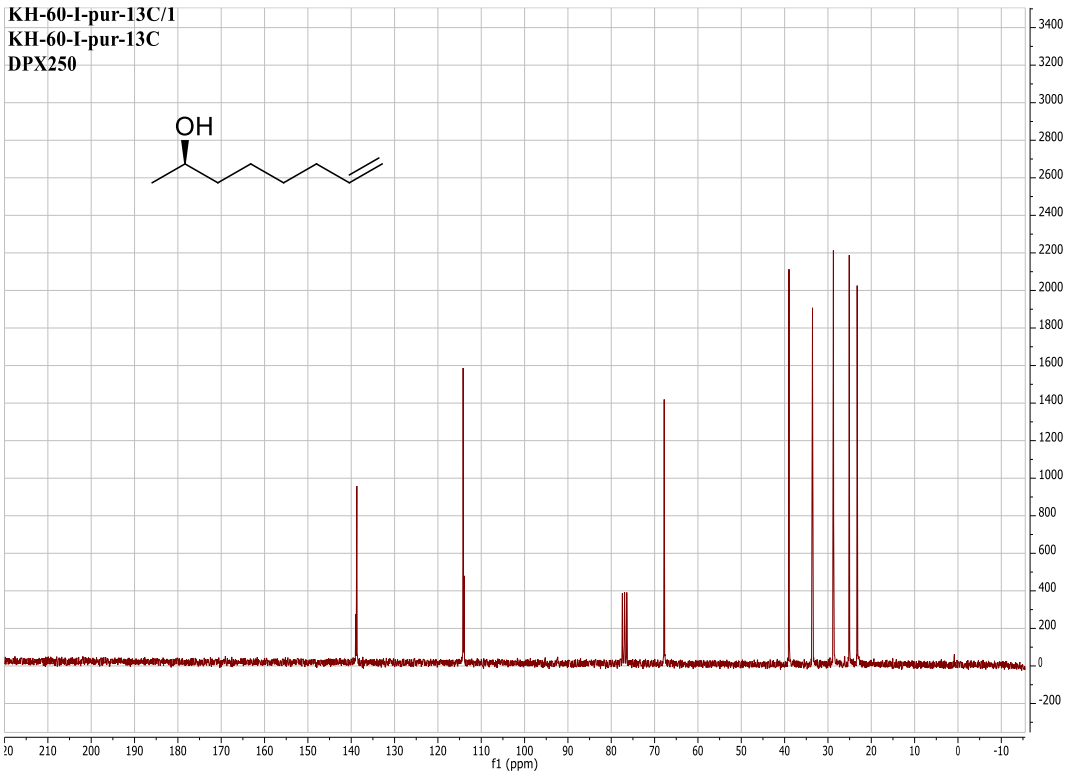

Spectral data for compound **1.1, n=1**:

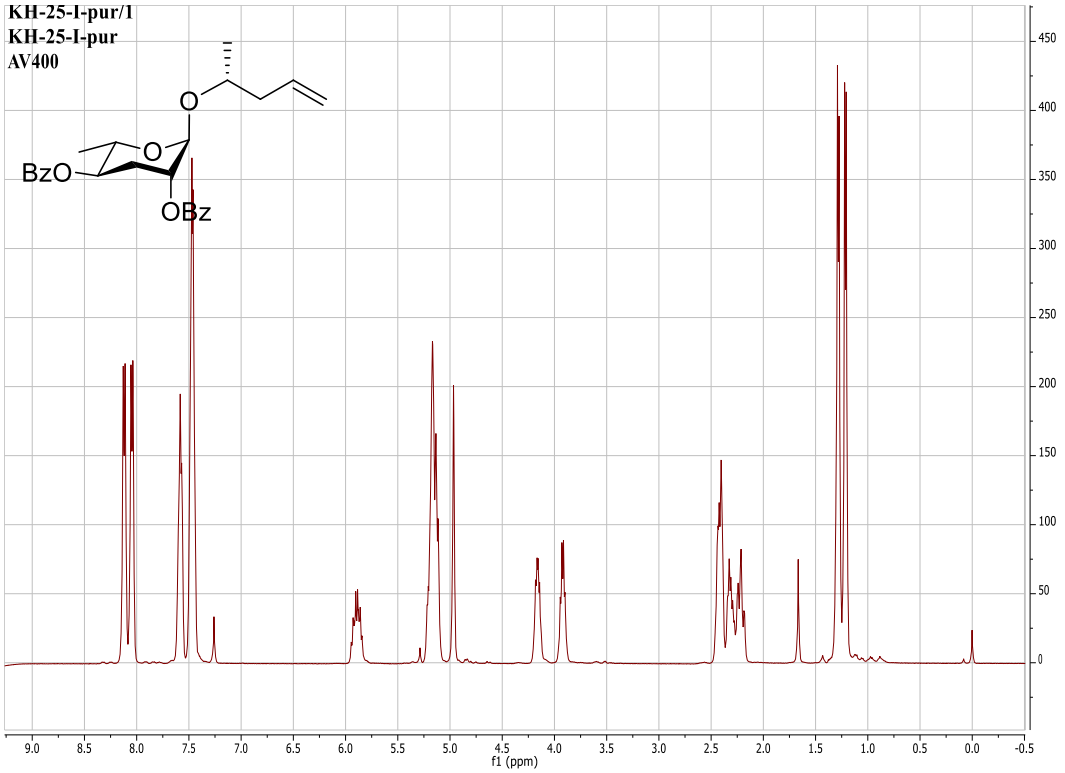

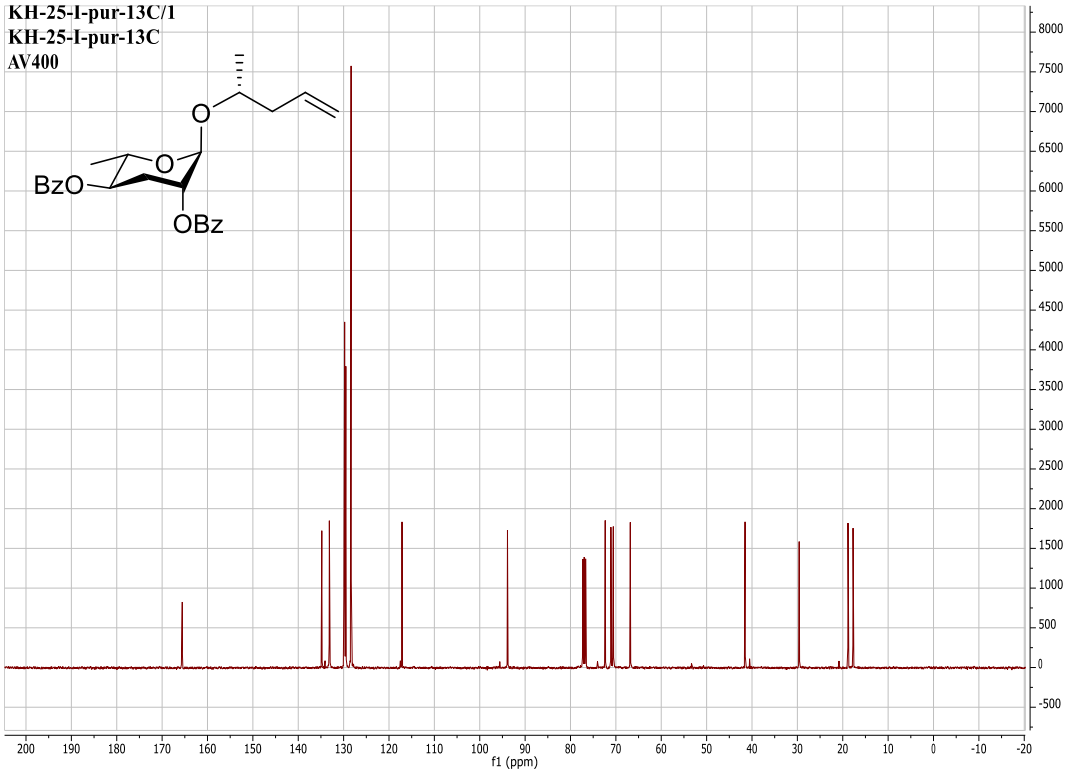

Spectral data for compound **1.1, n=2**:

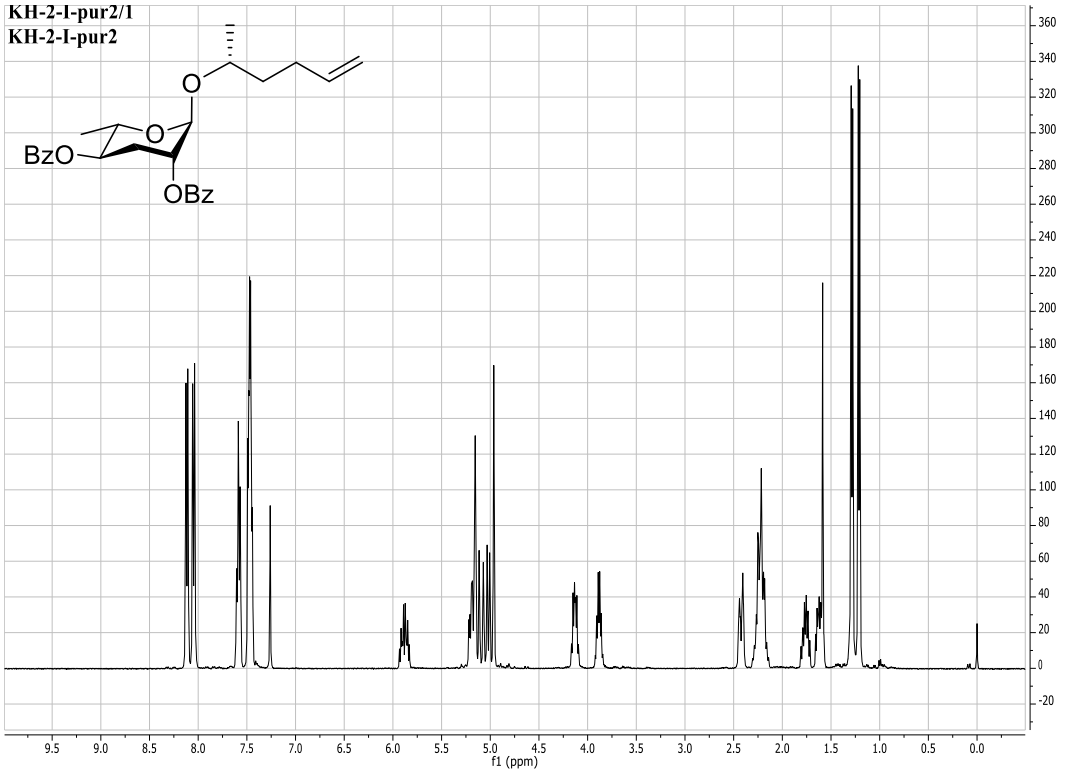

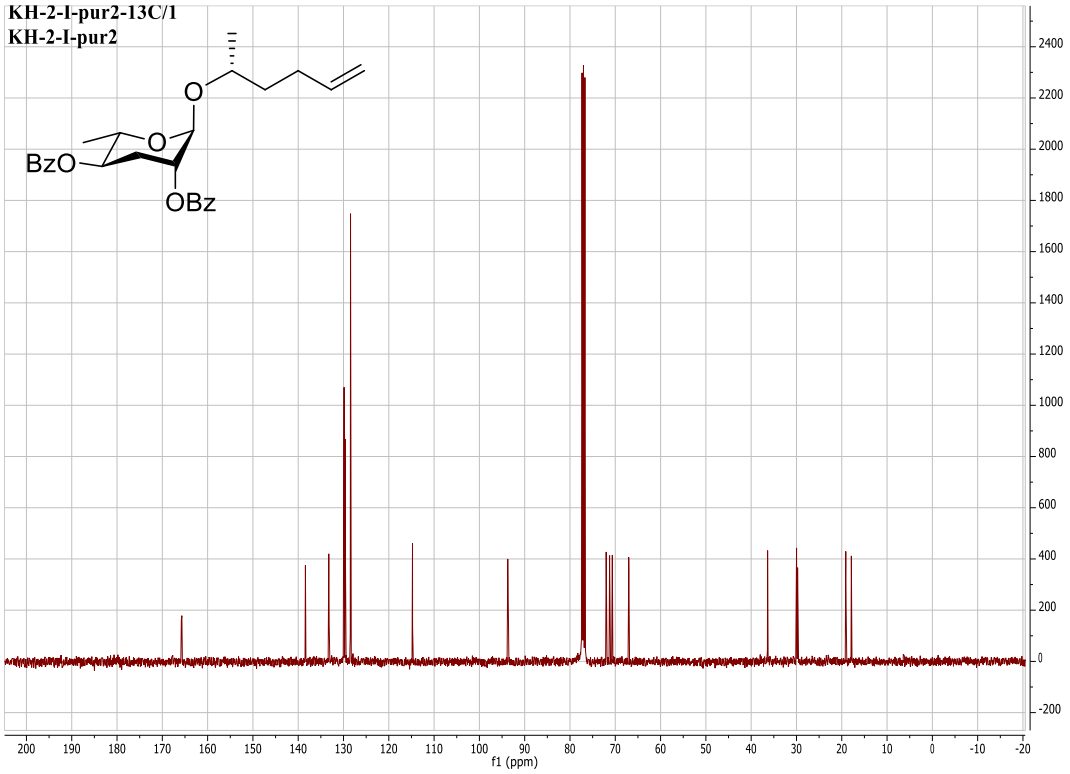

Spectral data for compound **1.1, n=3**:

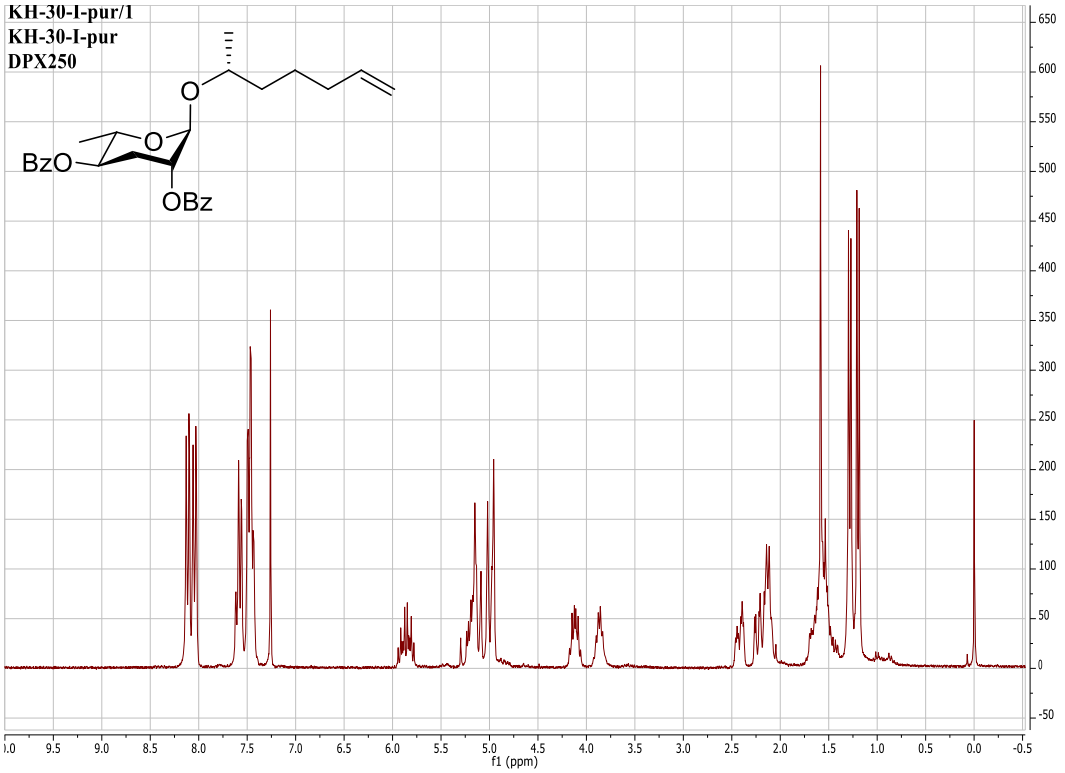

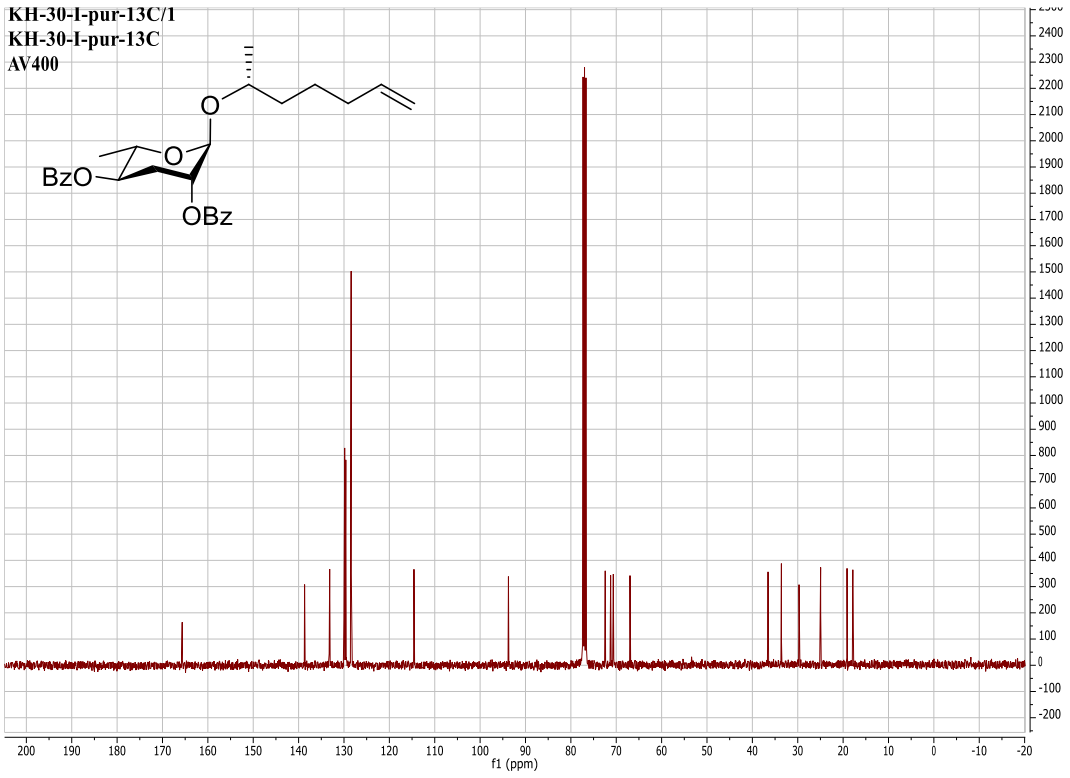

Spectral data for compound **1.1, n=4**:

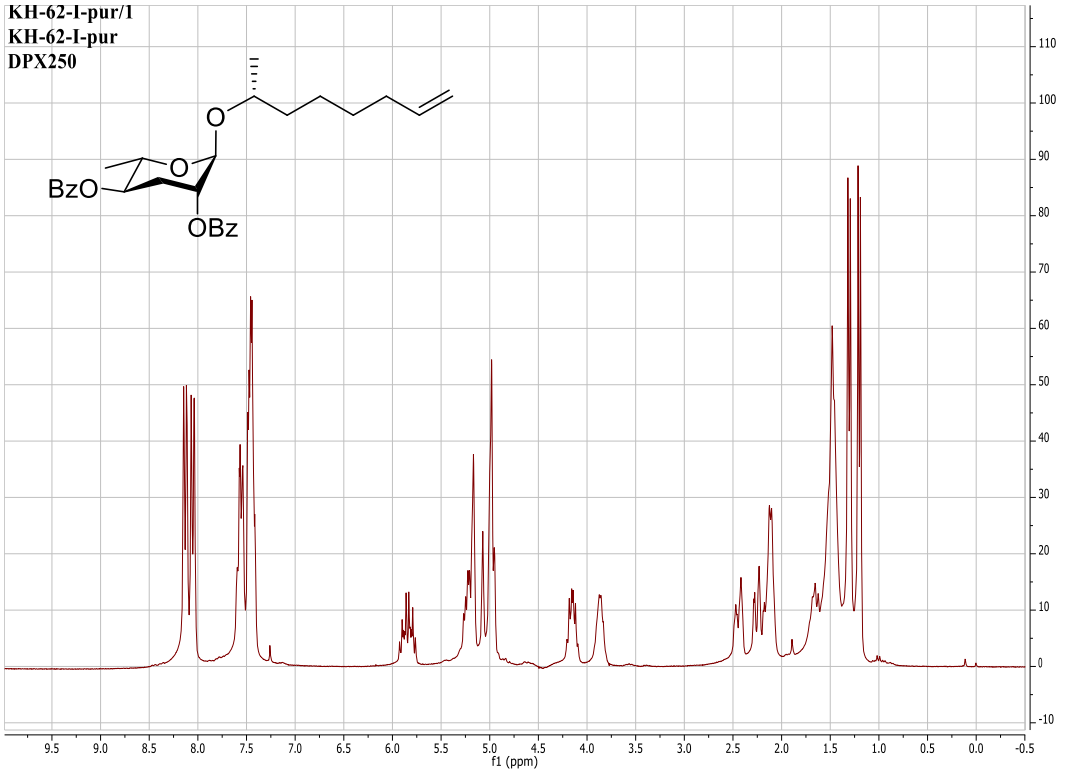

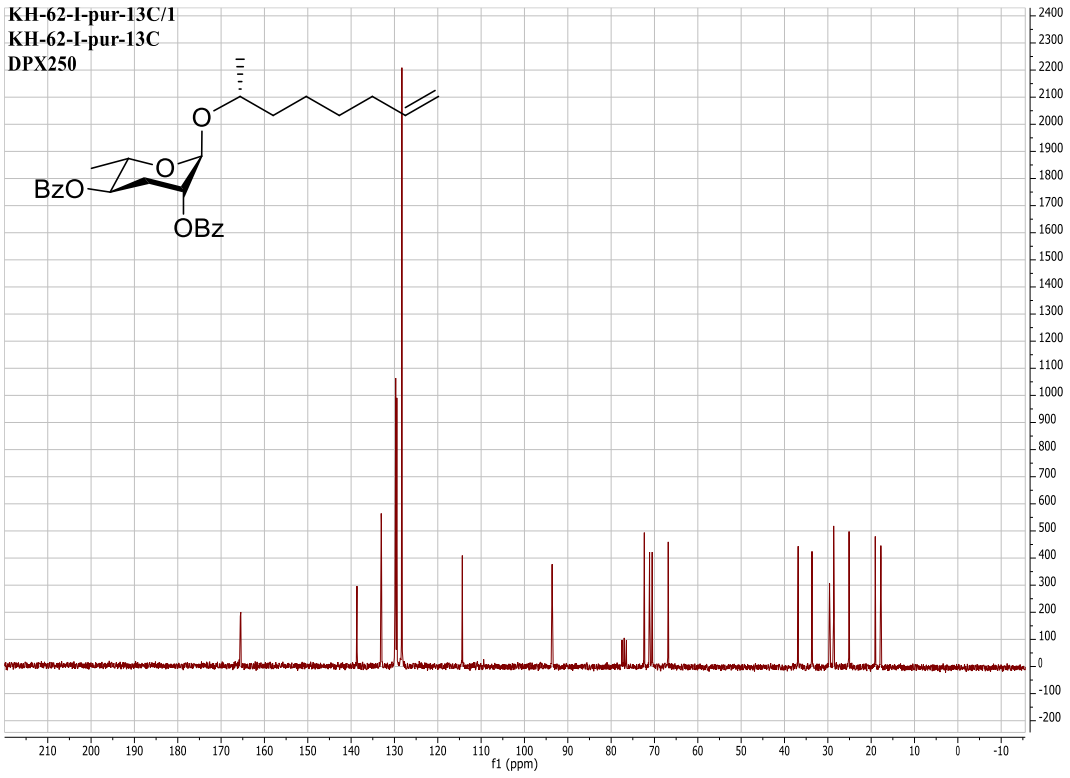

Spectral data for compound **1.4**:

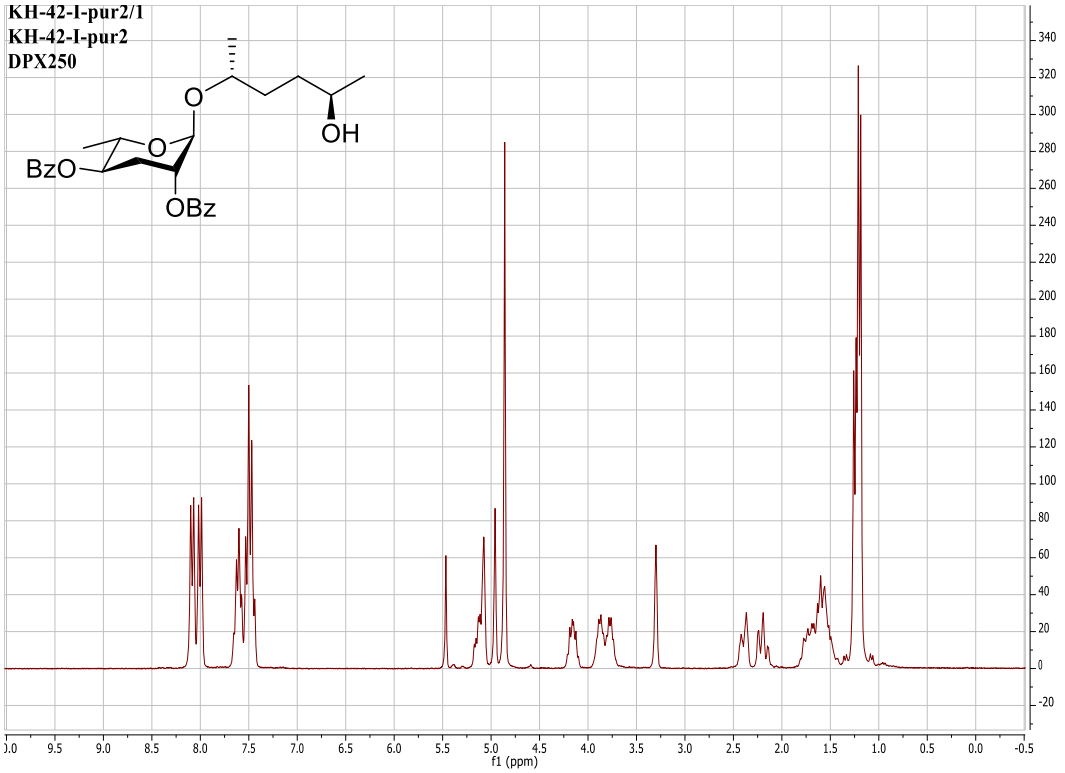

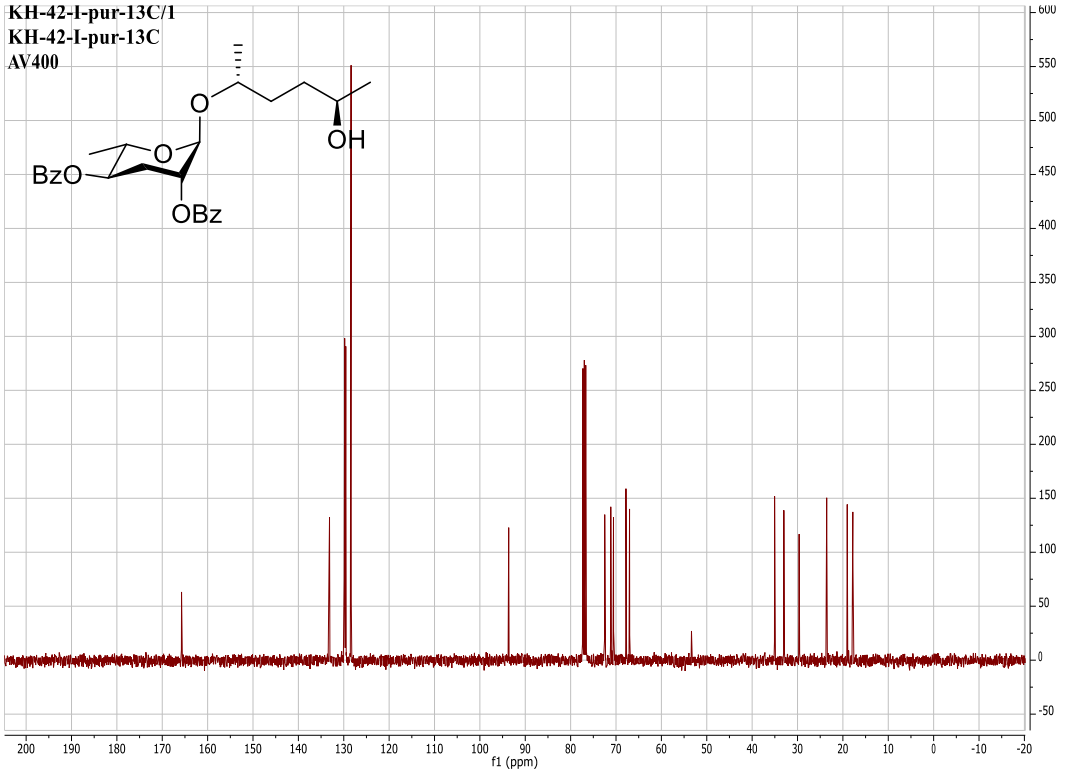

Spectral data for compound **1.5**:

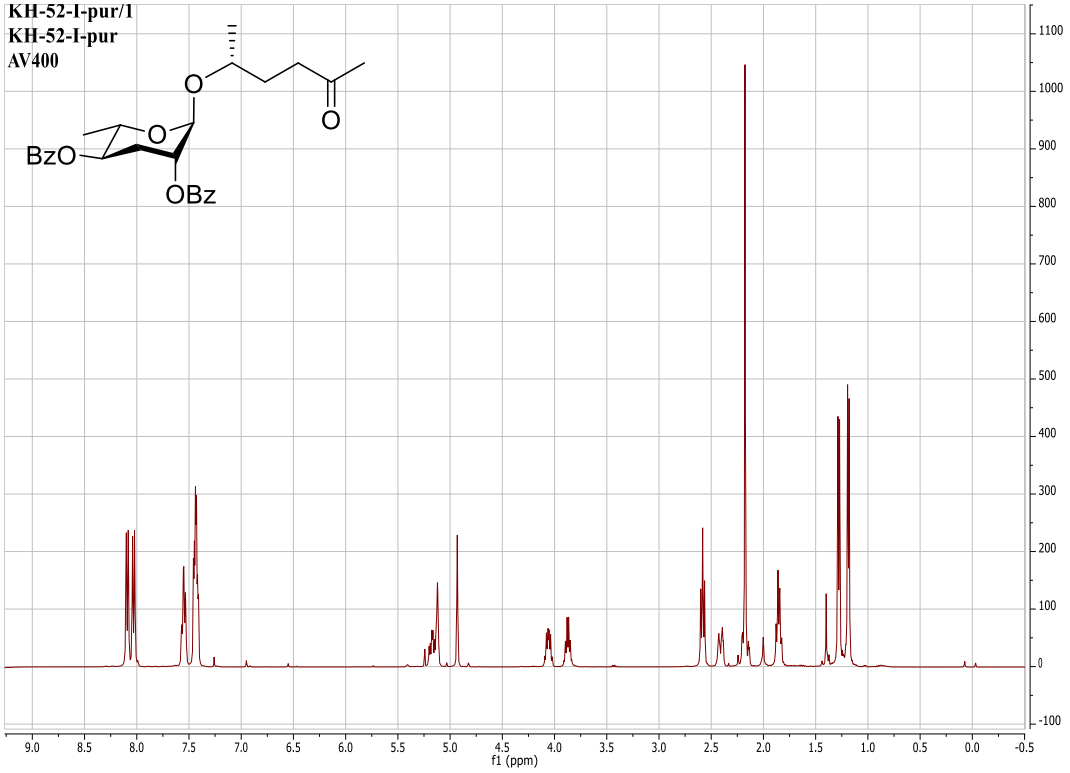

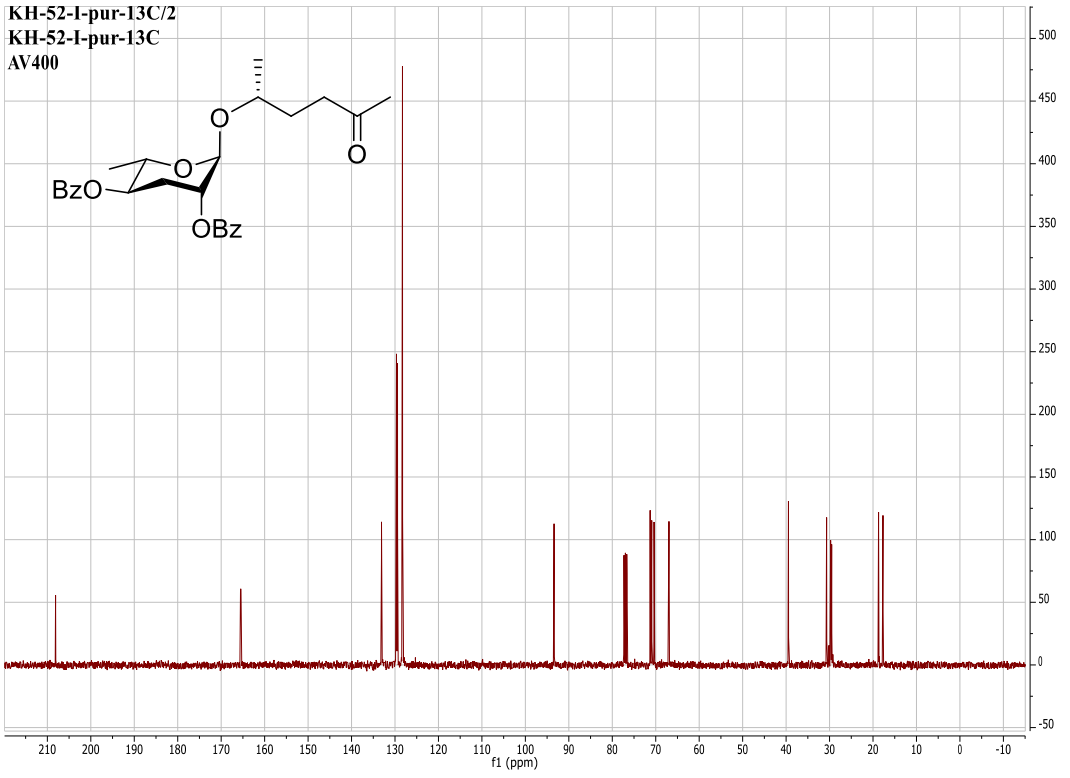

Spectral data for compound **1.2, n=1**:

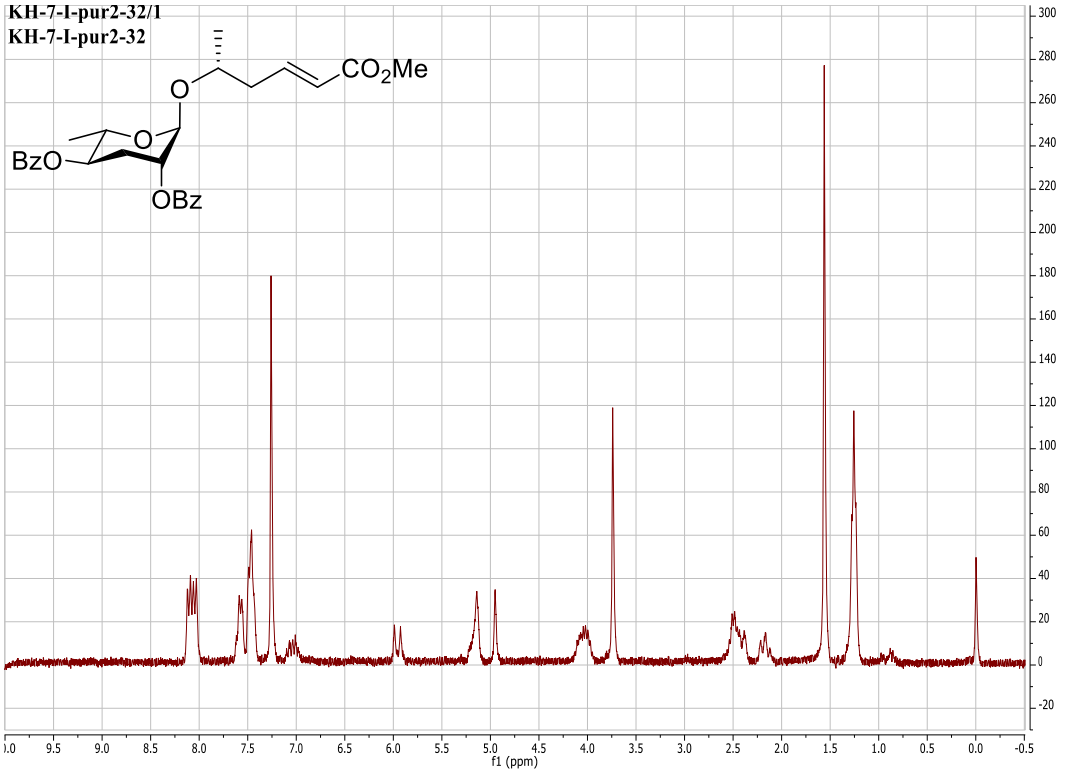

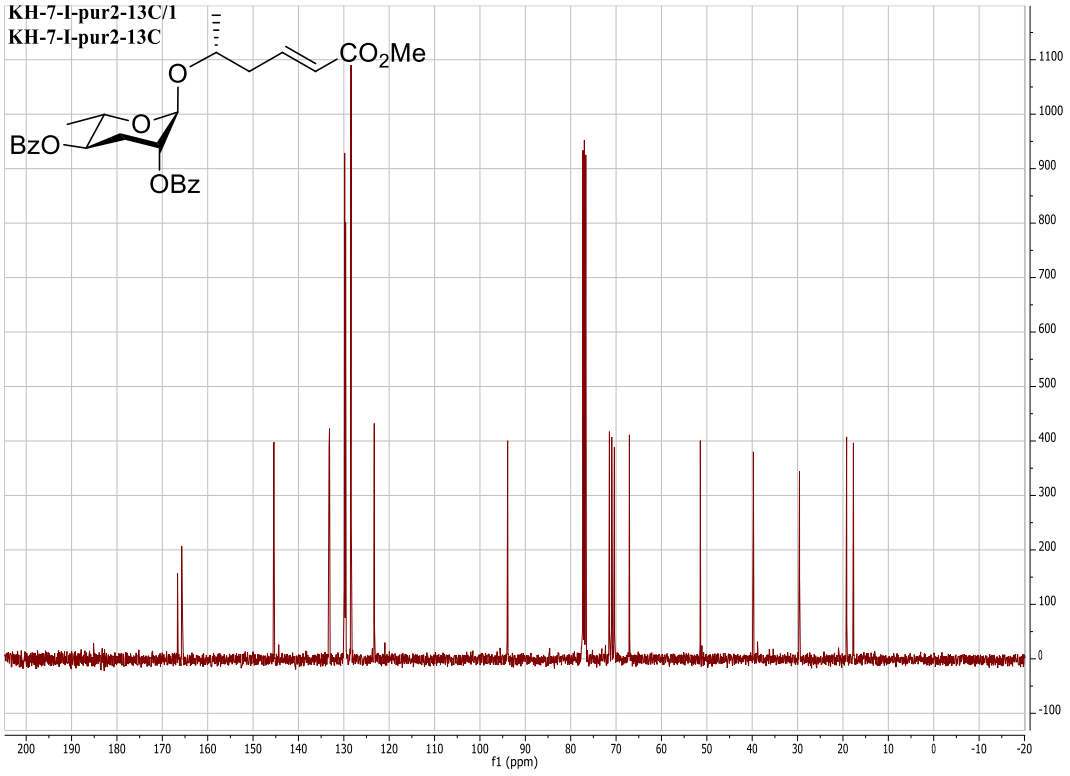

Spectral data for compound **1.2, n=2**:

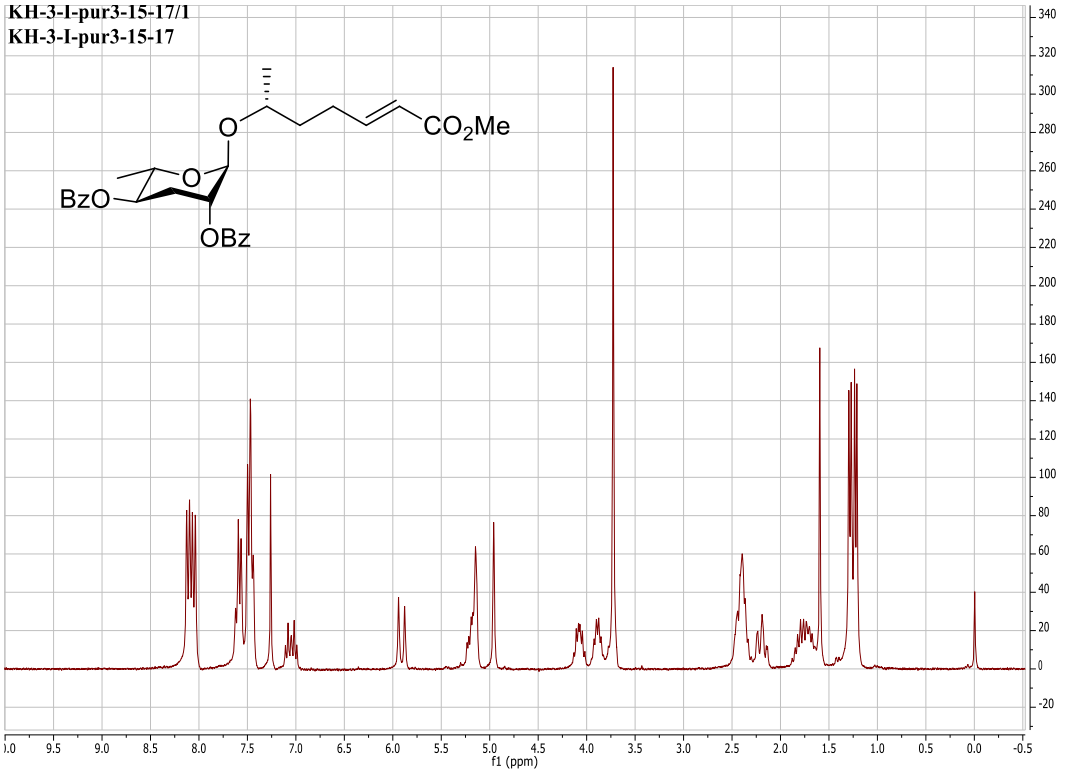

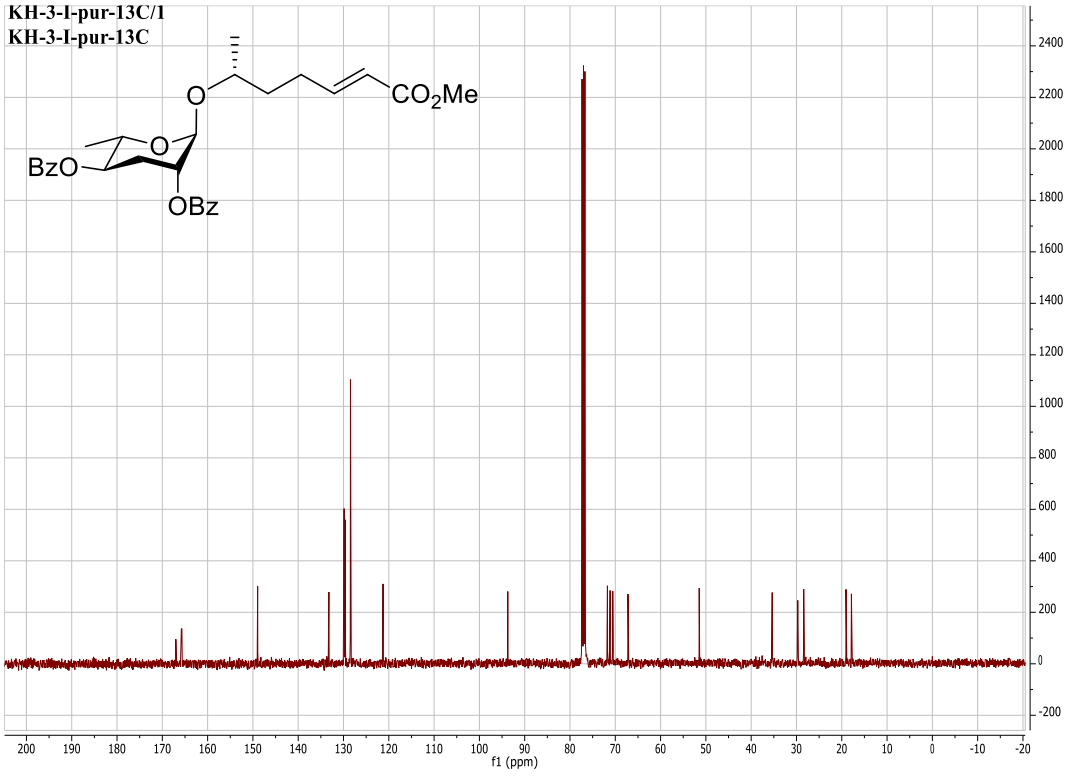

Spectral data for compound **1.2, n=3**:

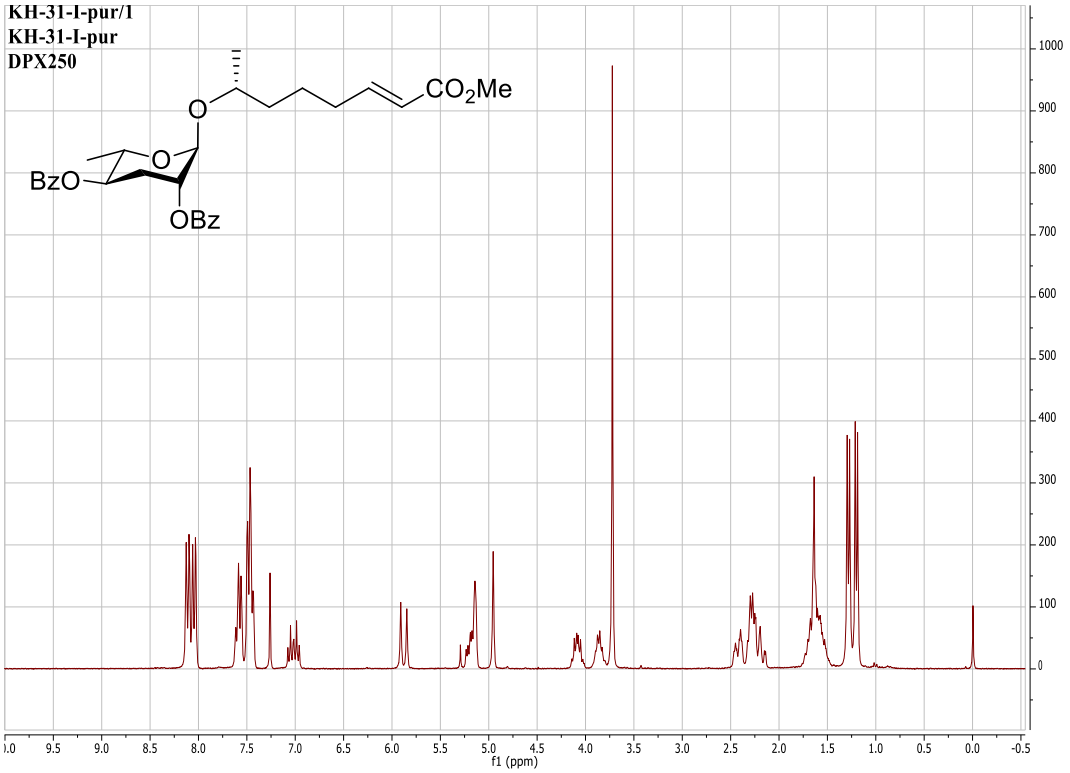

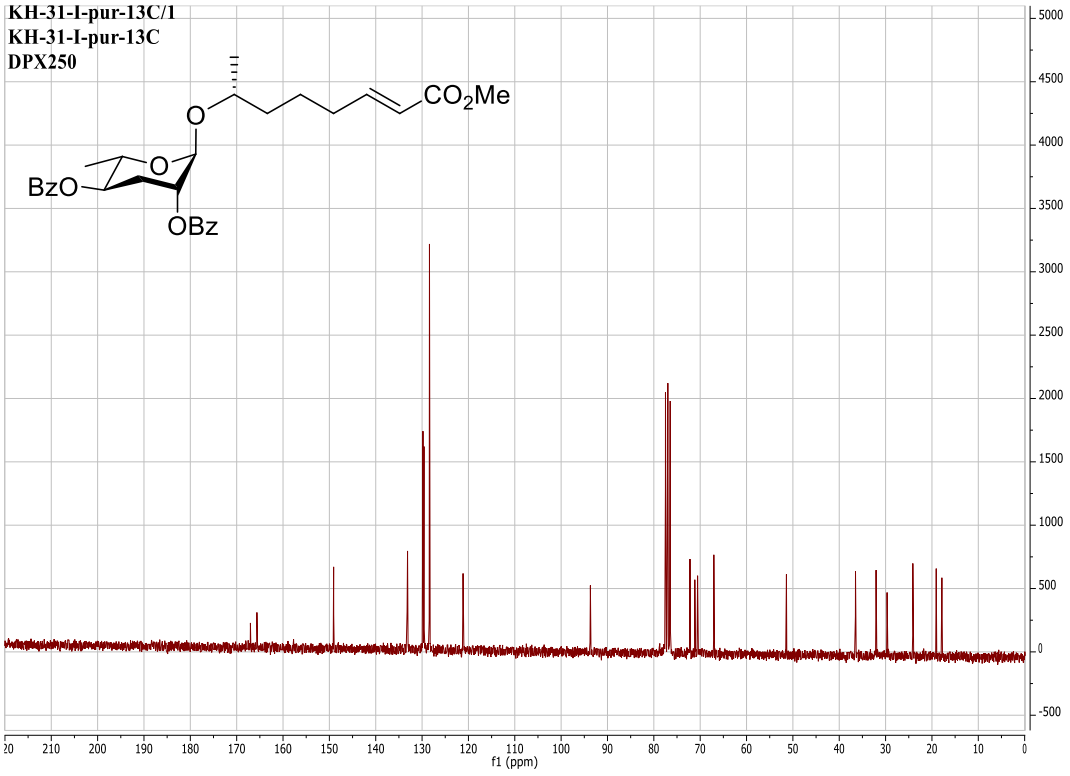

Spectral data for compound **1.2, n=4**:

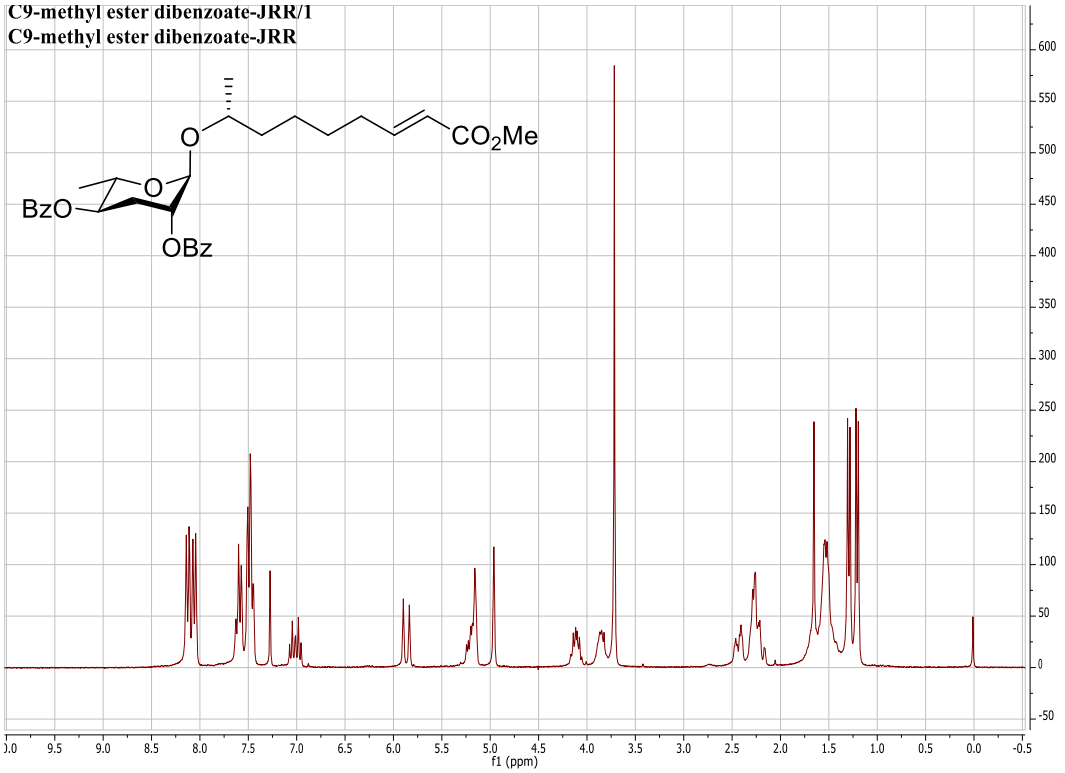

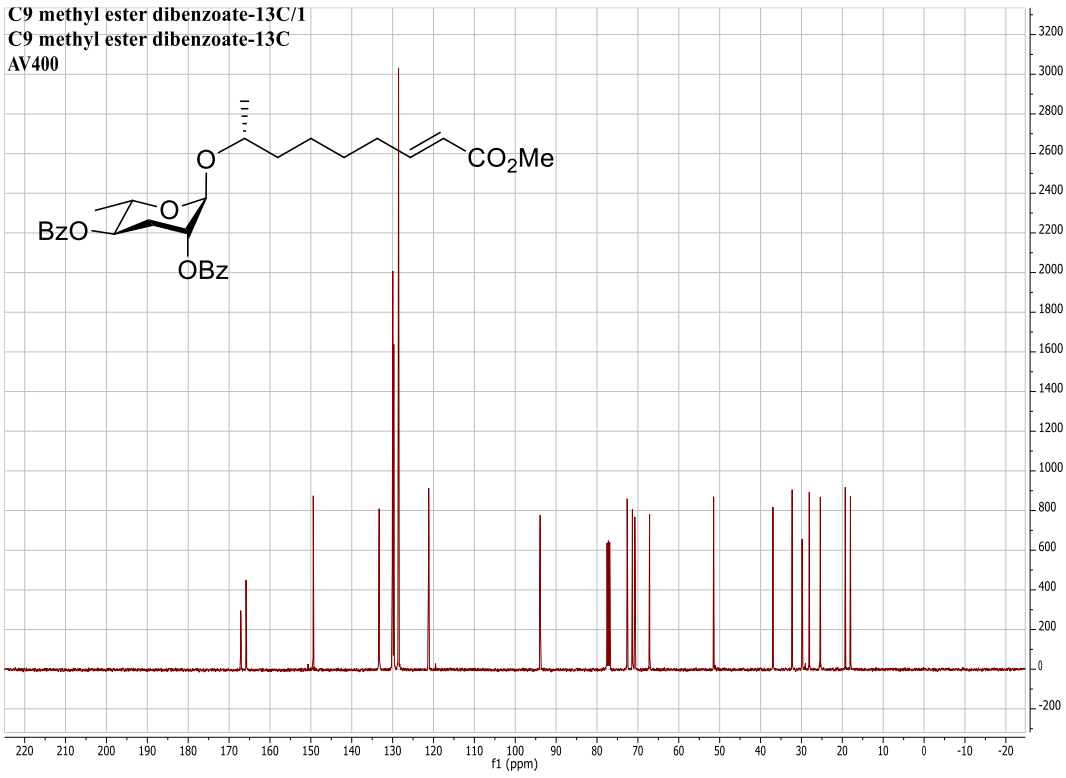

Spectral data for compound **1.3, n=1**:

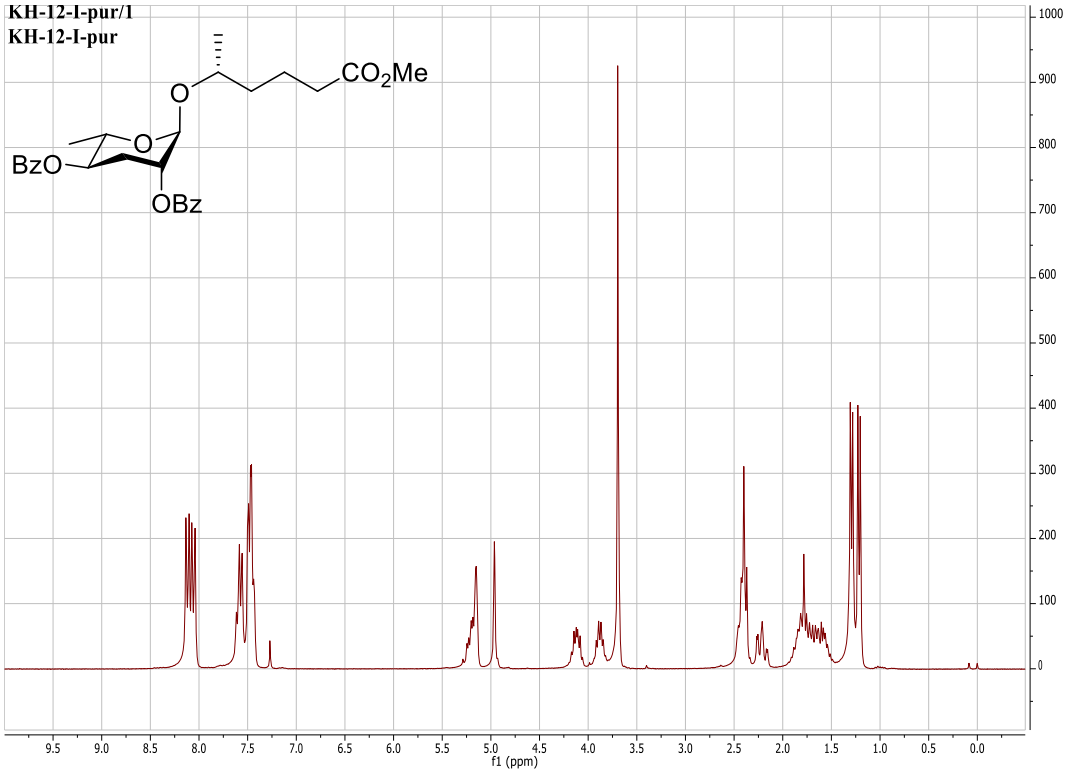

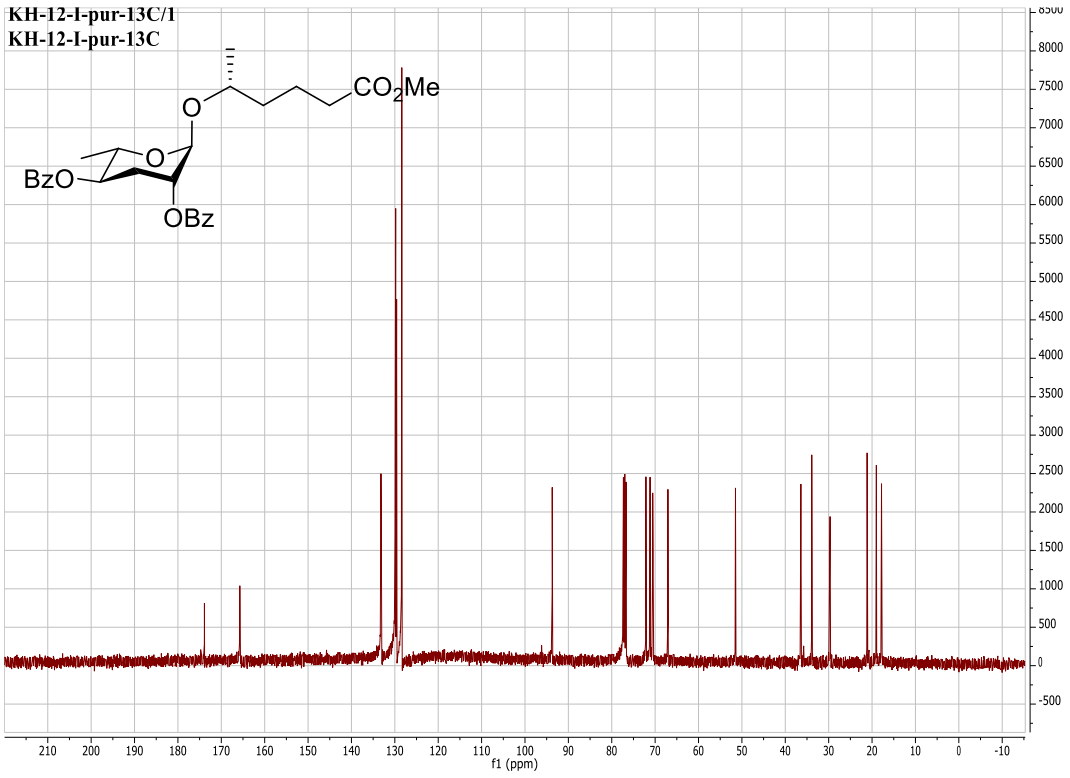

Spectral data for compound **1.3, n=2**:

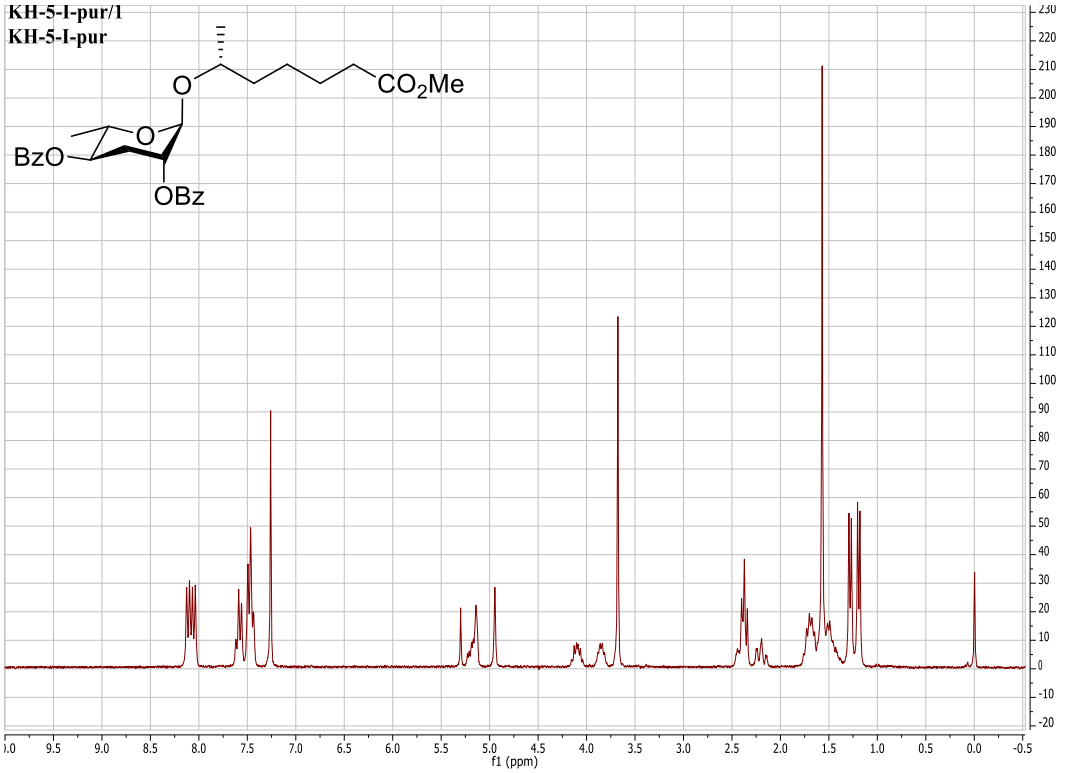

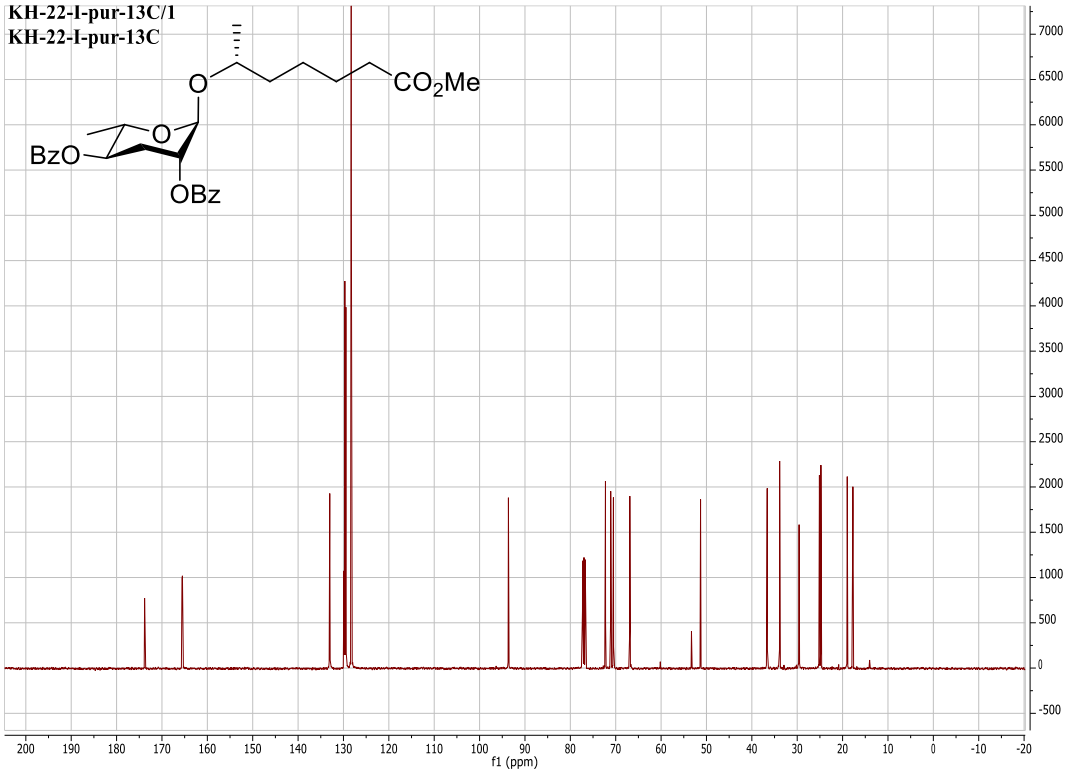

Spectral data for compound **1.3, n=3**:

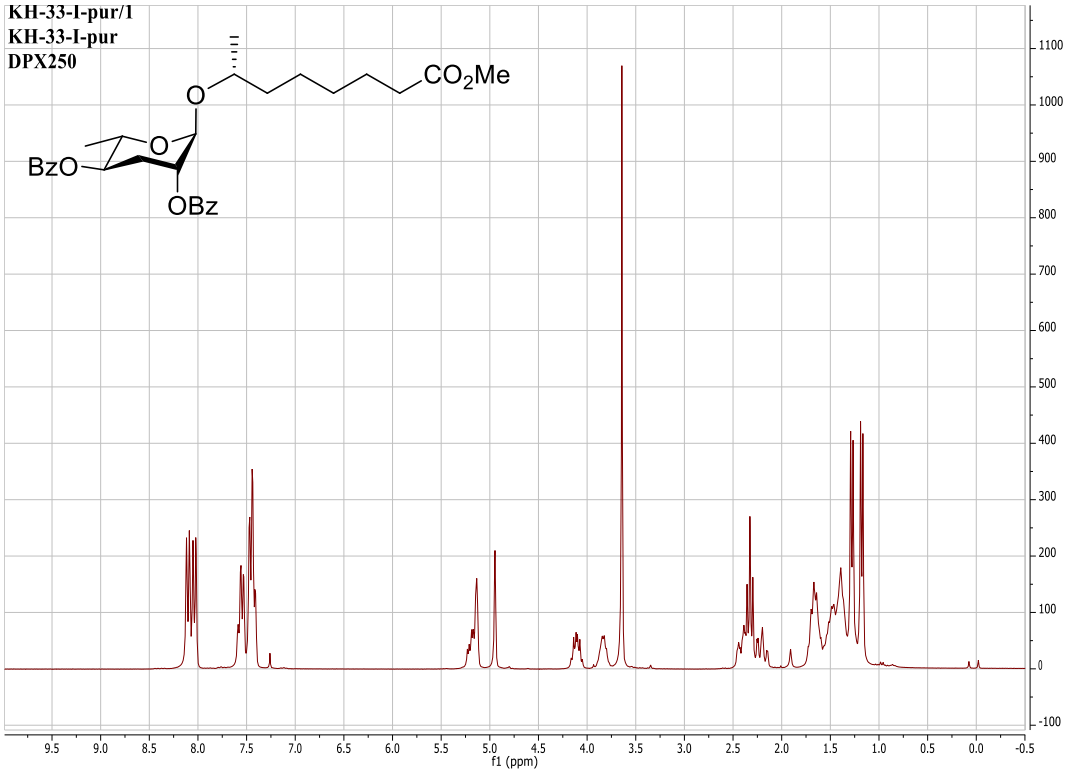

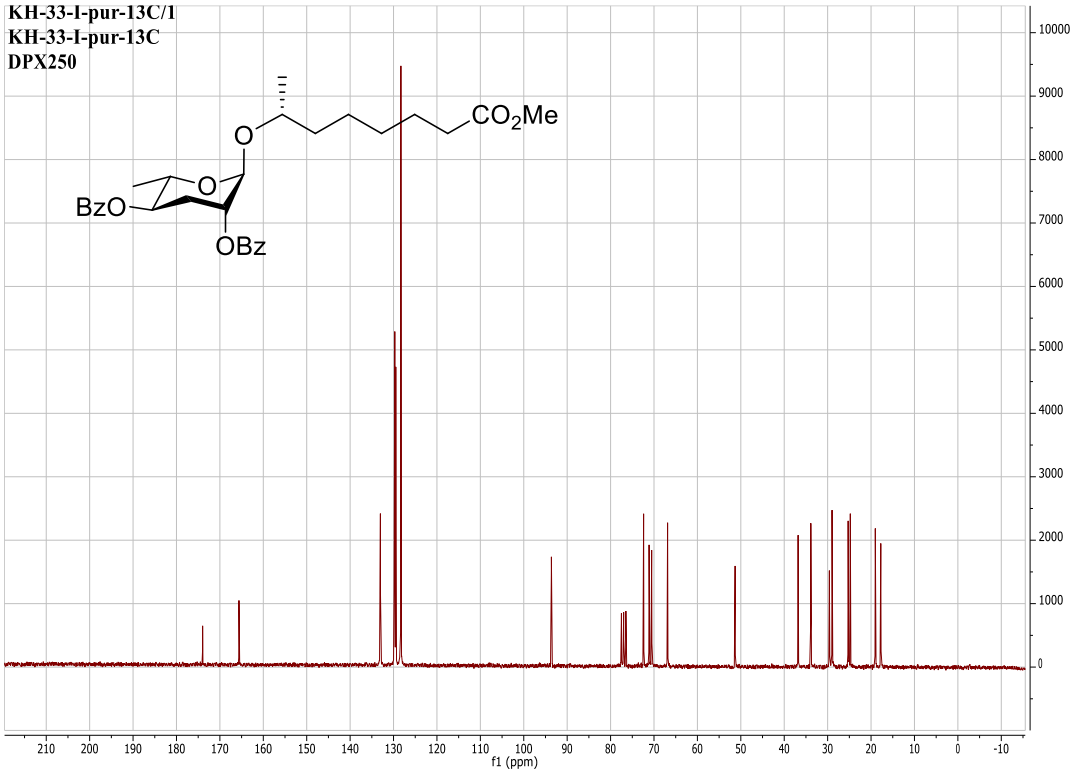

Spectral data for compound **1.3, n=4**:

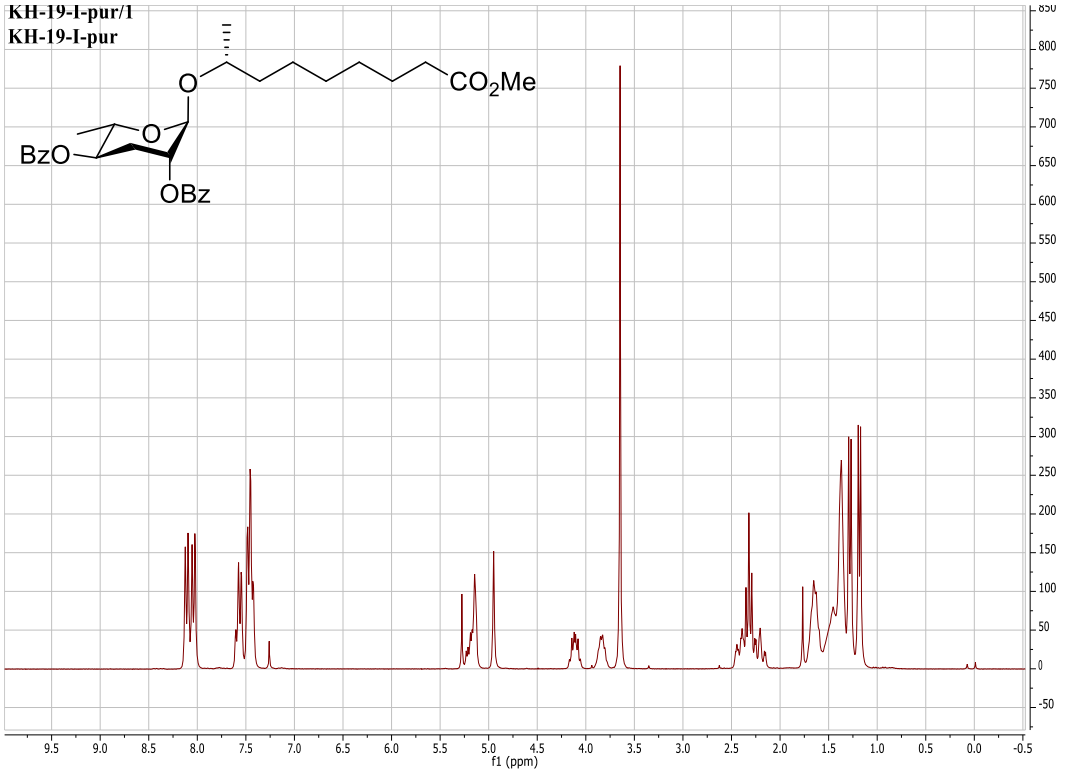

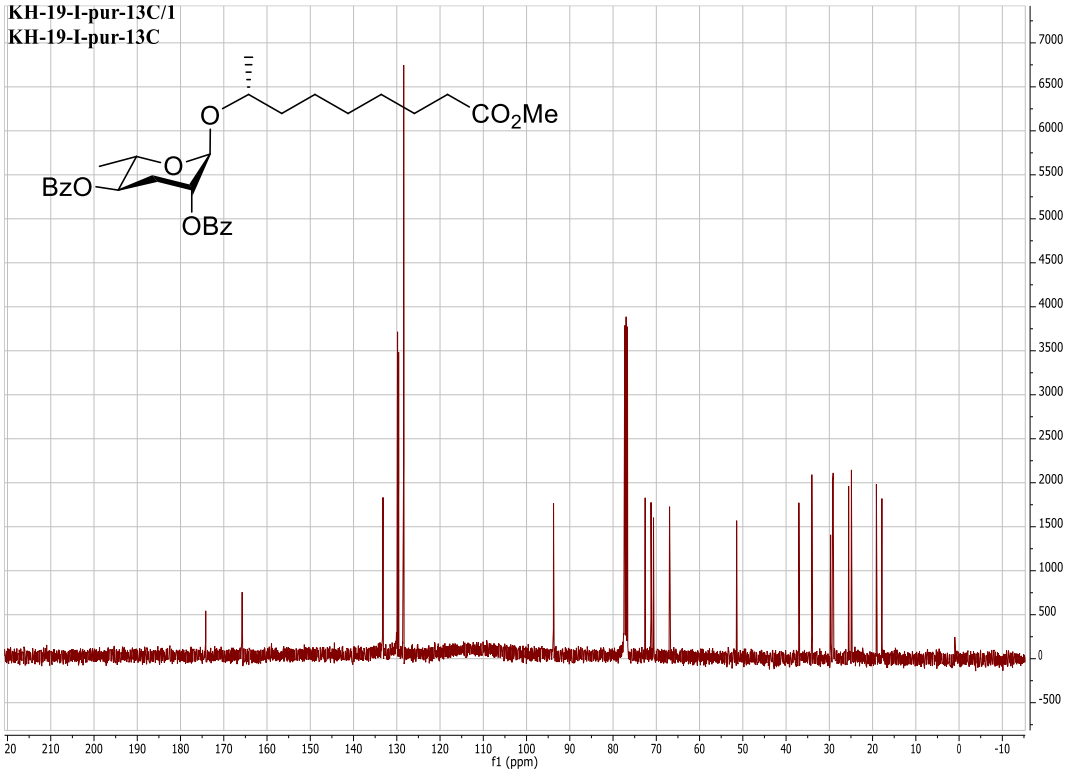

Spectral data for compound **asc-ΔC6**:

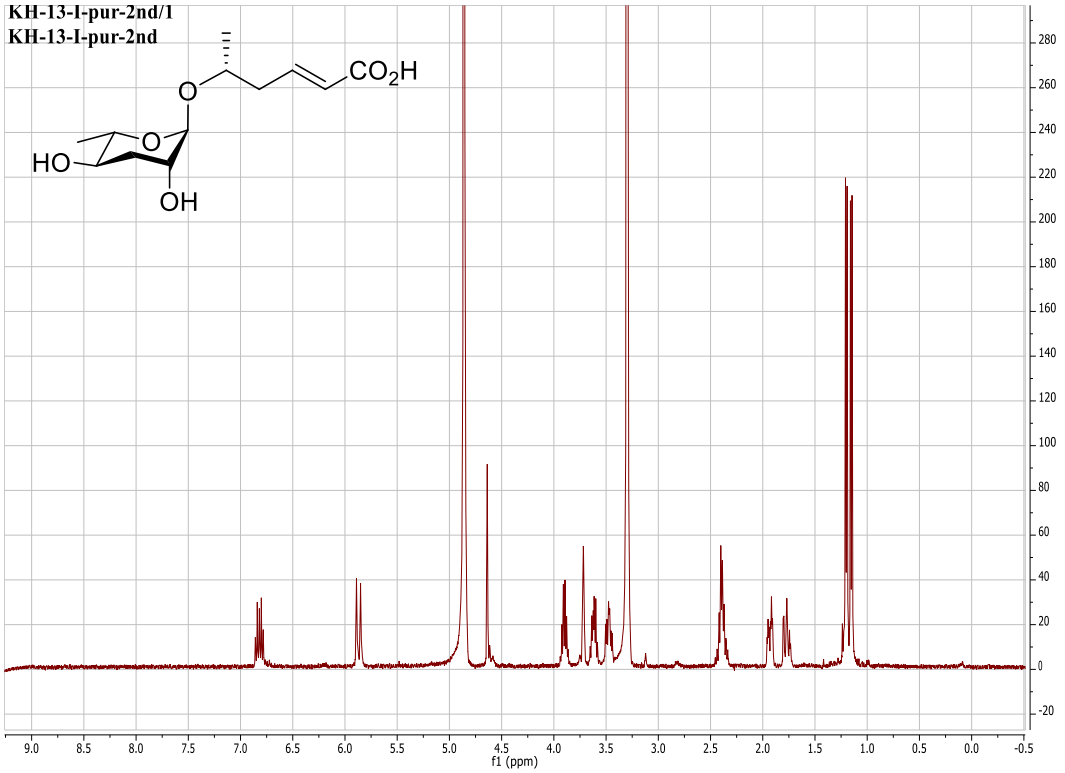

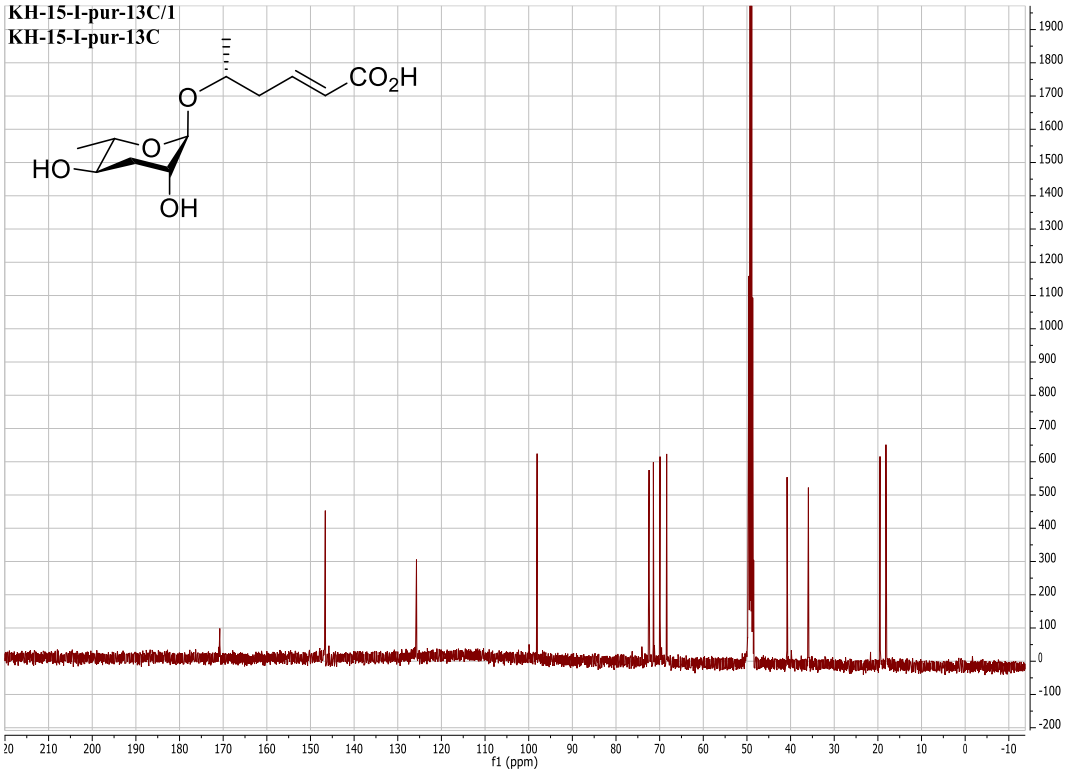

Spectral data for compound **asc-ΔC7**:

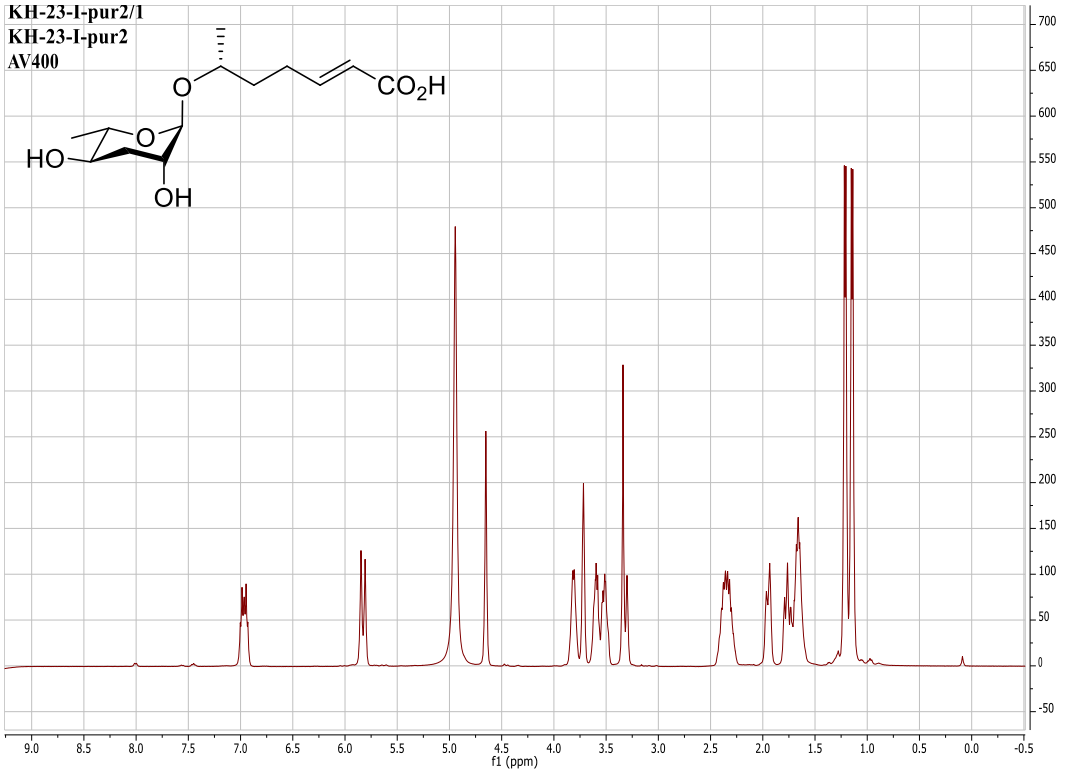

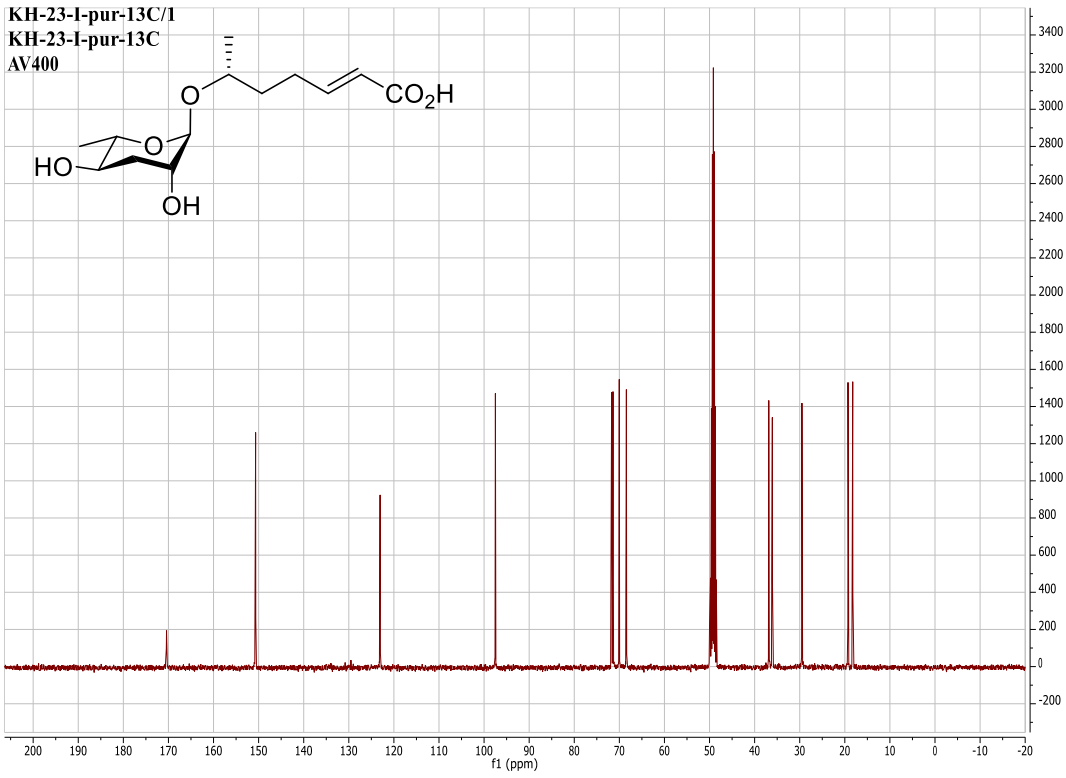

Spectral data for compound **asc-ΔC8**:

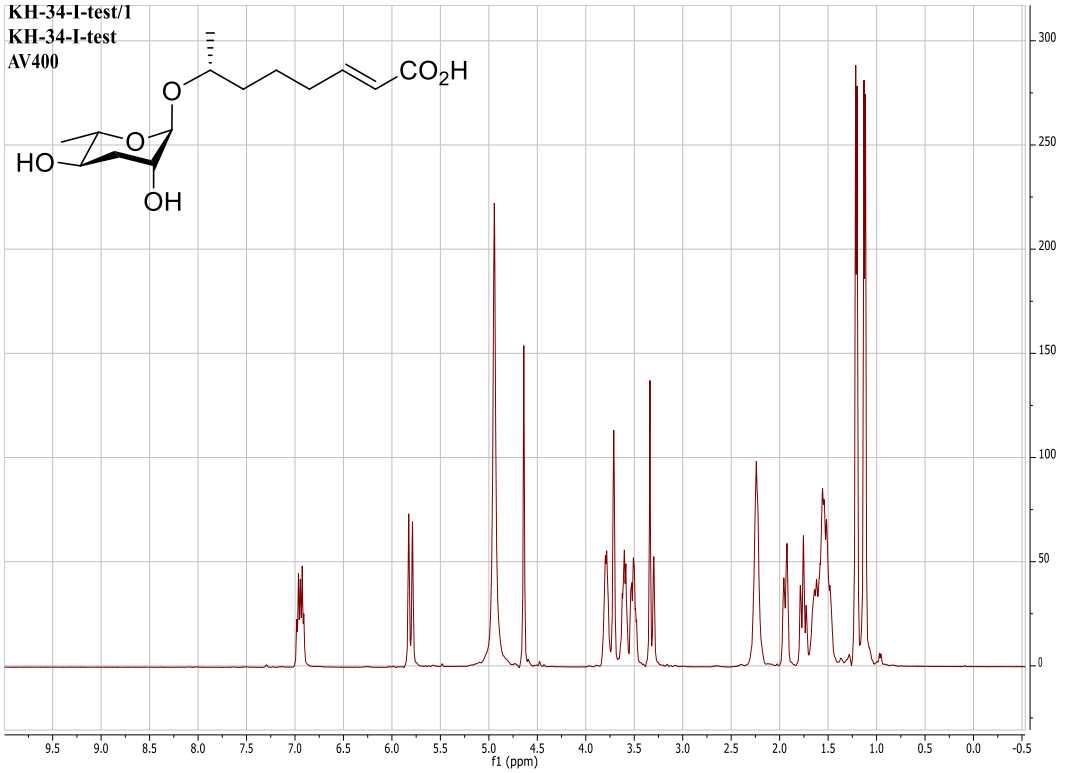

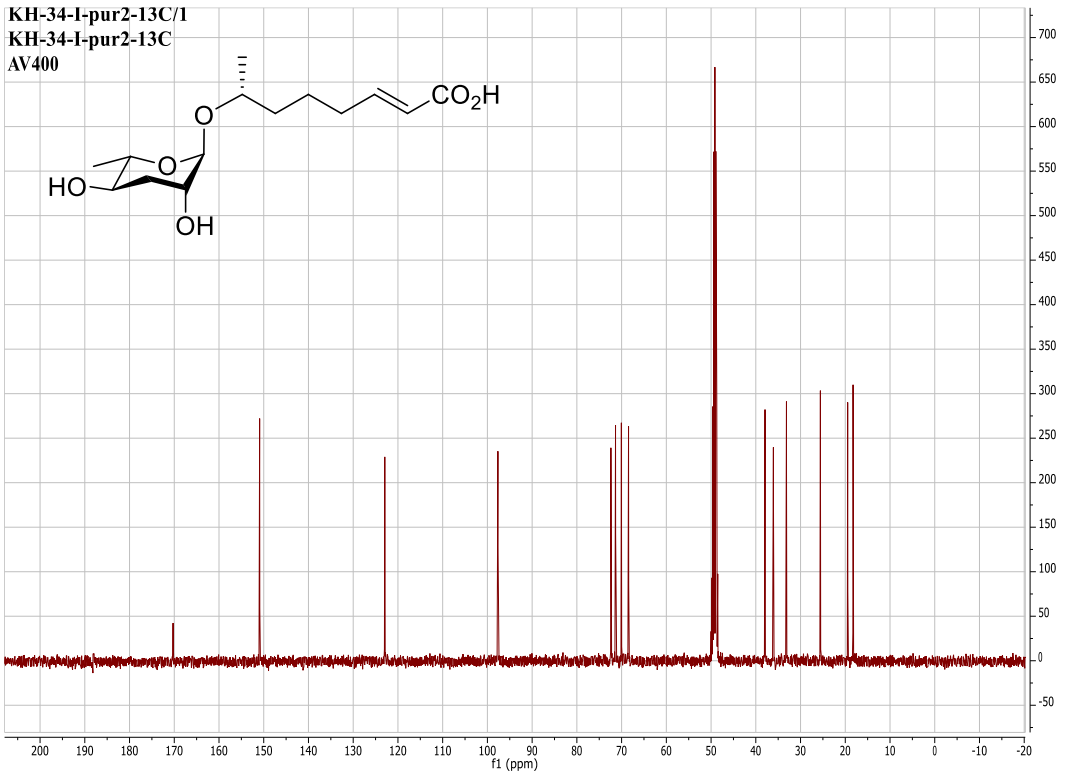

Spectral data for compound **asc-ΔC9**:

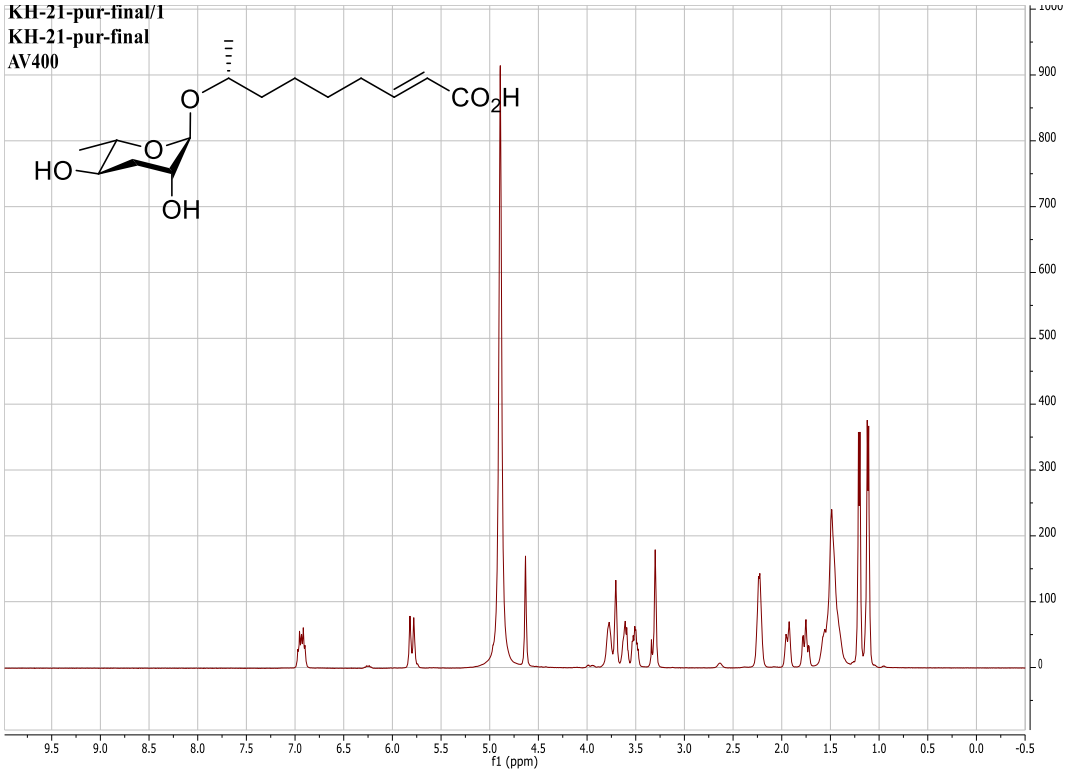

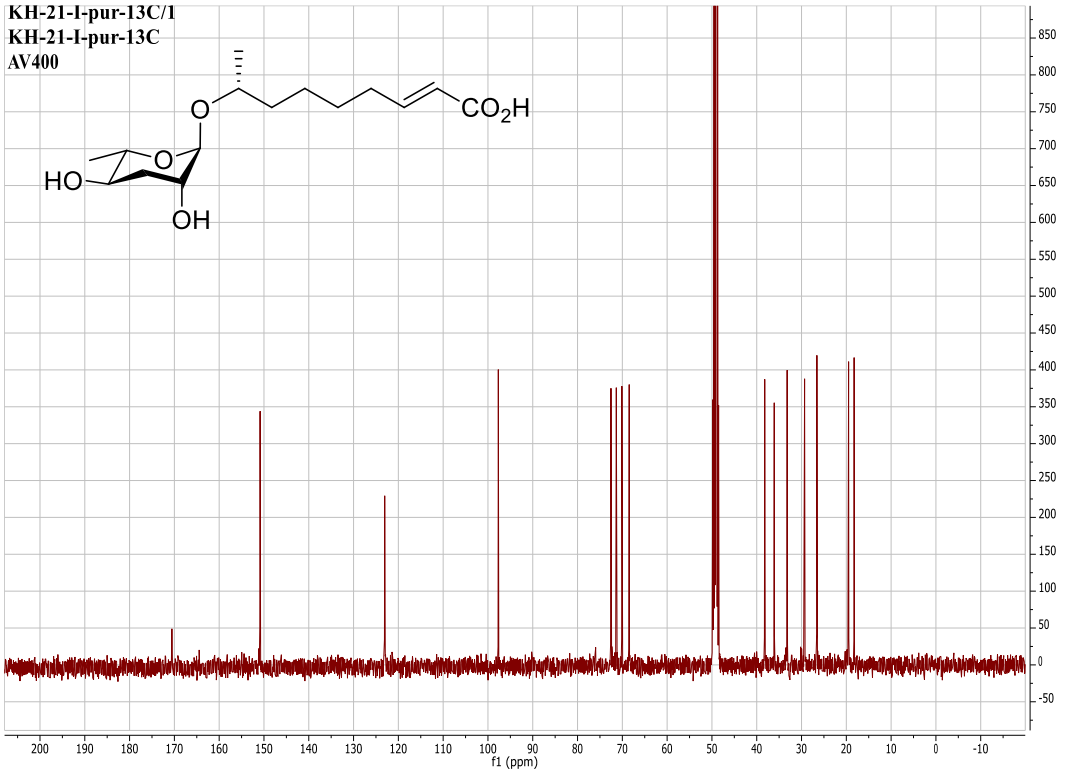

Spectral data for compound **asc-C6**:

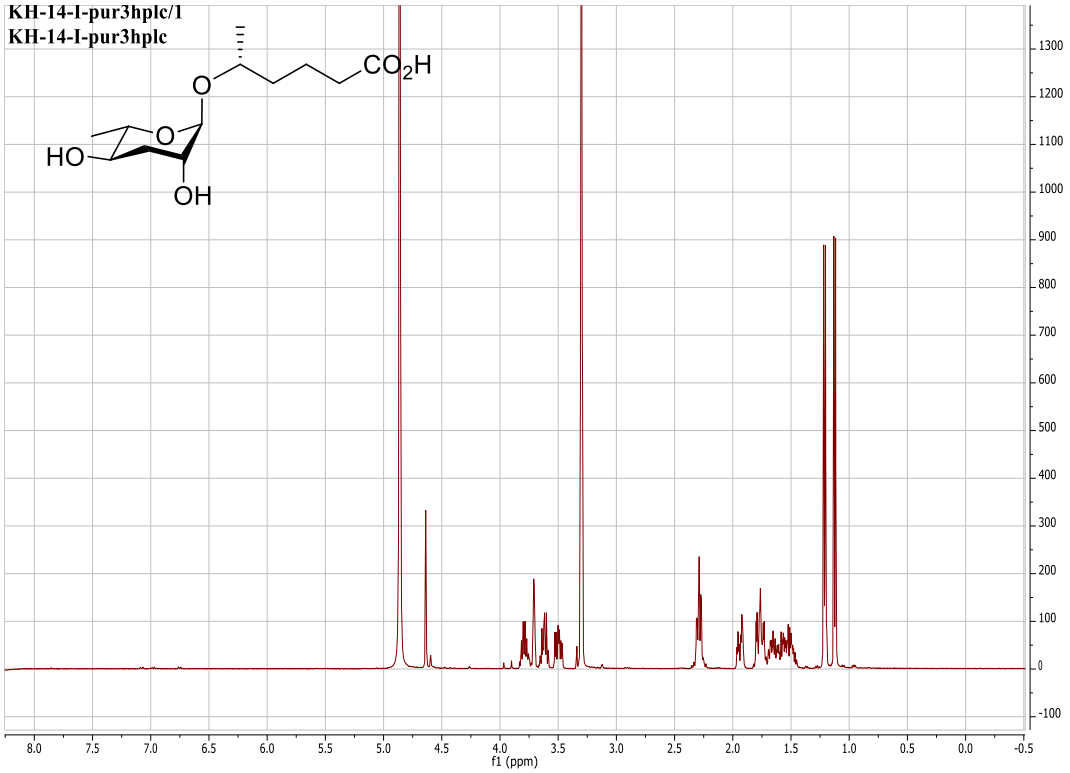

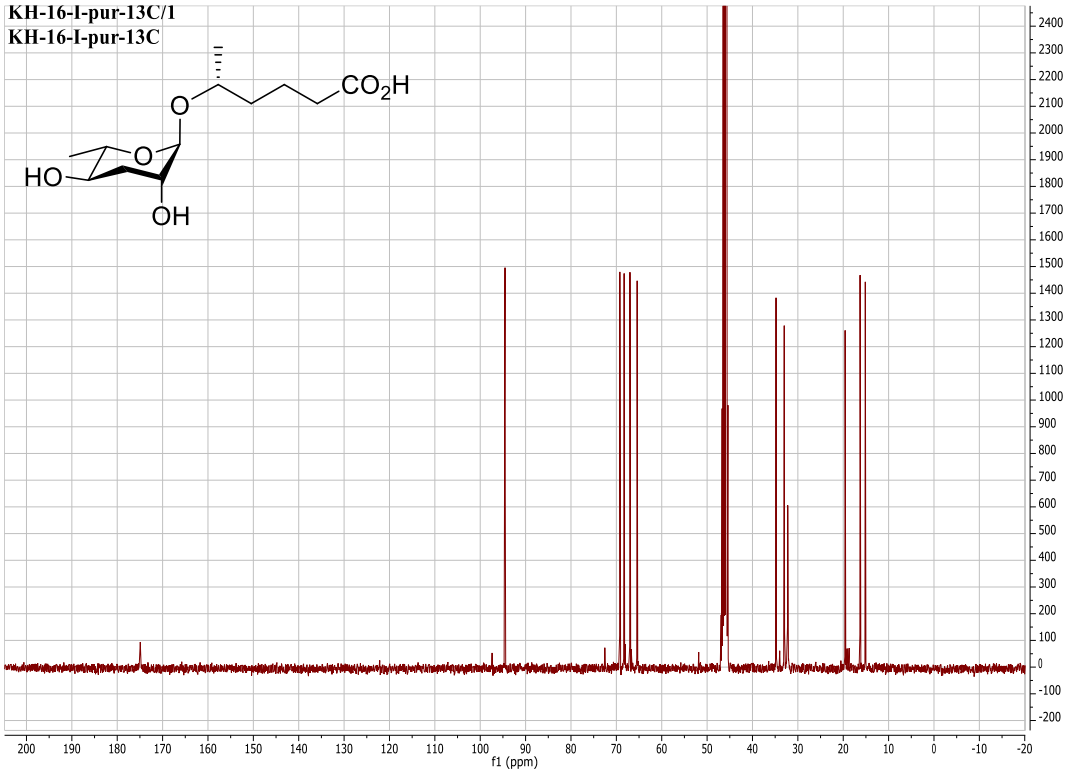

Spectral data for compound **asc-C7**:

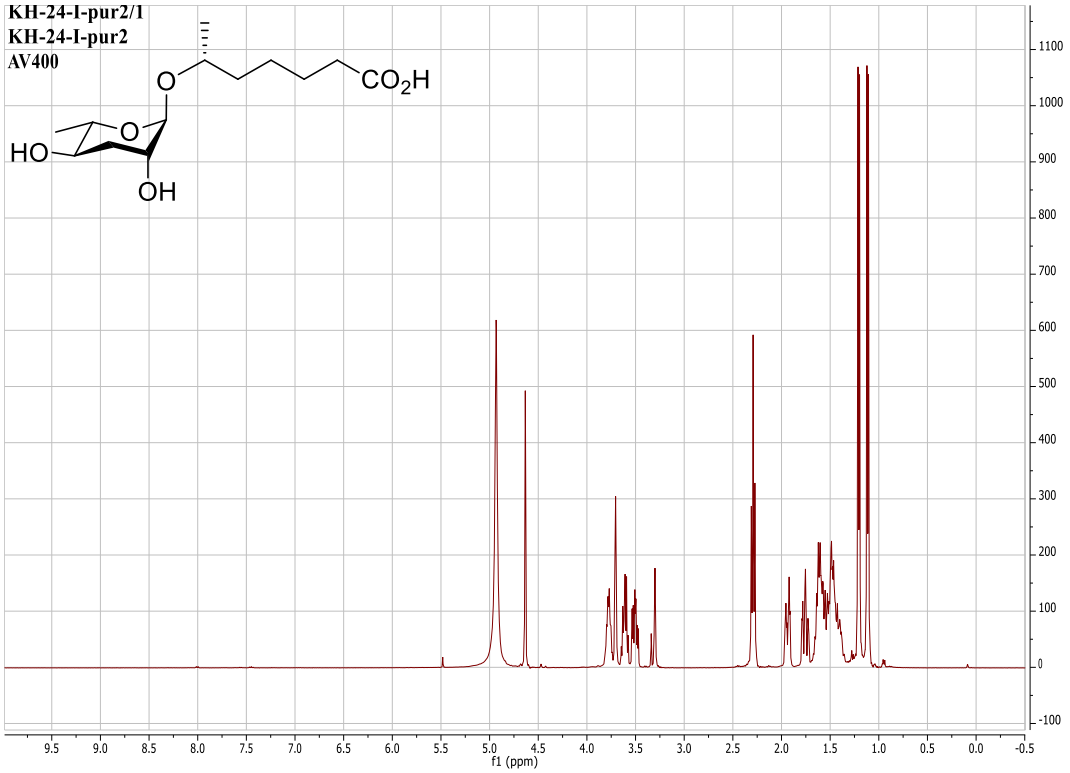

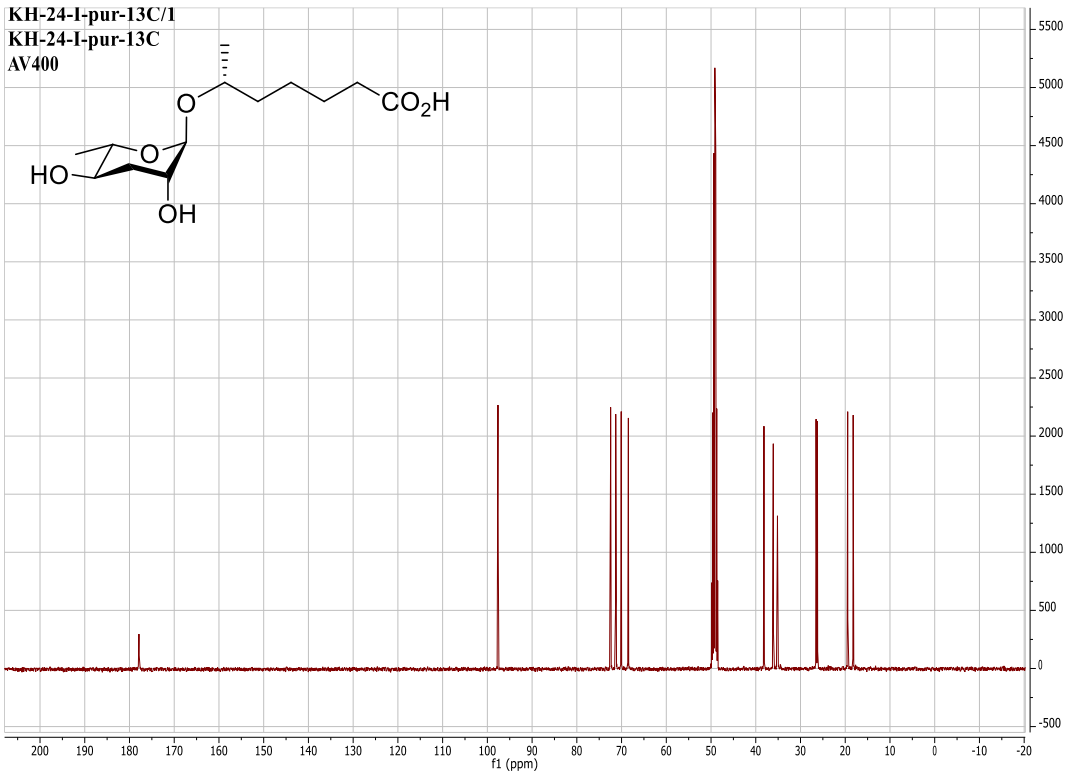

Spectral data for compound **asc-C8**:

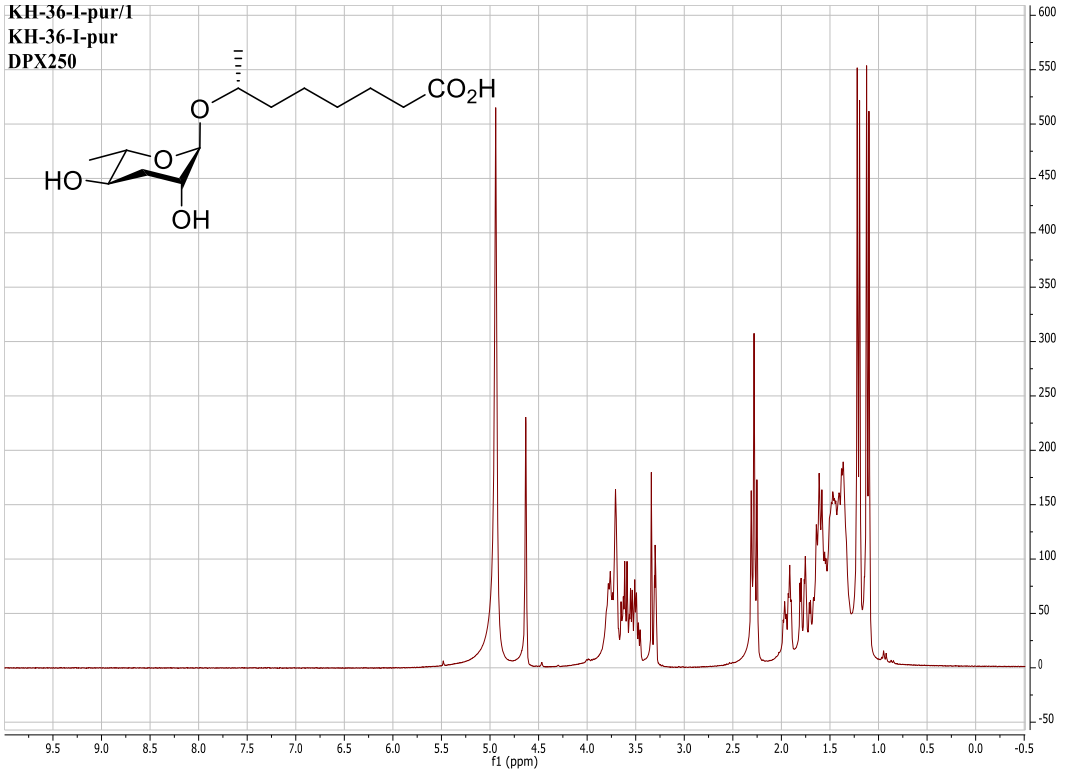

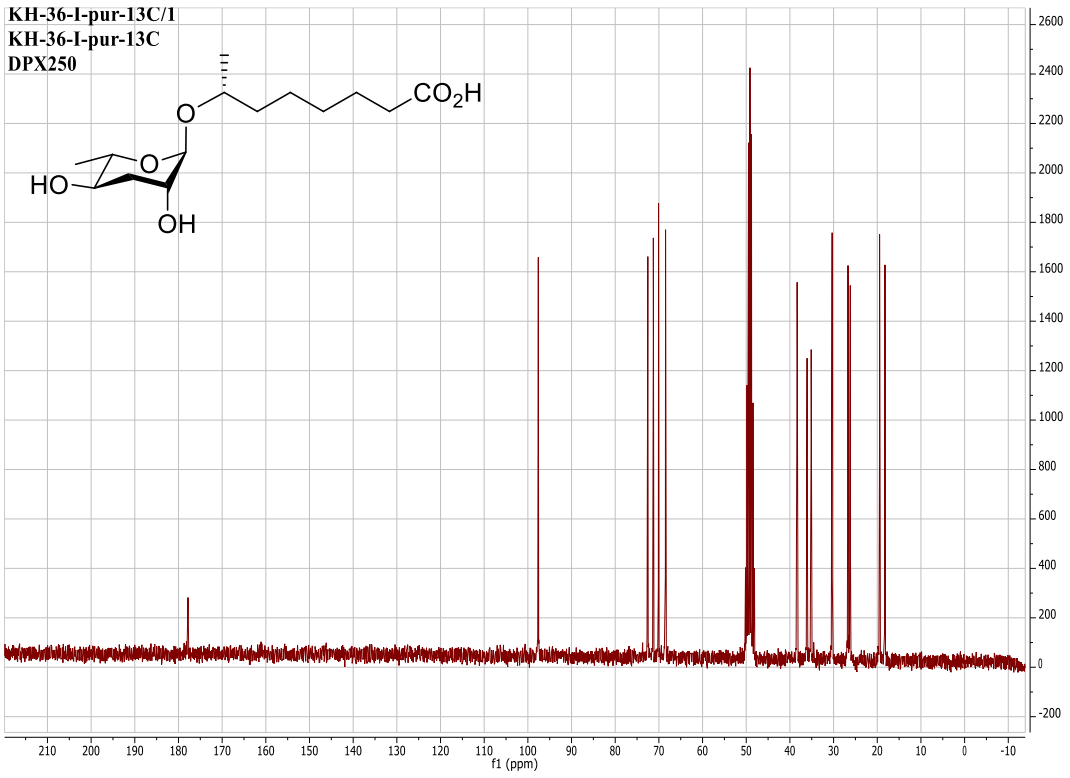

Spectral data for compound **asc-C9**:

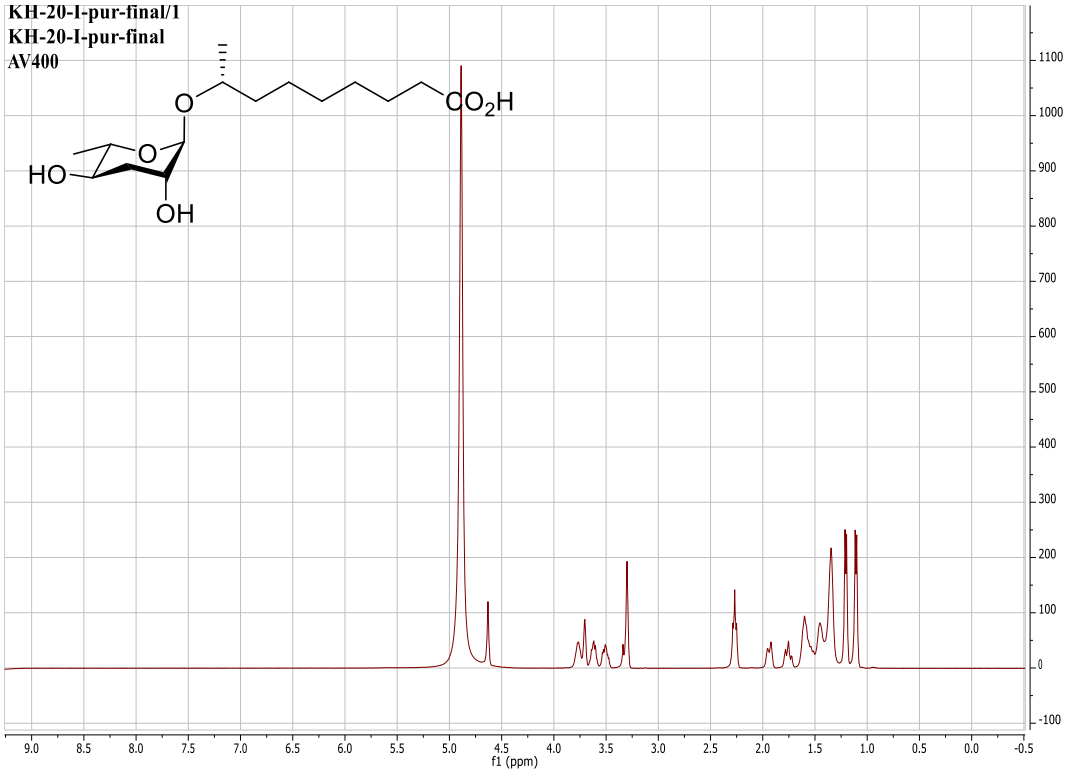

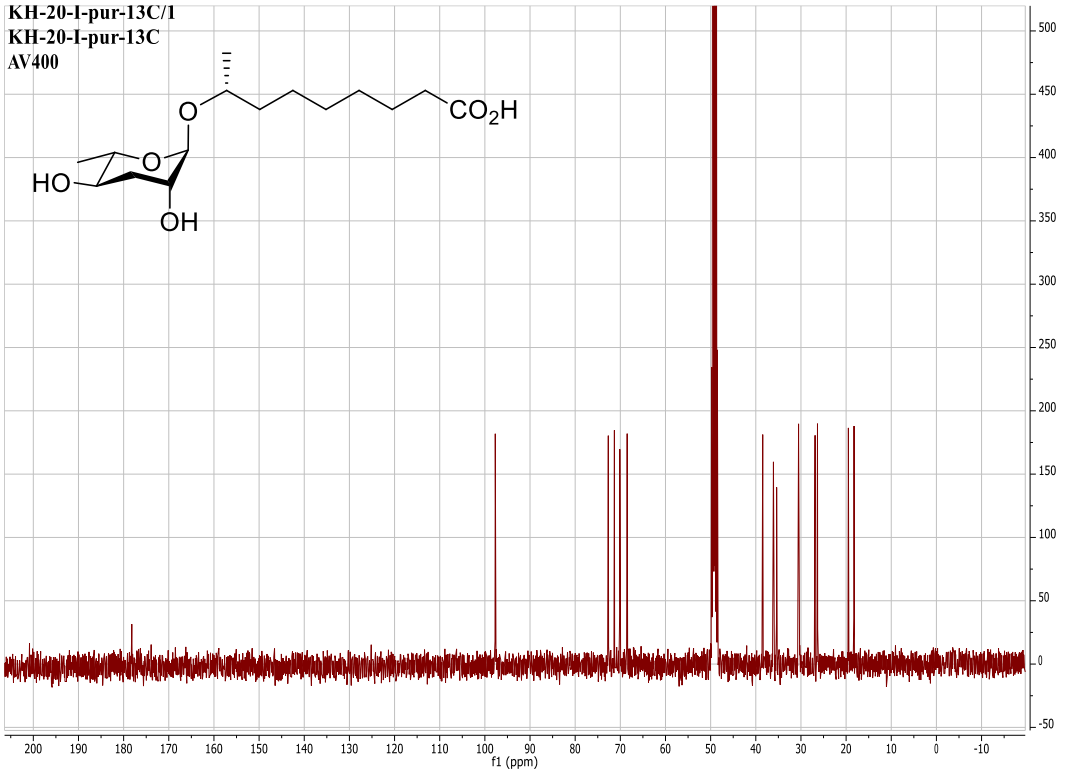

Spectral data for compound **1.10, n=1**:

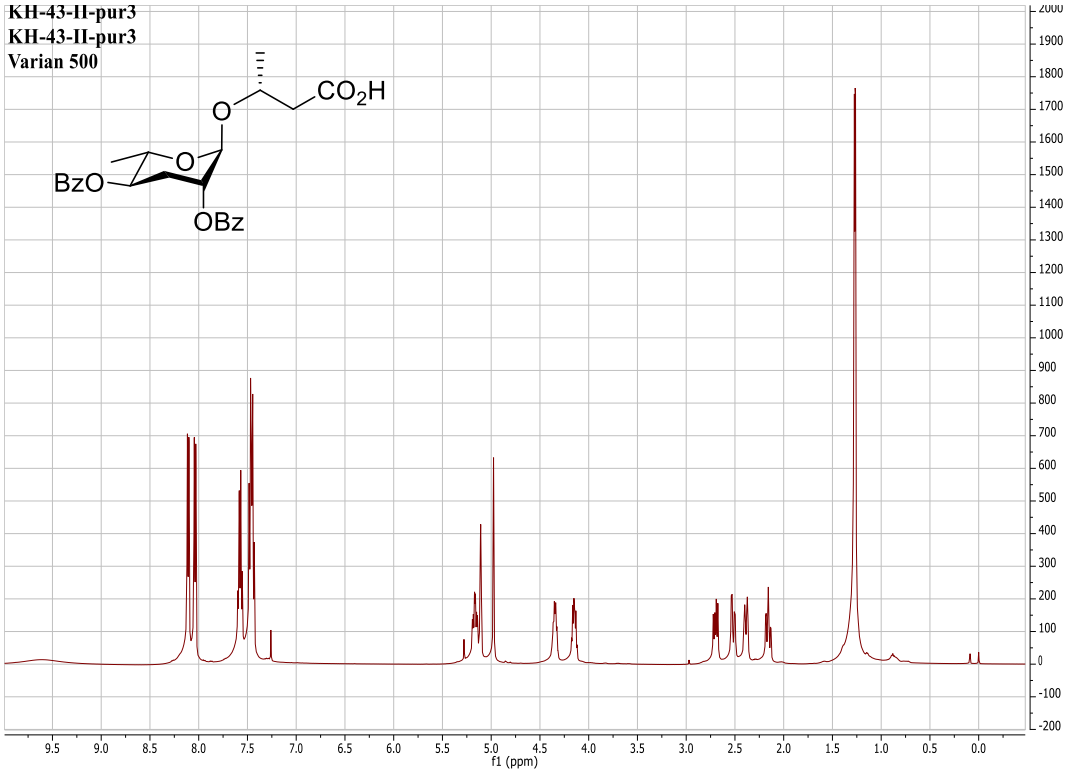

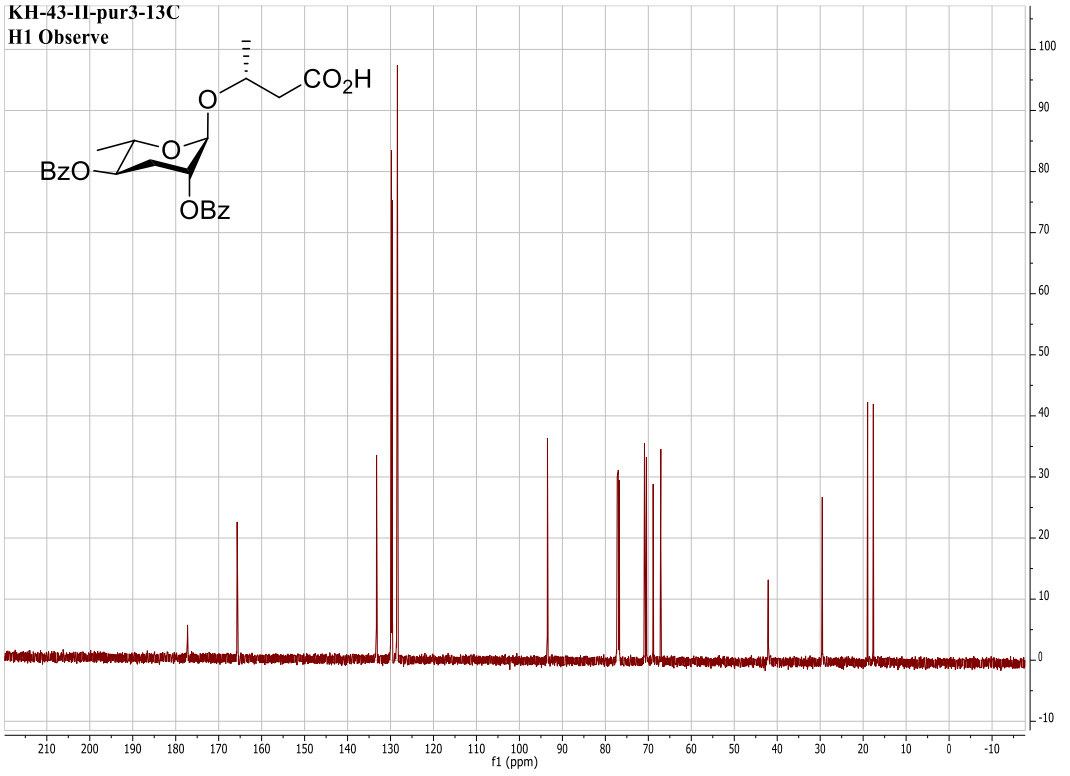

Spectral data for compound **1.10, n=2**:

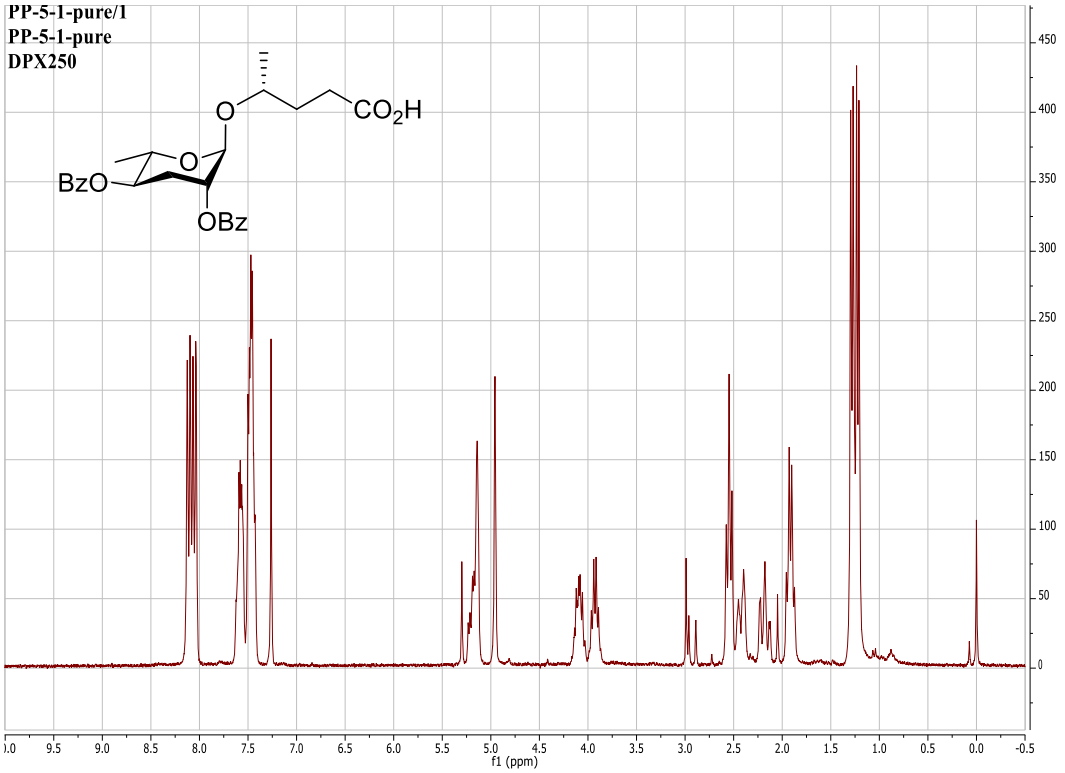

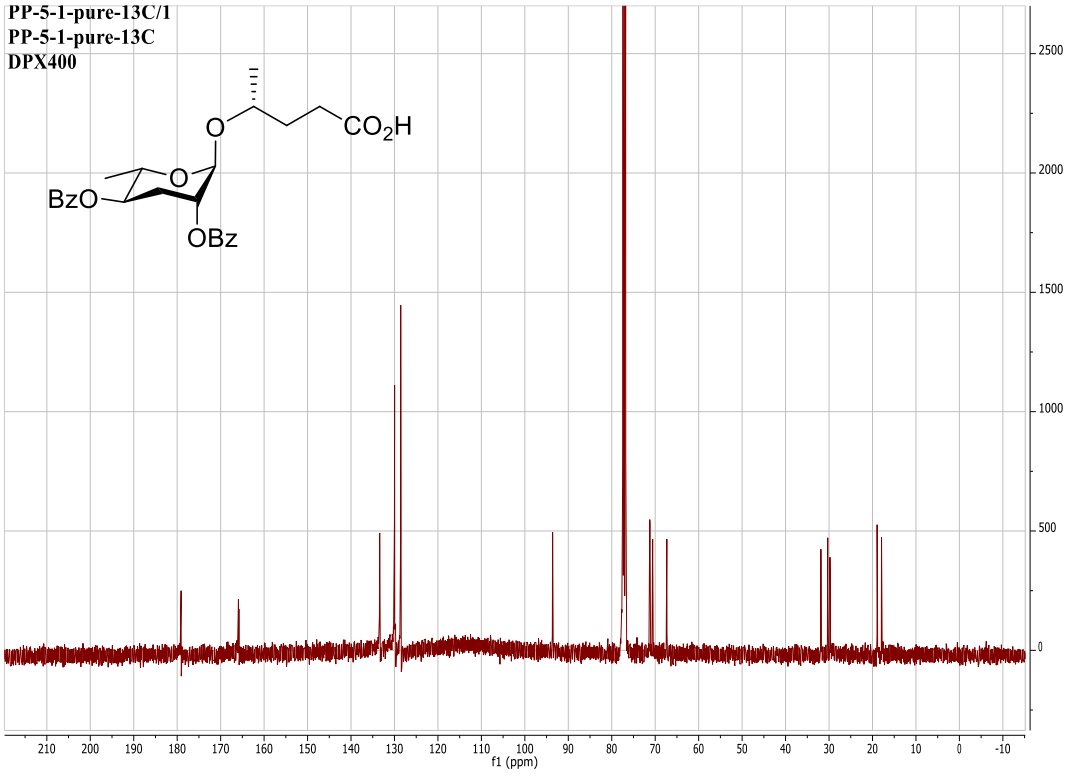

Spectral data for compound **asc-C4**:

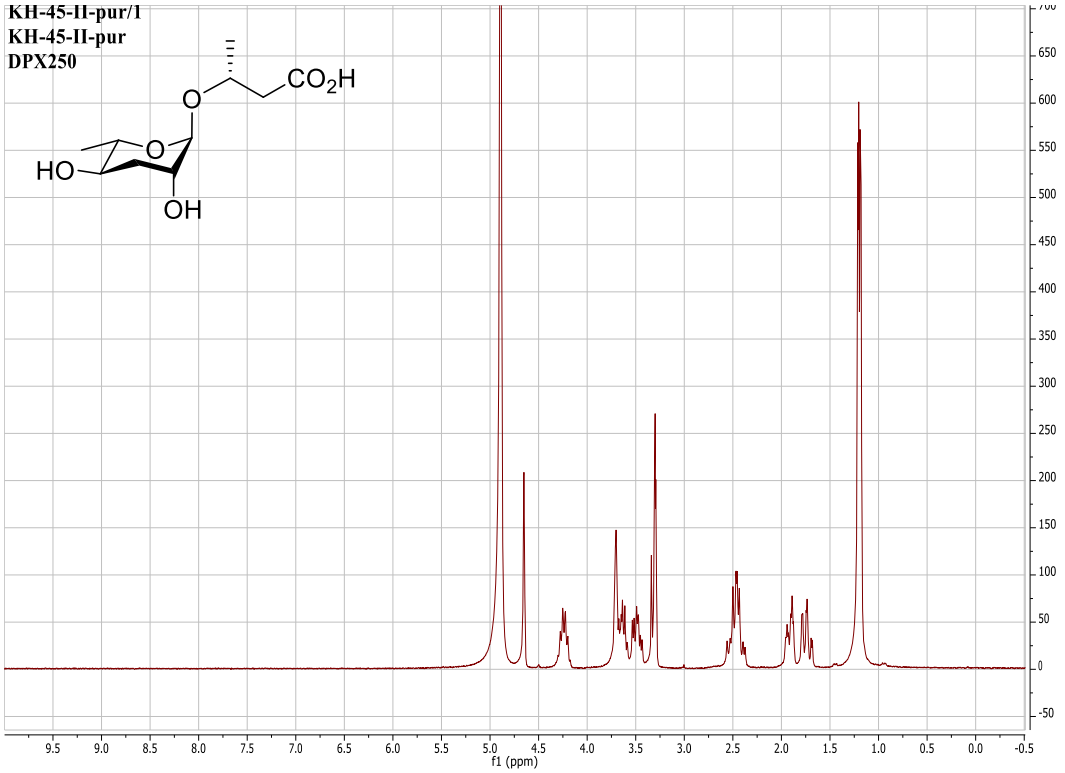

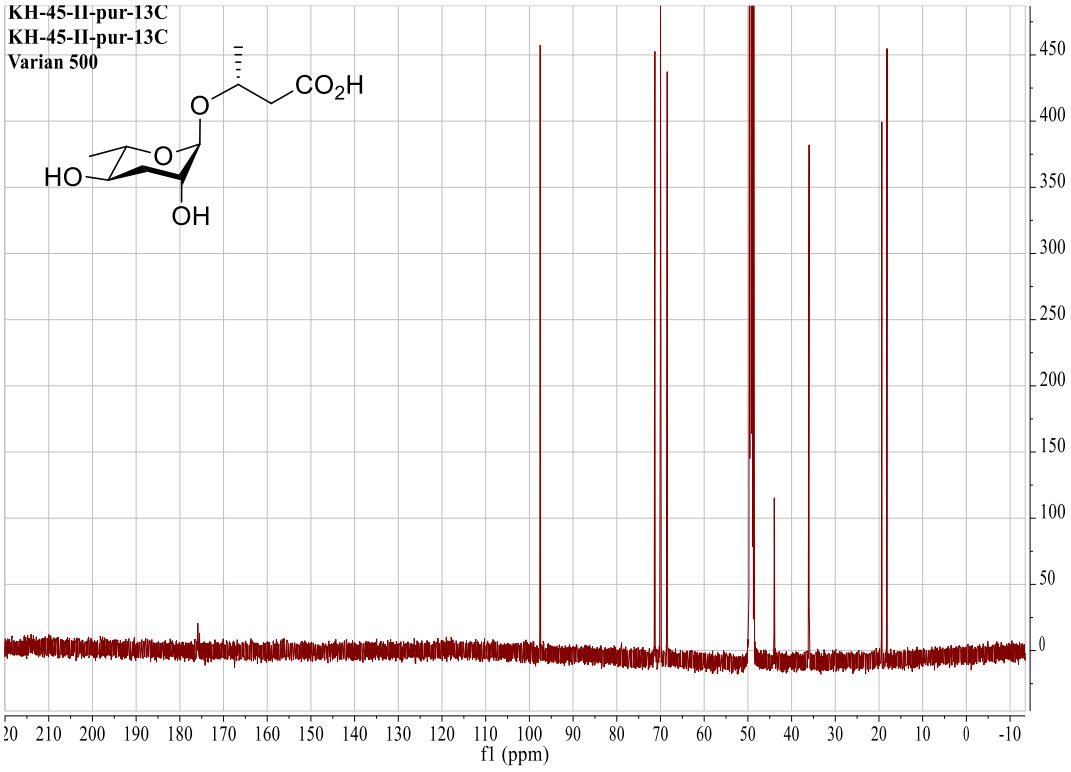

Spectral data for compound **asc-C5**:

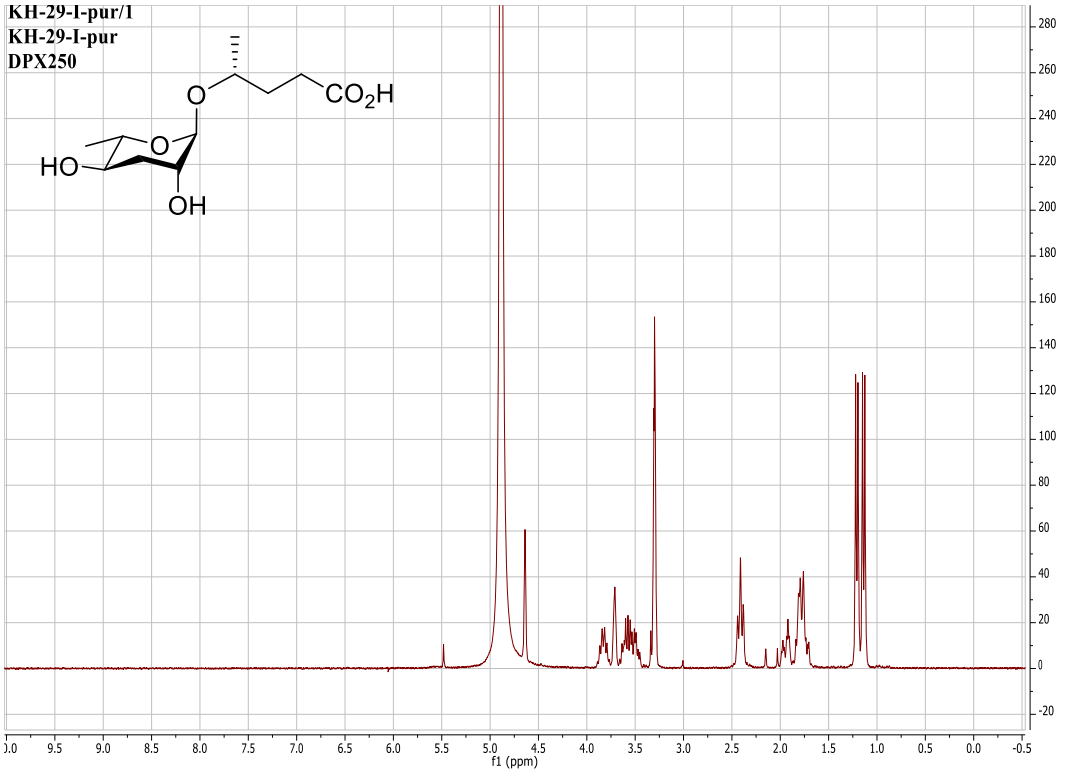

Spectral data for compound **asc-C6-MK:**

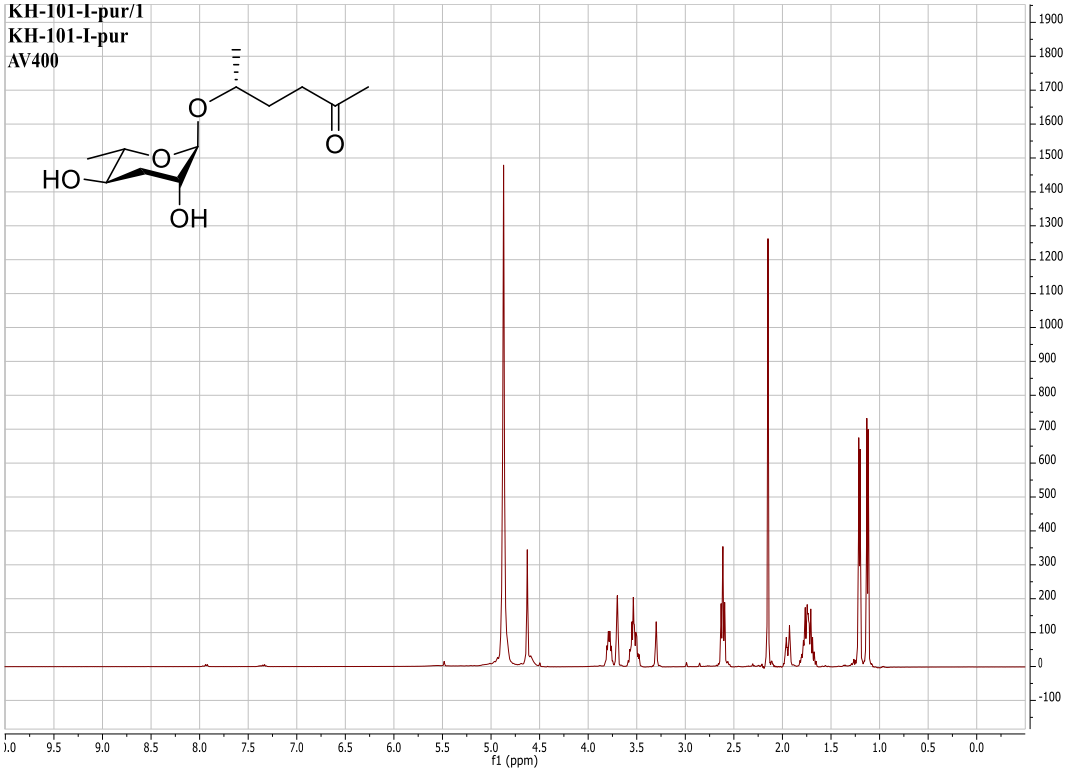

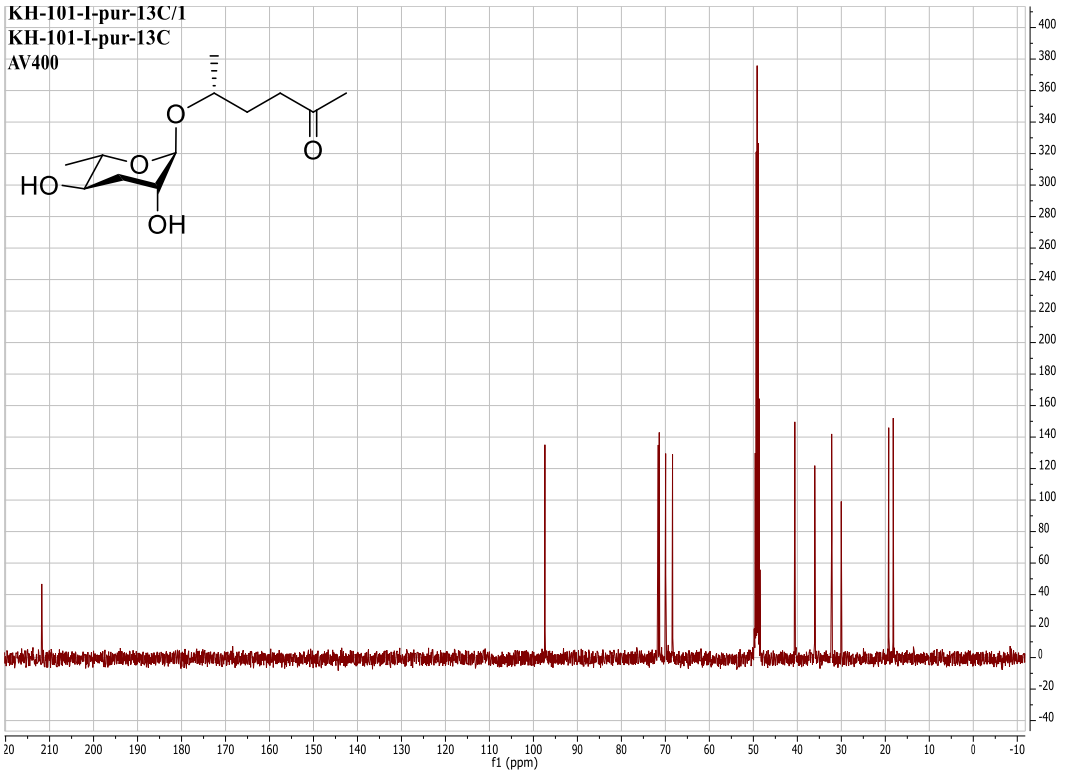

Spectral data for compound **1.6**:

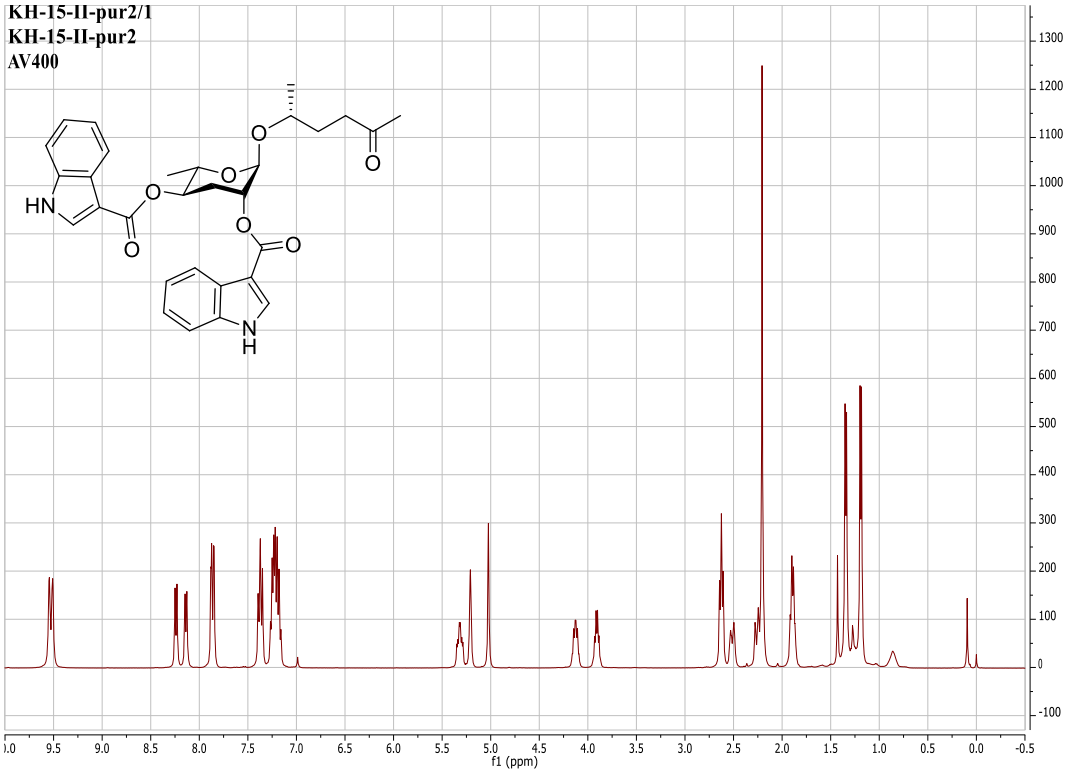

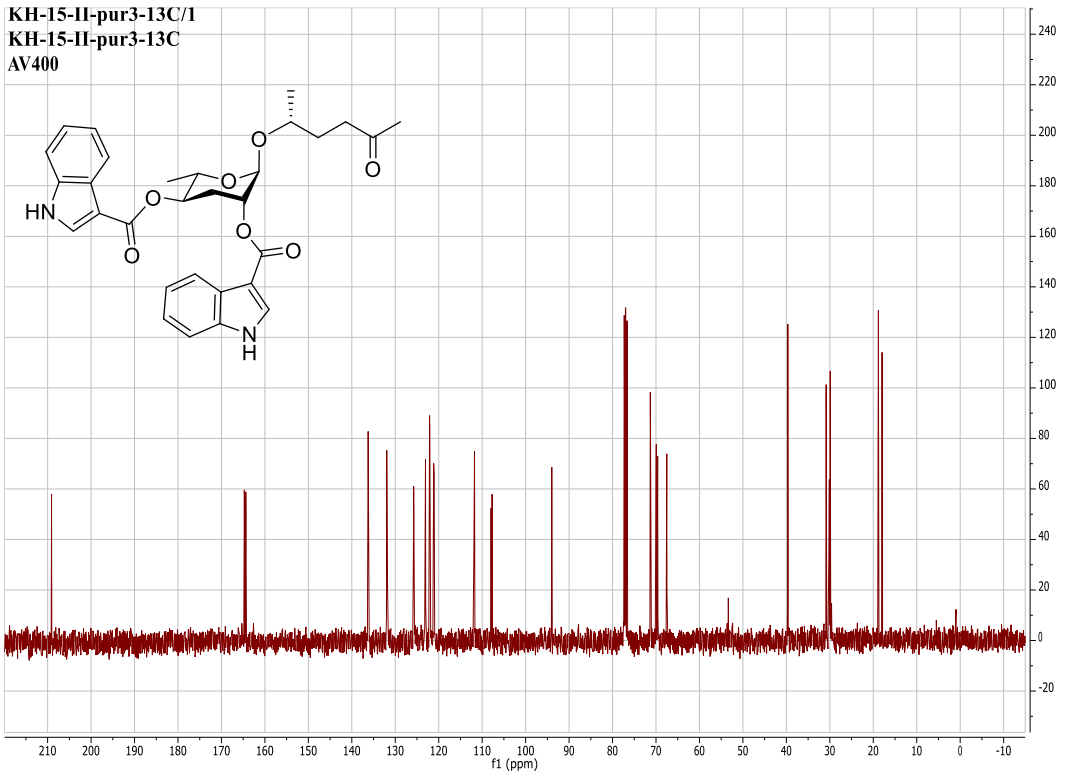

Spectral data for compound **IC-asc-C6-MK:**

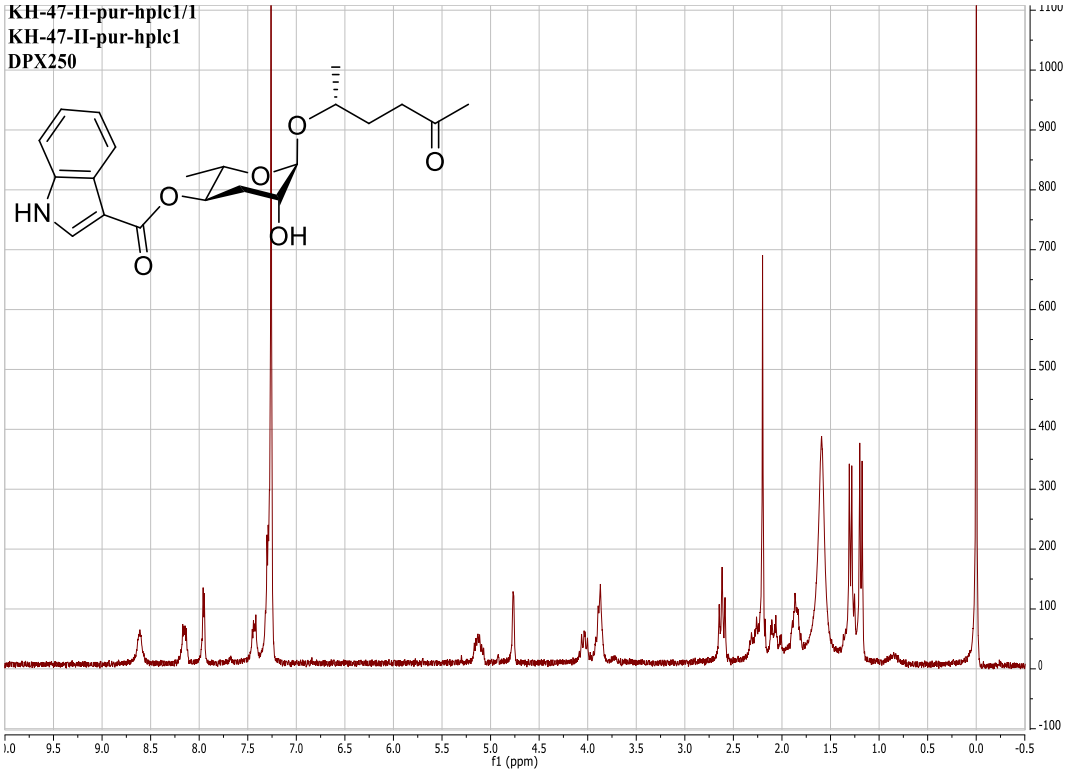

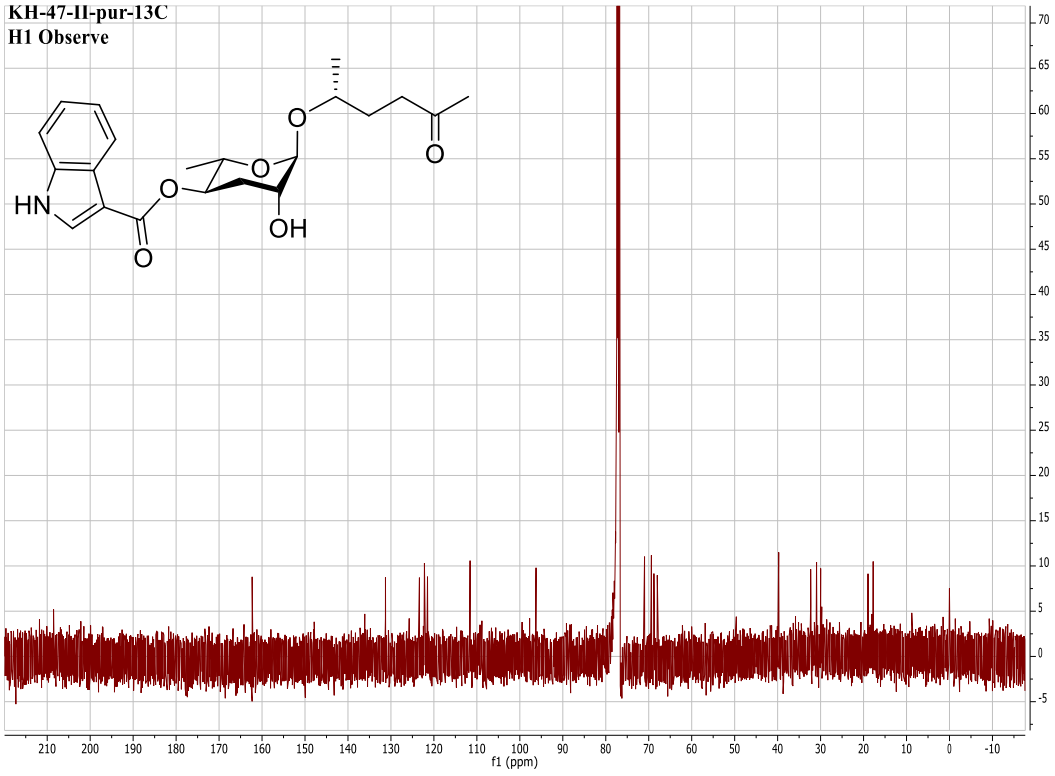

Spectral data for compound **1.7**:

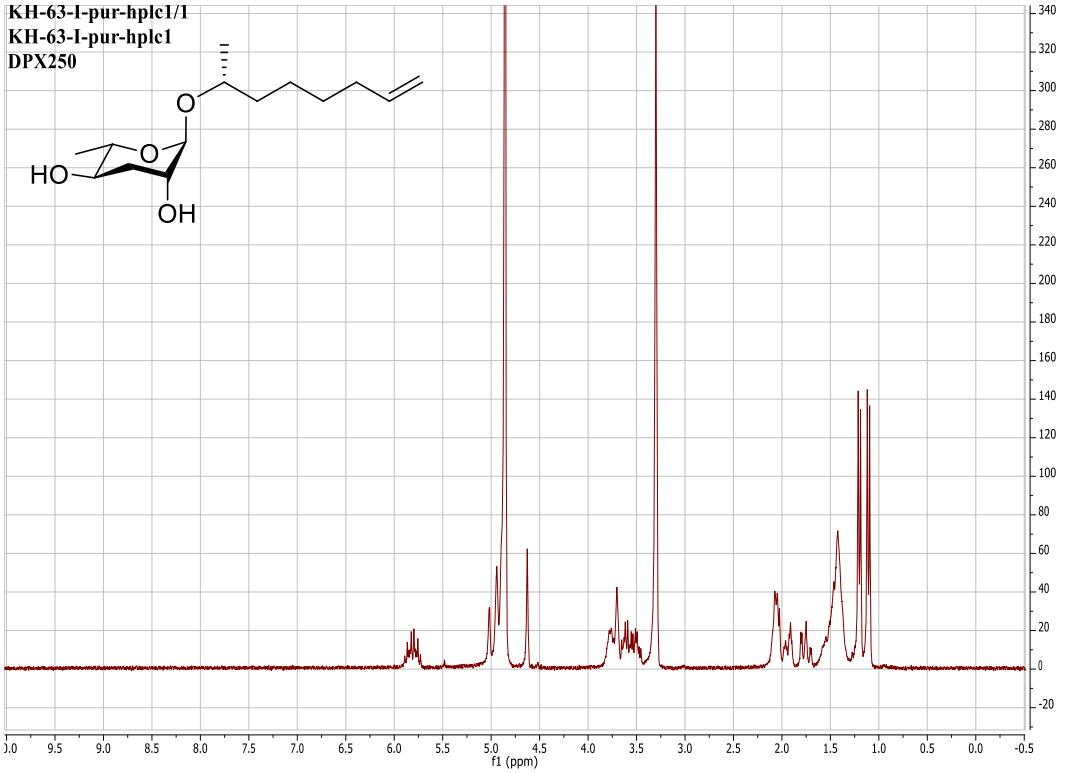

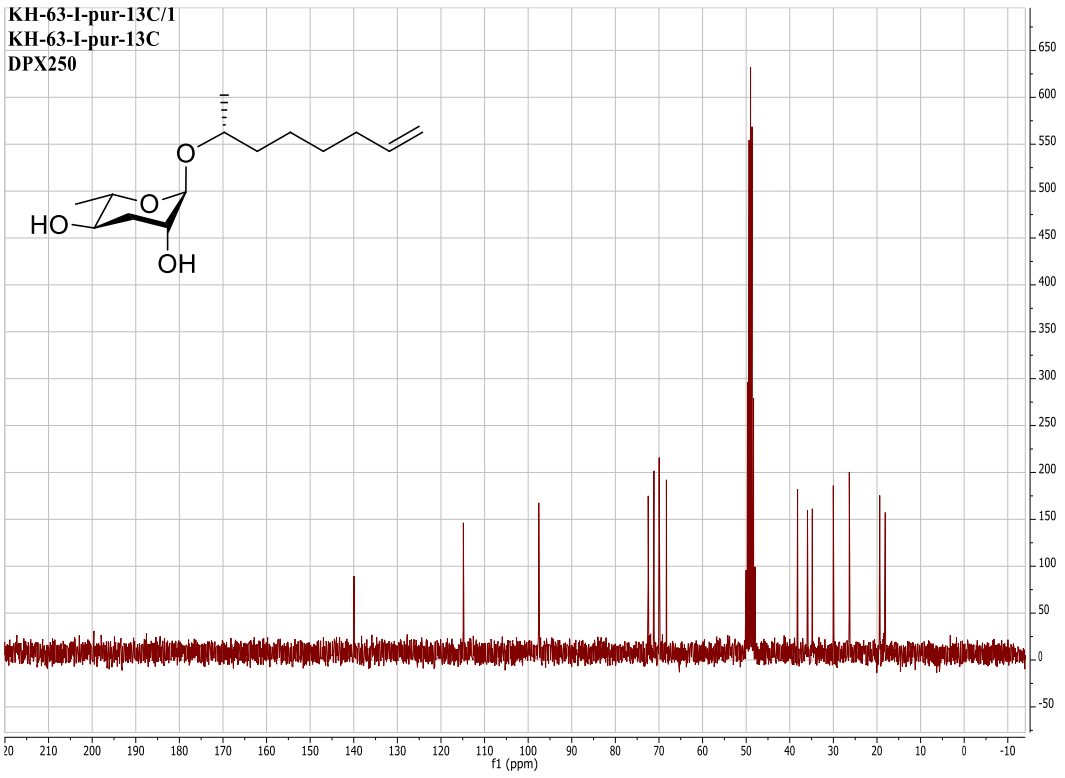

Spectral data for compound **1.8**:

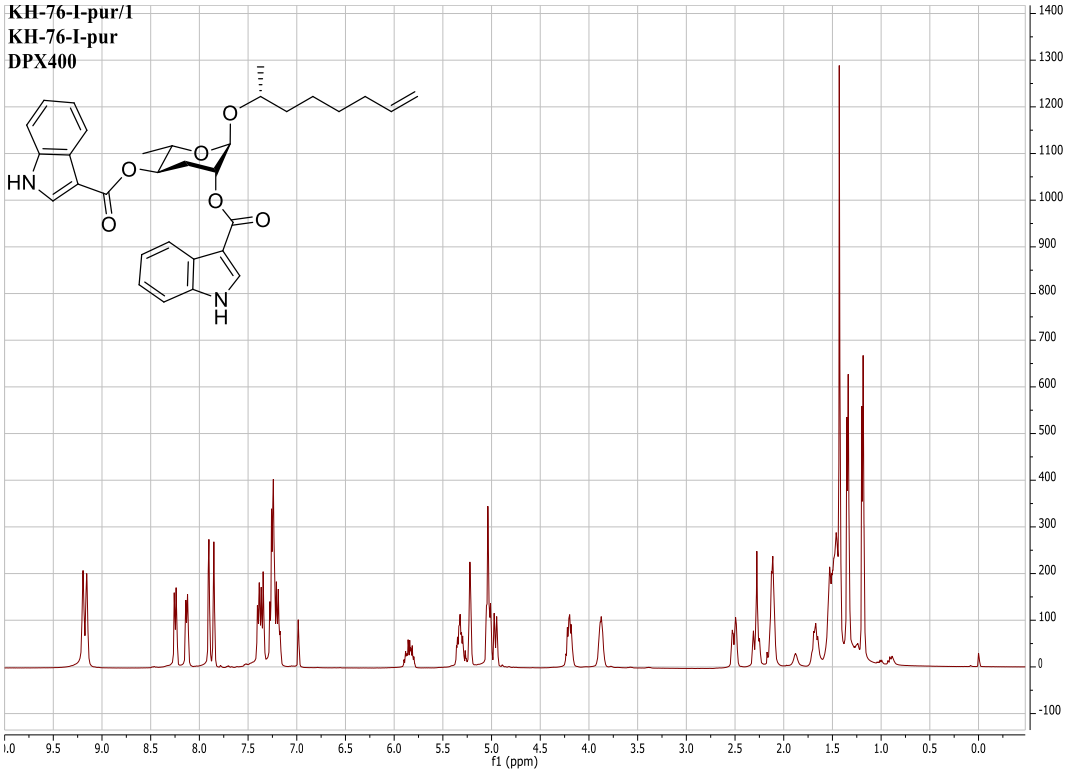

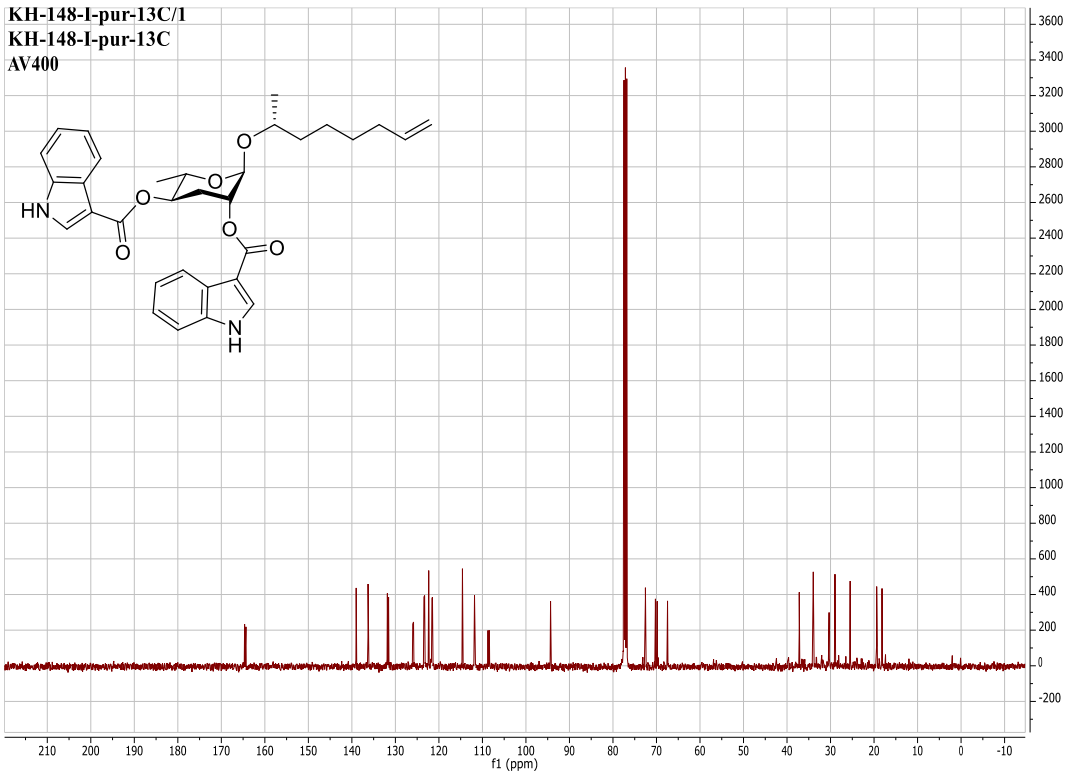

Spectral data for compound **1.9:**

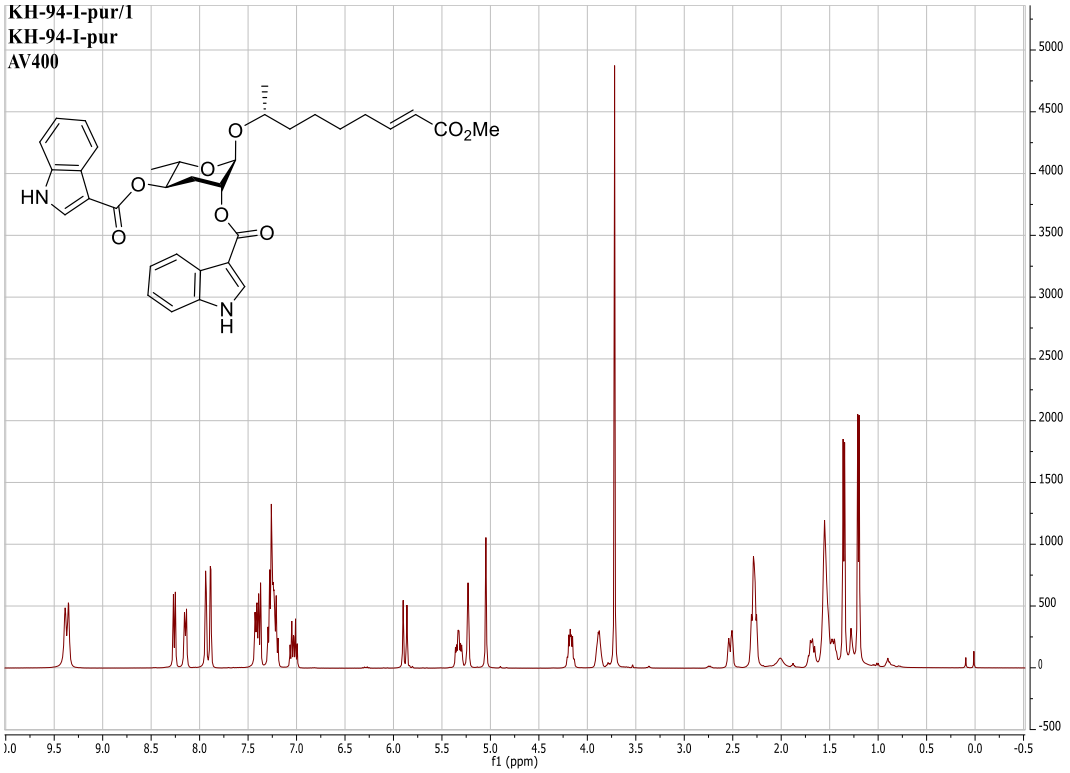

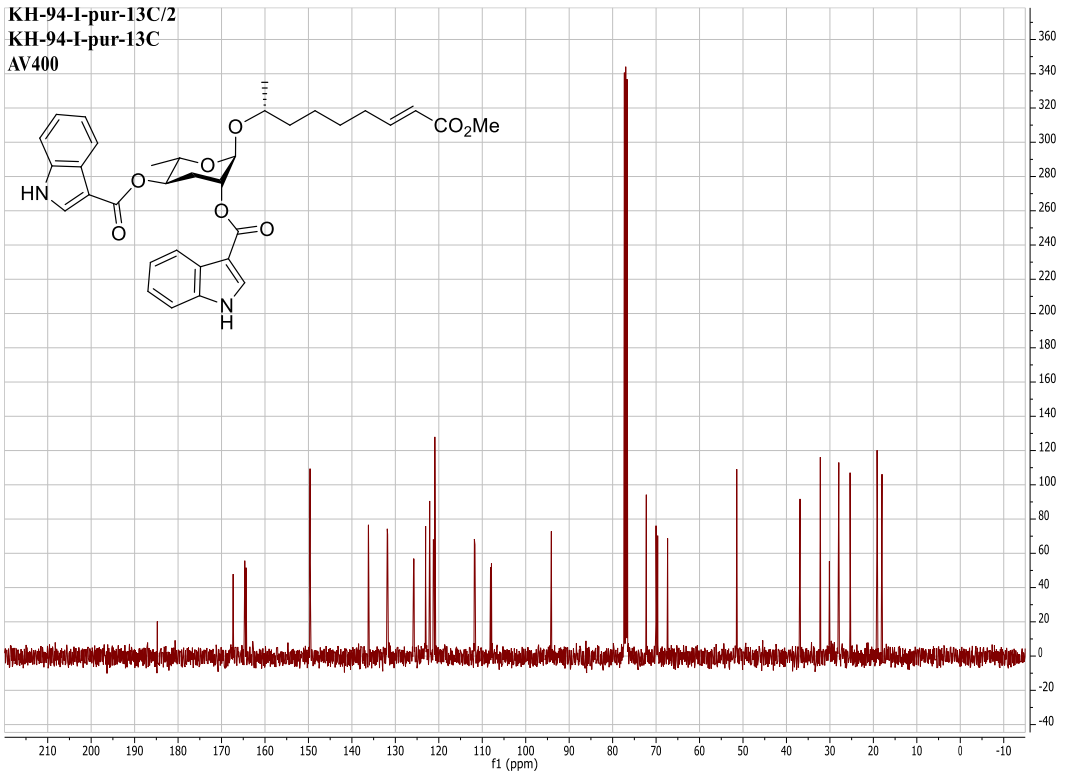

Spectral data for compound **IC-asc-ΔC9:**

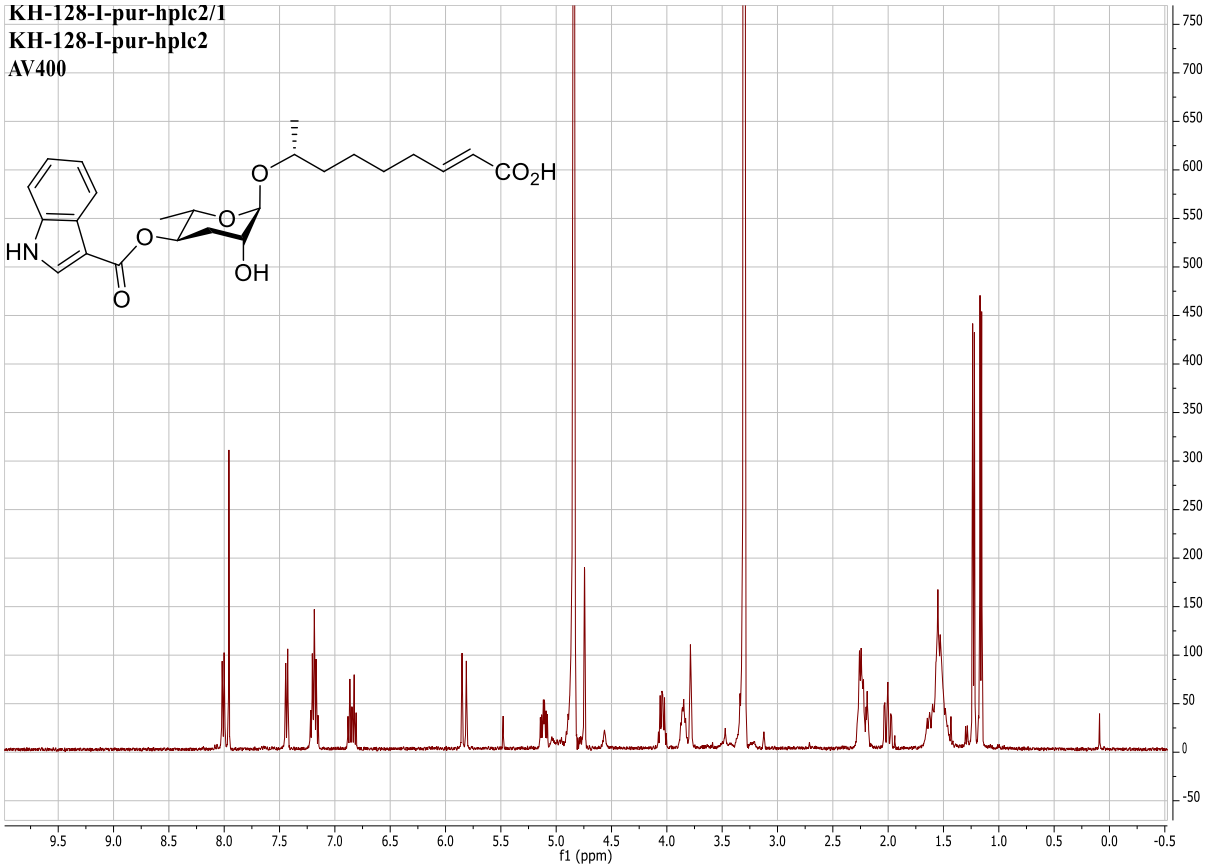

APPENDIX C: NMR SPECTRA OF COMPOUNDS FOUND IN CHAPTER 3

Spectral data for compound **3.8**:

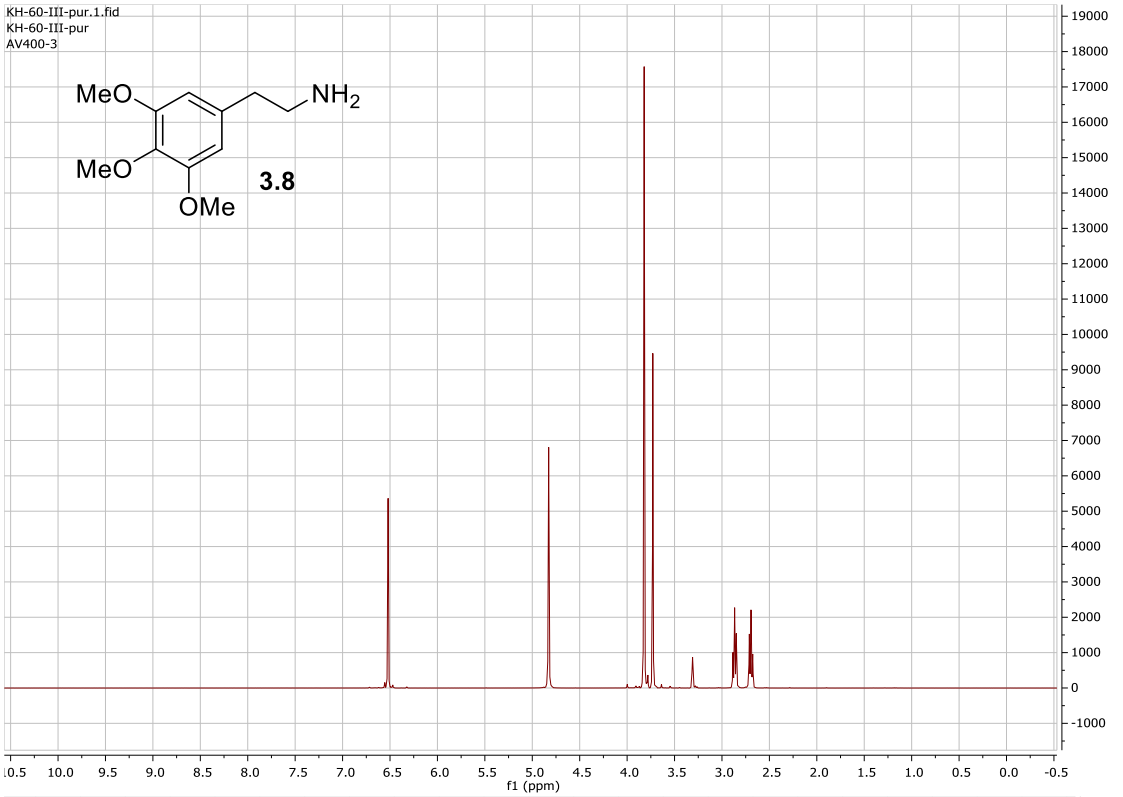

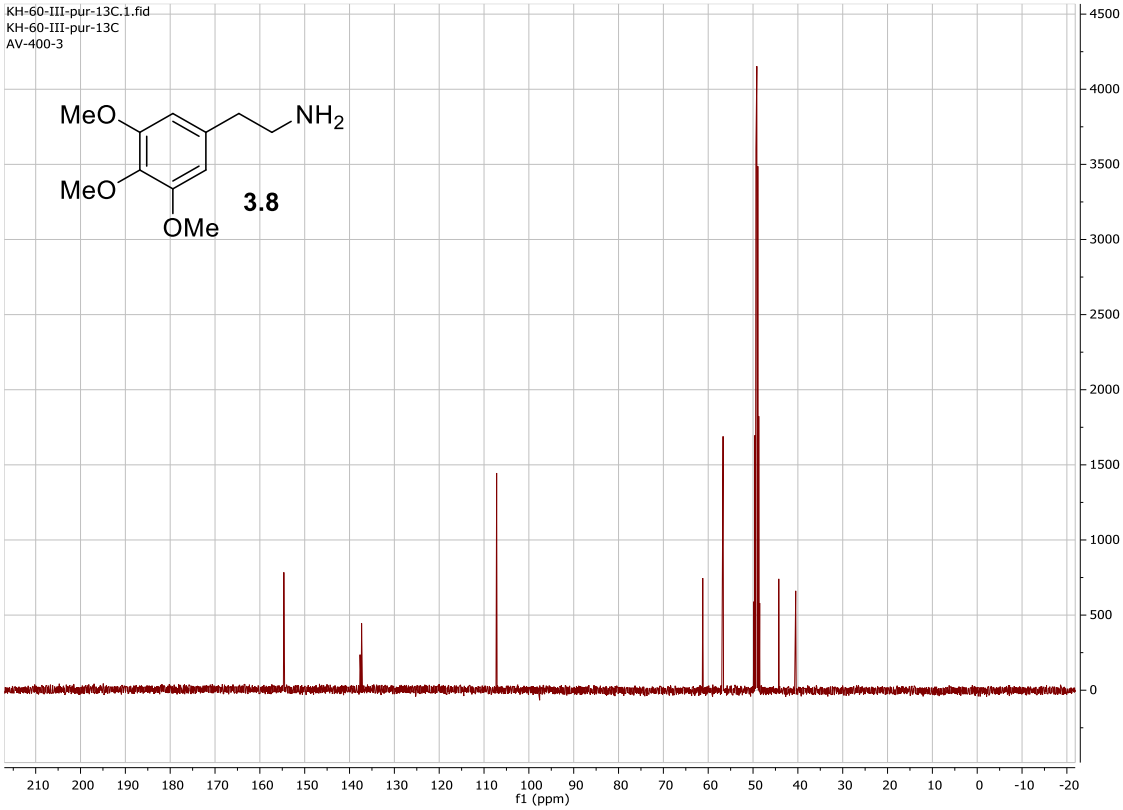

Spectral data for compound **3.8a**:

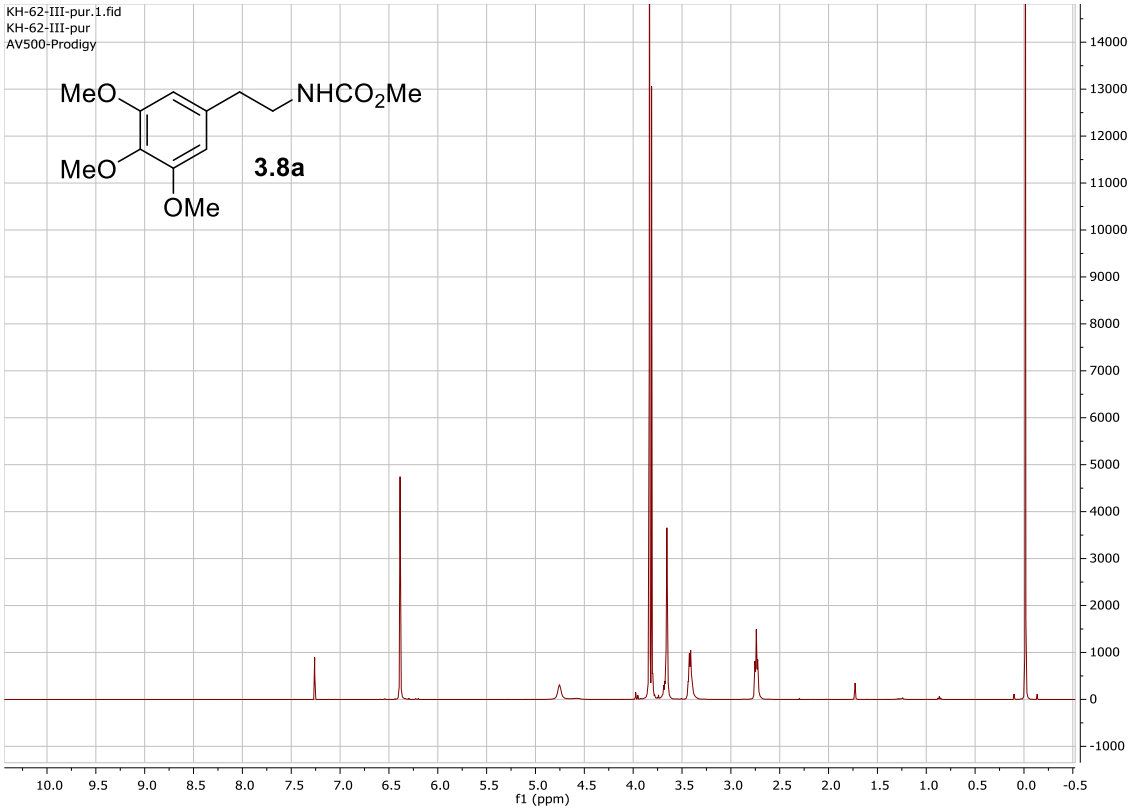

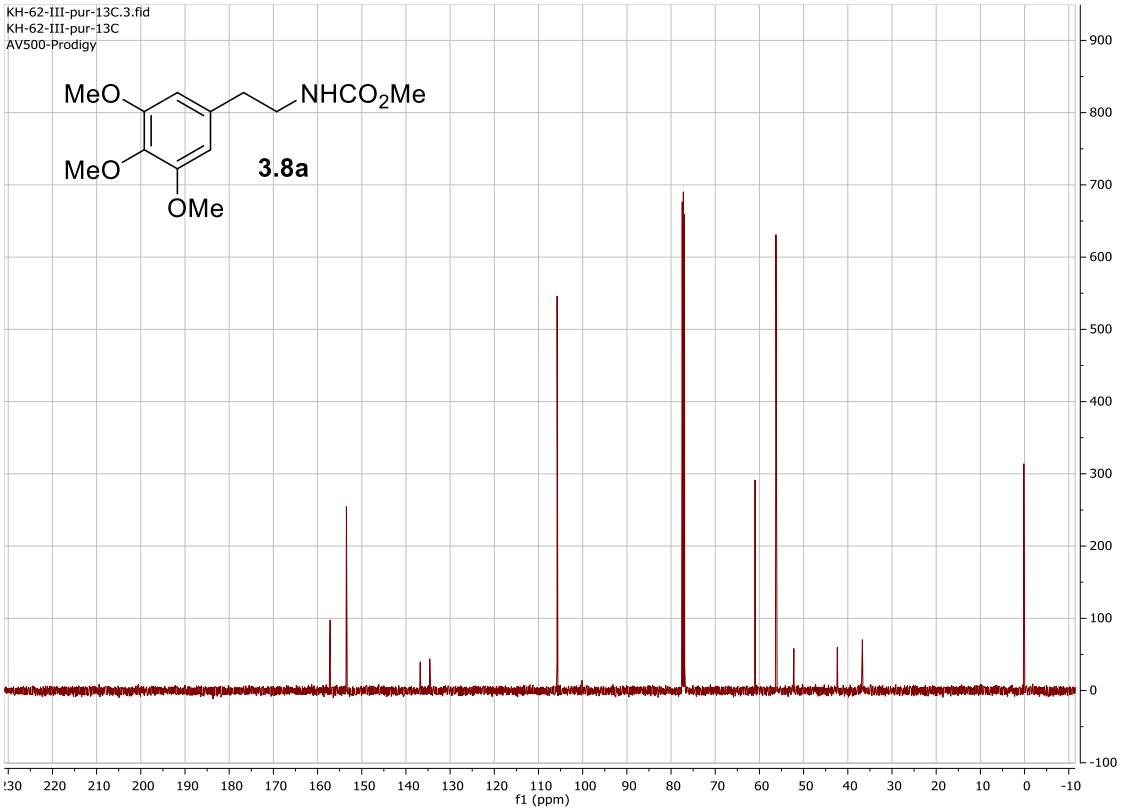

Spectral data for compound **3.9**:

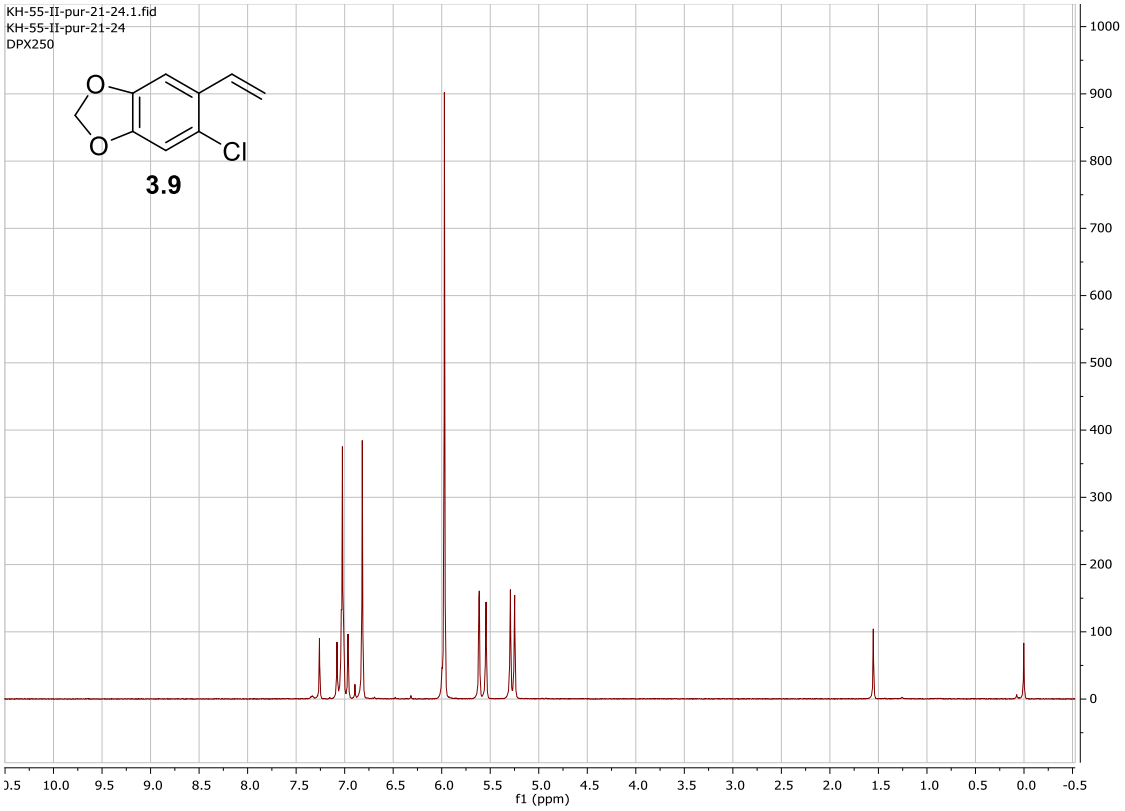

Spectral data for compound **3.11**:

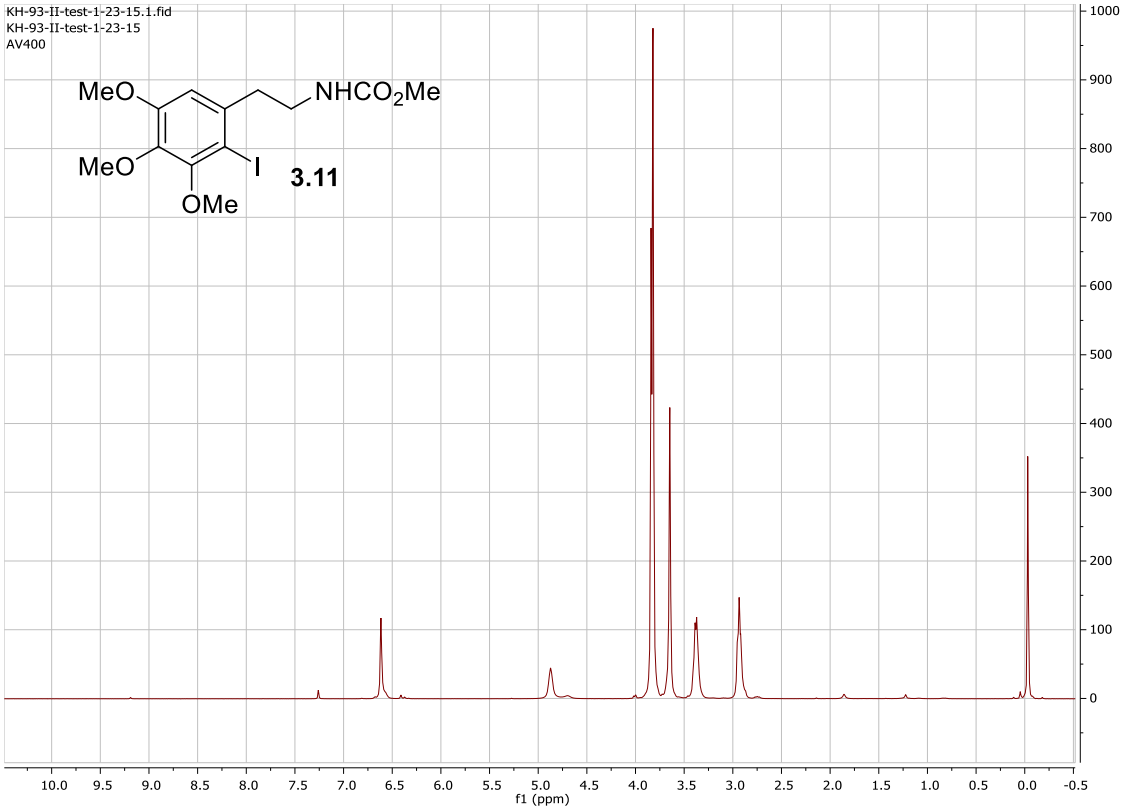

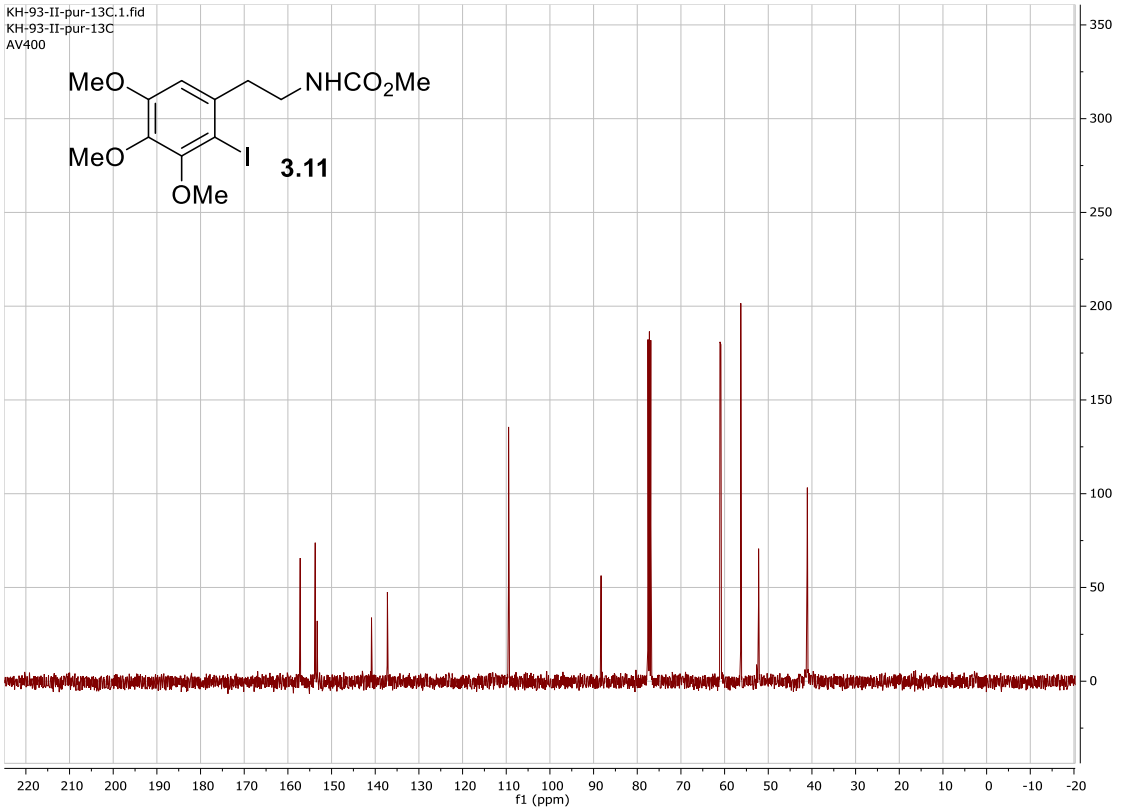

Spectral data for compound **3.12**:

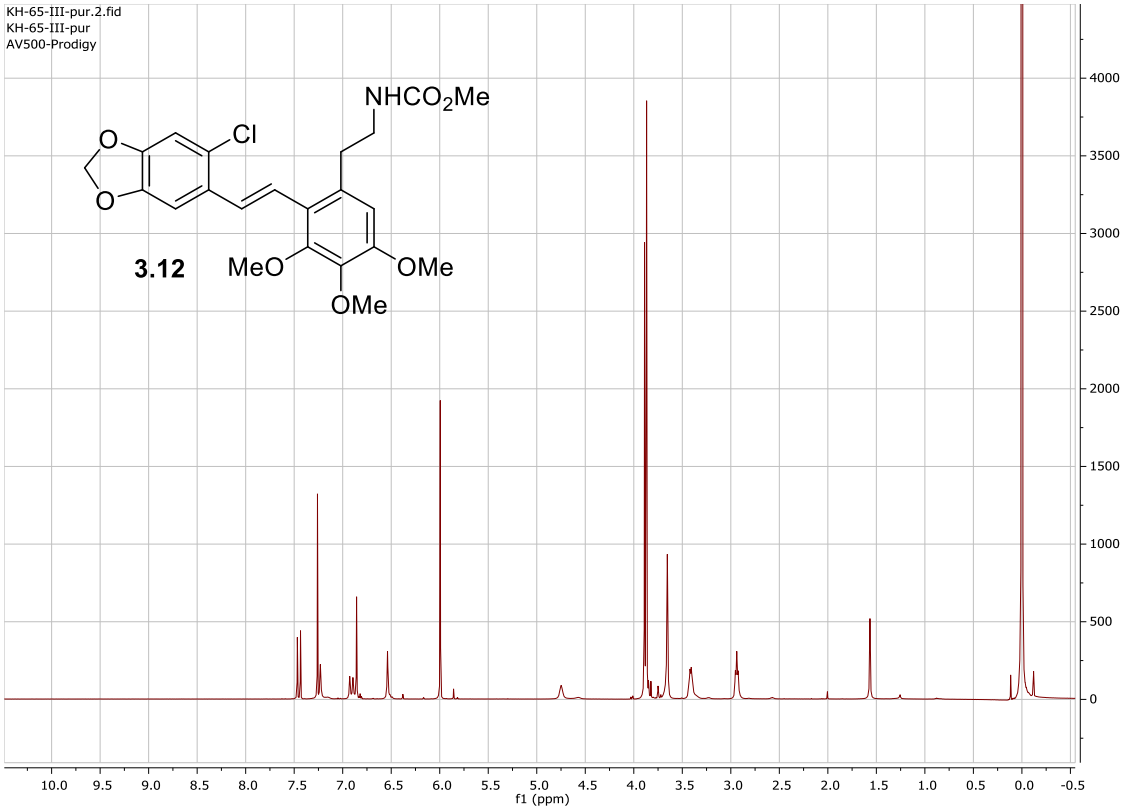

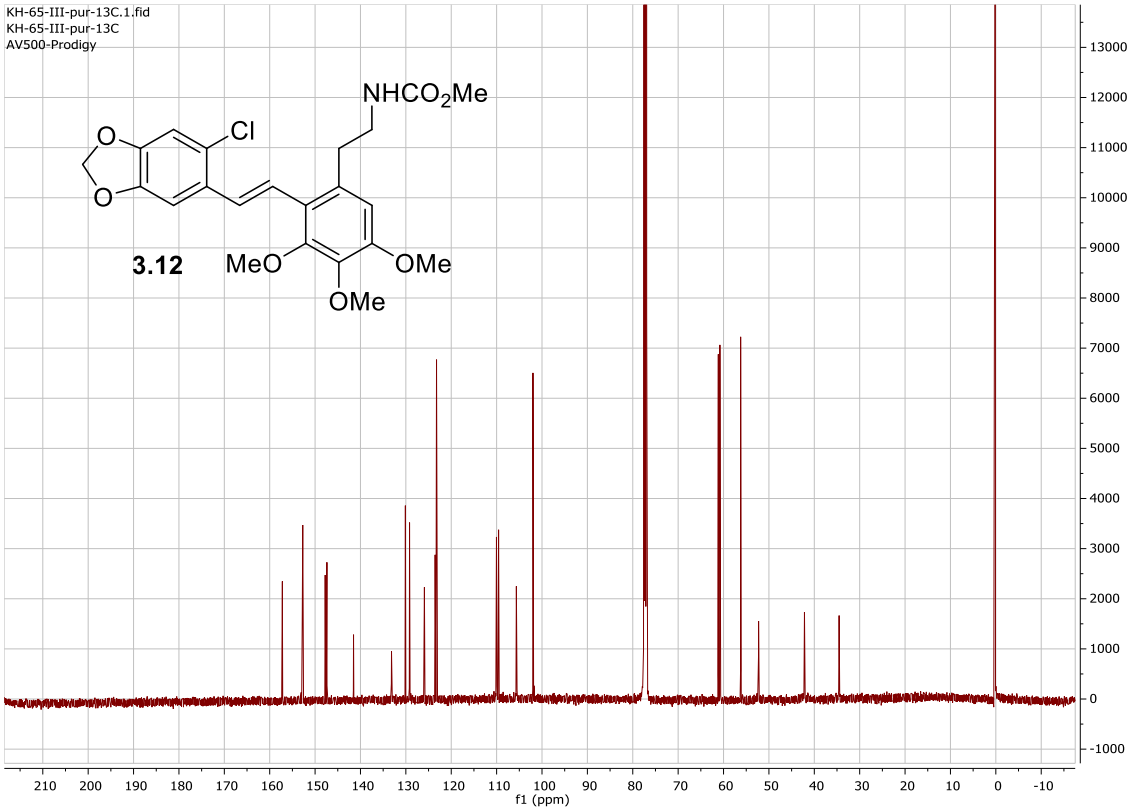

Spectral data for compound **3.5a**:

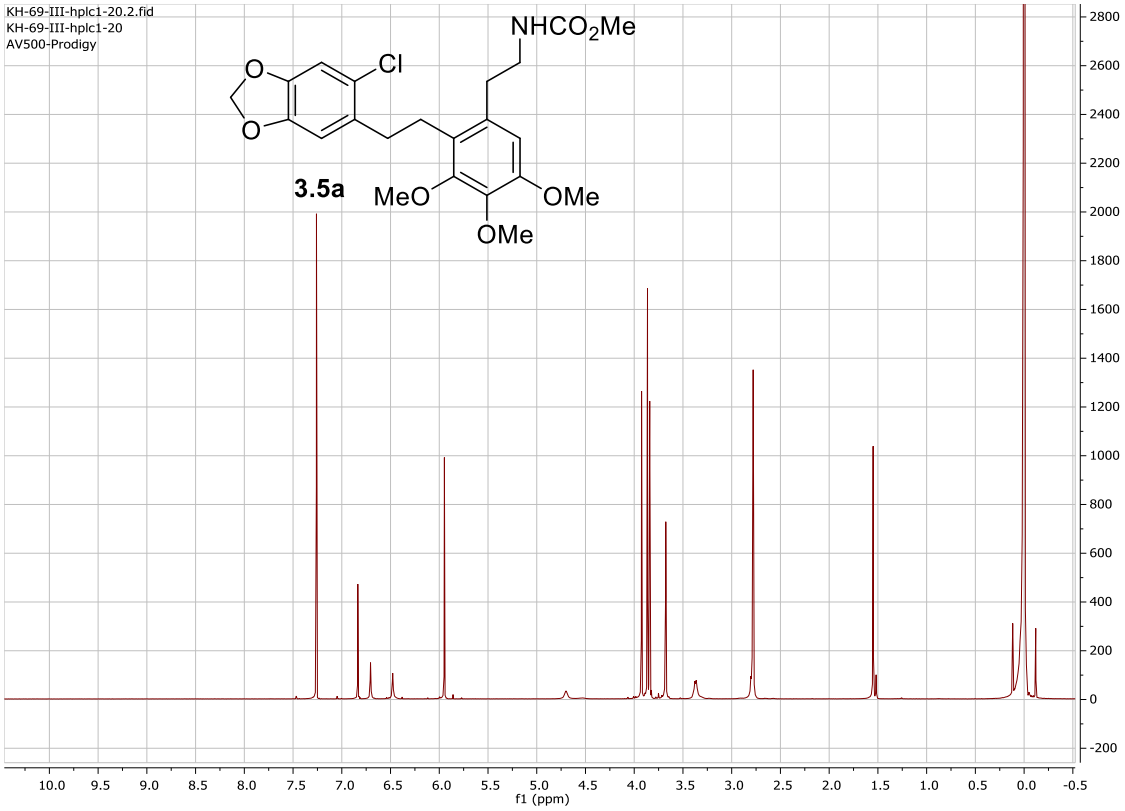

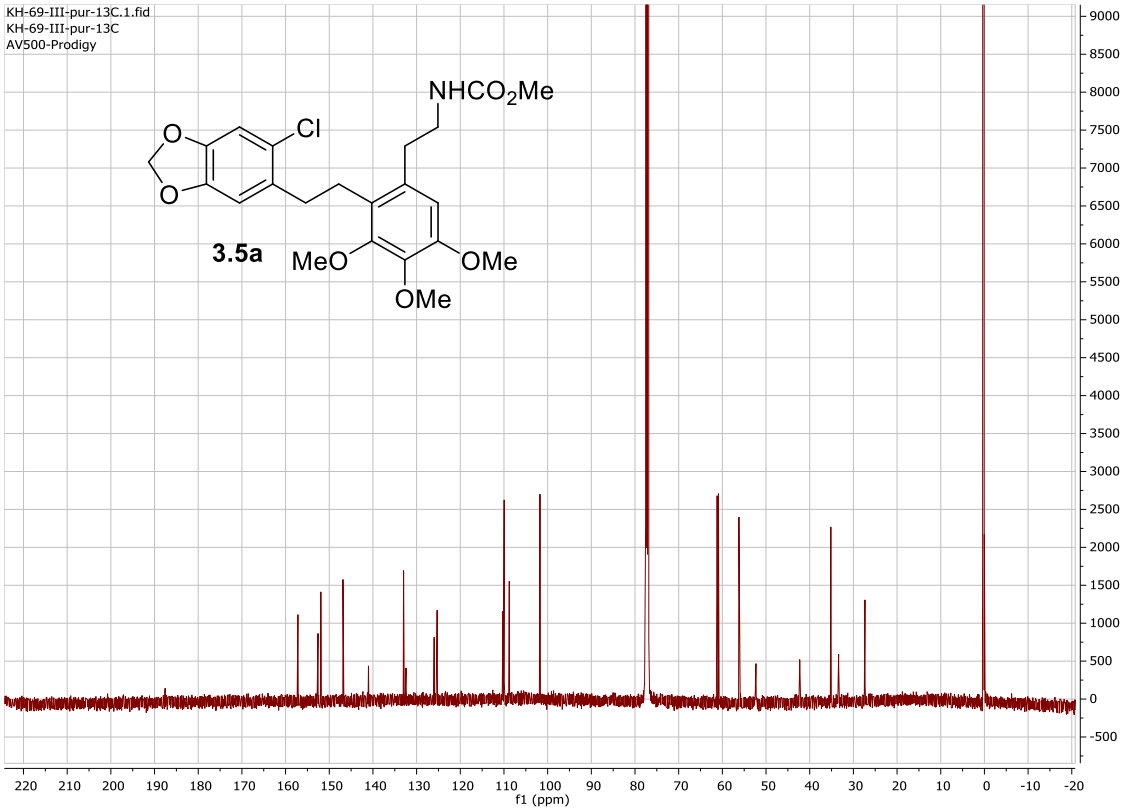

Spectral data for compound **3.12**:

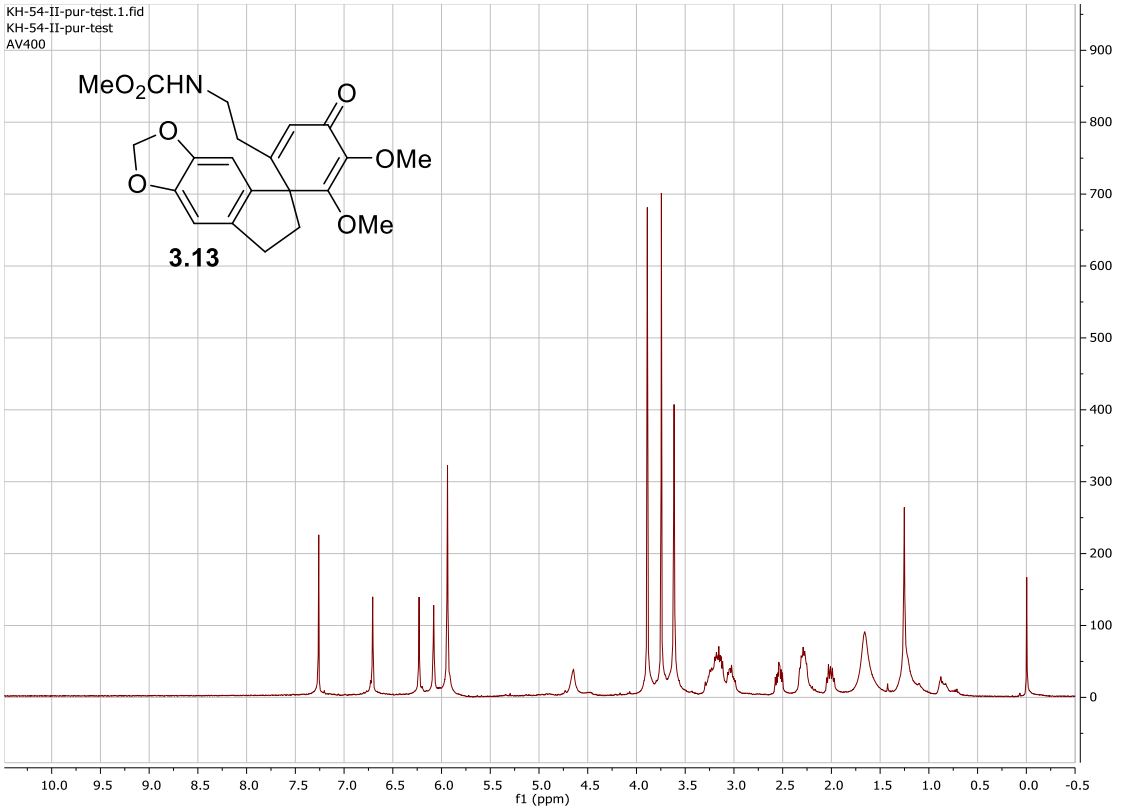

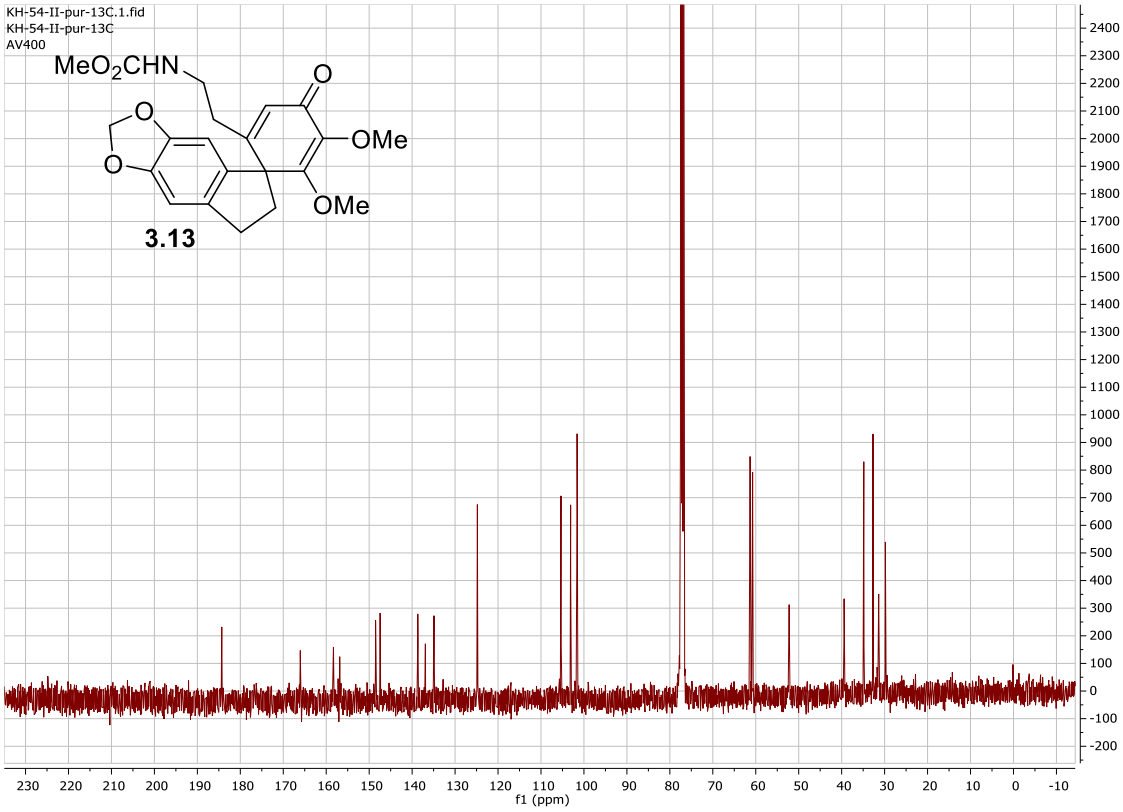

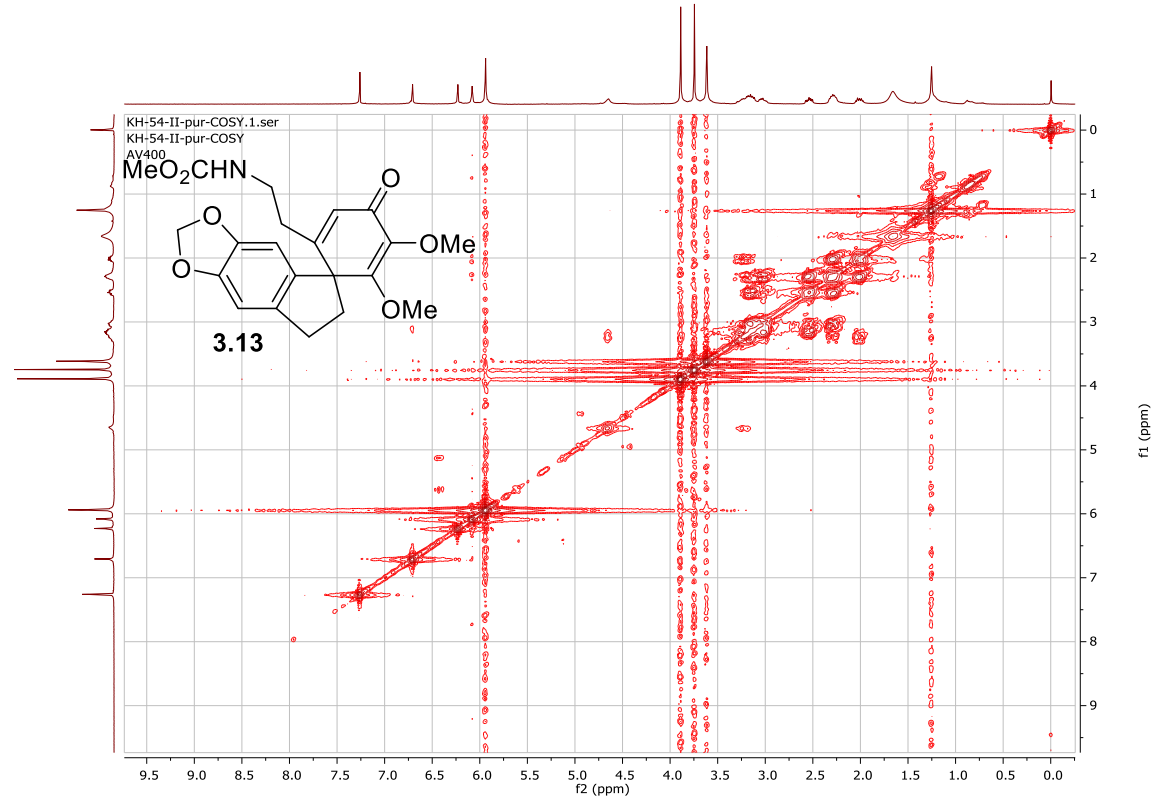
KH-54-II-pur-COSY.1.ser
KH-54-II-pur-COSY
AV400
MeO2CHN
O
O
O
OMe
OMe
3.13
f2 (ppm)
f1 (ppm)

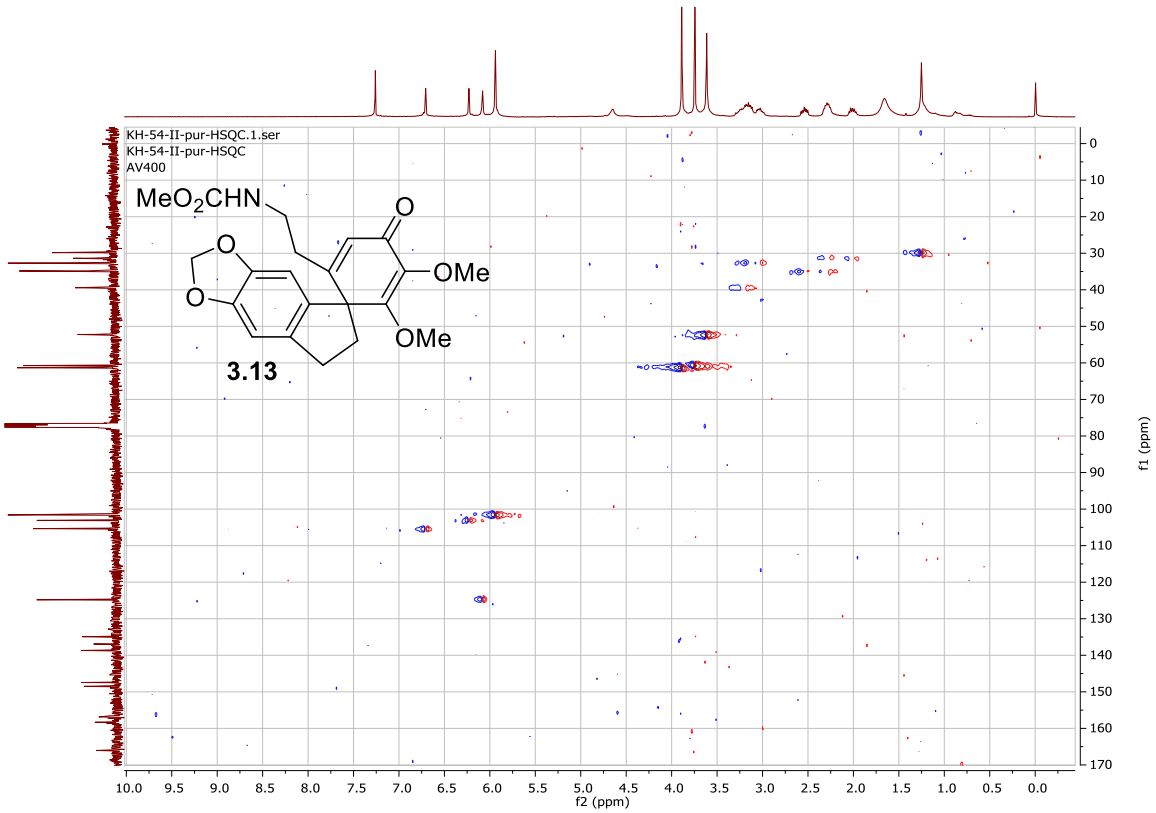
KH-54-II-pur-HSQC.1.ser
KH-54-II-pur-HSQC
AV400
MeO2CHN
O
O
O
OMe
OMe
3.13
f2 (ppm)
f1 (ppm)

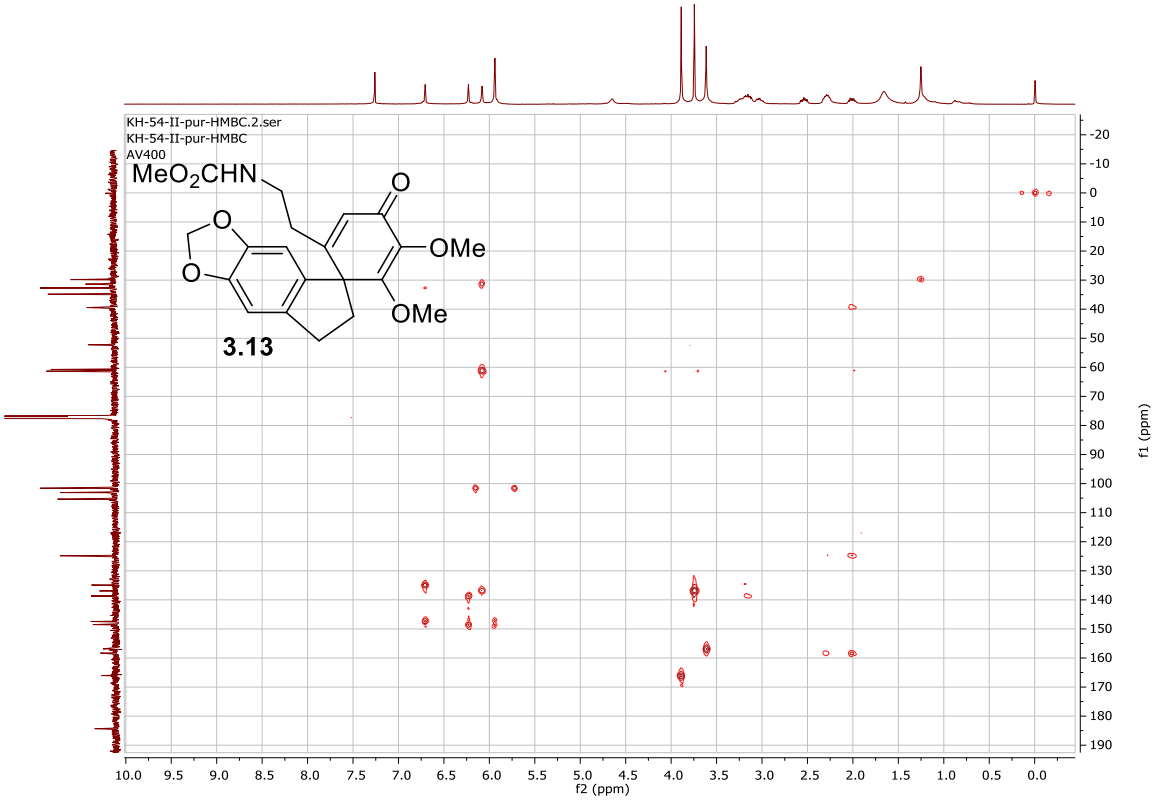
KH-54-II-pur-HMBC.2.ser
KH-54-II-pur-HMBC
AV400
MeO2CHN
O
O
O
OMe
OMe
3.13
f2 (ppm)
f1 (ppm)

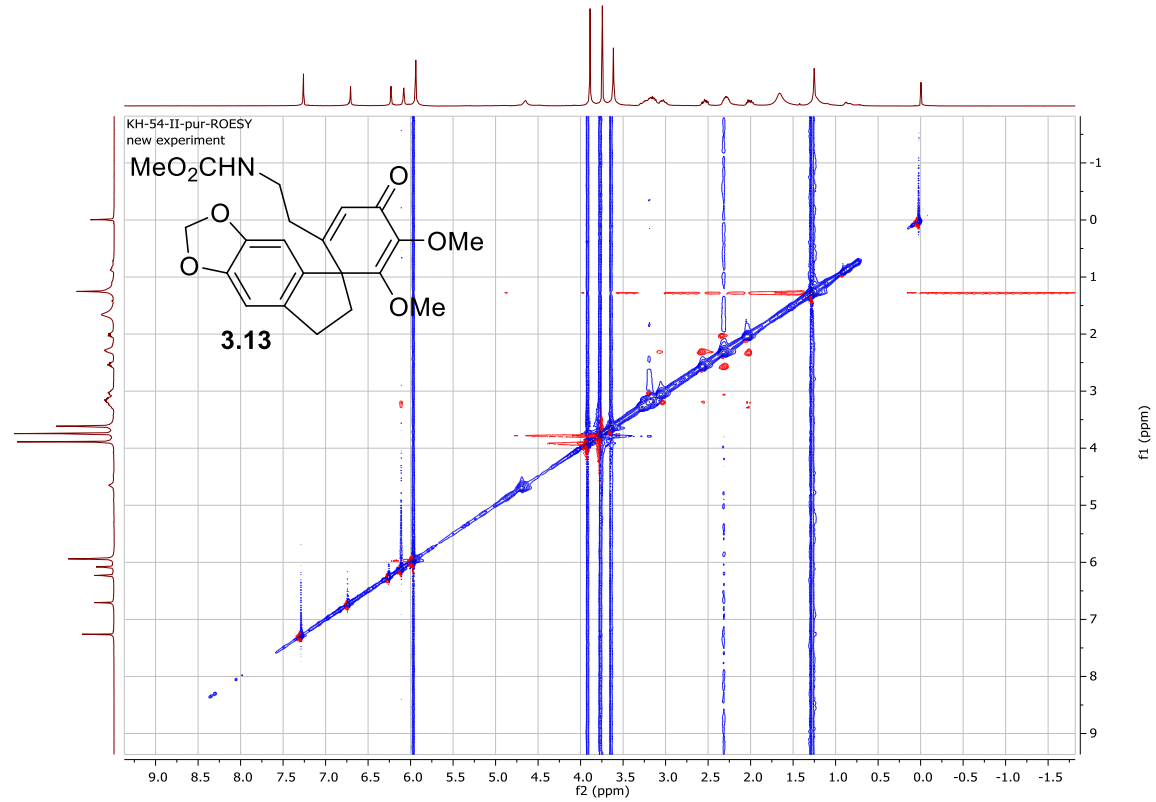
KH-54-II-pur-ROESY
new experiment
MeO2CHN
O
O
O
OMe
OMe
3.13
f2 (ppm)
f1 (ppm)

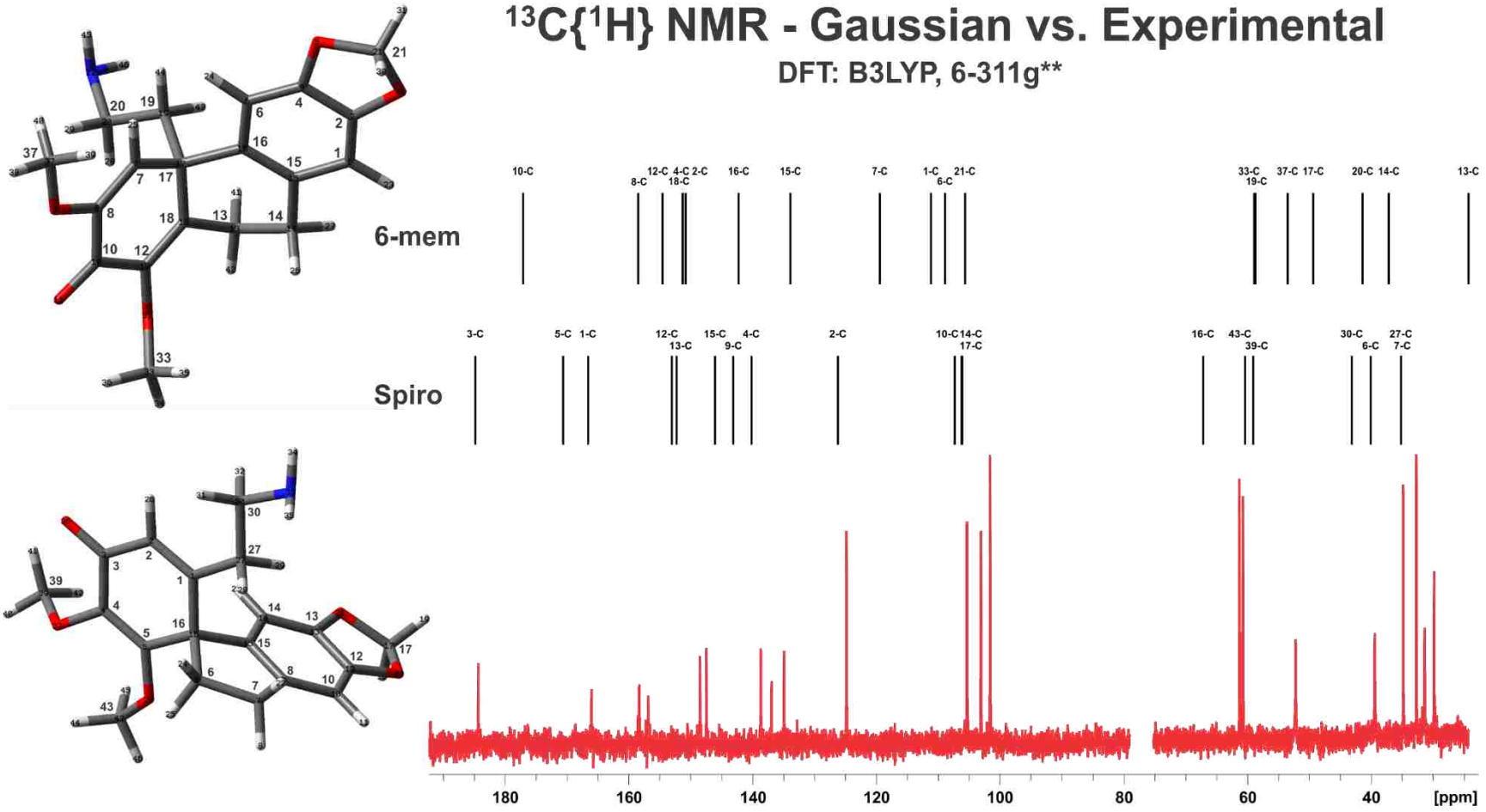
13C{1H} NMR - Gaussian vs. Experimental
DFT: B3LYP, 6-311g**
6-mem
Spiro
10-C
8-C
12-C
4-C
18-C
2-C
16-C
15-C
7-C
1-C
6-C
21-C
33-C
19-C
37-C
17-C
20-C
14-C
13-C
3-C
5-C
1-C
12-C
13-C
15-C
9-C
4-C
2-C
10-C
14-C
17-C
16-C
43-C
39-C
30-C
6-C
27-C
7-C
180
160
140
120
100
80
60
40
[ppm]

APPENDIX D: NMR SPECTRA OF COMPOUNDS FOUND IN CHAPTER 4

Spectral data for compound **4.5**:

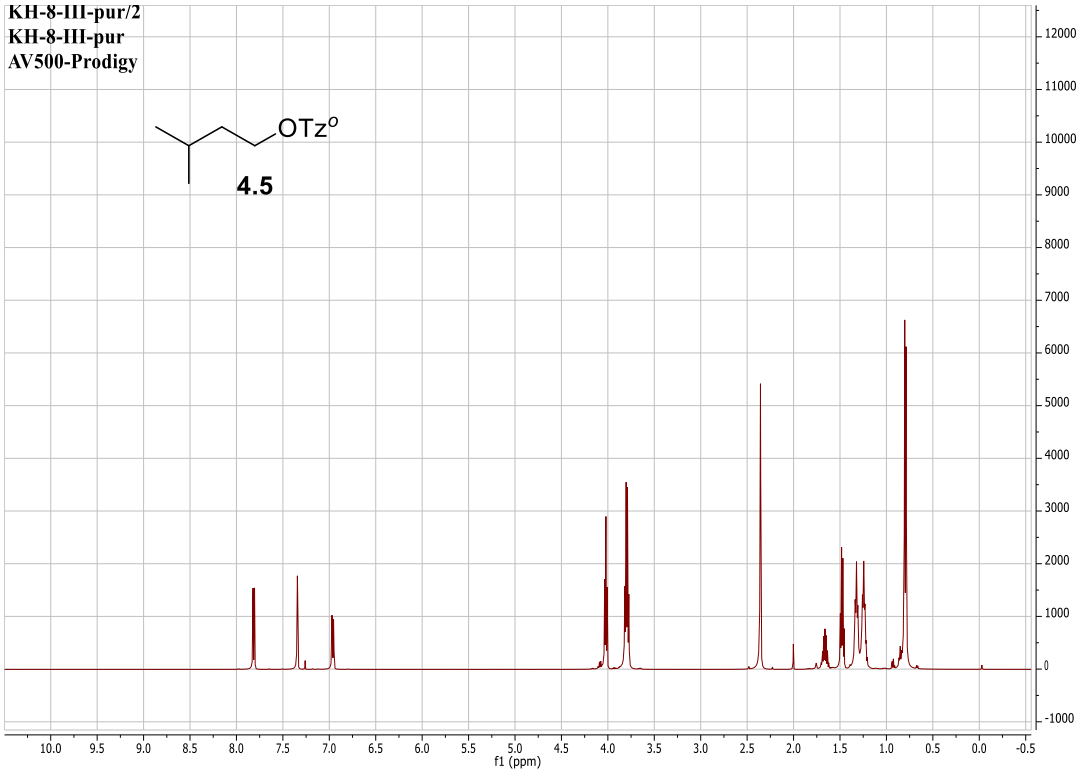

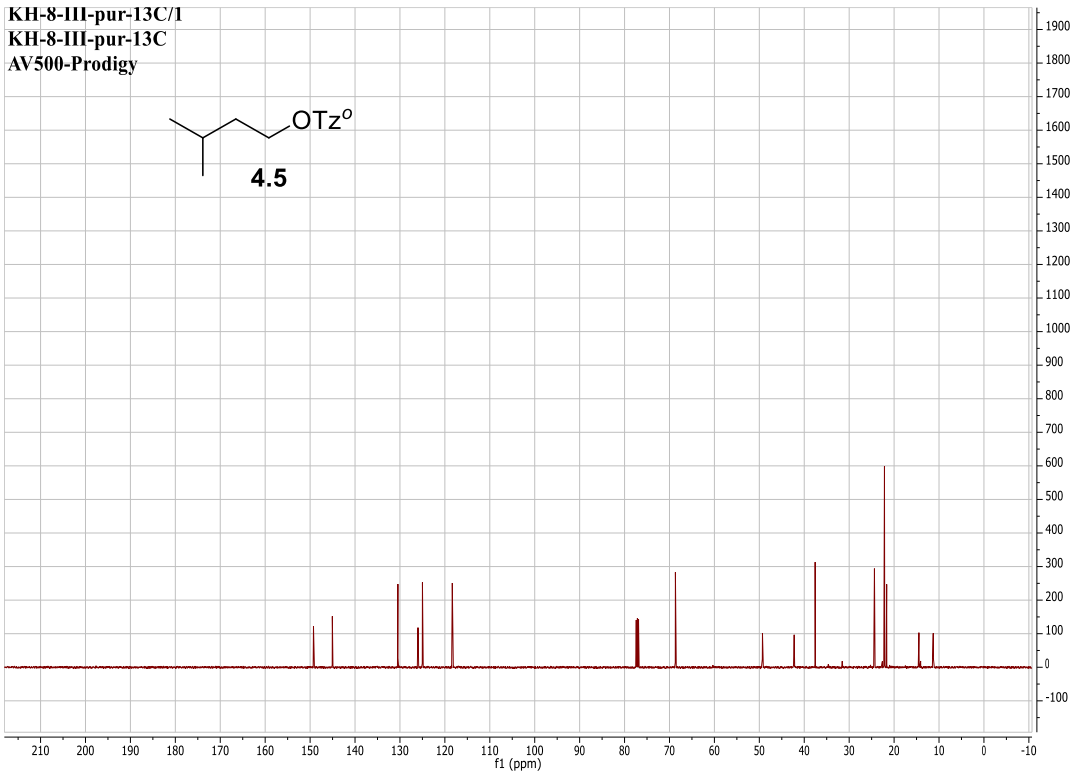

Spectral data for compound **4.10**:

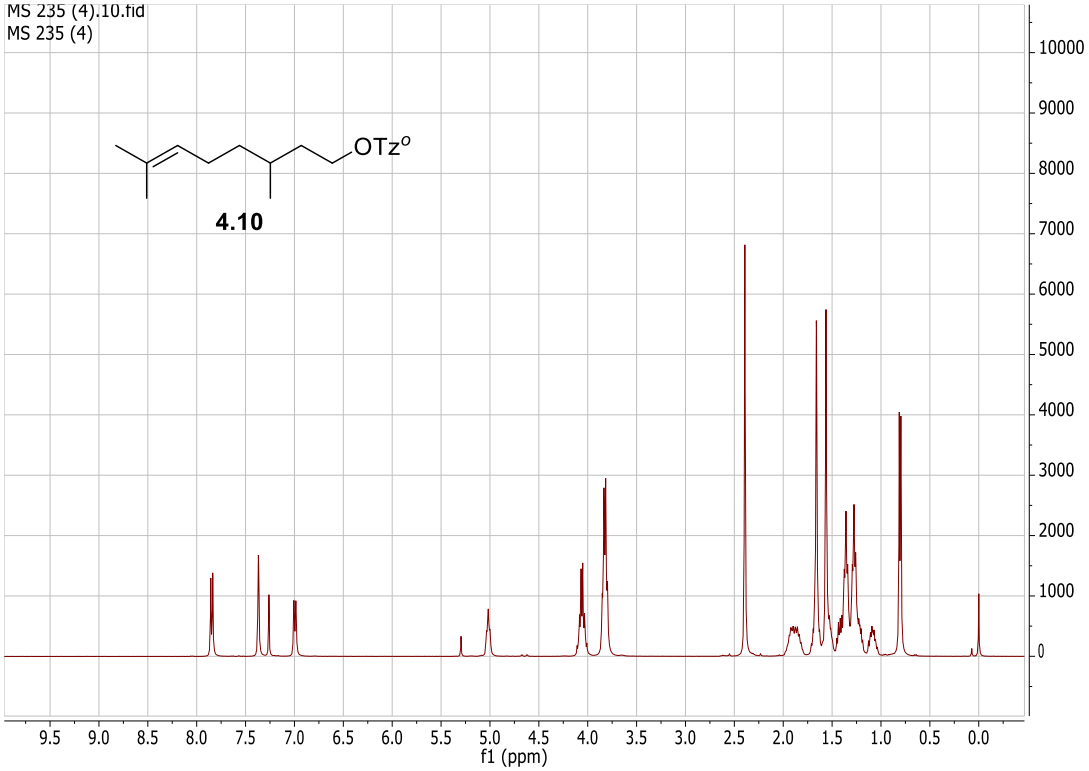

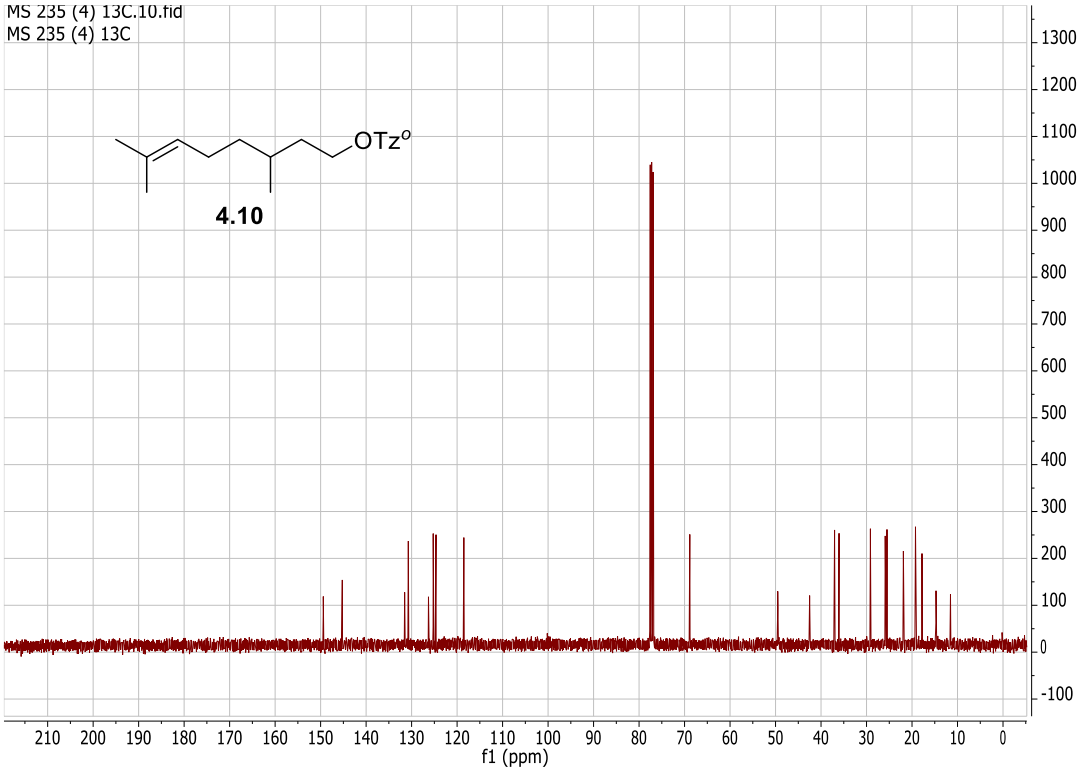

Spectral data for compound **4.12**:

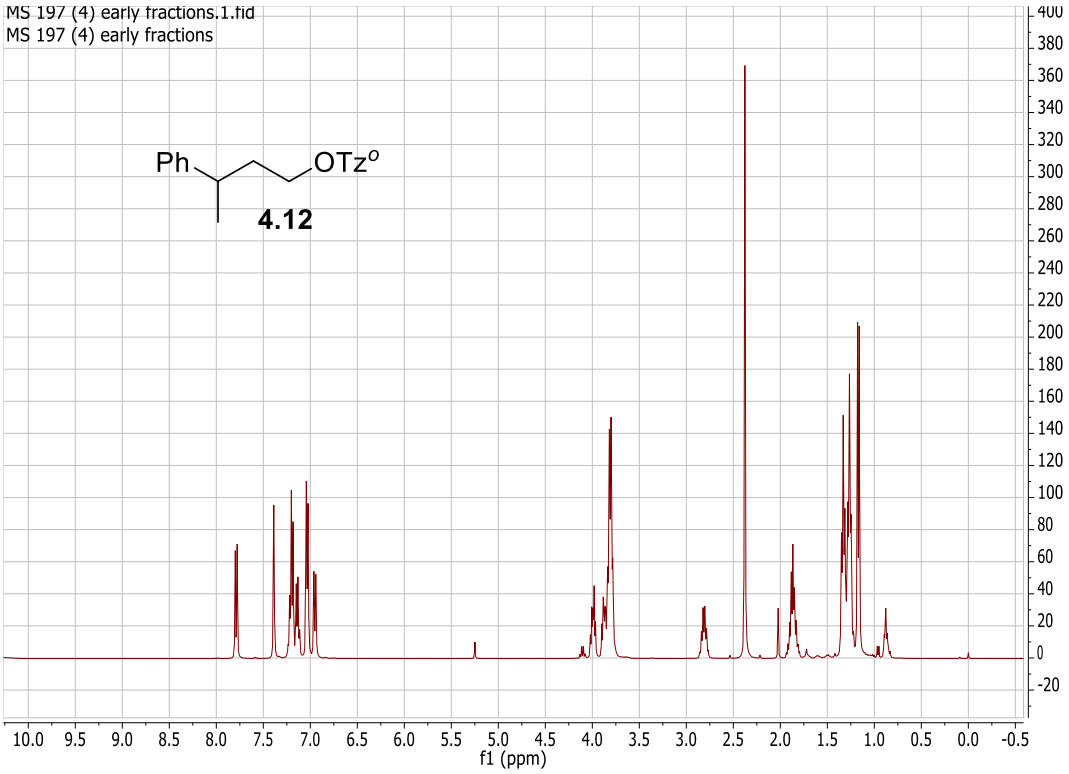

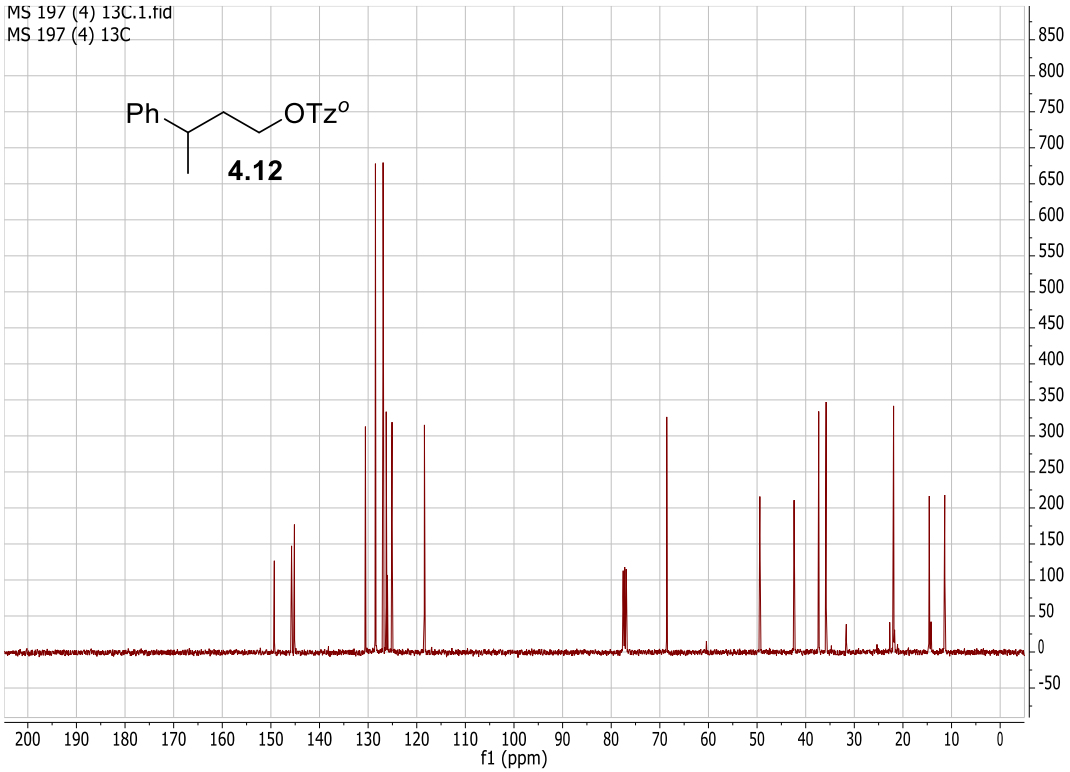

Spectral data for compound **4.13**:

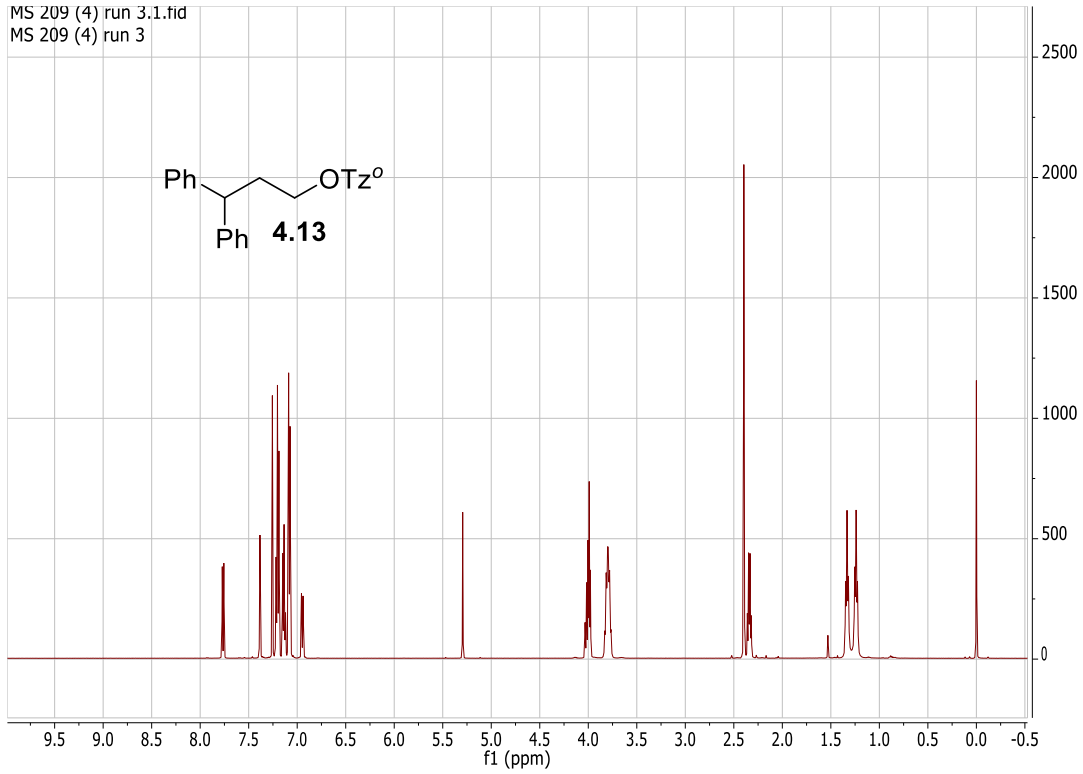

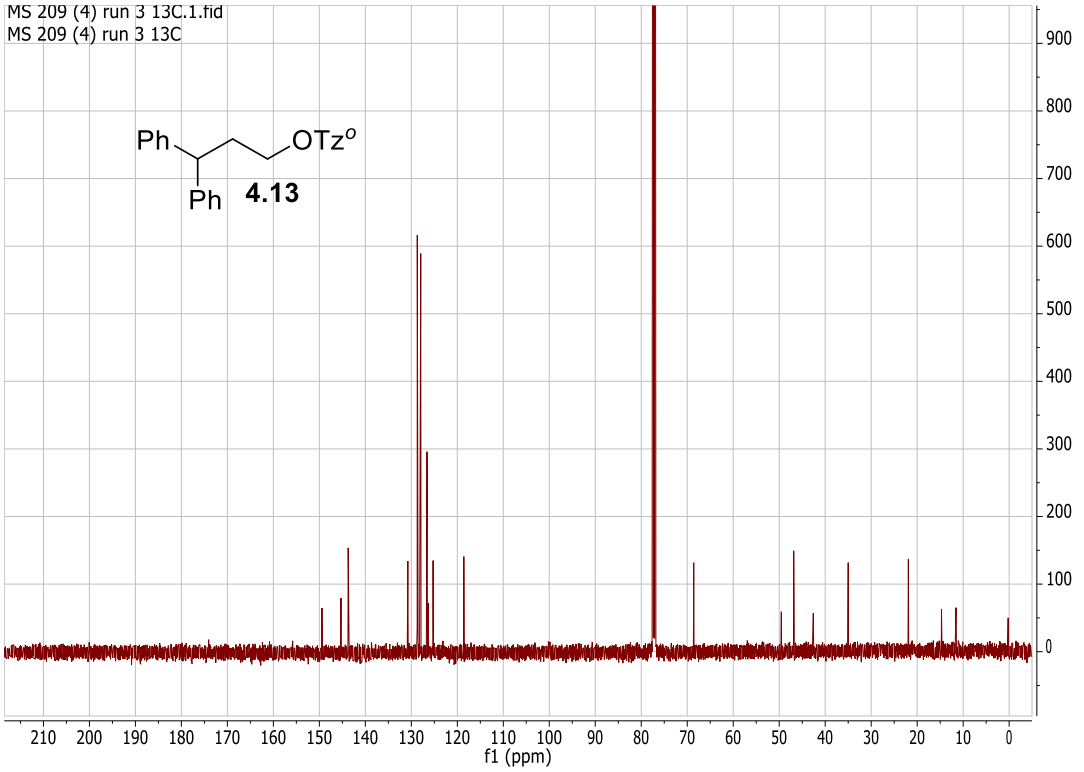

Spectral data for compound **des-methyl-4.14**:

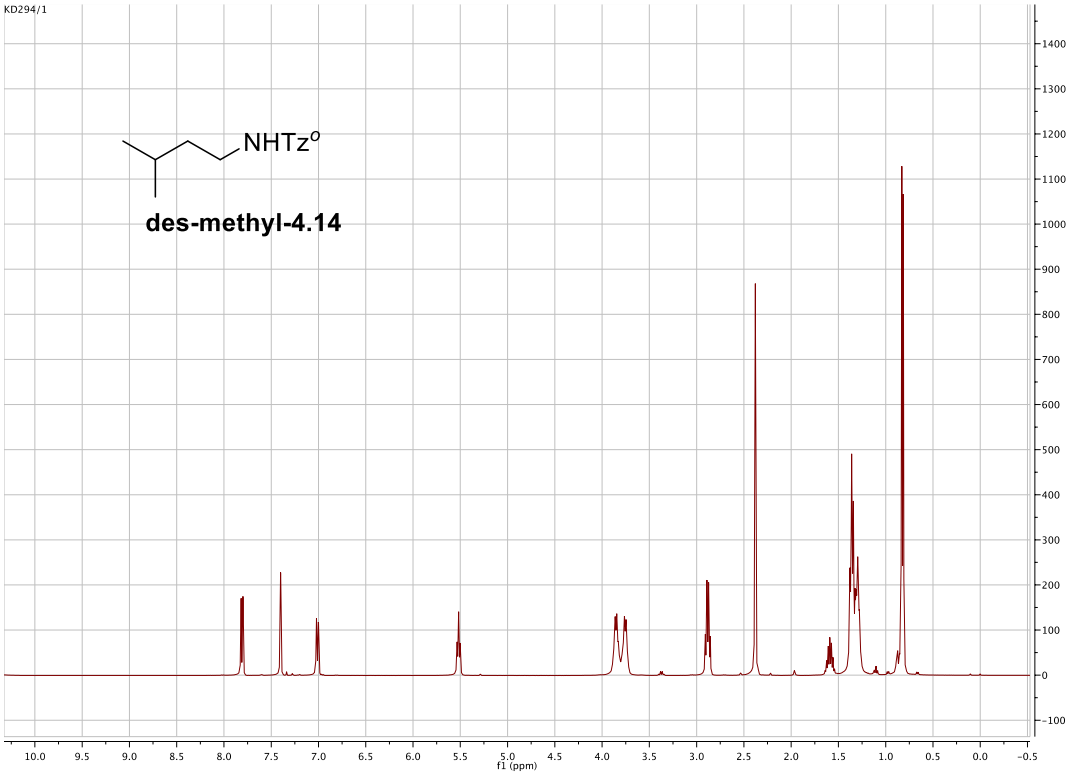

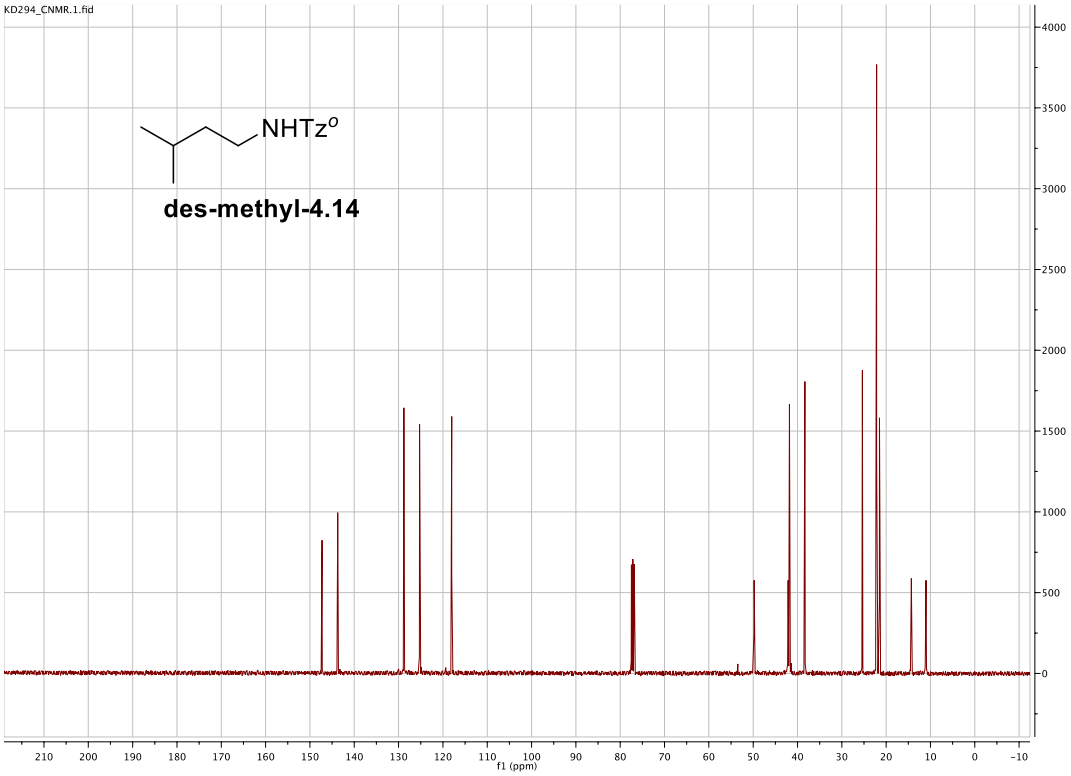

Spectral data for compound **4.14**:

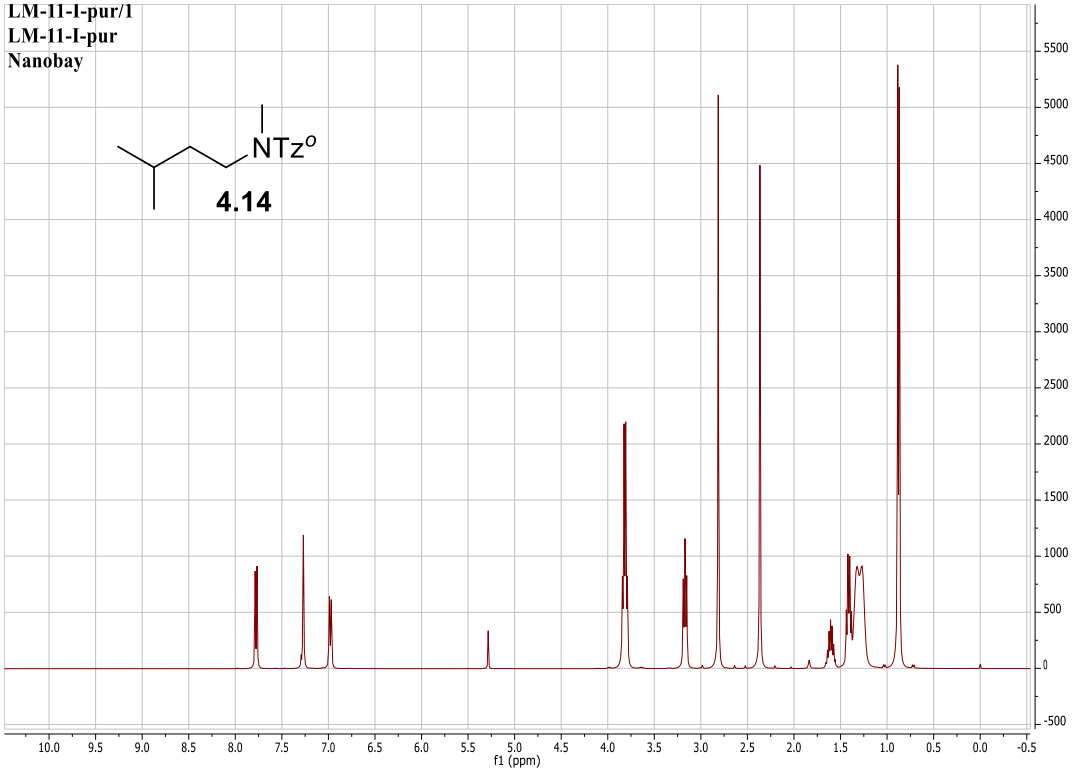

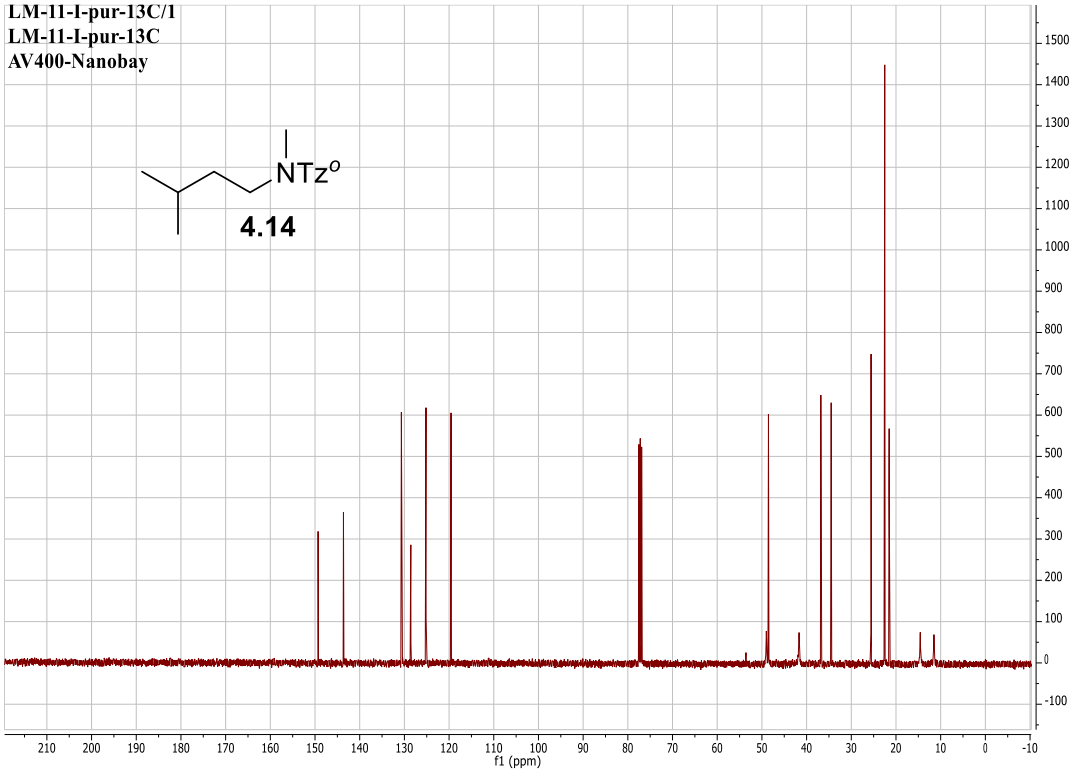

Spectral data for compound **des-methyl-4.15**:

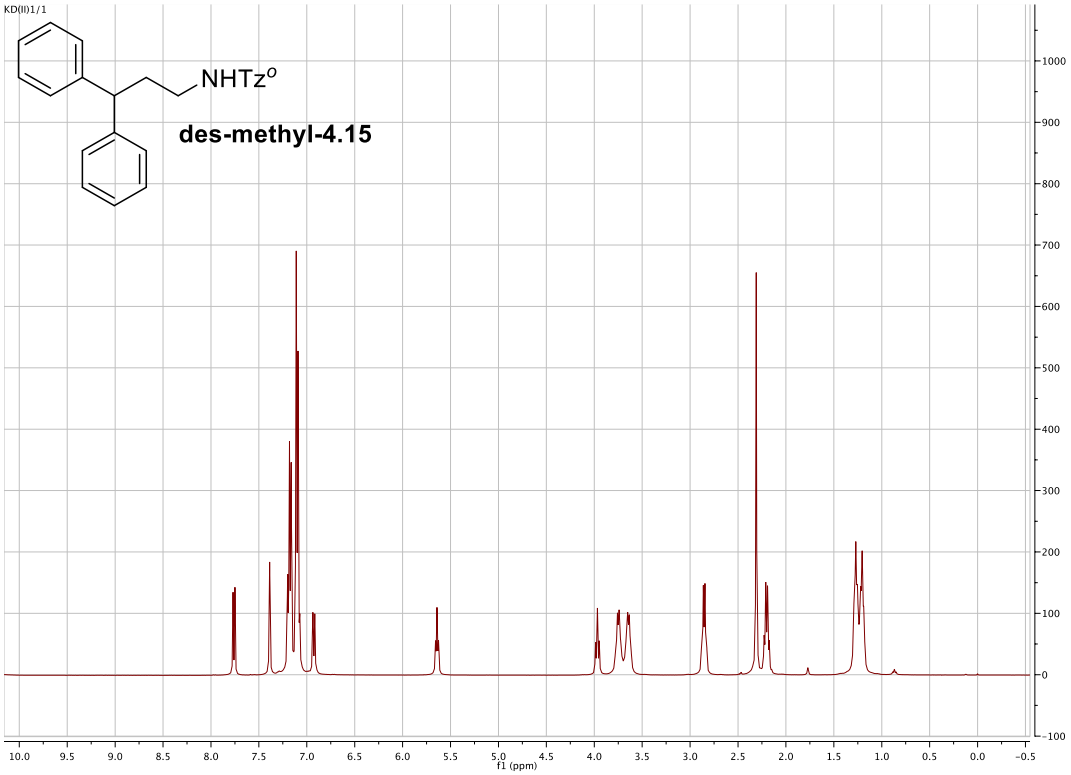

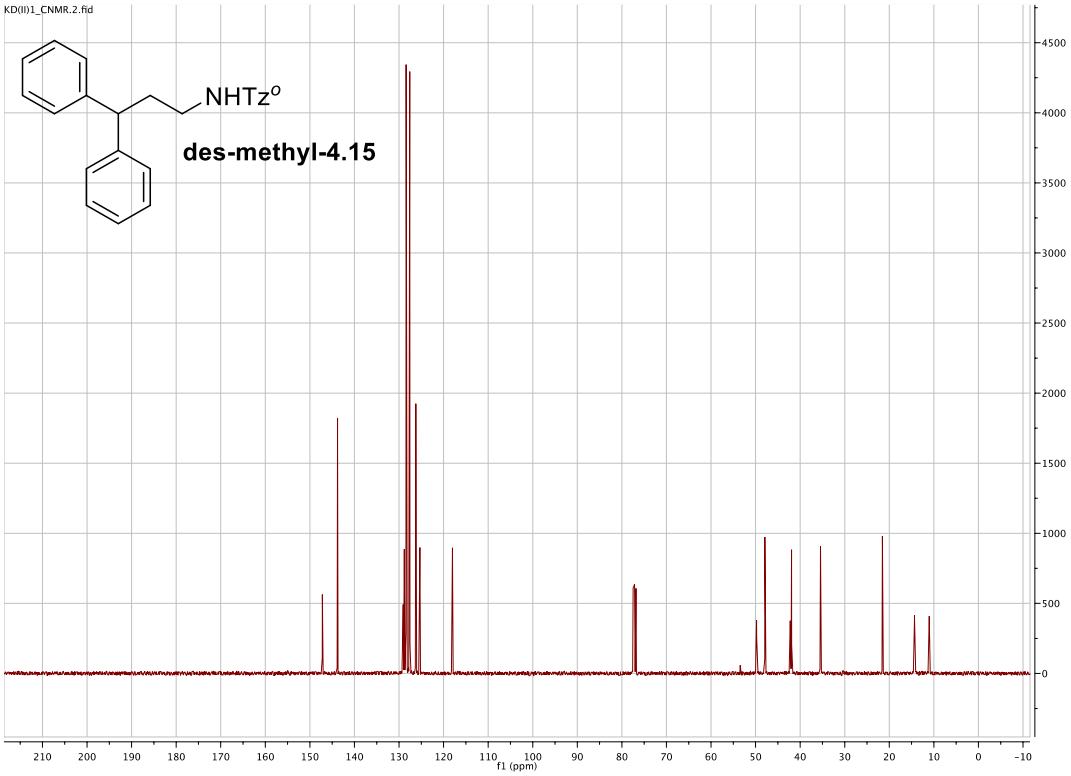

Spectral data for compound **4.15**:

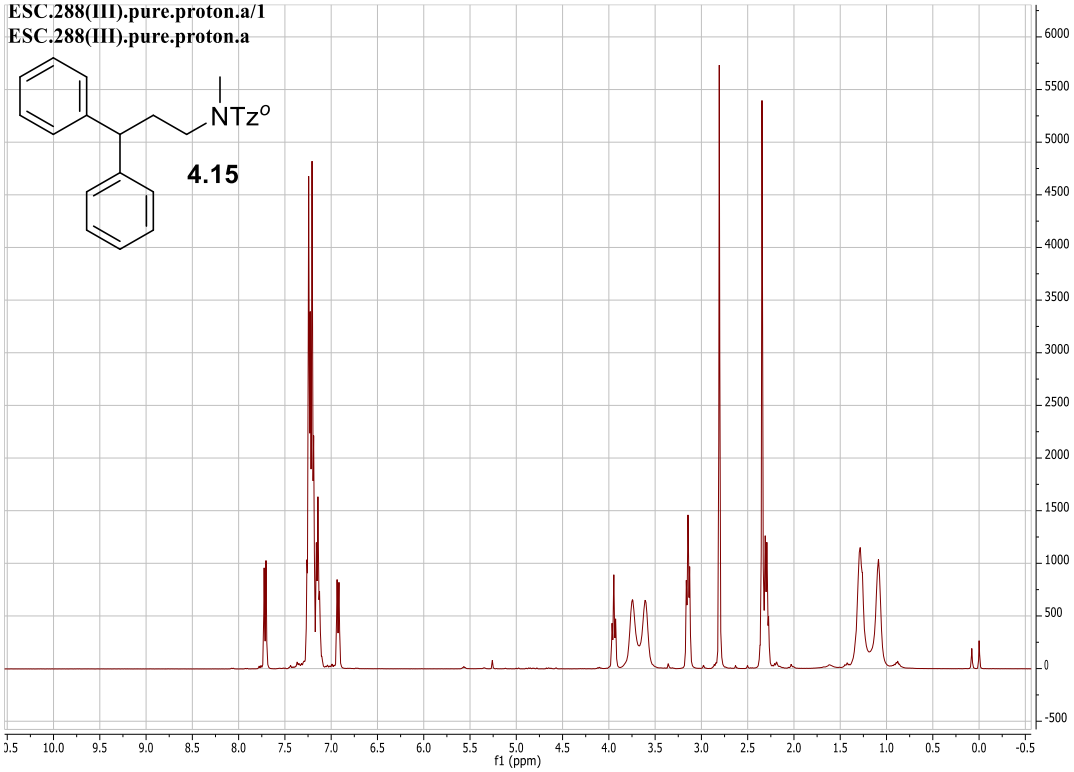

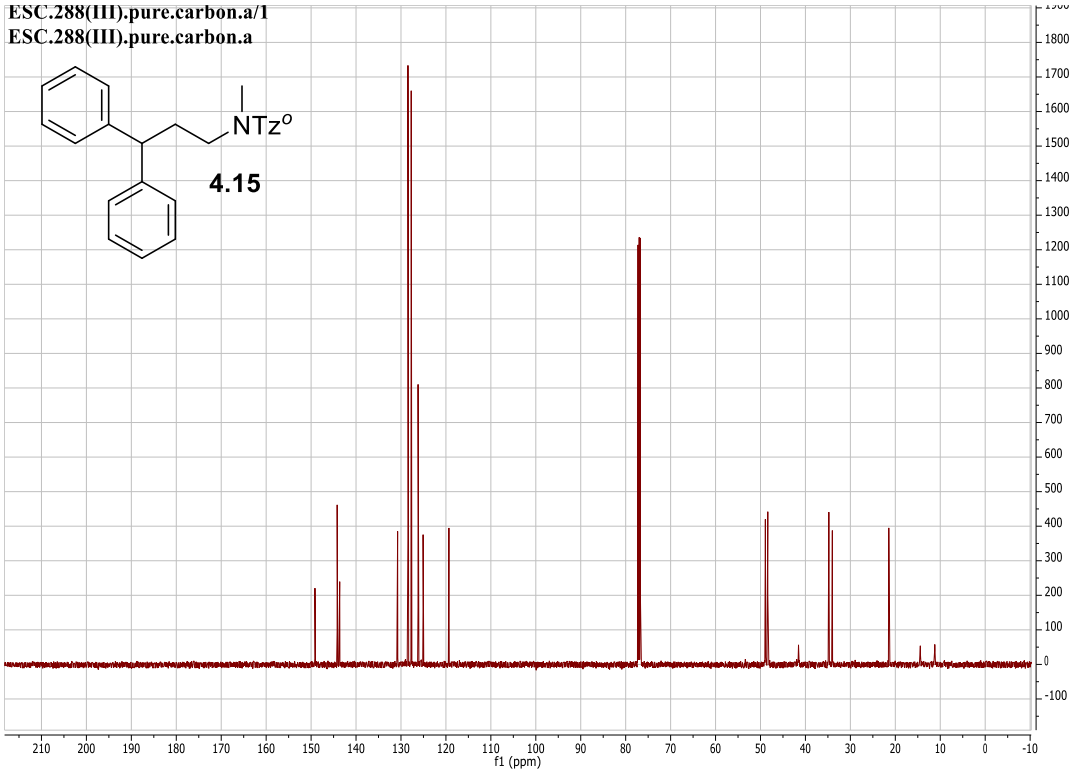

Spectral data for compound **4.16**:

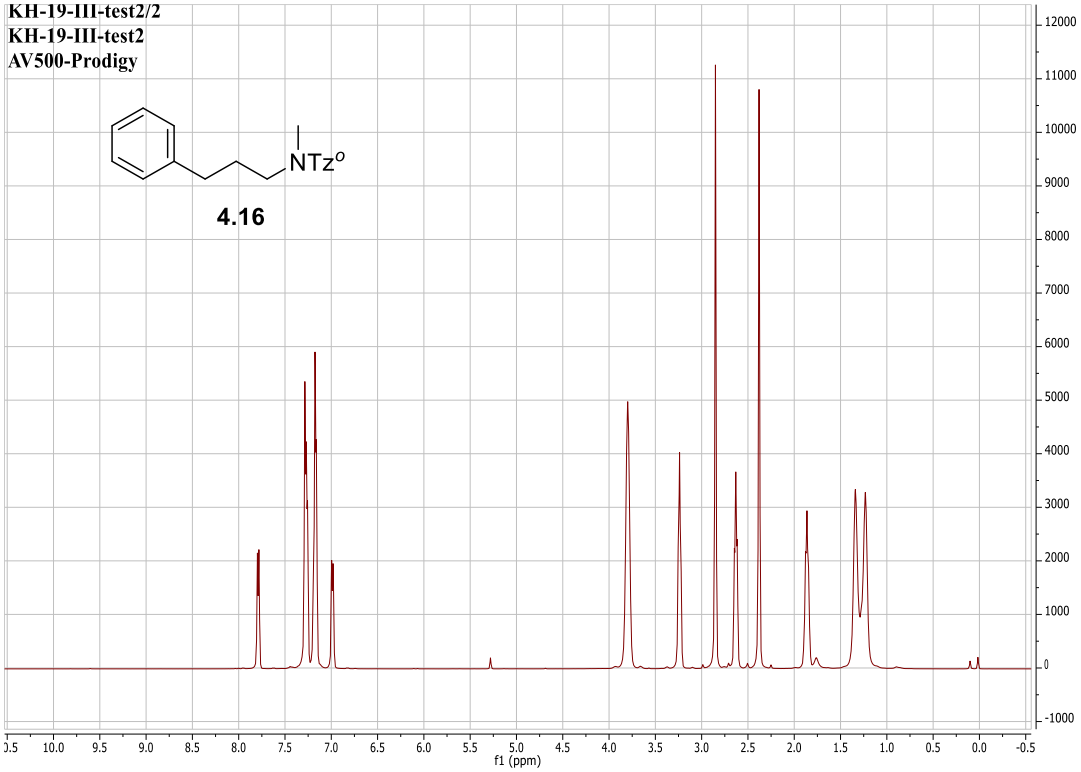

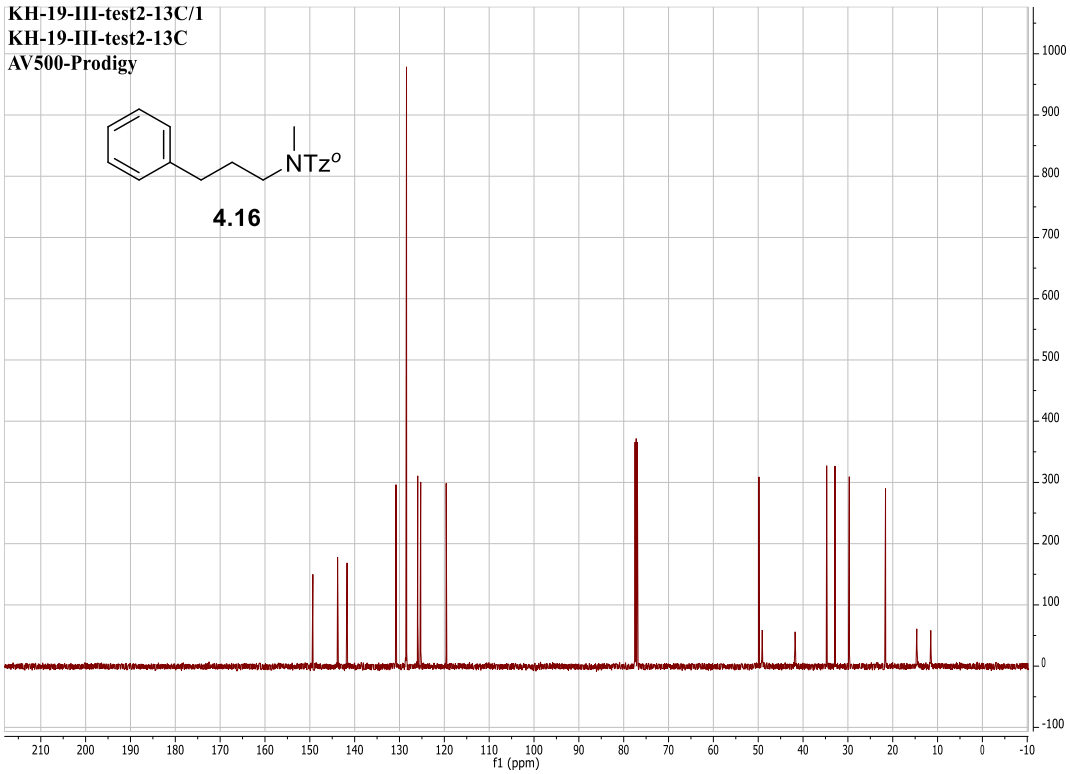

Spectral data for compound **4.17**:

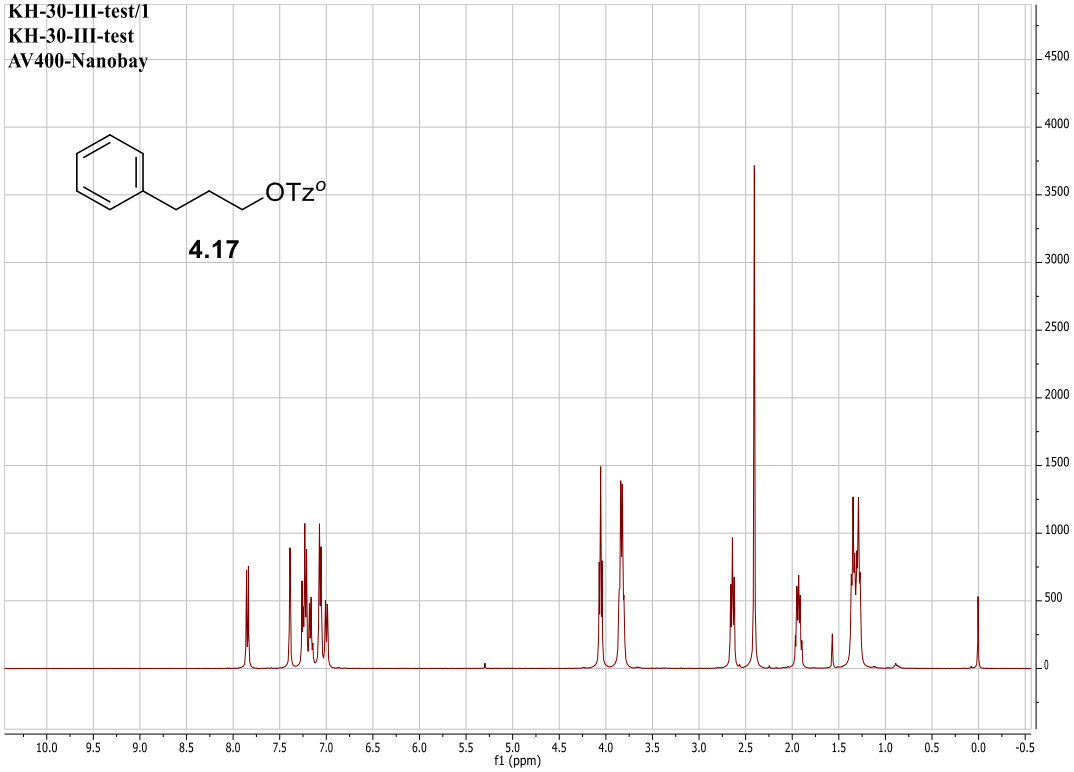

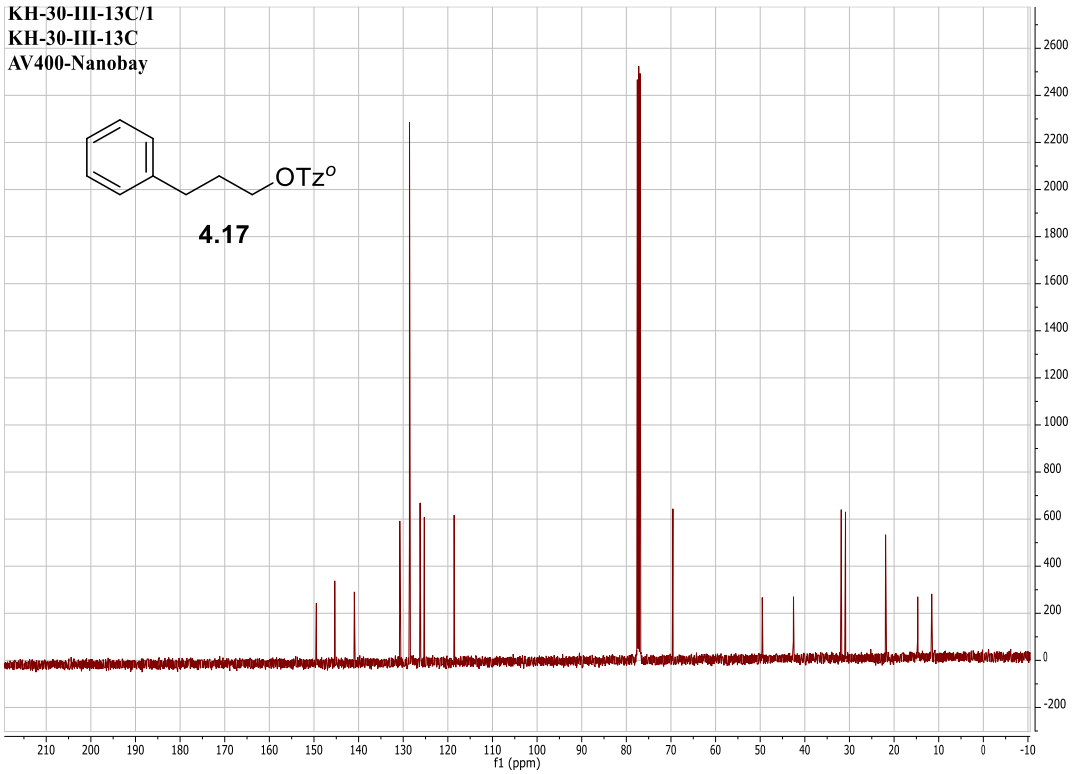

Spectral data for compound **4.18**:

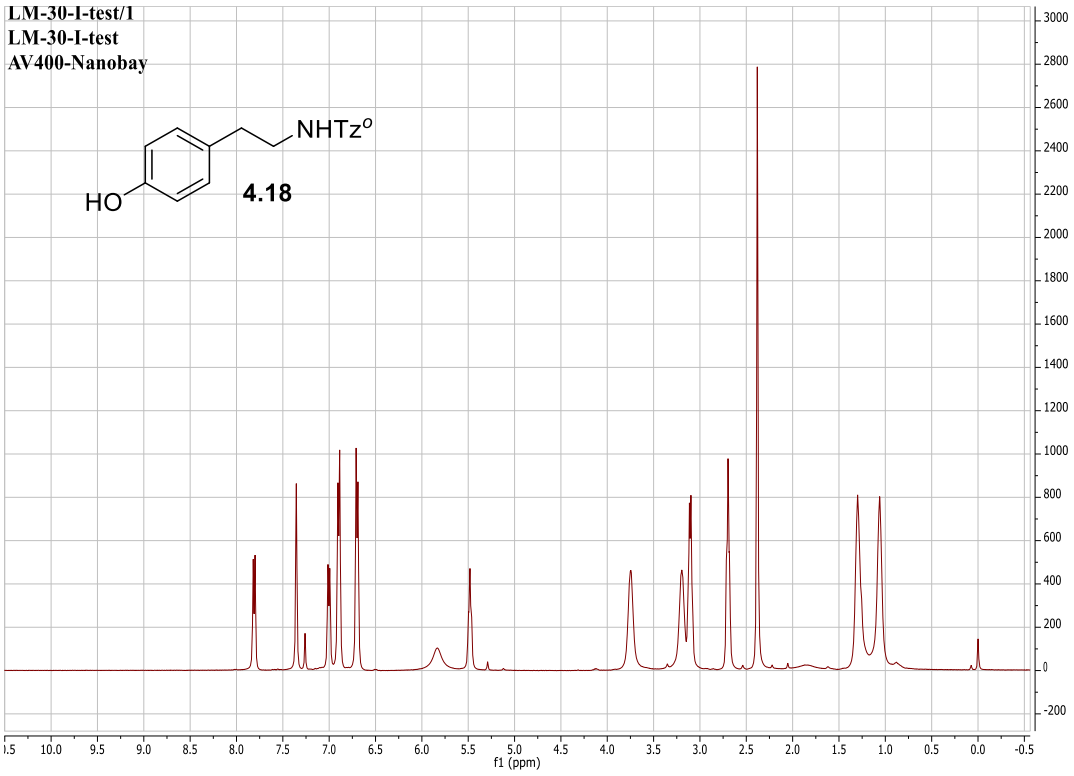

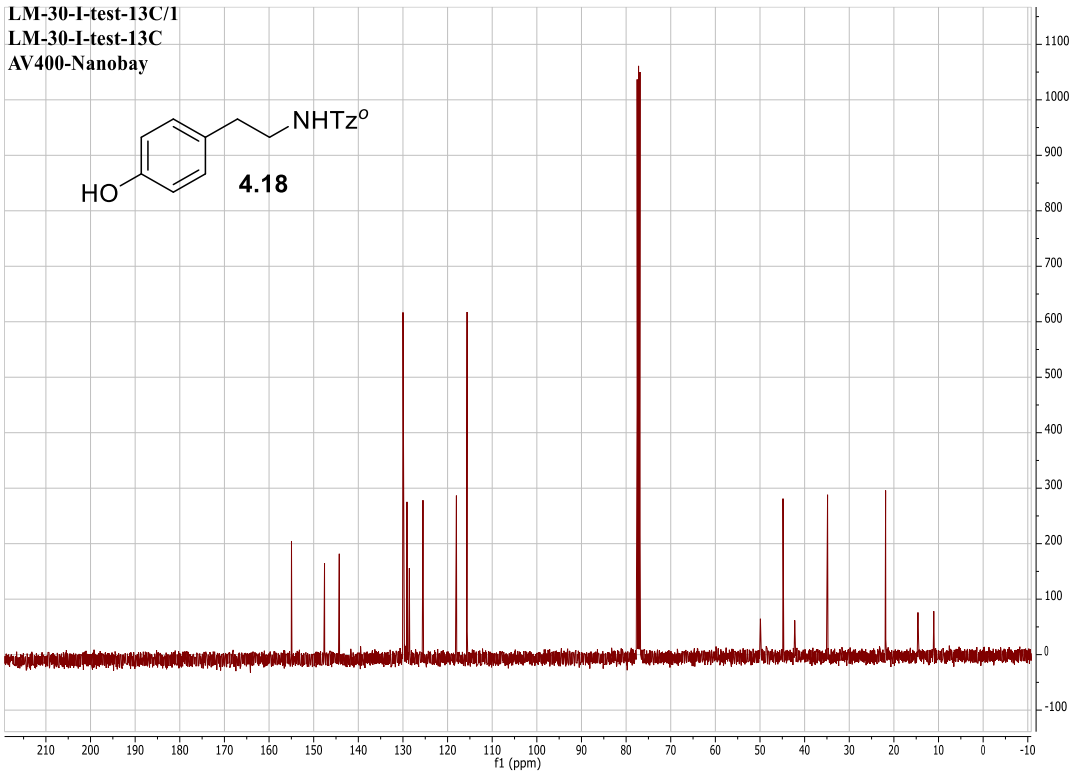

Spectral data for compound **4.5a**:

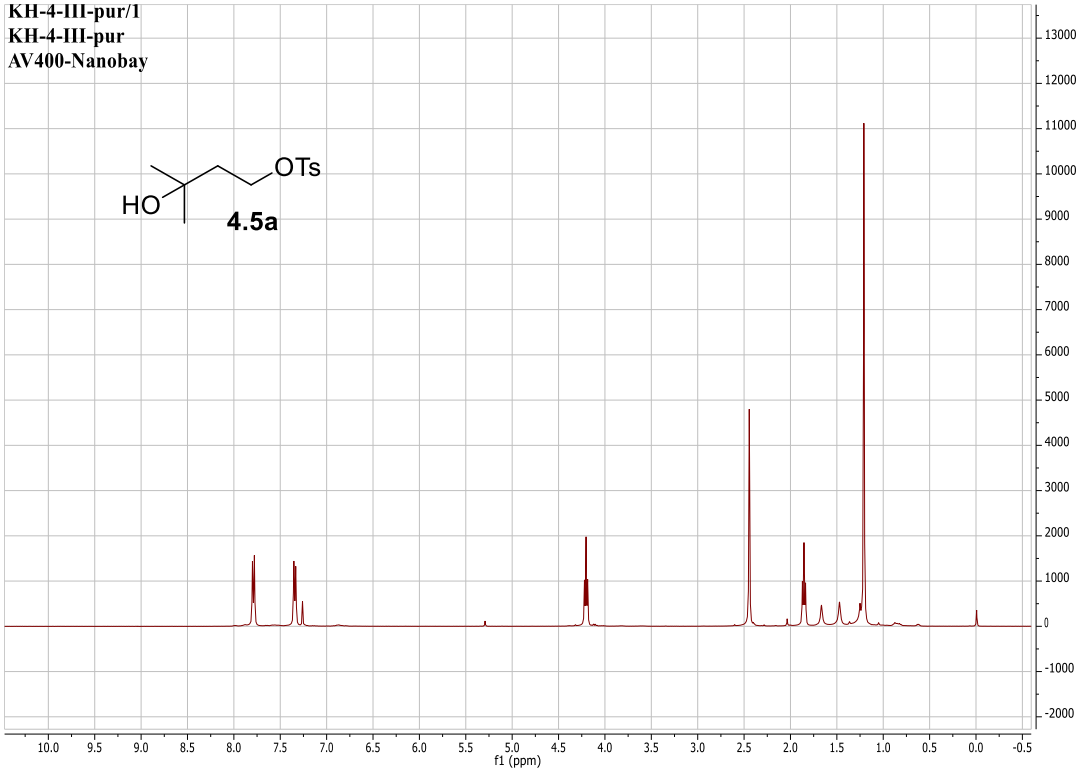

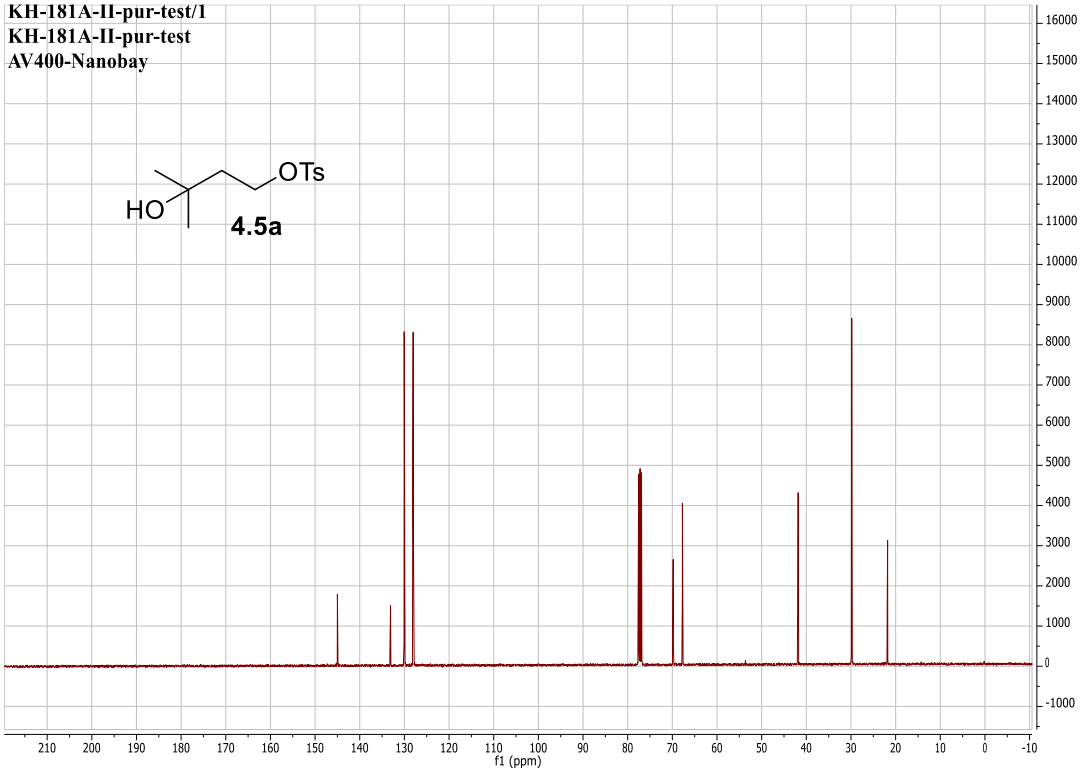

Spectral data for compound **4.5c**:

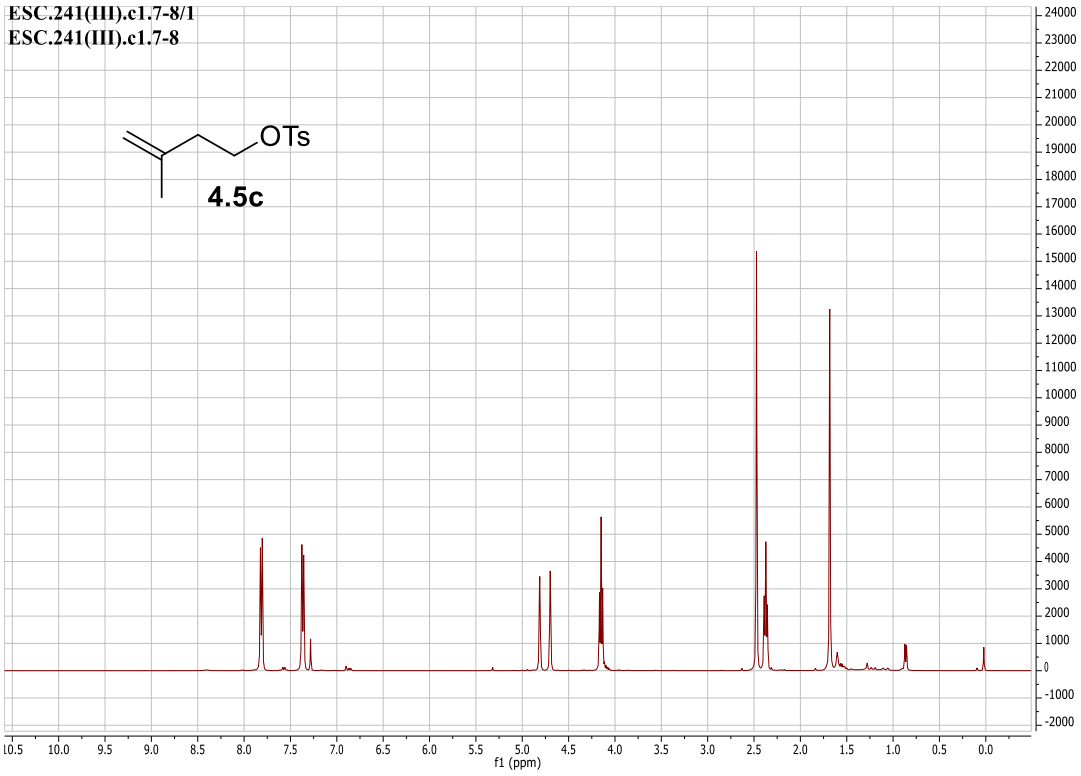

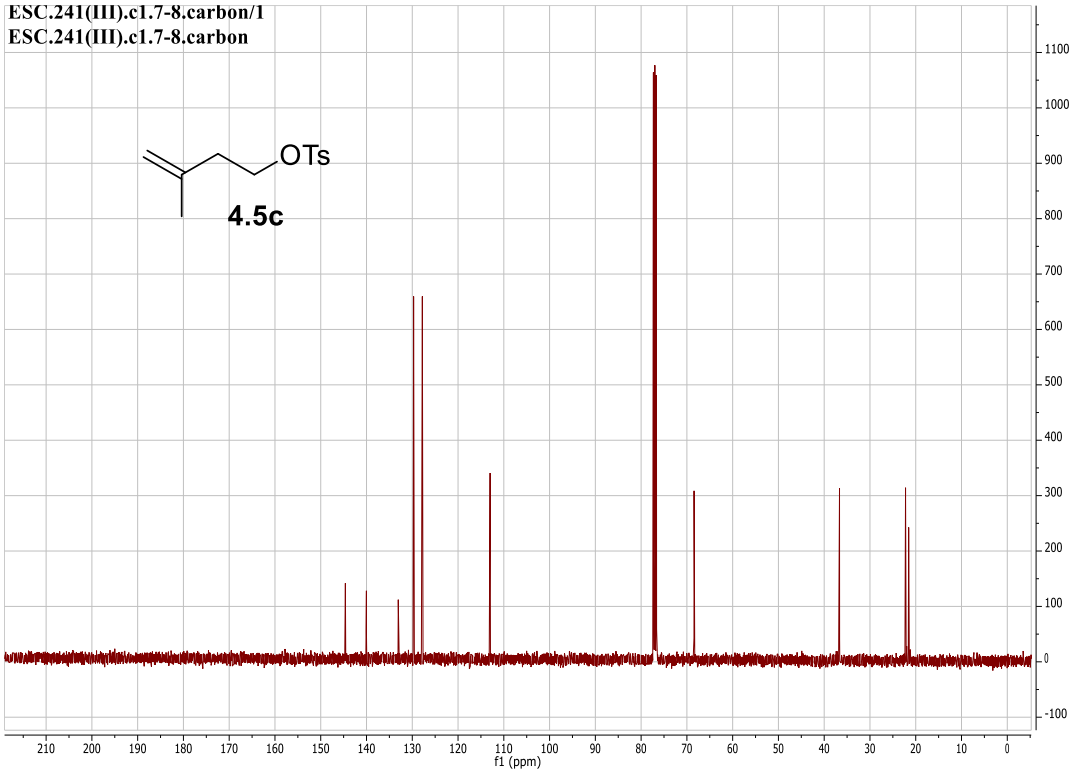

Spectral data for compound **4.6a**:

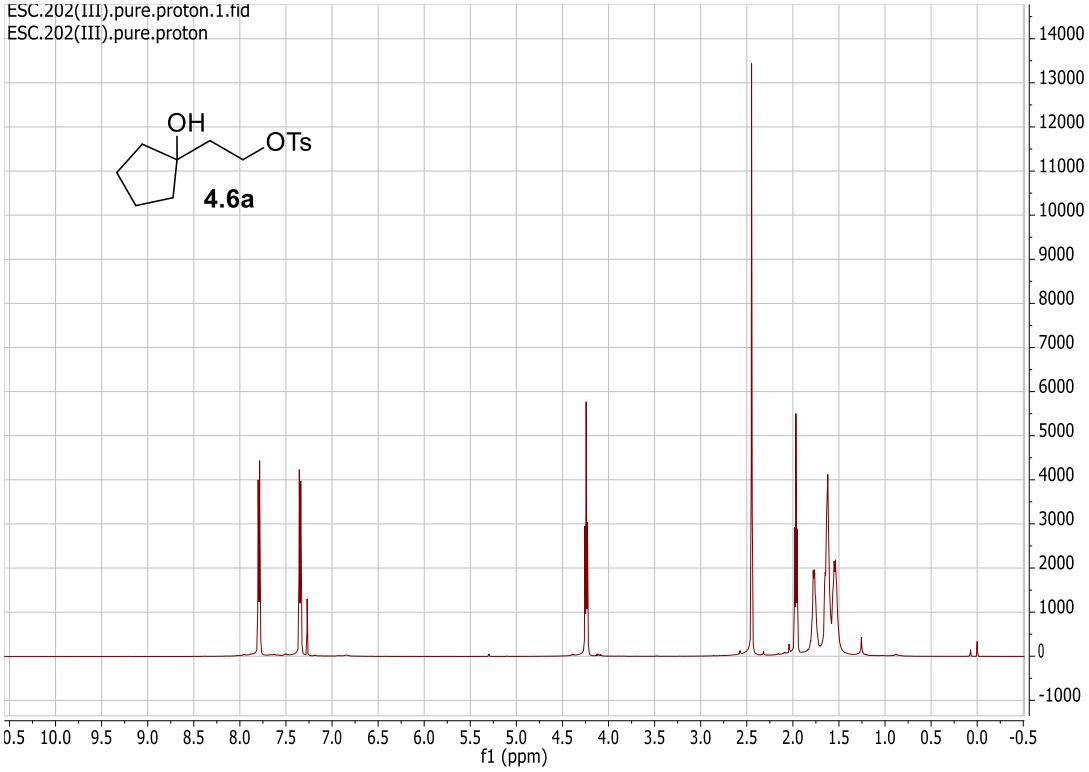

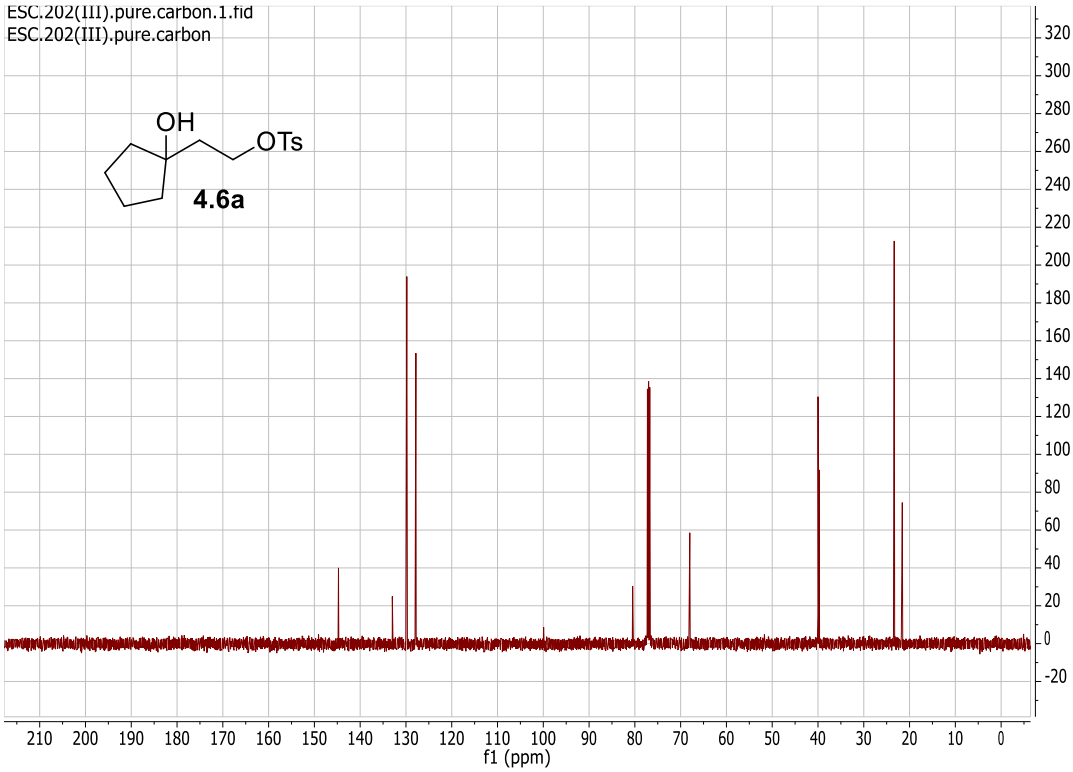

Spectral data for compound **4.7a**:

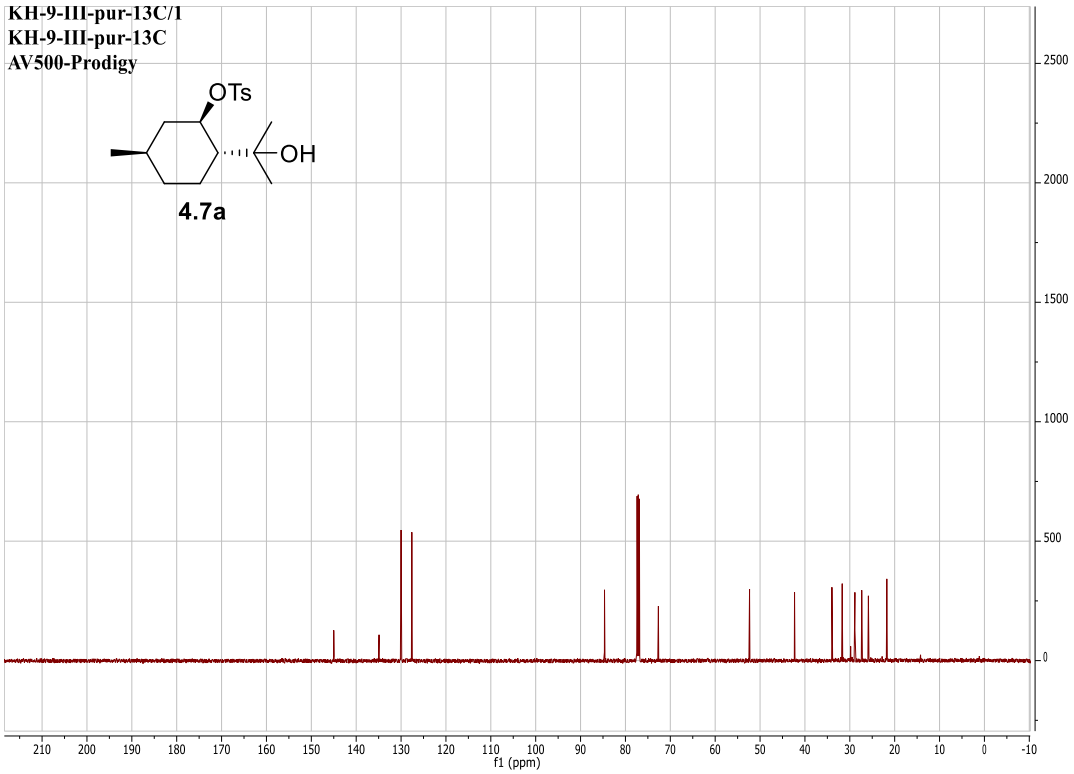

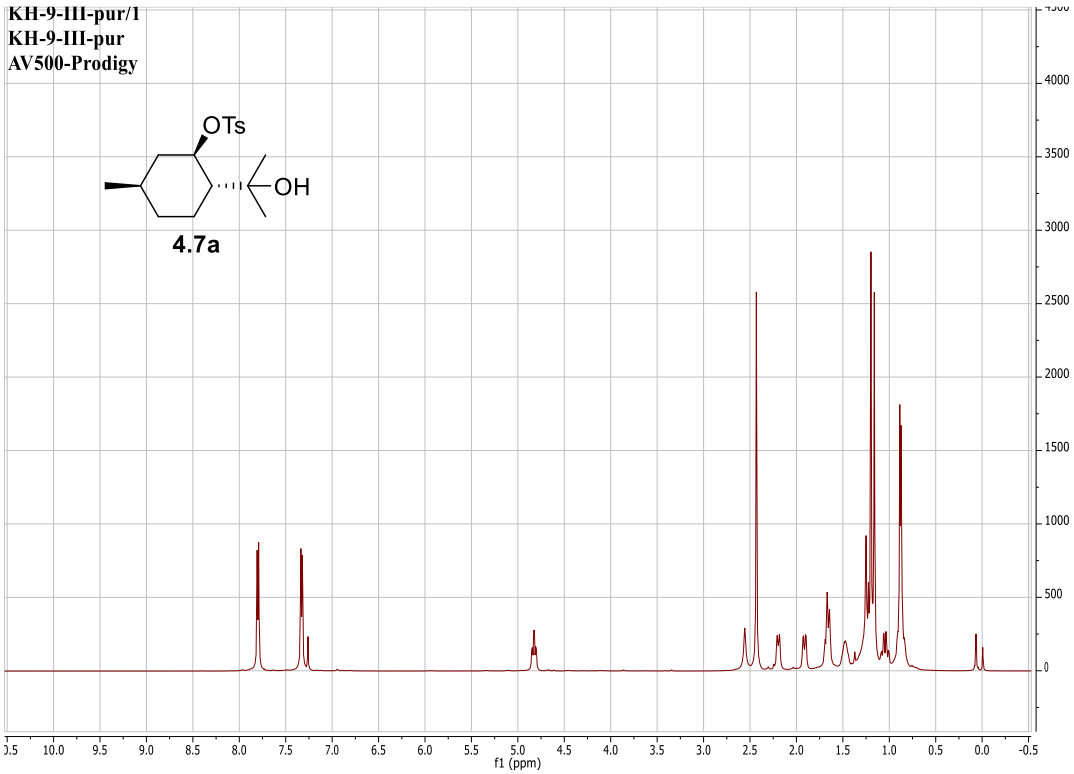

Spectral data for compound **4.10a**:

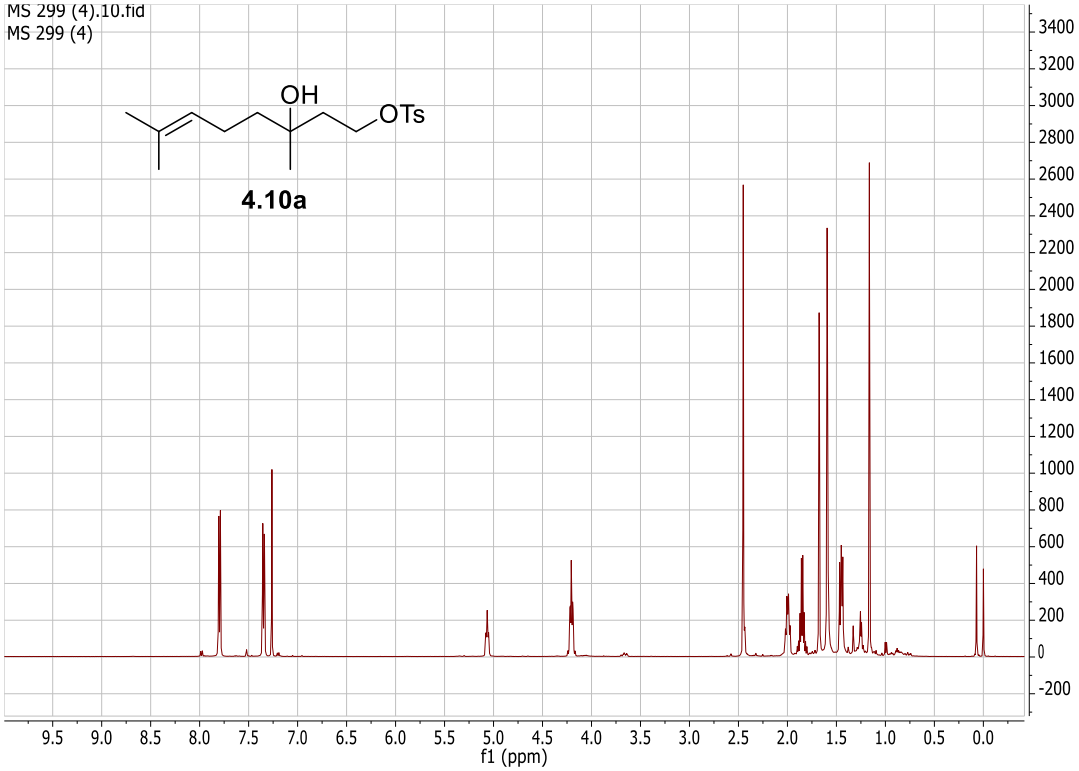

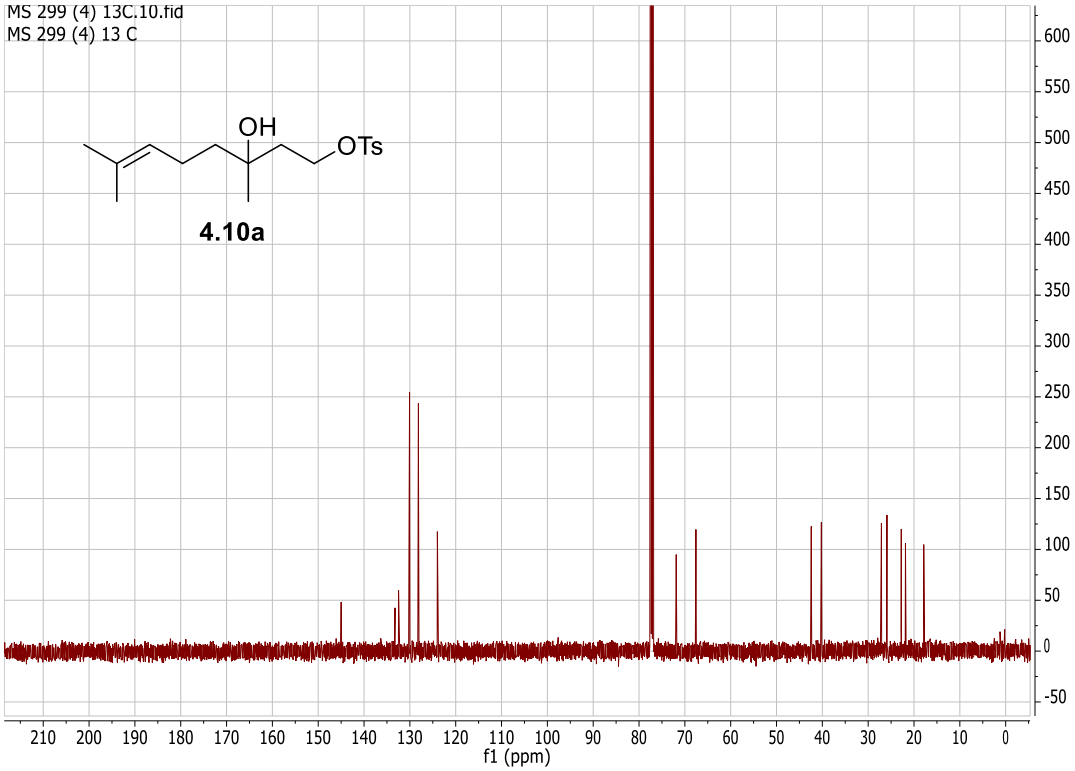

Spectral data for compound **4.11a**:

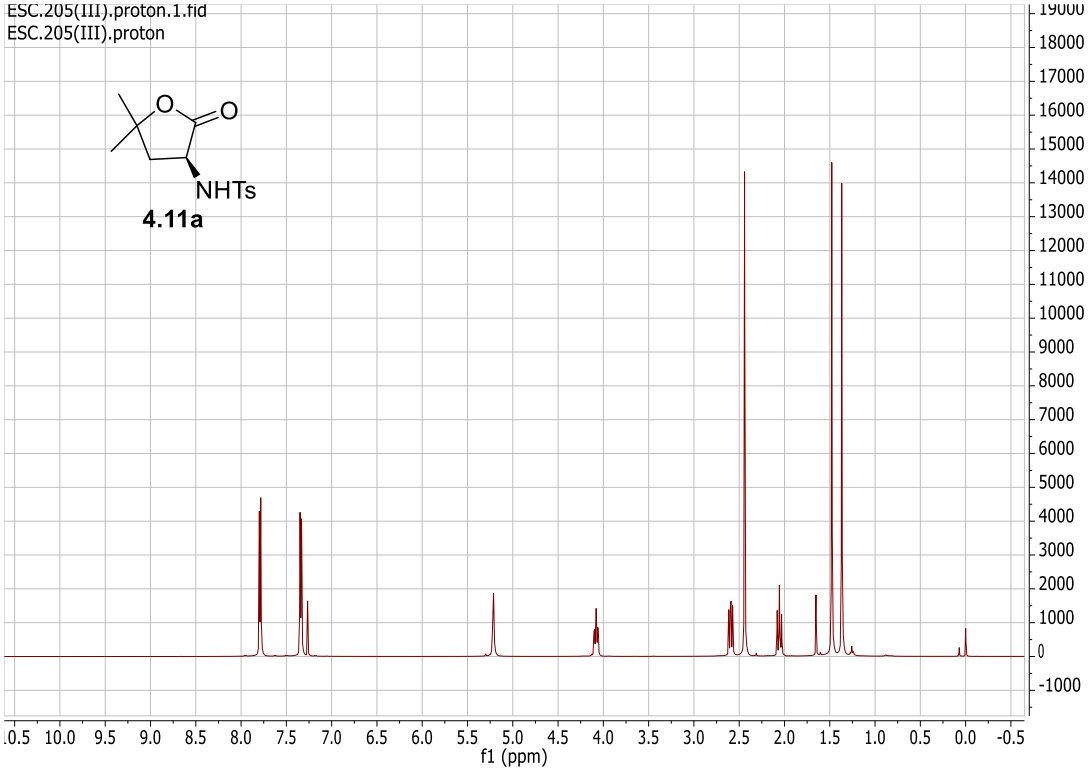

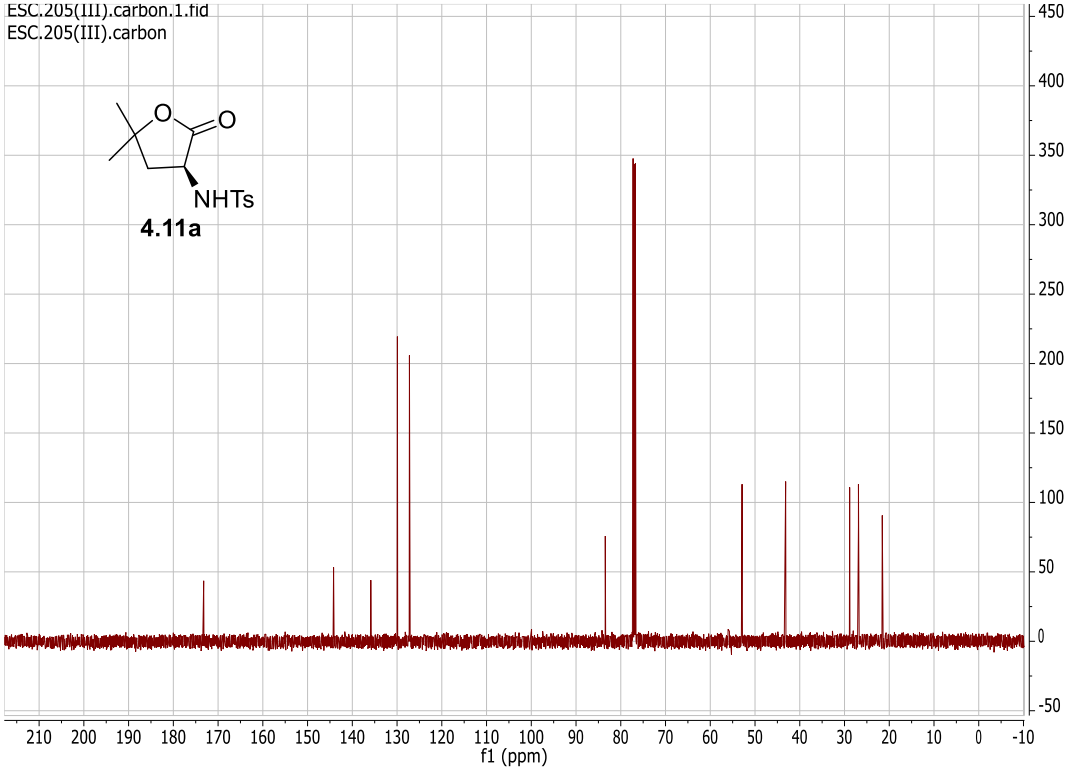

Spectral data for compound **4.12a**:

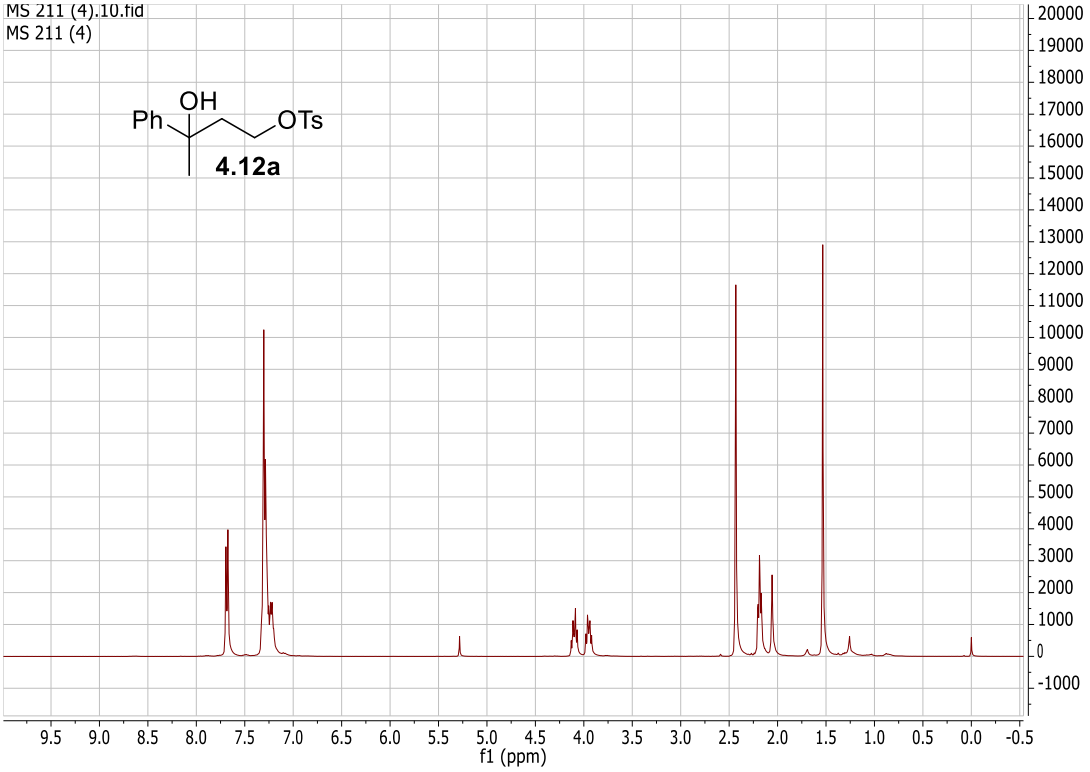

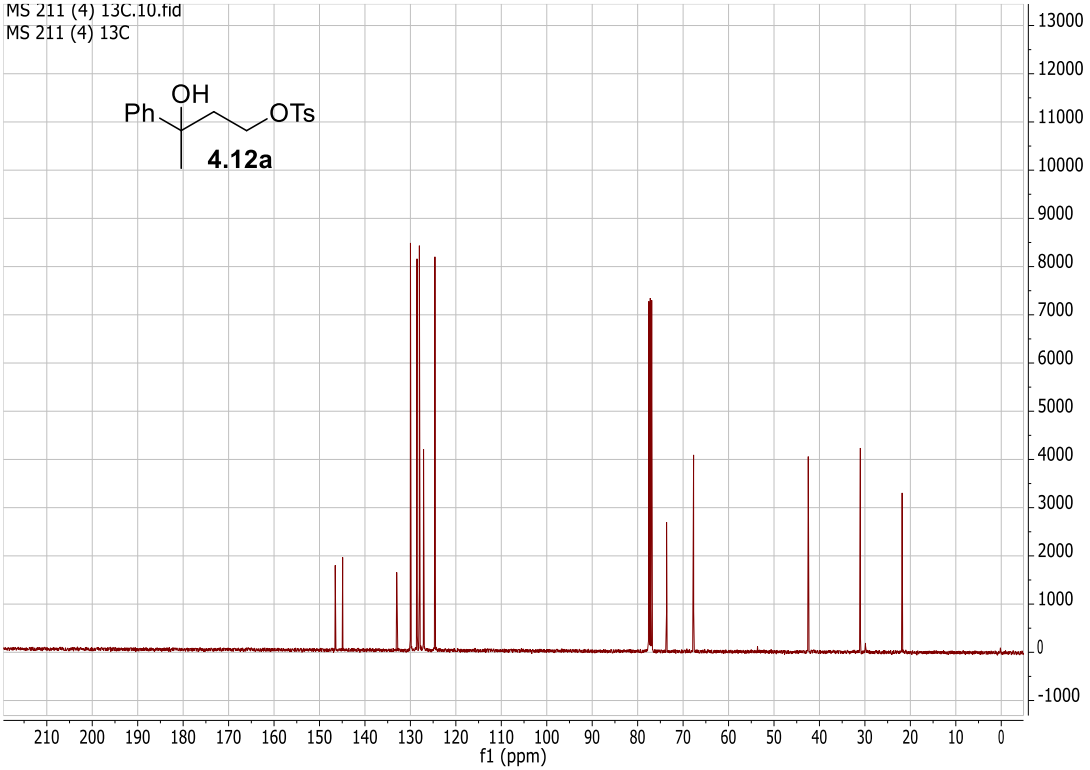

Spectral data for compound **4.13a**:

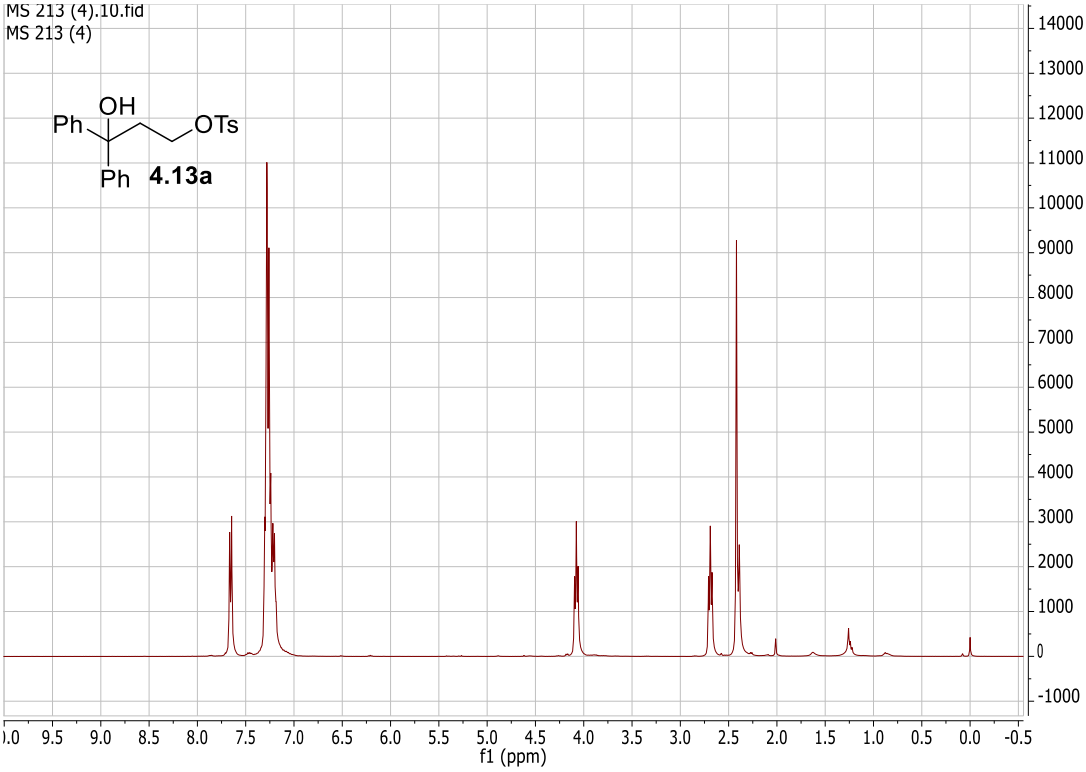

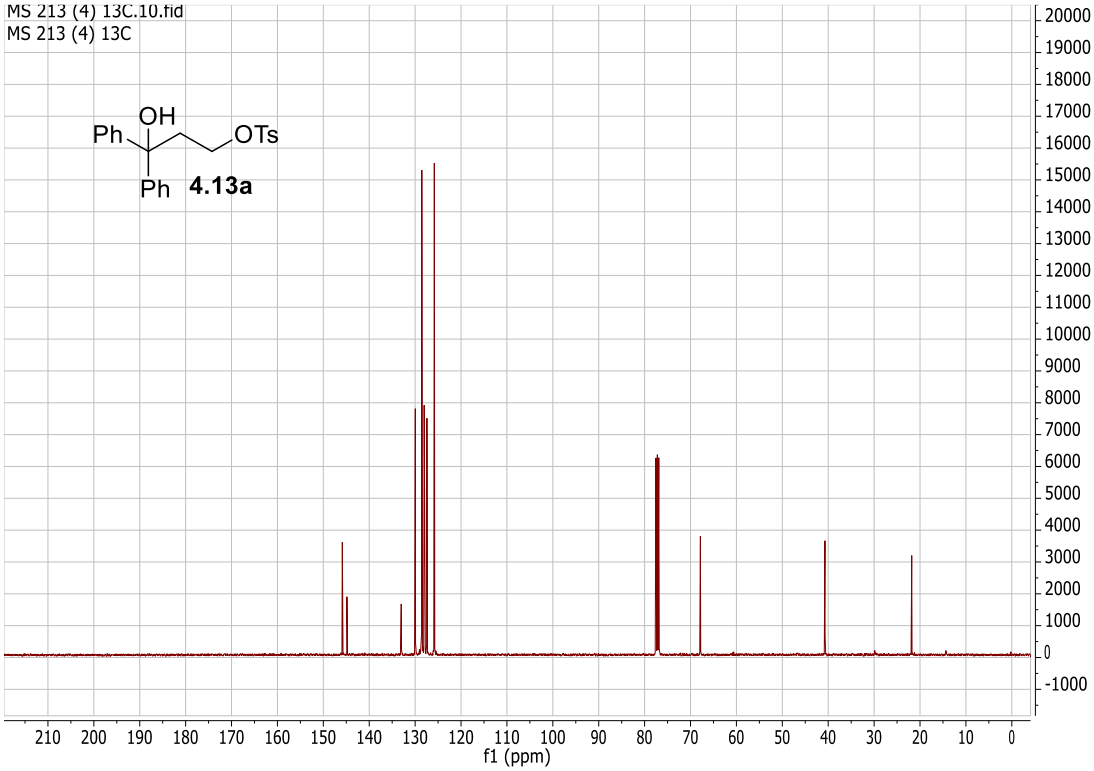

Spectral data for compound **4.14a**:

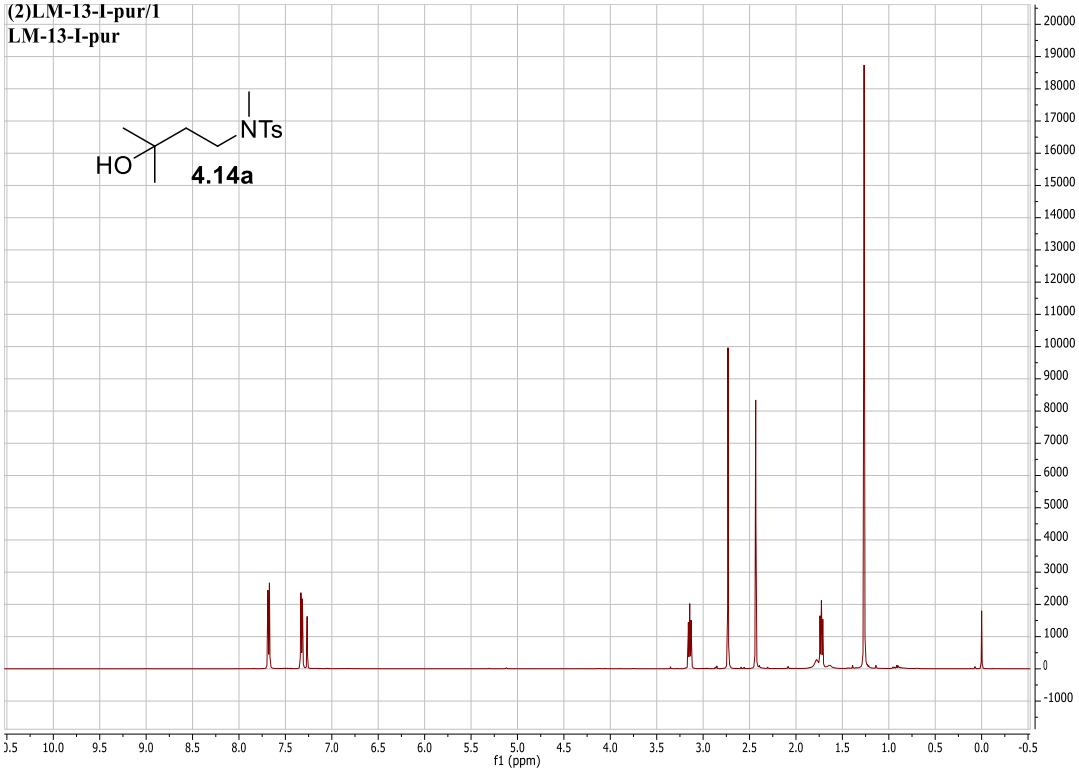

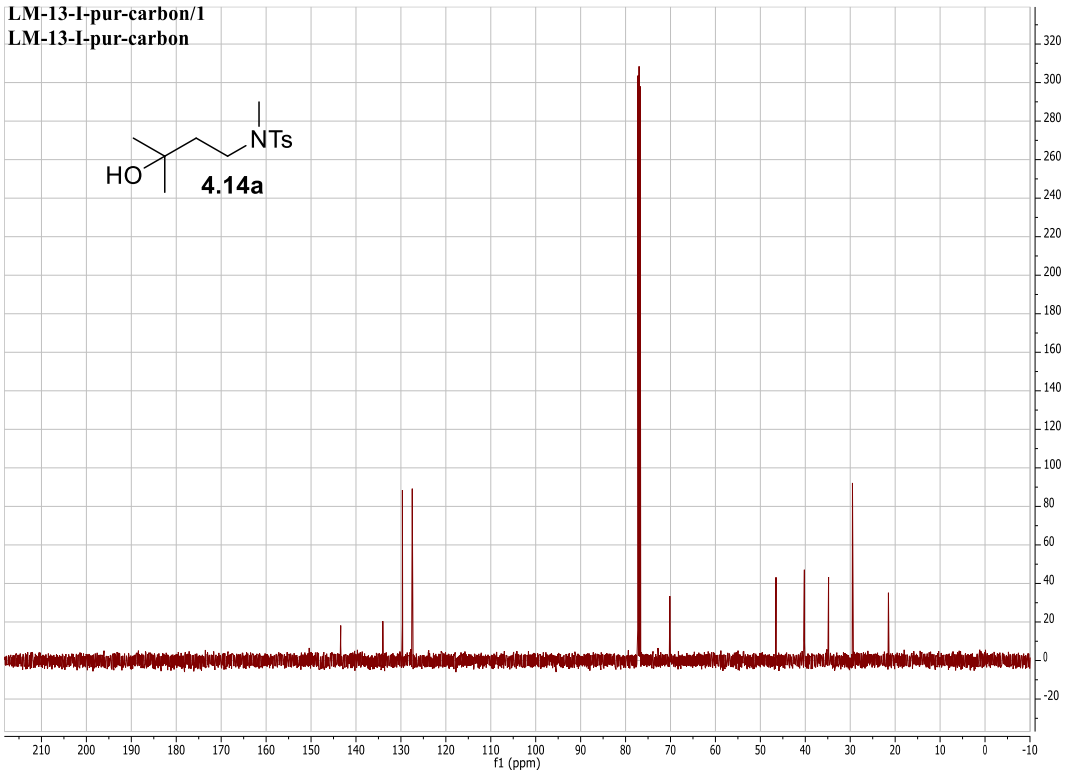

Spectral data for compound **4.15a**:

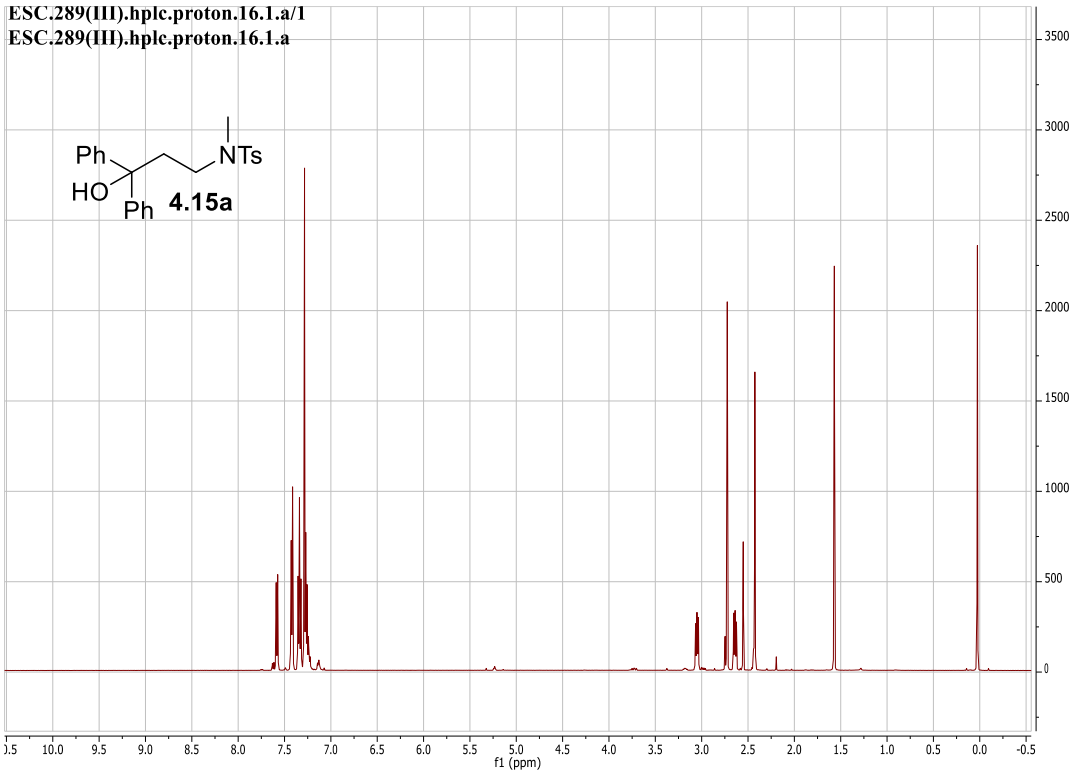

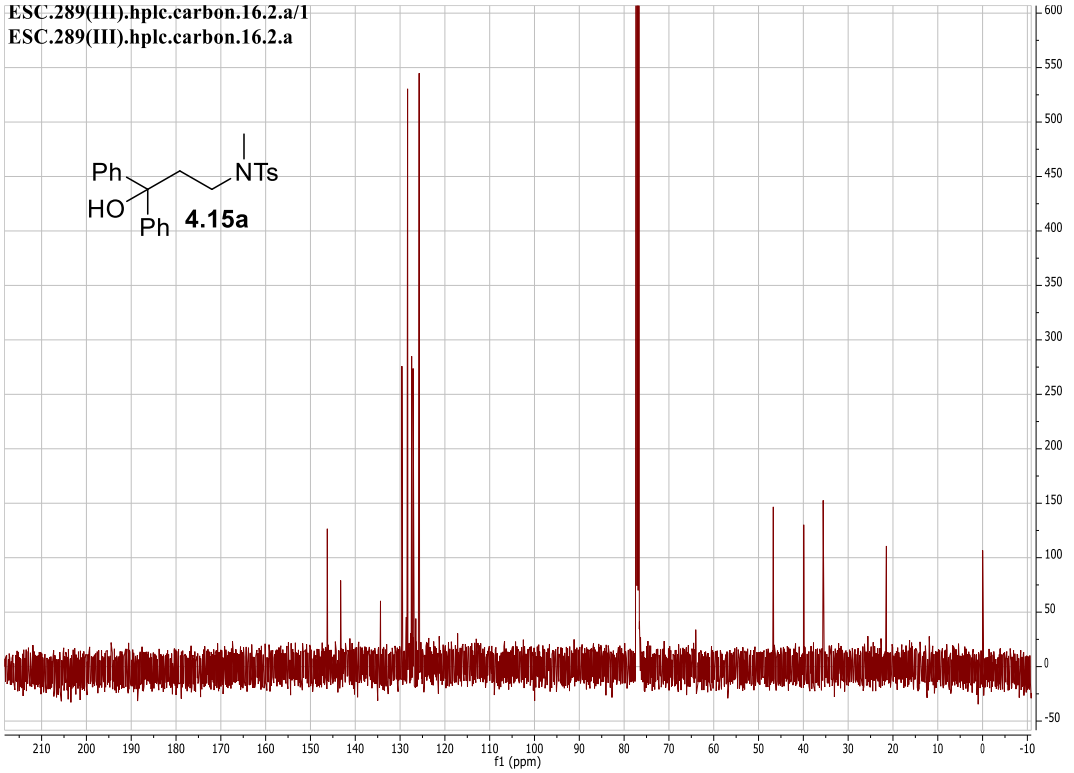

Spectral data for compound **4.16a**:

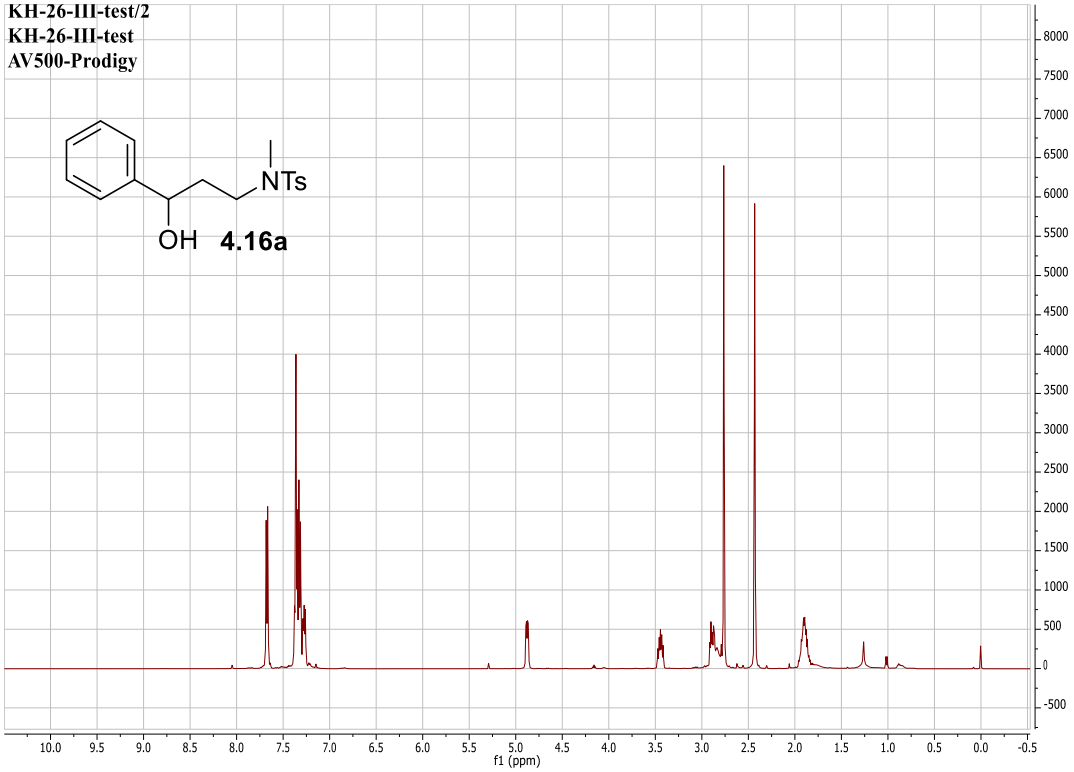

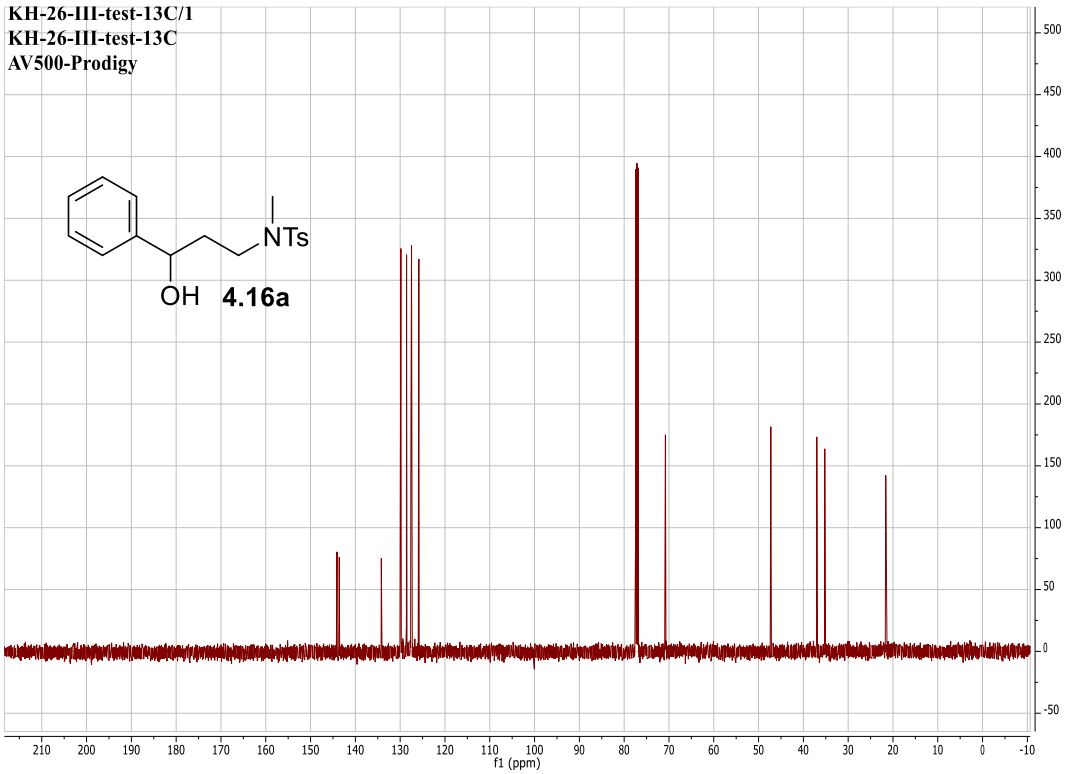

Spectral data for compound **4.18a**:

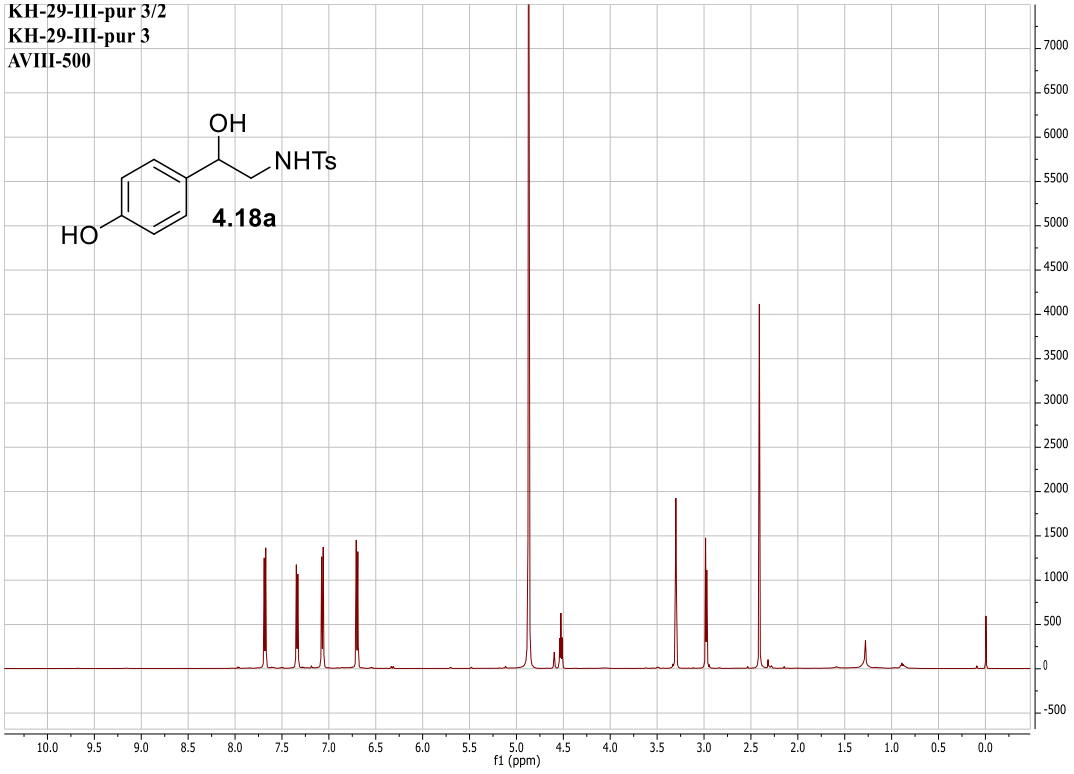

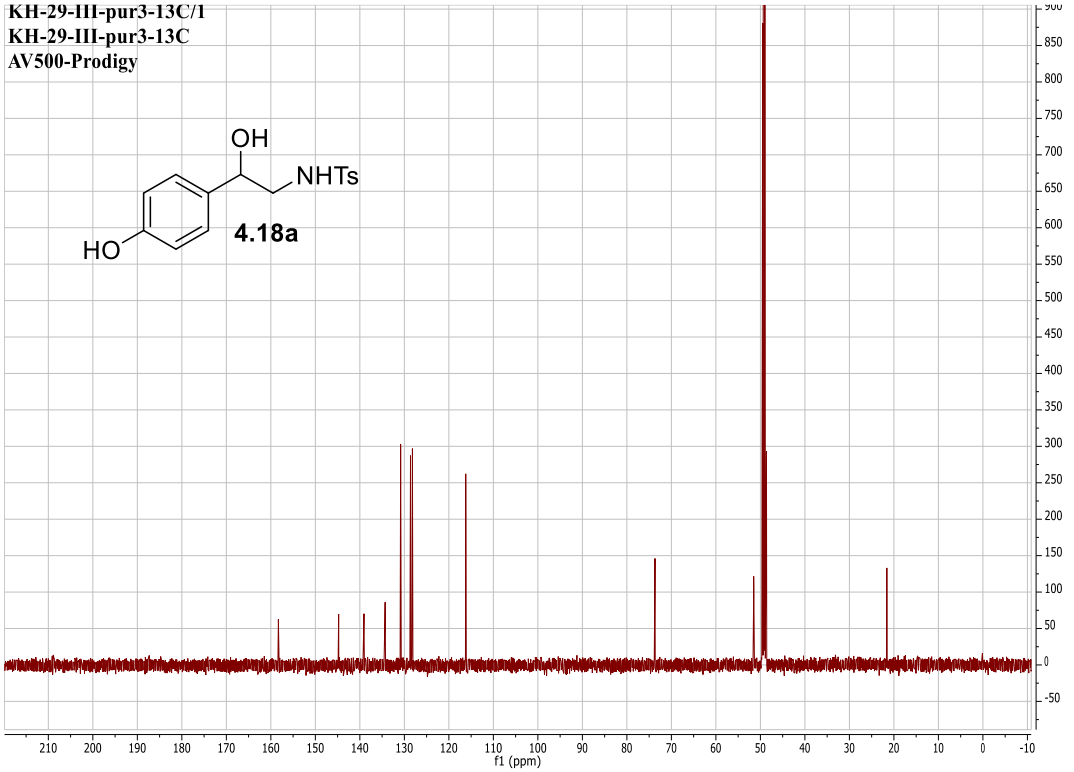

Spectral data for compound **4.5d**:

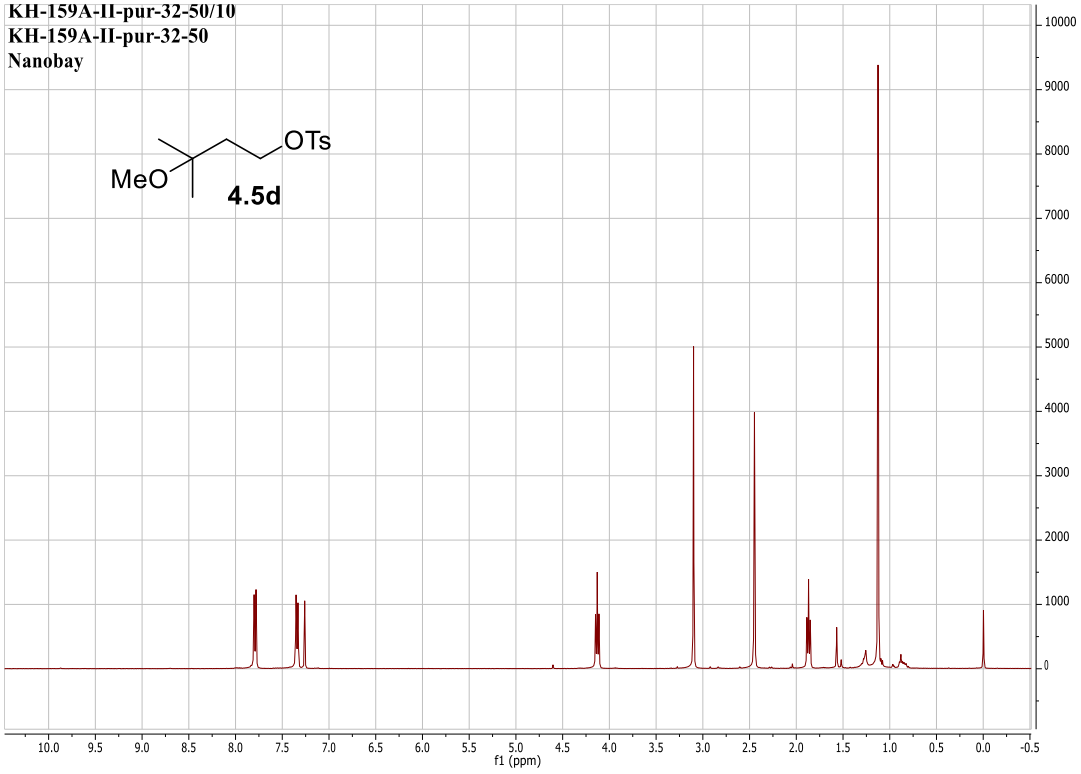

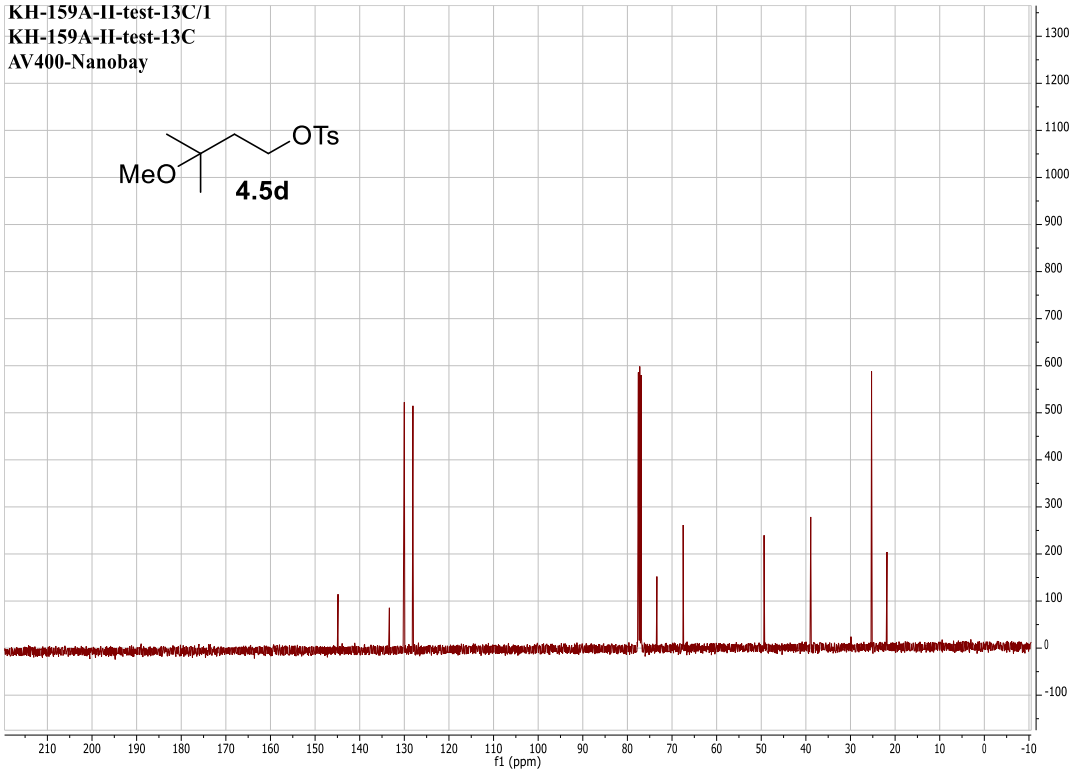

Spectral data for compound **4.6d**:

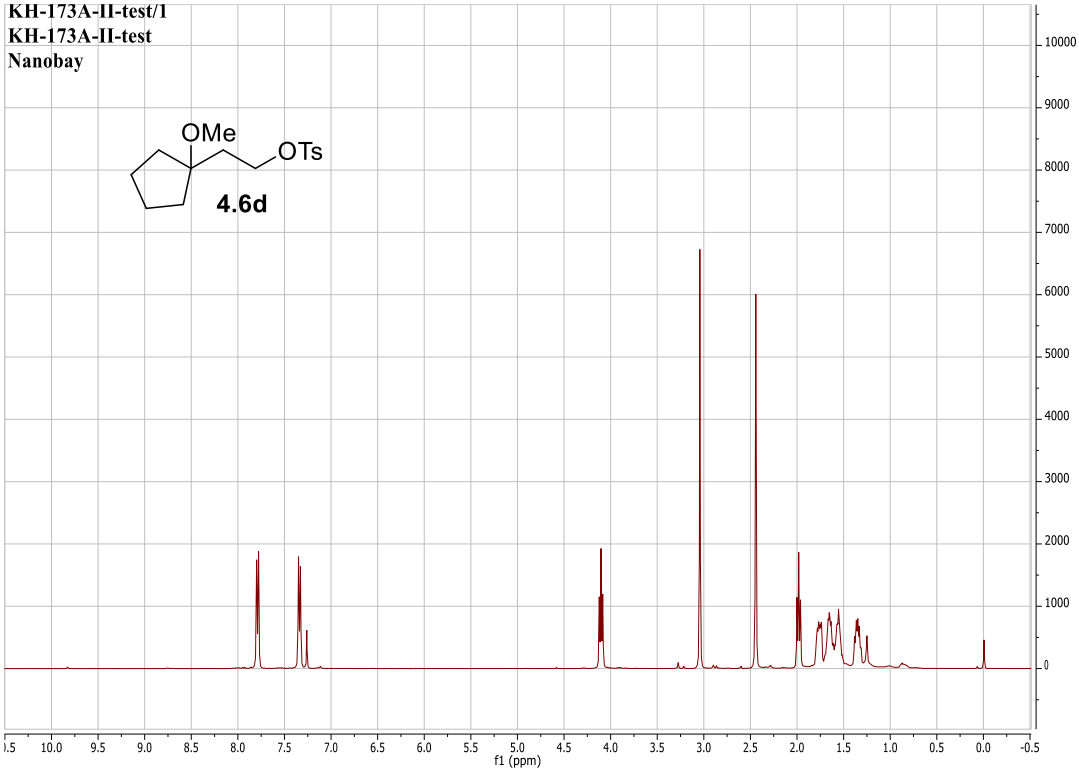

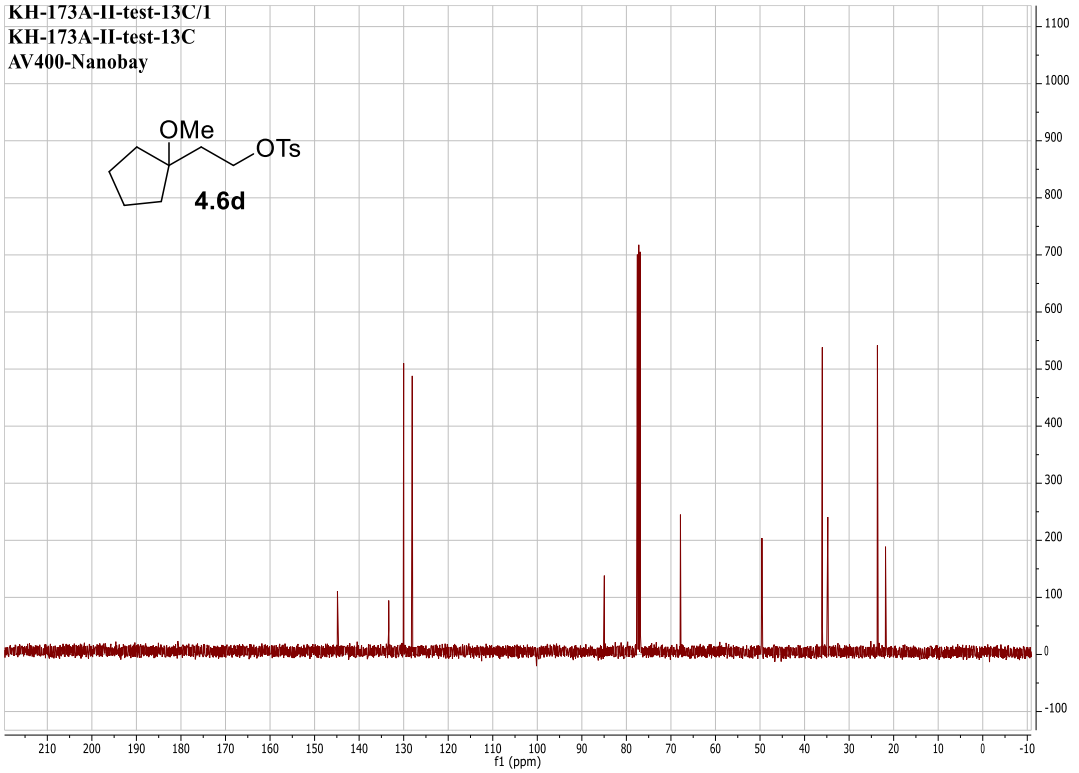

Spectral data for compound **4.19**:

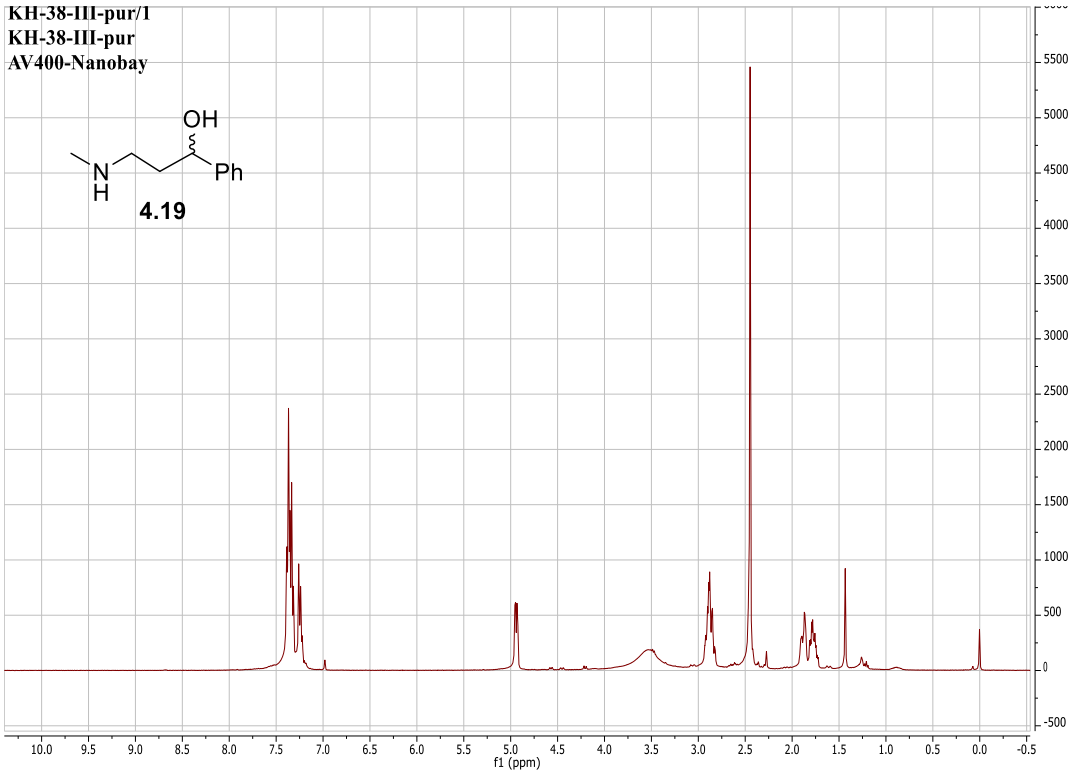

Spectral data for **fluoxetine**:

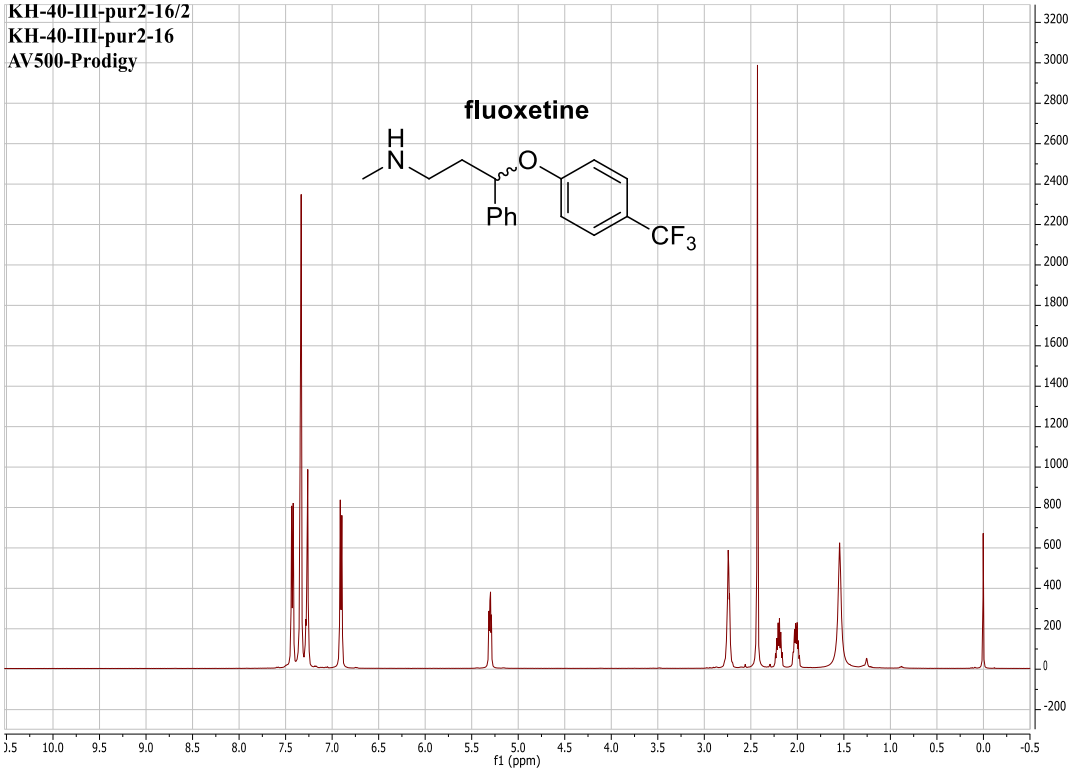

Spectral data for **fluoxetine HCl**:

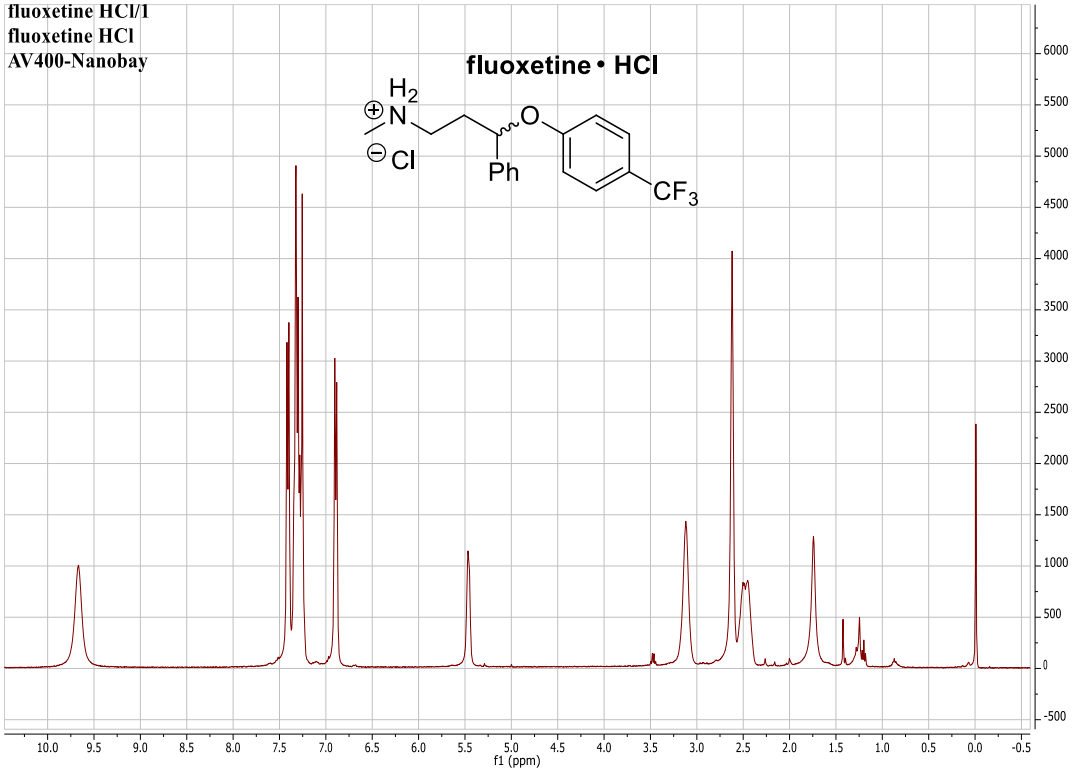

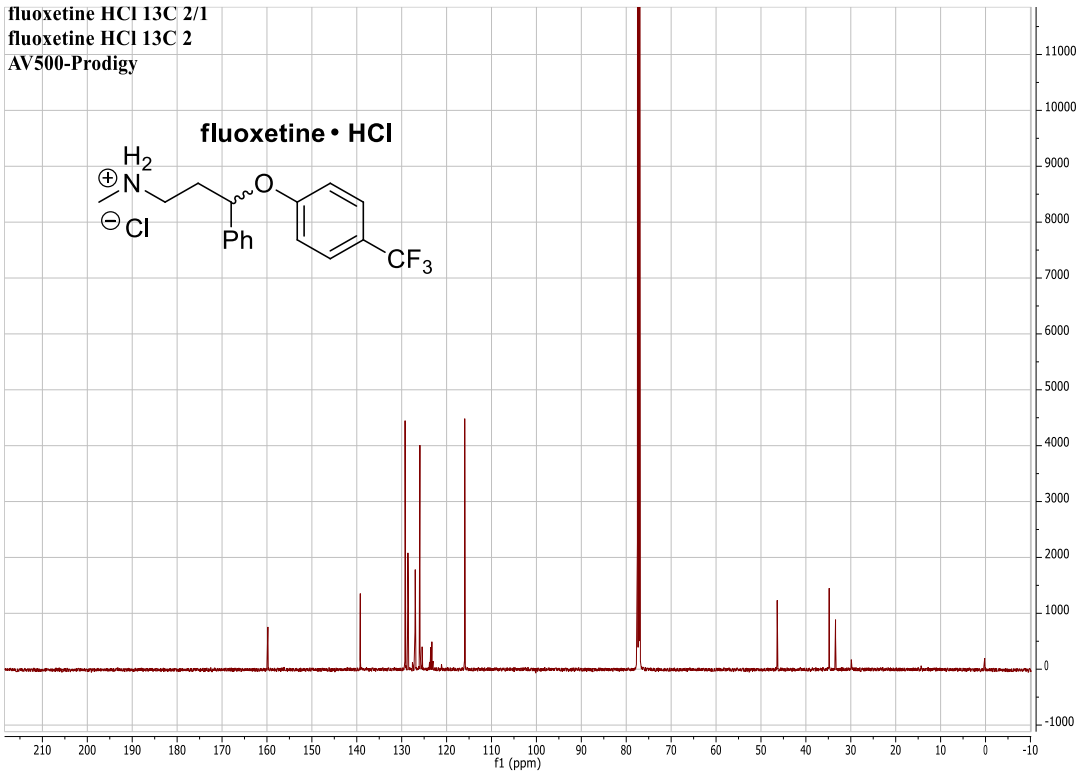

Spectral data for compound **4.5e**:

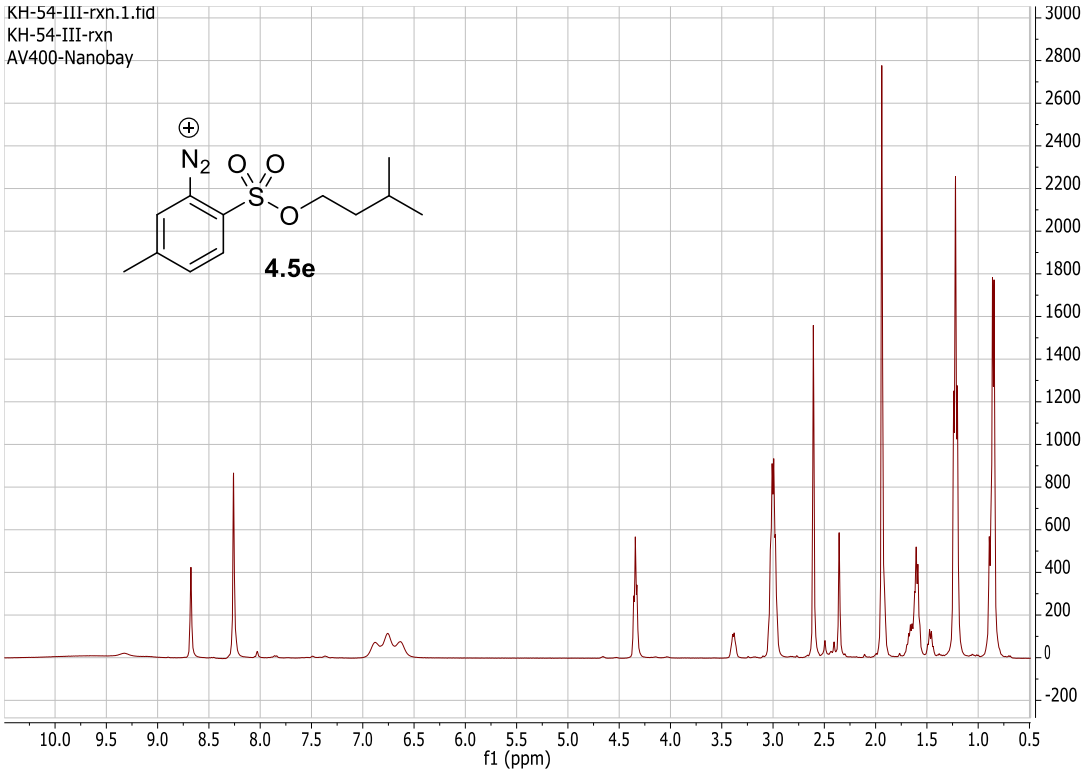

VITA

Kyle Allen Hollister was born in Lakeland, Florida to Stephen K. Hollister and Karen J. Hollister in 1987. He completed his primary education by graduating as valedictorian from Lakeland Senior High School in 2005. The following summer, he enrolled at the University of Florida, where he studied Chemical Engineering and graduated with his Bachelor of Science degree in May, 2010. He then traveled to Louisiana State University in August 2010 to pursue his doctoral degree in the Department of Chemistry. In the winter of 2010, he joined the research group of Dr. Justin R. Ragains and is currently a candidate for the degree of Doctor of Philosophy in Chemistry, to be awarded December 2015.